

Attachment 3C



Engineering and constructing a better tomorrow

June 29, 2009

Mr. Harry Manolopoulos
Project Procurement Specialist
Bechtel Power Corporation
5275 Westview Drive
Frederick, Maryland 21703

**Subject: Intake Samples Laboratory Test Data Report
Calvert Cliffs Nuclear Power Plant Unit 3
Bechtel Job No. 25237
Bechtel Purchase Order No. 25237-103-POA-CY05-00001
MACTEC Project Number 6234-08-4783**

Dear Mr. Manolopoulos:

MACTEC Engineering and Consulting, Inc. (MACTEC) has provided laboratory testing services for the above-referenced project. The testing was done as requested by Bechtel and includes classification, index property, and dynamic properties testing of the provided Intake samples. The tested materials were delivered to MACTEC in undisturbed Shelby tubes. A total of 10 tubes were tested. The requested testing was outlined on a Bechtel Geotechnical Laboratory Test Assignment Schedule dated April 2, 2009 (Rev. 1) as part of Bechtel Purchase Order No. 25237-103-POA-CY05-00001.

The samples were delivered by MACTEC to the Houston, Texas geotechnical laboratory of Fugro Consultants, Inc. (Fugro). Fugro performed the testing working under a subcontract to MACTEC. Initially, each sample was x-rayed and the results of the x-rays were submitted to Bechtel prior to testing. Approval to proceed with the sample extrusion and testing was provided by Bechtel via email on April 10, 2009.

The results of the following laboratory testing of the Intake samples are presented on the attached sheets for your review:

- Moisture Content – ASTM D2216-05
- Unit Weight – ASTM D2166-06
- Specific Gravity – ASTM D854-06
- Gradation – ASTM D422-63(2007)e1 and ASTM D6913-04e1
- Organic Content – ASTM D2974-07
- Atterberg Limits – ASTM D4318-05
- Carbonate Content – ASTM D4373-02(2007)
- Resonant Column Torsional Shear (RCTS) (Fugro Procedure HGL-876, Rev. 1)

This laboratory data report consists of the following:

- Cover letter dated June 22, 2009,

MACTEC Engineering and Consulting, Inc.

2801 Yorkmont Road, Suite 100 • Charlotte, NC 28208 • Phone: 704.357.8600

June 29, 2009

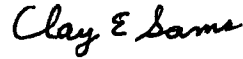
- Attachment 1: Resonant Column / Torsional Shear (RCTS) Test Results Report, prepared by Fugro Consultants, Inc. dated June 18, 2009.

We have enjoyed assisting you on this phase of the project and look forward to continuing to serve as your geotechnical and laboratory testing consultant on the remainder of this project.

Very truly yours,
MACTEC ENGINEERING AND CONSULTING, INC.



Steven E. Kiser
Project Manager



Clay E. Sams
Senior Principal



Engineering and constructing a better tomorrow

ATTACHMENT 1

RESONANT COLUMN / TORSIONAL SHEAR (RCTS) TEST RESULTS DATA REPORT

**CALVERT CLIFFS COL
BECHTEL JOB NO. 25237**

**REPORT PREPARED BY FUGRO CONSULTANTS, INC.
FUGRO REPORT NO. 0411-09-1734**

REPORT DATED JUNE 18, 2009



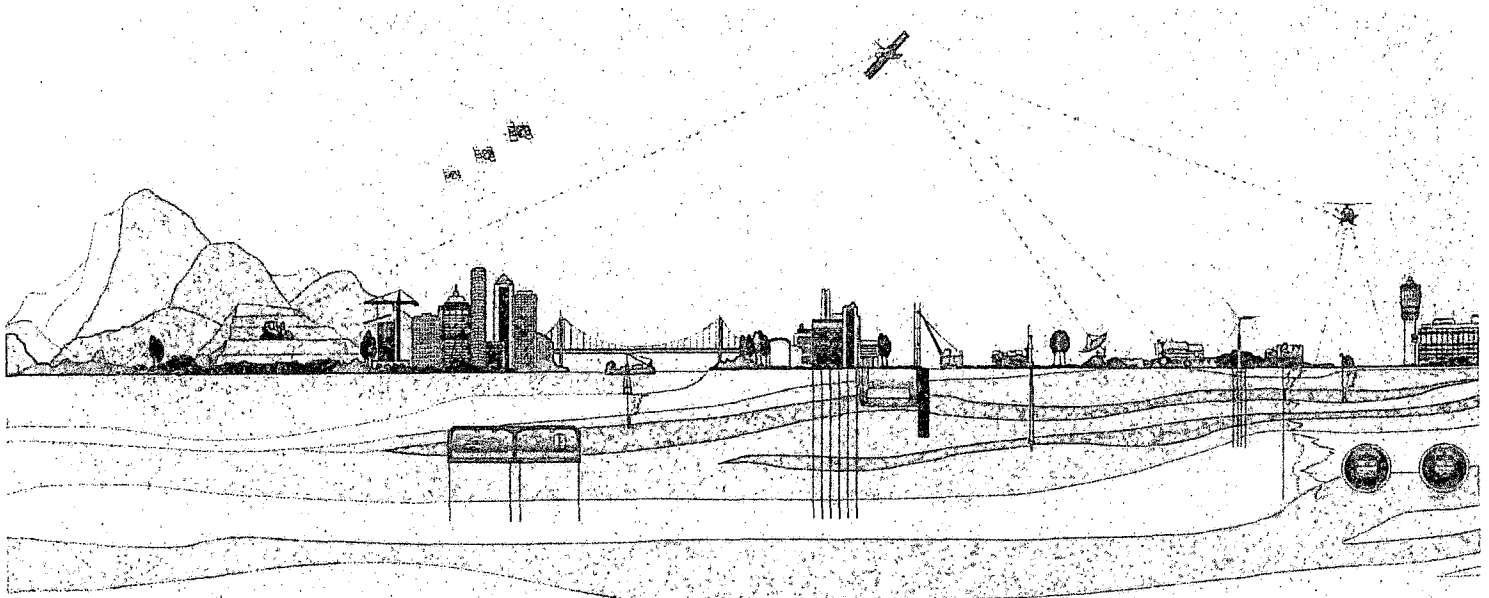
CALVERT CLIFFS NPP
RESONANT COLUMN / TORSIONAL
SHEAR (RCTS) TEST RESULTS

PREPARED FOR: MACTEC

PREPARED BY: FUGRO CONSULTANTS INC.

DATE: June 18, 2009

FUGRO#0411-09-1734



Revised By:
Michael S. Howell
Mark O. Hood 6-22-09



June 18, 2009

Mr. Steven E. Kiser, P.E.
MACTEC Engineering and Consulting, Inc.
2801 Yorkmont Road, Suite 100
Charlotte, NC 28208

6100 Hillcroft (77081)
P.O. Box 740010
Houston, Texas 77274
Tel: 713-369-5400
Fax: 713-369-5518

RE: RCTS Reports For The Calvert Cliffs Project

Dear Mr. Kiser:

Fugro has completed the ten (10) RCTS tests for the Calvert Cliffs project. This submission includes the following items (in hardcopy and CD-ROM):

- Index properties summary, and
- Appendices A through J for each test.

Each individual appendix consists of the following items:

- One (1) cover sheet,
- Up to twenty (20) Figures,
- Five (5) Tables, and
- One (1) grain size plot.

We appreciate this opportunity to be of continued service to MACTEC, Inc. We look forward to working with you in future projects.

Very truly yours,

Fugro Consultants, Inc.

A handwritten signature in black ink, appearing to read "Jiewu Meng".

Jiewu Meng, PhD, P.E.
Project Engineer

A handwritten signature in black ink, appearing to read "Maurice N. Morvant".

Maurice N. Morvant
Assistant Manager

Enclosures



SECTION 1

INTRODUCTION

General:

This report presents the results of resonant column and torsional shear (RCTS) geotechnical testing program performed by the Houston Geotechnical Testing Laboratory of Fugro Consultants, Inc. for MACTEC Engineering and Consulting, Inc (MACTEC) Project Number 6234-08-4783. The testing program was conducted on intake samples provided by MACTEC.

The laboratory testing results contained in this report were completed based on our scope of services as established through submitted work instructions from MACTEC. We have prepared this report exclusively for MACTEC to assist in their Calvert Cliffs project. We intend for this report, including all illustrations, to be used in its entirety. Data as presented in this report should be used along with other available information.

Report Format:

This report is organized into three (3) main sections. This section provides introductory information, describes the scope of the testing program, and highlights specific test procedures. Sections 2 and 3 describe the test procedures and present results from individual test types in tabular and graphical forms. The following presents the individual sections of this report:

- Section 1: Introduction
- Section 2: RCTS Test Procedures
- Section 3: Index Properties and RCTS Characteristics

Purpose and Scope of Testing Program:

The purpose of this laboratory testing program is to determine physical and engineering properties of ten (10) tube samples taken from the project site. Purposes and Scopes of the individual test types are to determine engineering properties of selected materials as follows:

- Index properties and grain size distribution.
- Dynamic properties under various confining pressures.

The following number and type of index and engineering property tests were performed as part of the scope of work.

- Ten (10) grain size & hydrometer analysis tests.
- Ten (10) Atterberg limits tests.
- Ten (10) specific gravity tests.
- Ten (10) organic content tests.

- Ten (10) calcium carbonate tests.

The following basic physical property determinations were performed in conjunction with each engineering property test specimen.

- Water Content
- Total Unit Weight

Test Procedures:

Fugro conducted this service under MACTEC's QA program. MACTEC audited Fugro's QA program and provided additional QA requirements through a procurement agreement with Fugro. Equipment calibrations provided traceability to NIST standards or physical constants. Equipment calibration records were provided separately to MACTEC.

The testing was conducted following the procedures provided in MACTEC's Work Instruction For Laboratory Testing, Revisions 1, dated April 27, 2009. Fugro received soil tubes for testing as delivered by MACTEC via FedEx under Chain of Custody. The tubes were stored upright, in a temperature controlled environment at Fugro's facility following MACTEC's instructions. Prior to testing, the tubes were X-rayed for quality identification following ASTM D4452.

The index properties were tested on trimmings and take-downs of Resonant Column and Torsional Shear (RCTS) samples. The ASTM test methods specified in the work instructions are summarized below.

- *Moisture Content* – ASTM D2216 Standard Test Methods for Laboratory Determination of Water (Moisture) Content of Soil and Rock by Mass.
- *Atterberg Limits* – ASTM D4318 Standard Test Methods for Liquid Limit, Plastic Limit, and Plasticity Index of Soils.
- *Specific Gravity* – ASTM D854 Standard Test Methods for Specific Gravity of Soil Solids by Water Pycnometer.
- *Organic Content* – ASTM D2974 Standard Test Methods for Moisture, Ash, and Organic Matter of Peat and Other Organic Soils.
- *Calcium Carbonate* – ASTM D4373 Standard Test Method for Rapid Determination of Carbonate Content of Soils.
- *Particle Size Analysis* – ASTM D422 Standard Test Method for Particle-Size Analysis of Soils.
- *Sieve Analysis* – ASTM D6913 Standard Test Methods for Particle-Size Distribution (Gradation) of Soils Using Sieve Analysis.

In addition, Unified Soil Classification System (USCS) symbols were assigned to the samples per ASTM D2487 Standard Practice for Classification of Soils for Engineering Purposes (Unified Soil Classification System)

The RCTS testing was performed following Technical Procedures for Resonant Column and Torsional Shear (RCTS) Testing of Soil and Rock Samples (Procedure PBRCTS01, Revision 4) as provided by MACTEC. These procedures are presented separately in Section 2 of this report.

SECTION 2

RCTS PROCEDURES

Fugro laboratory personnel used resonant column and torsional shear (RCTS) equipment to measure the material properties (shear modulus and material damping in shear) of soil specimens. The RCTS equipment used is of the fixed-free type, with the bottom of the specimen fixed and shear stress applied to the top.

Both the resonant column (RC) and torsional shear (TS) tests were performed in a sequential series on the same specimen over a shearing strain range from about 10-4% to about 1%, depending upon specimen stiffness.

The basic operational principle is to vibrate the cylindrical specimen in first-mode torsional motion. Harmonic torsional excitation is applied to the top of the specimen over a range in frequencies, and the variation of the acceleration amplitude of the specimen with frequency is obtained. Once first-mode resonance is established, measurements of the resonant frequency and amplitude of vibration are made. These measurements are then combined with equipment characteristics and specimen size to calculate shear wave velocity and shear modulus based on elastic wave propagation.

The RC test is based on the one-dimensional wave equation derived from the theory of elasticity. The shear modulus is obtained by measuring the first-mode resonant frequency while material damping is evaluated from either the free-vibration decay curve or from the width of the frequency response curve at the so-called half power points. In the TS test, the actual stress-strain hysteresis loop is determined by means of measuring the torque-twist curve. Shear modulus is calculated from the slope of the hysteresis loop, and the damping ratio is calculated using the area of the hysteresis loop compared to the triangle made by the slope of the hysteresis loop and a line passing horizontally through the origin. The primary difference between the two types of tests is the excitation frequency. In the RC test, frequencies above 20 Hz are generally required and inertia of the specimen and drive system is considered when analyzing the measurements. The TS test is associated with slow cyclic loading frequencies generally below 10 Hz and inertia is not considered in the data analysis.

Equipment wise, the RCTS apparatus consists of four basic subsystems which are: 1) a confinement system, 2) a drive system, 3) a height-change measurement system, and 4) a motion monitoring system. The test apparatus is automated so that a microcomputer controls the test and collects the data. Compressed air is used to confine isotropically the specimen in the stainless steel confining chamber. The drive system consists of a drive plate, magnets, drive coils, a power amplifier and a signal generating source. The magnets are fixed to the drive plate and the drive coils encircle the ends of the magnets such that the drive plate excites the soil specimen in torsional motion when a current is passed through the coils. The height change of the specimen is measured by a linear variable differential transformer to determine the changes in the length and

mass of the specimen during consolidation or swell, and to calculate change in the mass moment of inertia, mass density, and void ratio during testing.

RCTS testing was performed on each soil specimen at selected confining pressures of 0.25, 0.5, 1, 2, and 4 times the estimated effective stress. Testing at each successive stage (i.e., confining pressure condition) occurred after the specimens were allowed to consolidate at each pressure step. The soil specimen is sealed in a membrane and pore pressure in the specimen is vented to atmospheric pressure. In general, the rate of consolidation decreased with increasing confining pressure for each specimen, and cohesive soil specimens longer to consolidate than granular soils. Consolidation times range from about 1 day up to about 1 week. Fugro laboratory personnel analyzed the resulting stress/strain curve to determine when the sample was sufficiently consolidated for testing.

At each level of shear strain amplitude, the shear modulus (G) and material damping ratio (λ) were determined. For each consolidation stage, the maximum shear modulus (G_{max}) and minimum material damping ratio (λ_{min}) were determined, along with some values of G and λ versus strain amplitude. Typically in the 0.25, 0.5, 1, 2, and 4 times consolidation stages, a less than 0.001% shear strain amplitude is generally applied throughout each of the testing sequence. In the 1 and 4 consolidation stages, additional levels of shear strain amplitude are applied, up to that obtainable by the equipment. In each consolidation stage, after testing at the maximum strain amplitude, additional values of G were determined to monitor specimen recovery.

Because different frequencies are applied in the RC and TS tests, different motion monitoring systems are used. The motion monitoring system in the RC test consists of an accelerometer, a charge amplifier, and a data acquisition system (DAQ). The motion monitoring system in the TS test consists of two proximator probes, an operational amplifier, a DC power supply, a U-shaped target and a digital data acquisition system to monitor torque-twist hysteresis loops of the specimen.

SECTION 3

INDEX PROPERTIES AND RCTS CHARACTERISTICS

- Index Properties Summary
- Appendix A 773B-UD2
- Appendix B 773B-UD3
- Appendix C 773B-UD4
- Appendix D 773B-UD5
- Appendix E 773B-UD6
- Appendix F 773B-UD7
- Appendix G 773B-UD9
- Appendix H 773B-UD11
- Appendix I 773B-UD13
- Appendix J 773B-UD15

Table 1. Index Properties Summary
Calvert Cliffs COL Project (Fugro#0411-09-1734)

Appendix #	Boring #	Sample #	Depth (ft)	Type	Index Properties							
					Total Unit Weight (lb/ft ³)	Moisture Content (%) (ASTM D2216)	Liquid Limit (ASTM D4318)	Plastic Limit (ASTM D4318)	Specific Gravity (ASTM D854)	Organic Content (ASTM D2974)	Calcium Carbonate (ASTM D4373)	USCS Symbol (ASTM D2487)
A	773B	2	15.9	UD	125.7	23.3	Non Plastic		2.67	0.60	22	SM
B	773B	3	27.0	UD	111.6	35.0	55	22	2.61	1.64	13	SC
C	773B	4	37.0	UD	103.0	53.6	101	25	2.68	3.06	0	CH
D	773B	5	47.0	UD	110.9	34.1	46	20	2.65	1.64	5	SC
E	773B	6	57.0	UD	106.4	44.5	62	24	2.65	4.12	2	CH
F	773B	7	66.1	UD	110.1	33.5	87	23	2.64	2.62	2	CH
G	773B	9	87.0	UD	99.1	59.2	119	29	2.61	5.94	2	CH
H	773B	11	107.0	UD	102.5	55.1	109	27	2.60	5.10	3	CH
I	773B	13	127.0	UD	108.3	45.2	69	24	2.53	1.34	2	SC
J	773B	15	147.0	UD	101.5	52.3	102	75	2.48	2.16	2	CH

APPENDIX A

Specimen B-773B_2

Borehole B-773B

Sample 2

Depth = 15.9 ft (4.8 m)

Total Unit Weight = 125.7 lb/ft³

Water Content = 23.3 %

FUGRO JOB #: 0411-09-1734
Testing Station: RC5



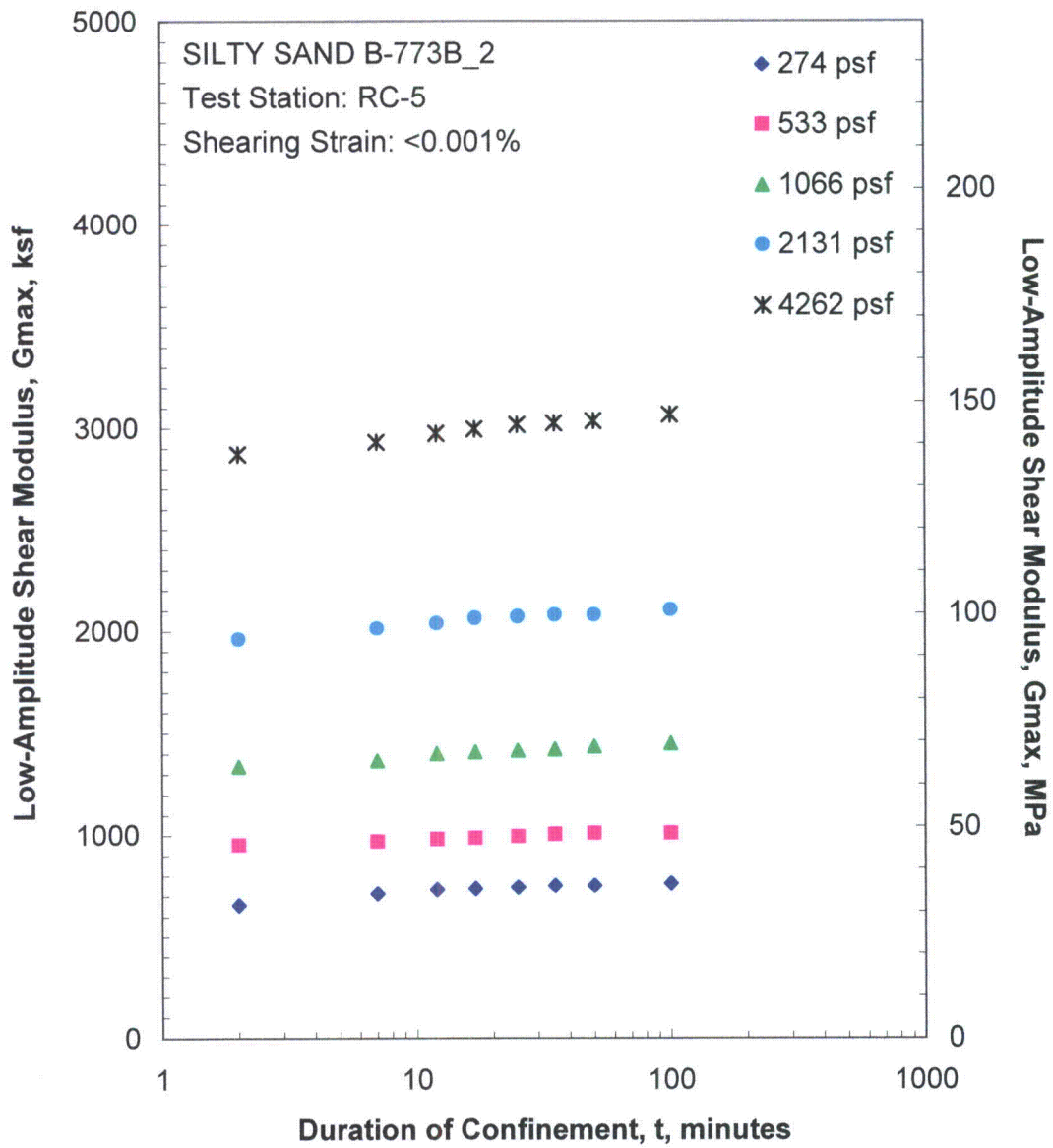


Figure A.1 Variation in Low-Amplitude Shear Modulus with Magnitude and Duration of Isotropic Confining Pressure from Resonant Column Tests

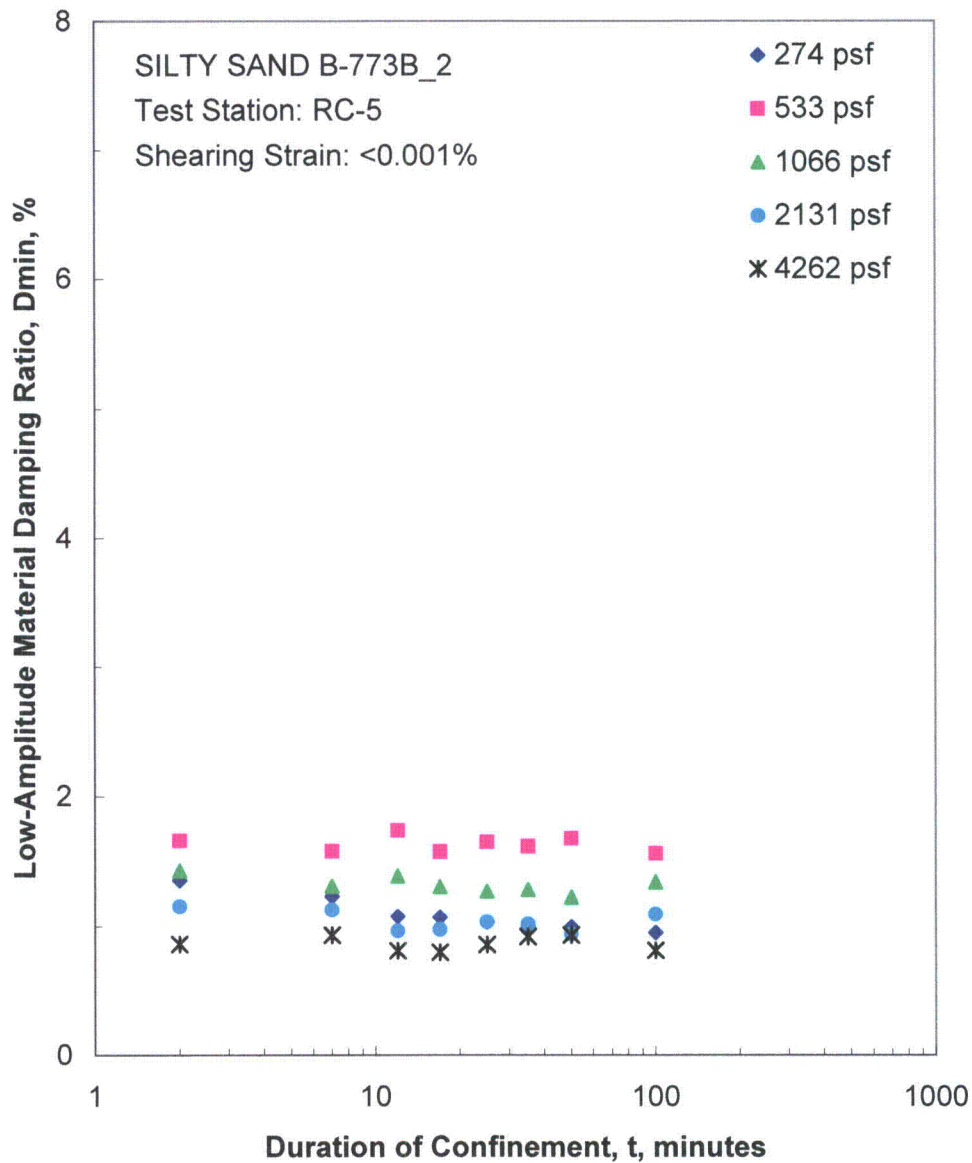


Figure A.2 Variation in Low-Amplitude Material Damping Ratio with Magnitude and Duration of Isotropic Confining Pressure from Resonant Column Tests

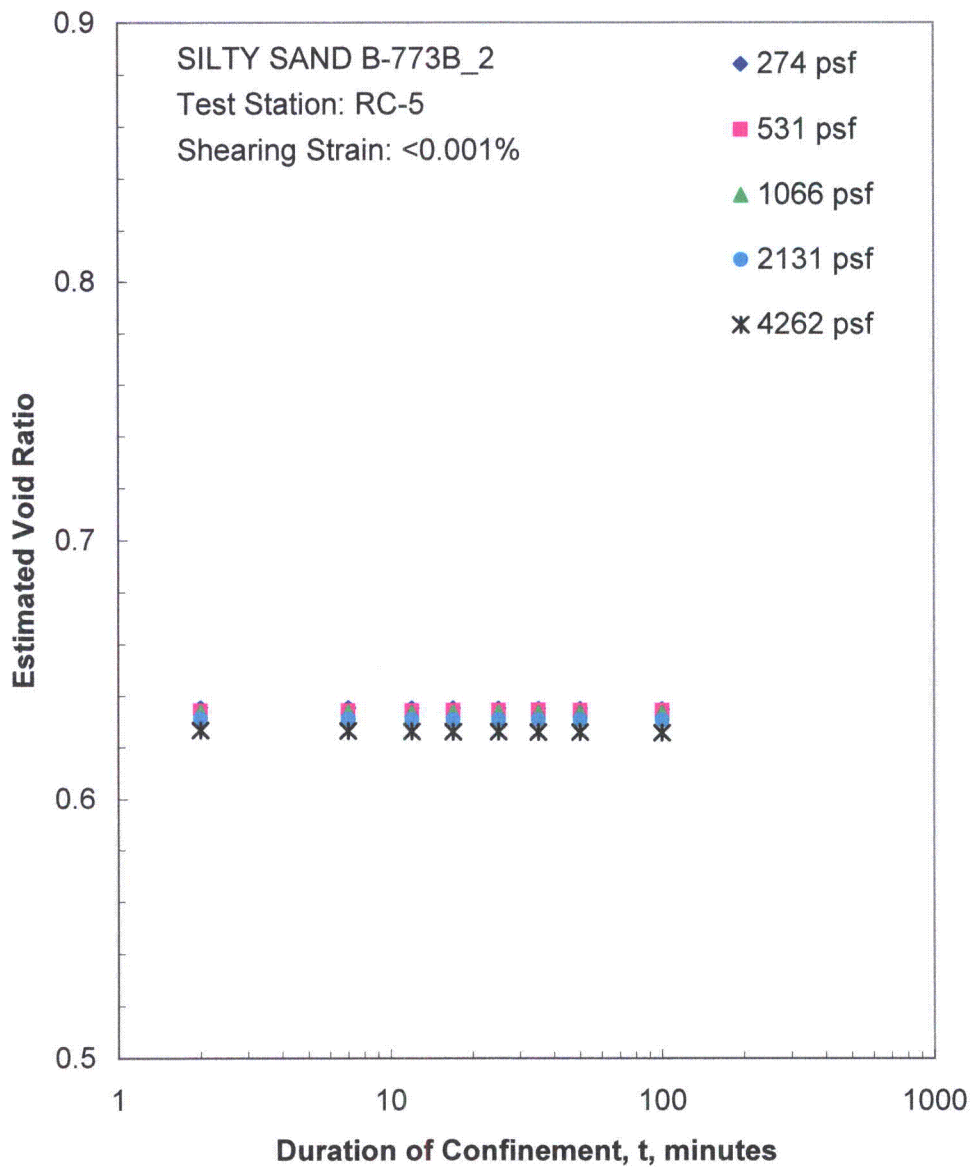


Figure A.3 Variation in Estimated Void Ratio with Magnitude and Duration of Isotropic Confining Pressure from Resonant Column Tests

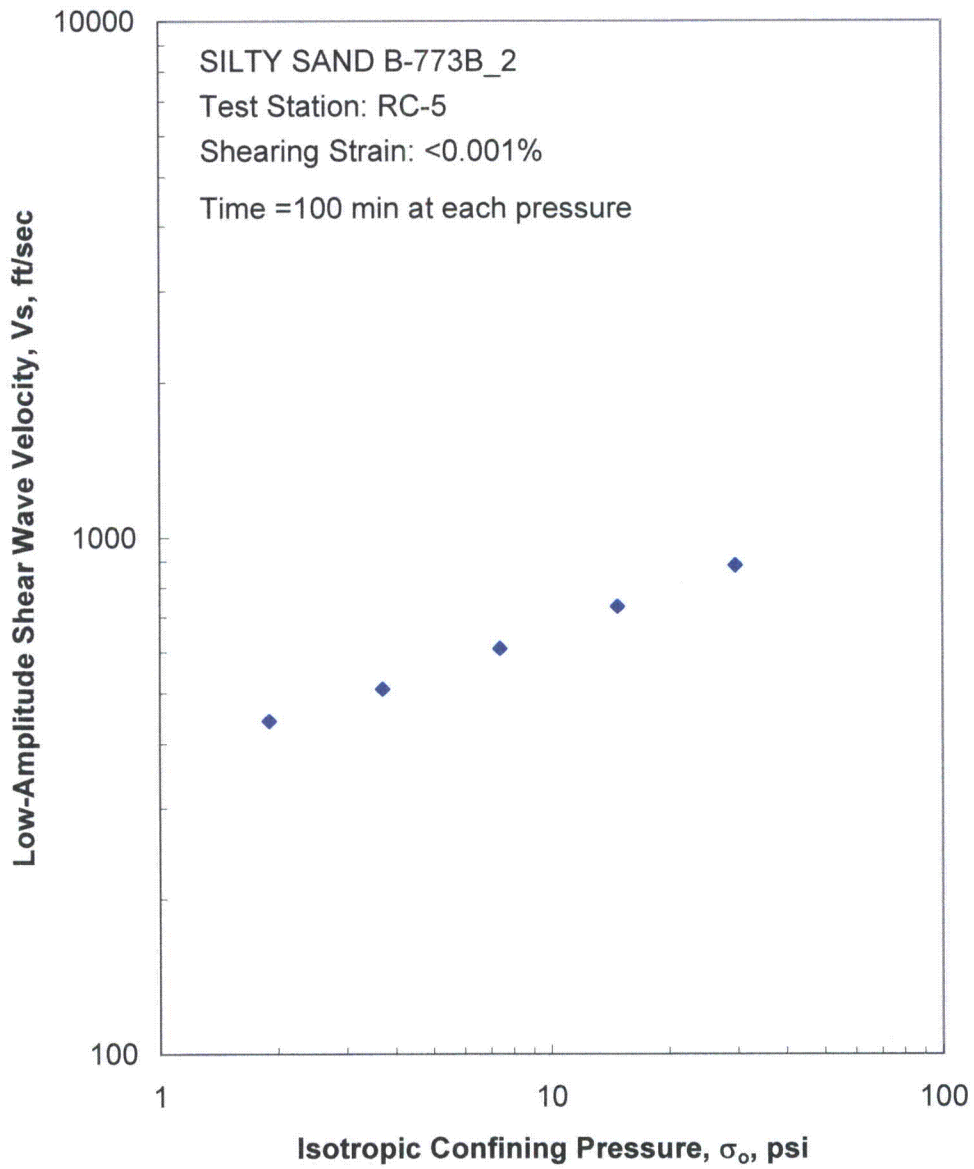


Figure A.4 Variation in Low-Amplitude Shear Wave Velocity with Isotropic Confining Pressure from Resonant Column Tests

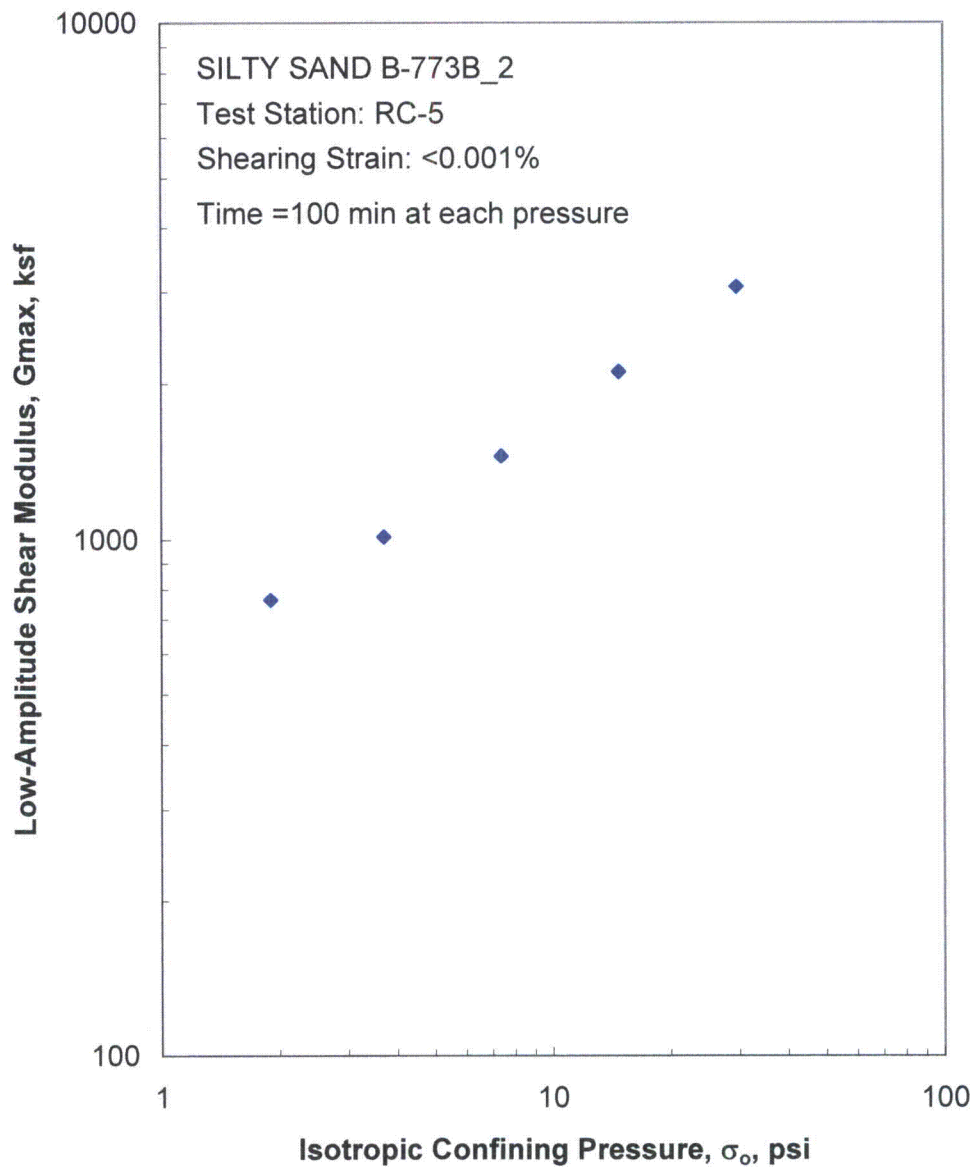


Figure A.5 Variation in Low-Amplitude Shear Modulus with Isotropic Confining Pressure from Resonant Column Tests

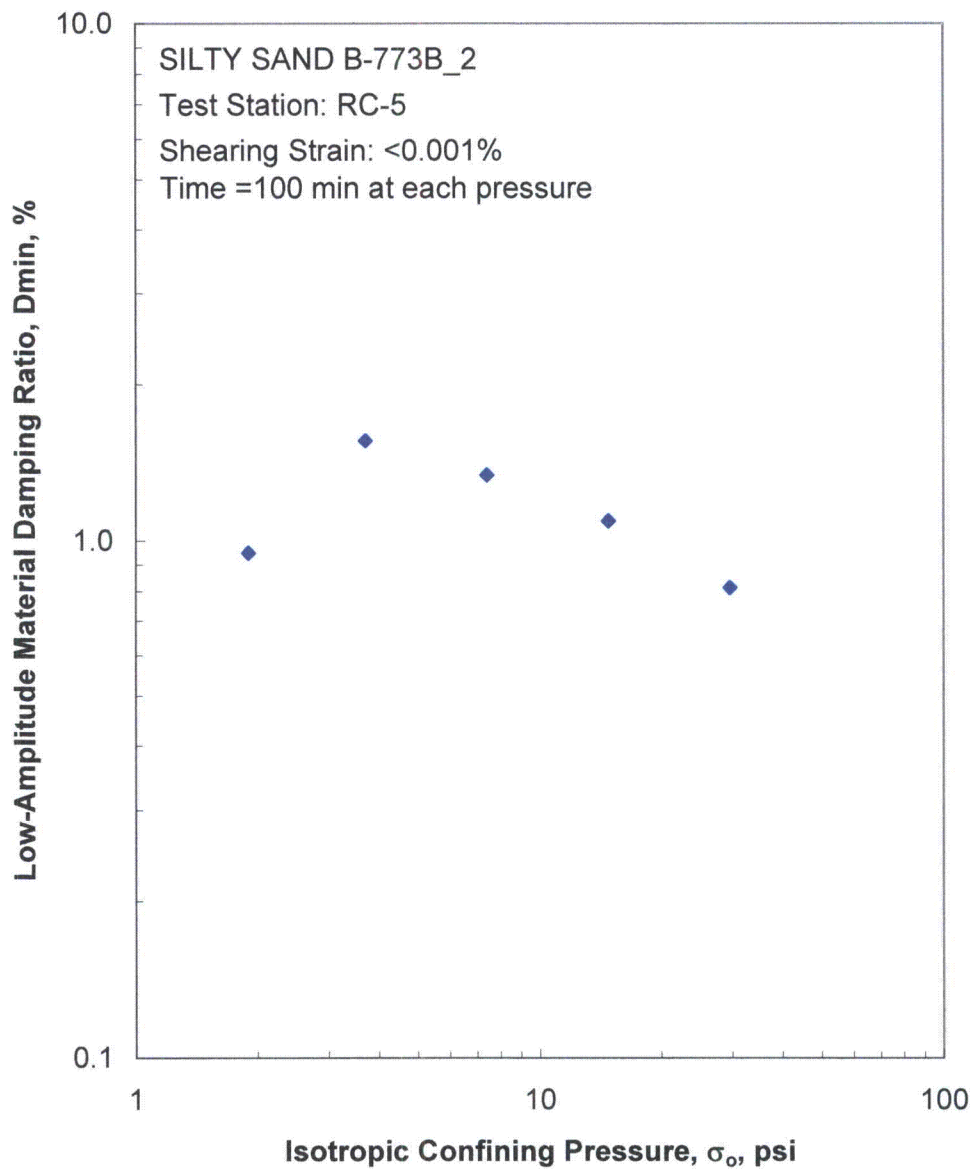


Figure A.6 Variation in Low-Amplitude Material Damping Ratio with Isotropic Confining Pressure from Resonant Column Tests

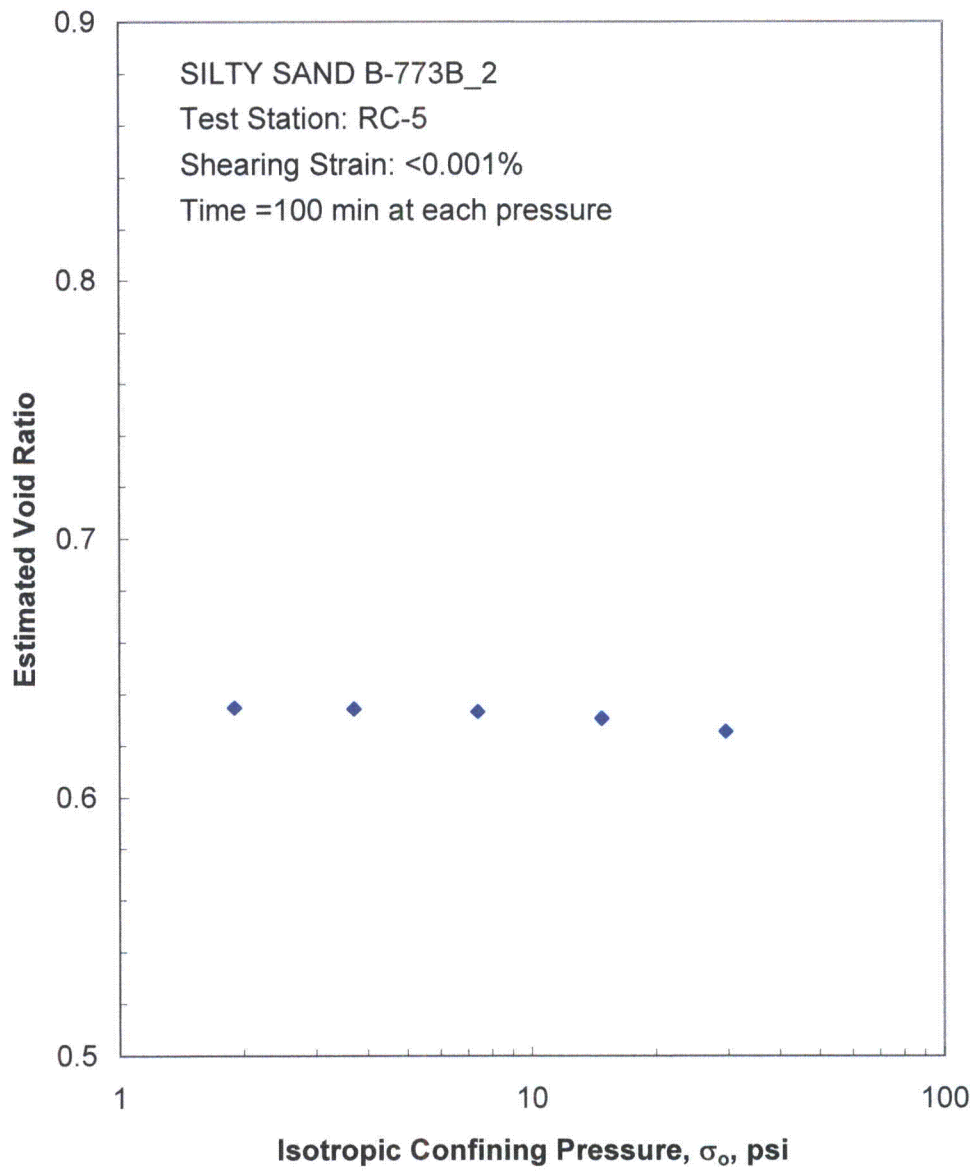


Figure A.7 Variation in Estimated Void Ratio with Isotropic Confining Pressure from Resonant Column Tests

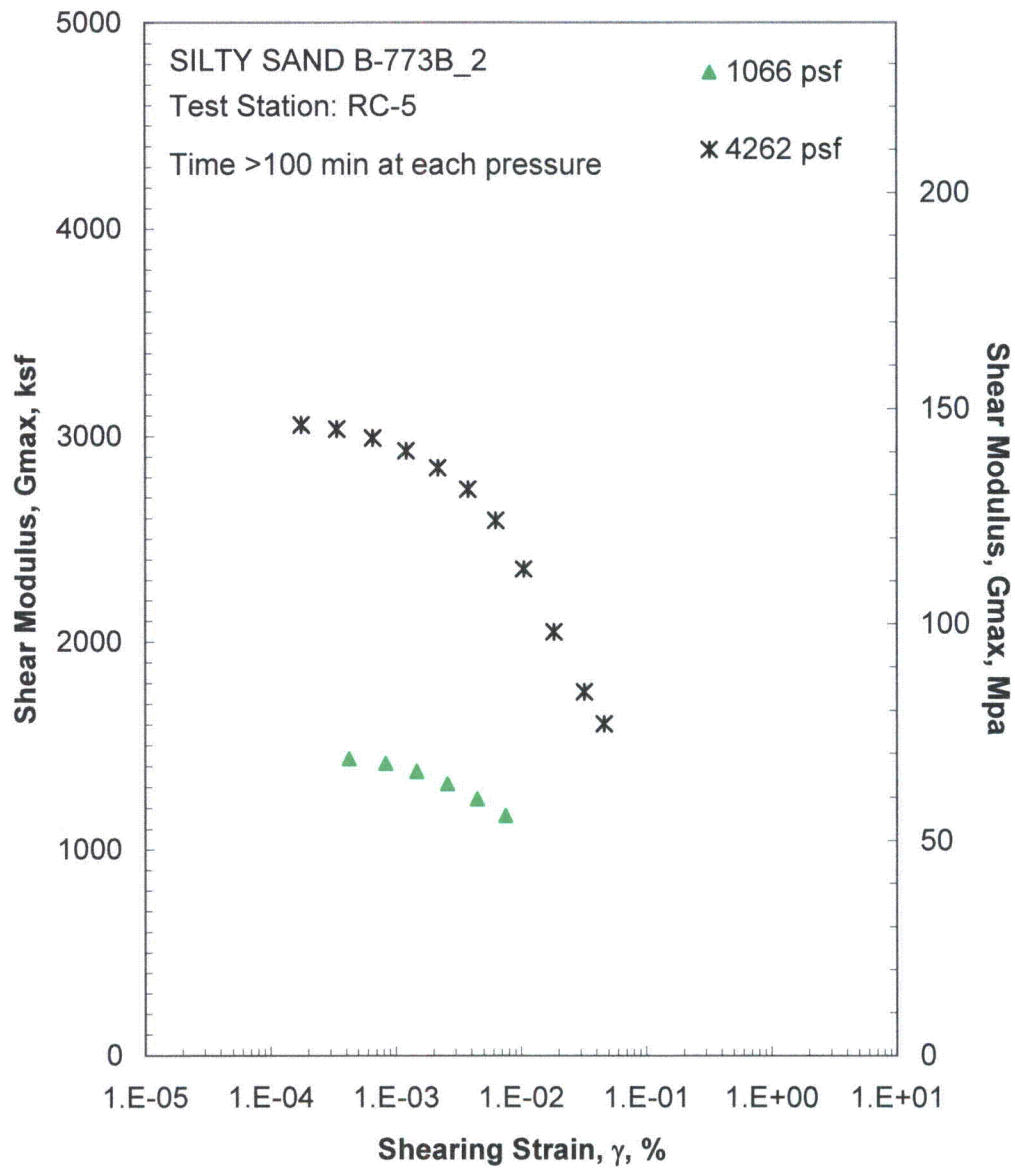


Figure A.8 Comparison of the Variation in Shear Modulus with Shearing Strain and Isotropic Confining Pressure from the Resonant Column Tests

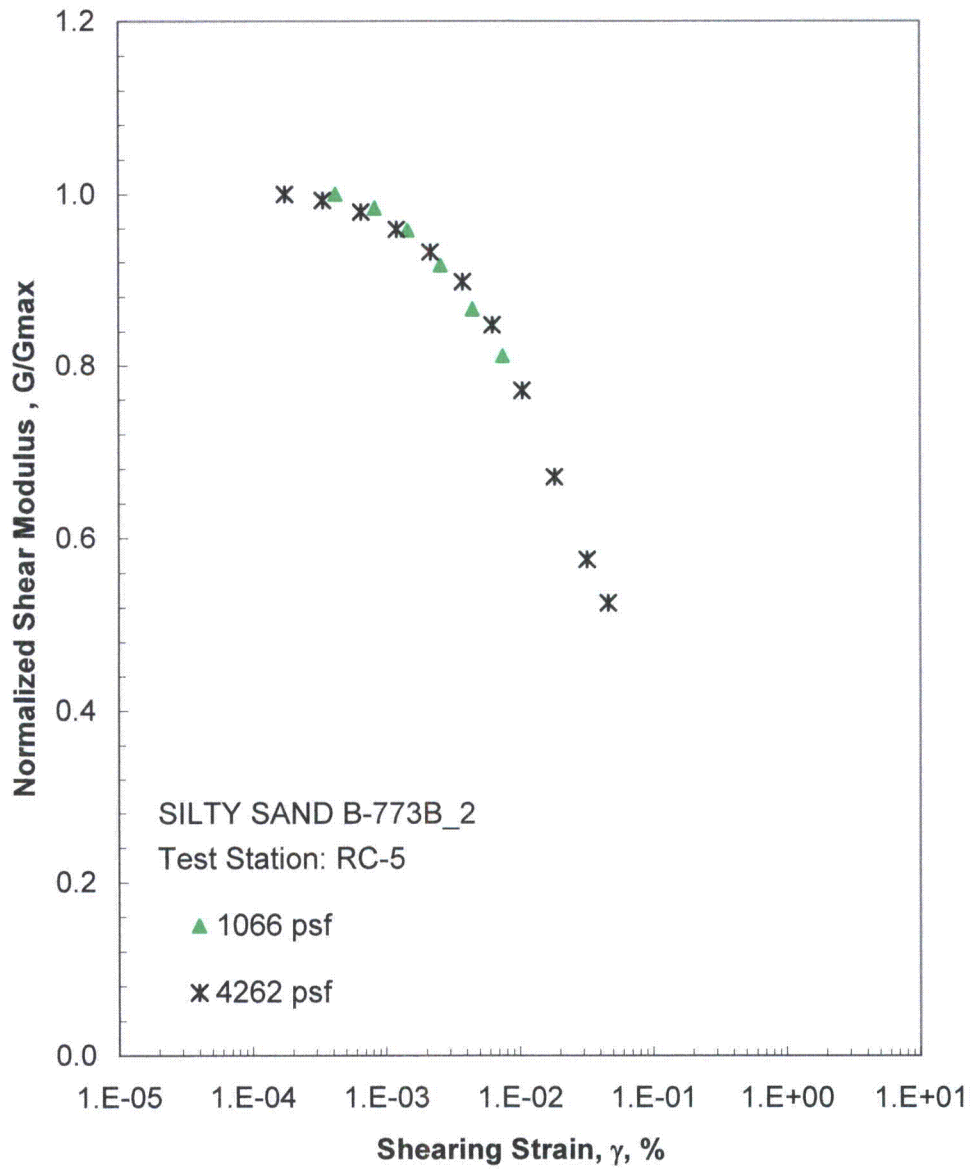


Figure A.9 Comparison of the Variation in Normalized Shear Modulus with Shearing Strain and Isotropic Confining Pressure from the Resonant Column Tests

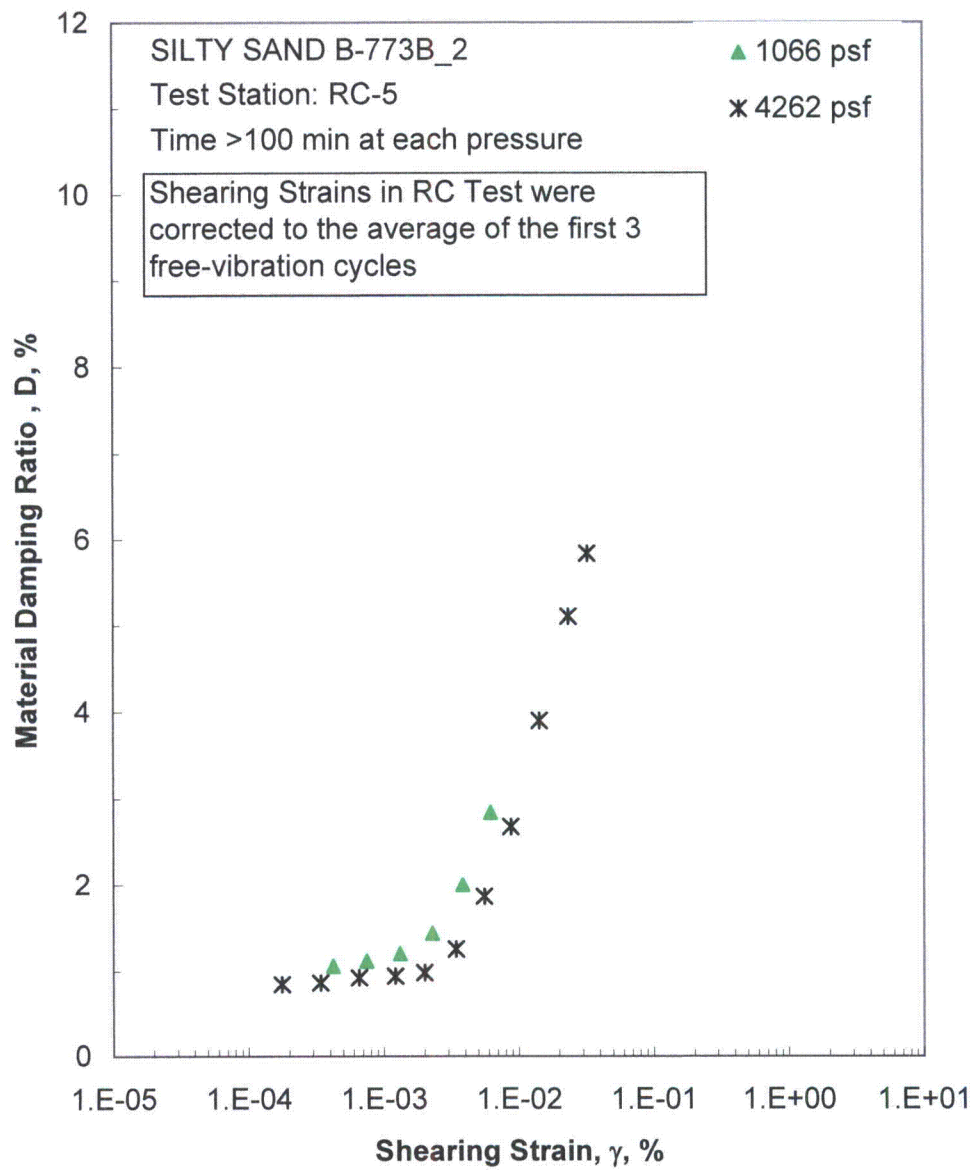


Figure A.10 Comparison of the Variation in Material Damping Ratio with Shearing Strain and Isotropic Confining Pressure from the Resonant Column Tests

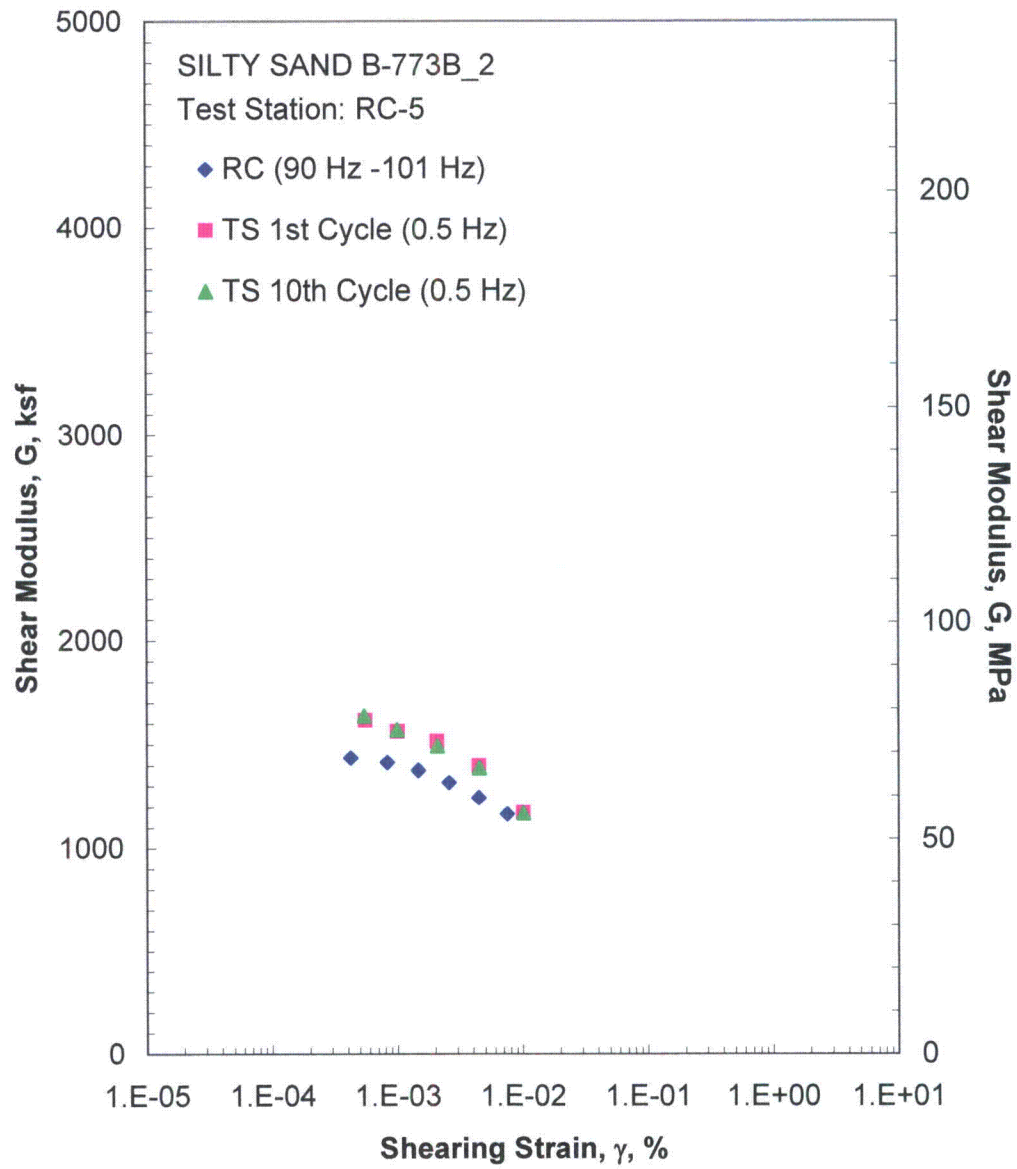


Figure A.11 Comparison of the Variation in Shear Modulus with Shearing Strain at an Isotropic Confining Pressure of 1066 psf from the Combined RCTS Tests

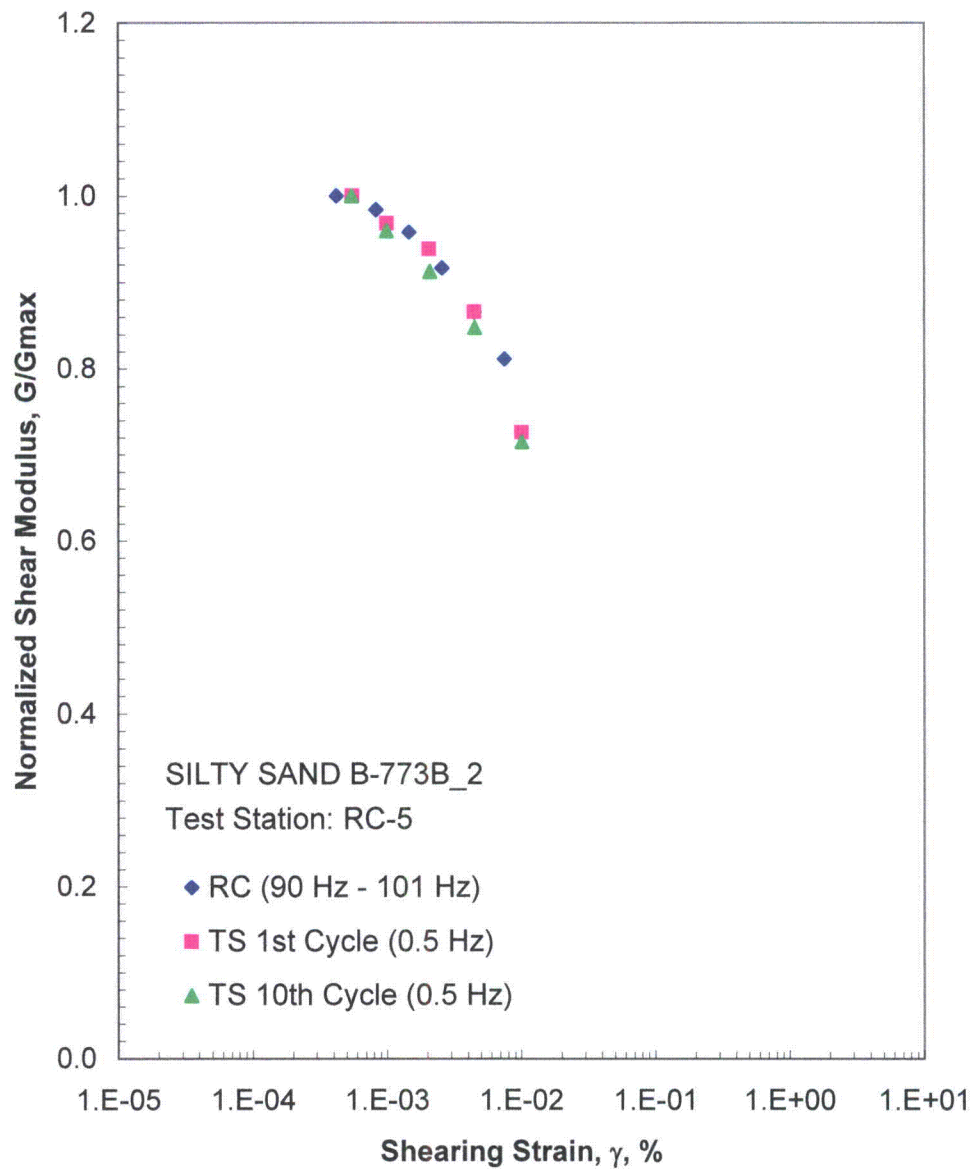


Figure A.12 Comparison of the Variation in Normalized Shear Modulus with Shearing Strain at an Isotropic Confining Pressure of 1066 psf from the Combined RCTS Tests

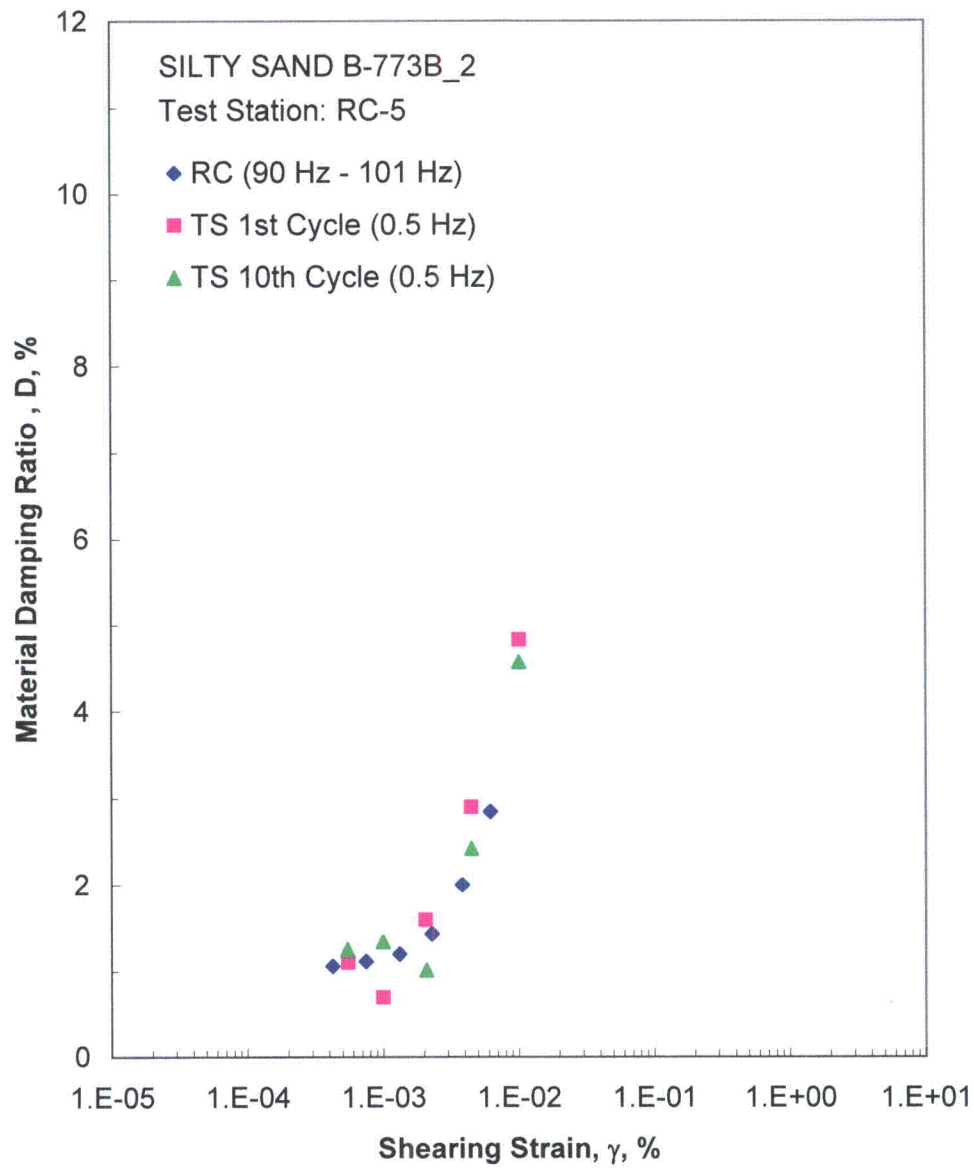


Figure A.13 Comparison of the Variation in Material Damping Ratio with Shearing Strain at an Isotropic Confining Pressure of 1066 psf from the Combined RCTS Tests

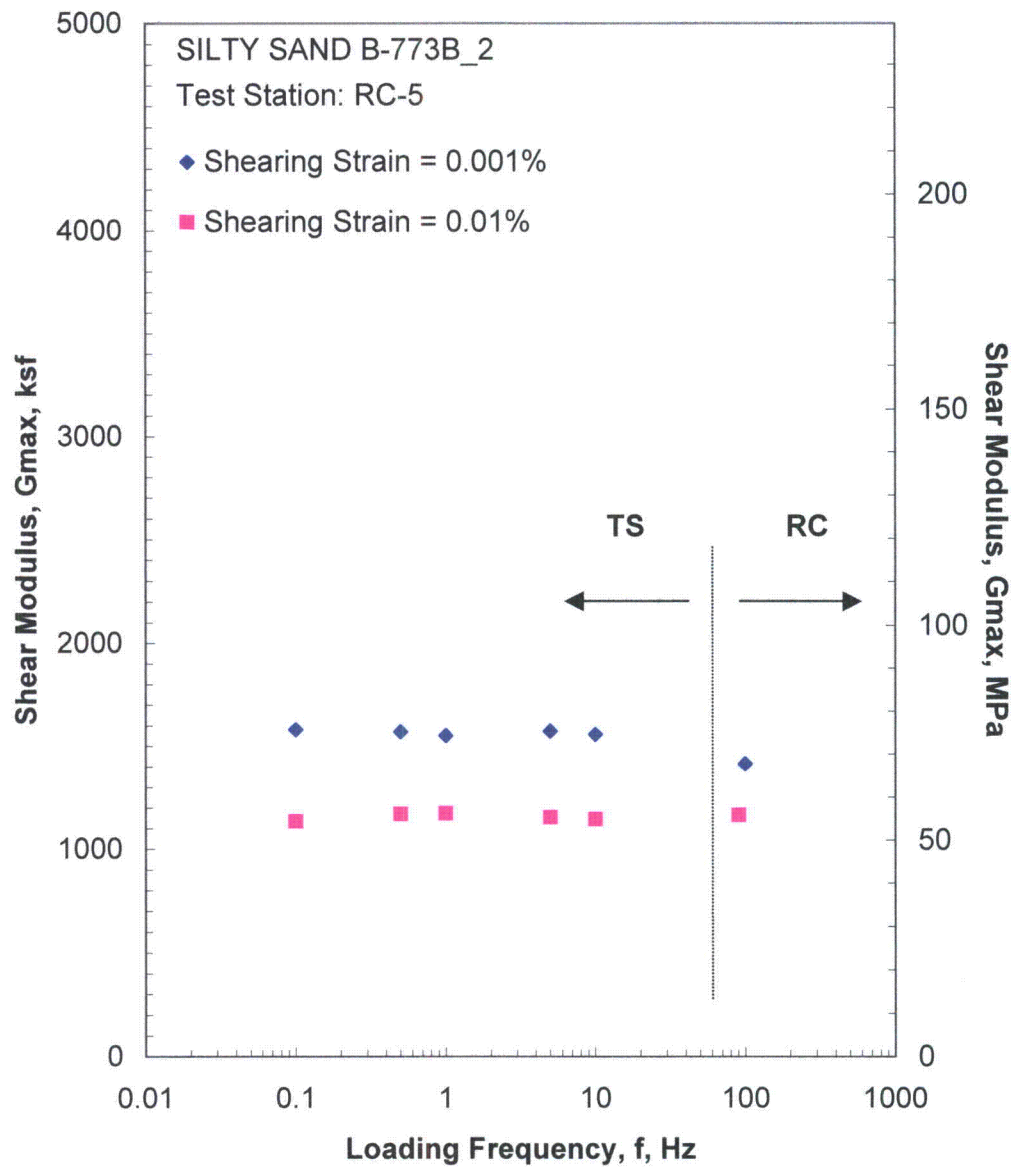


Figure A.14 Comparison of the Variation in Shear Modulus with Loading Frequency at an Isotropic Confining Pressure of 1066 psf from the Combined RCTS Tests

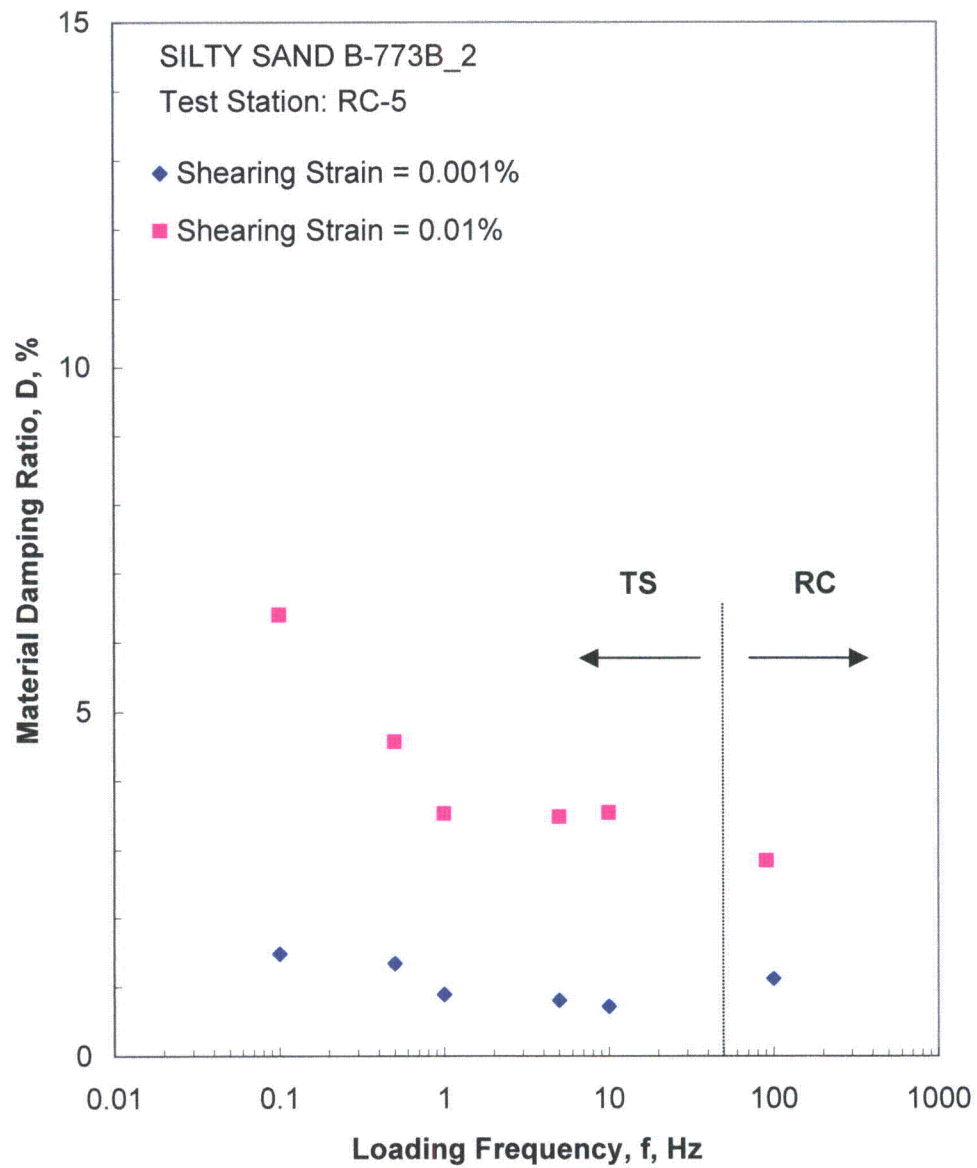


Figure A.15 Comparison of the Variation in Material Damping Ratio with Loading Frequency at an Isotropic Confining Pressure of 1066 psf from the Combined RCTS Tests

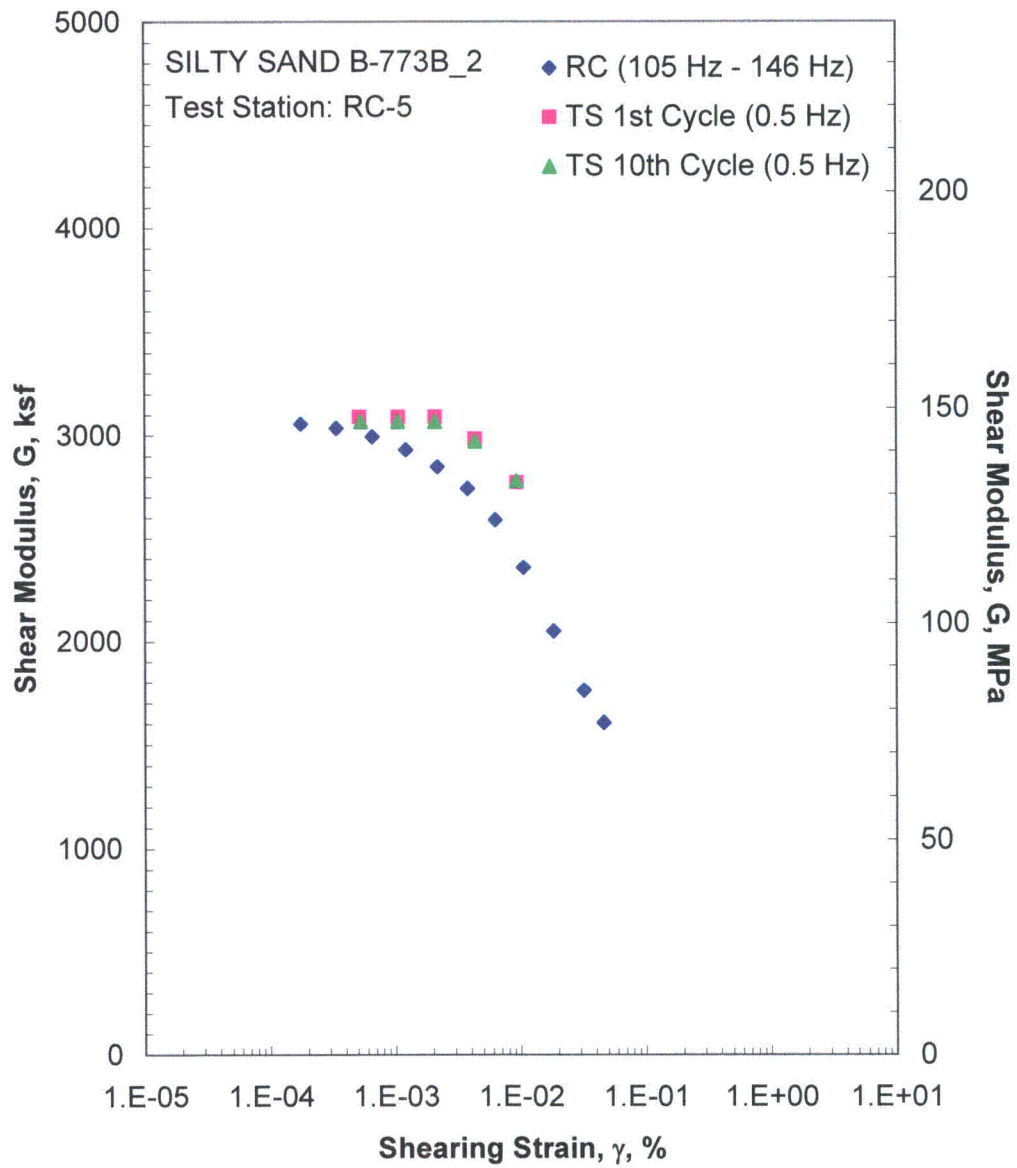


Figure A.16 Comparison of the Variation in Shear Modulus with Shearing Strain at an Isotropic Confining Pressure of 4262 psf from the Combined RCTS Tests

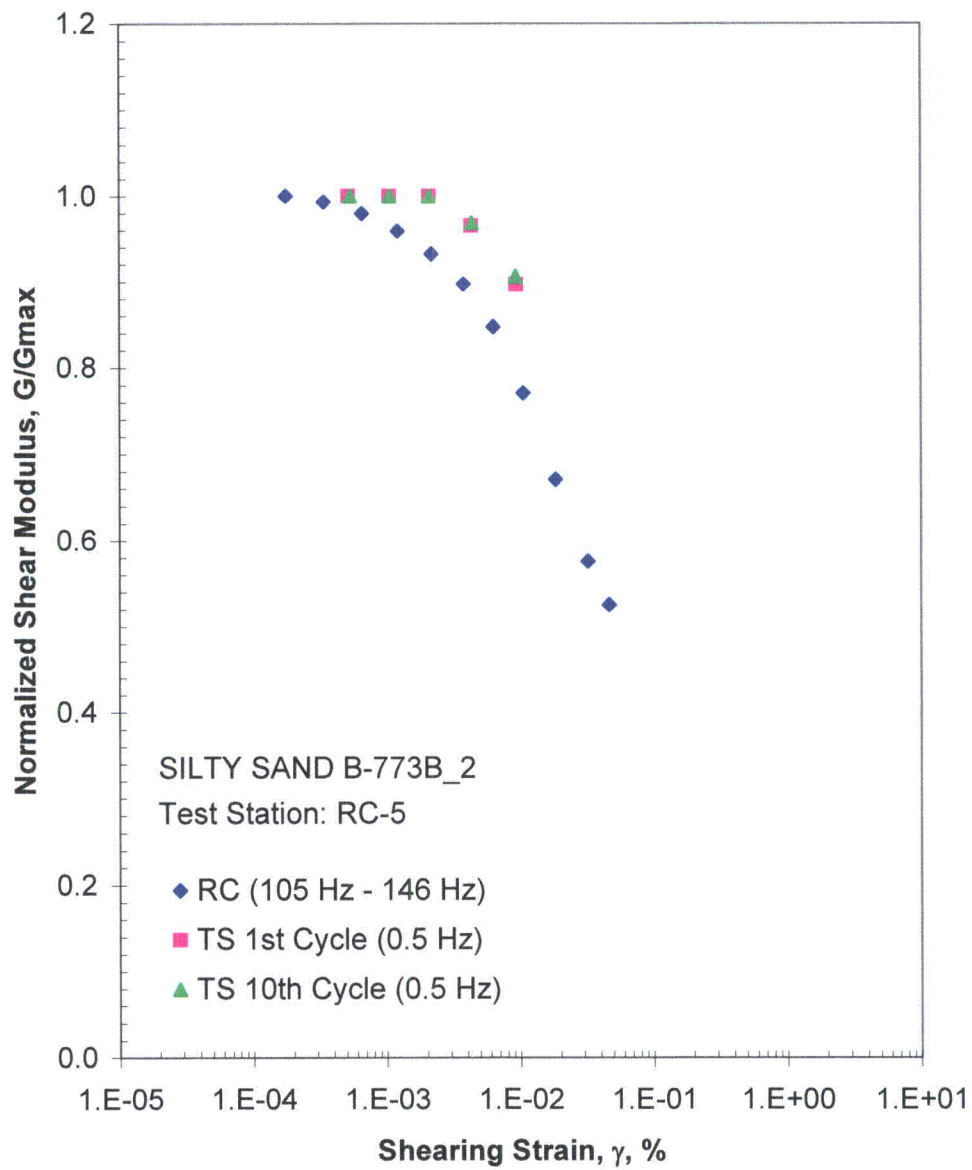


Figure A.17 Comparison of the Variation in Normalized Shear Modulus with Shearing Strain at an Isotropic Confining Pressure of 4262 psf from the Combined RCTS Tests

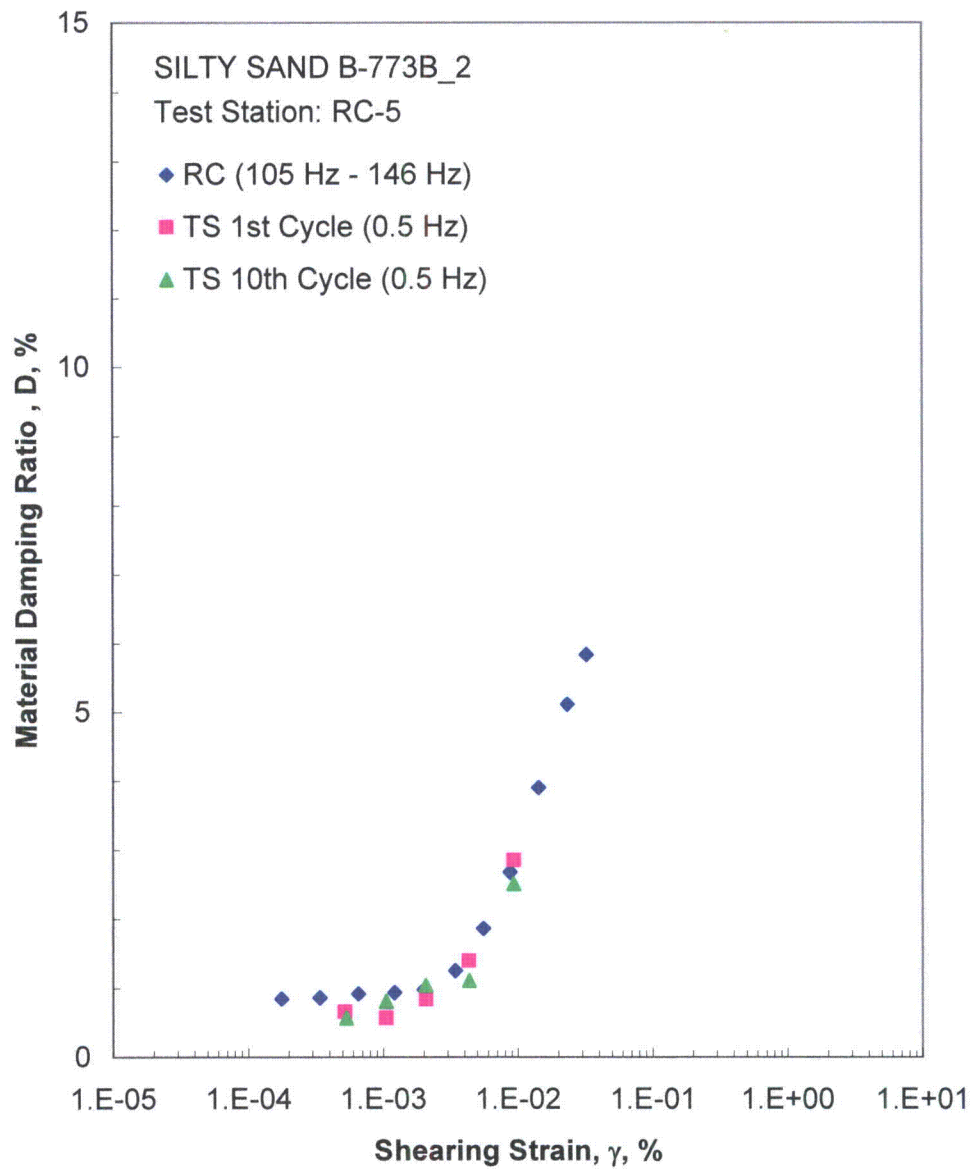


Figure A.18 Comparison of the Variation in Material Damping Ratio with Shearing Strain at an Isotropic Confining Pressure of 4262 psf from the Combined RCTS Tests

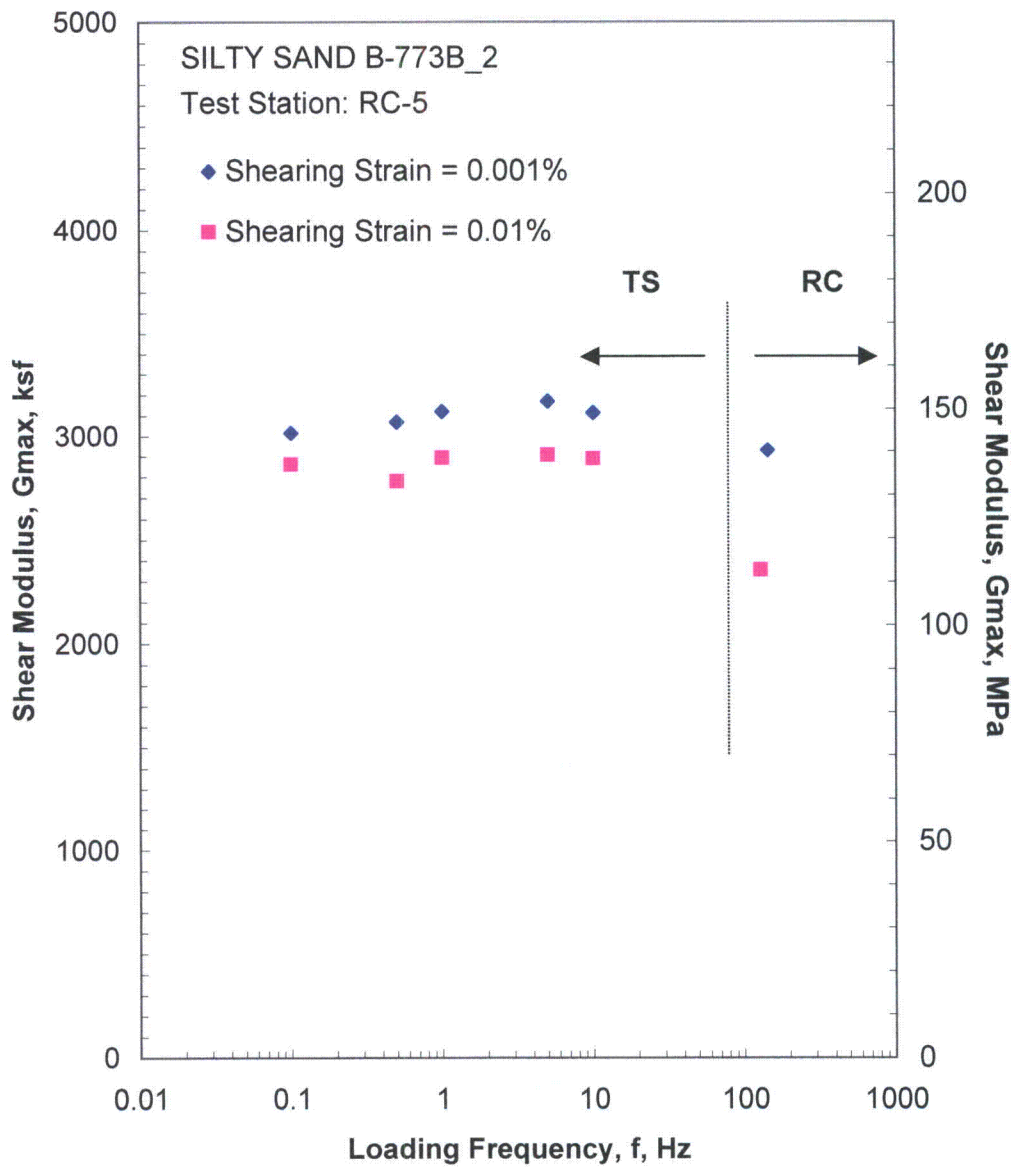


Figure A.19 Comparison of the Variation in Shear Modulus with Loading Frequency at an Isotropic Confining Pressure of 4262 psf from the Combined RCTS Tests

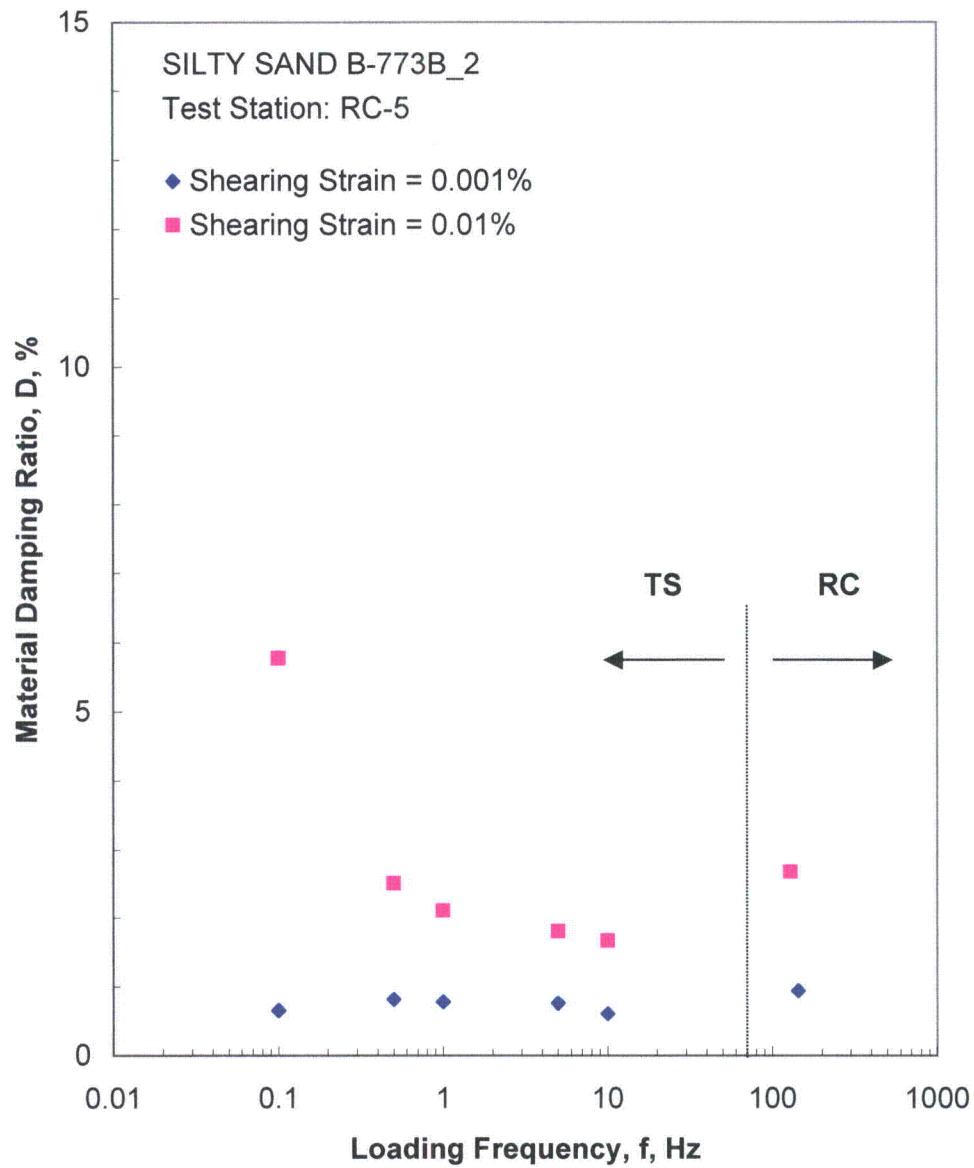


Figure A.20 Comparison of the Variation in Material Damping Ratio 4262 psf from the Combined RCTS Tests

Table A.1 Variation in Low-Amplitude Shear Wave Velocity, Low-Amplitude Shear Modulus, Low-Amplitude Material Damping Ratio and Estimated Void Ratio with Isotropic Confining Pressure from RC Tests of Specimen B-773B-2

Isotropic Confining Pressure, σ_o			Low-Amplitude Shear Modulus, G_{max}		Low-Amplitude Shear Wave Velocity, V_s	Low-Amplitude Material Damping Ratio, D_{min}	Estimated Void Ratio, e
(psi)	(psf)	(kPa)	(ksf)	(MPa)	(fps)	(%)	
2	274	13	762	37	441	0.95	0.63
4	533	25	1012	49	509	1.56	0.63
7	1066	51	1451	70	609	1.34	0.63
15	2131	102	2107	101	733	1.09	0.63
30	4262	204	3069	147	884	0.81	0.63

Table A.2 Variation in Shear Modulus and Material Damping Ratio with Shearing Strain from RC Tests of Specimen B-773B-2; Isotropic Confining Pressure, $\sigma_o = 1066$ psf

Peak Shearing Strain, %	Shear Modulus, G, ksf	Normalized Shear Modulus, G/G_{max}	Average ⁺ Shearing Strain, %	Material Damping Ratio ^x , D, %
4.22E-04	1437	1.00	4.22E-04	1.06
8.27E-04	1414	0.98	7.44E-04	1.12
1.46E-03	1376	0.96	1.32E-03	1.20
2.57E-03	1316	0.92	2.29E-03	1.43
4.47E-03	1244	0.87	3.84E-03	2.00
7.51E-03	1166	0.81	6.15E-03	2.84

⁺ Average Shearing Strain from the First Three Cycles of the Free Vibration Decay Curve

^x Average Damping Ratio from the First Three Cycles of the Free Vibration Decay Curve

Table A.3 Variation in Shear Modulus, Normalized Shear Modulus and Material Damping Ratio with Shearing Strain from TS Tests of Specimen B-773B-2; Isotropic Confining Pressure, $\sigma_0 = 1066$ psf

First Cycle				Tenth Cycle			
Peak Shearing Strain, %	Shear Modulus, G, ksf	Normalized Shear Modulus, G/G_{max}	Material Damping Ratio, D, %	Peak Shearing Strain, %	Shear Modulus, G, ksf	Normalized Shear Modulus, G/G_{max}	Material Damping Ratio, D, %
5.52E-04	1615	1.00	1.10	5.44E-04	1637	1.00	1.25
9.97E-04	1563	0.97	0.69	9.93E-04	1570	0.96	1.34
2.06E-03	1515	0.94	1.59	2.09E-03	1493	0.91	1.01
4.46E-03	1399	0.87	2.89	4.49E-03	1388	0.85	2.42
1.01E-02	1172	0.73	4.83	1.01E-02	1169	0.71	4.57

Table A.4 Variation in Shear Modulus and Material Damping Ratio with Shearing Strain from RC Tests of Specimen B-773B-2; Isotropic Confining Pressure, $\sigma_0 = 4262$ psf

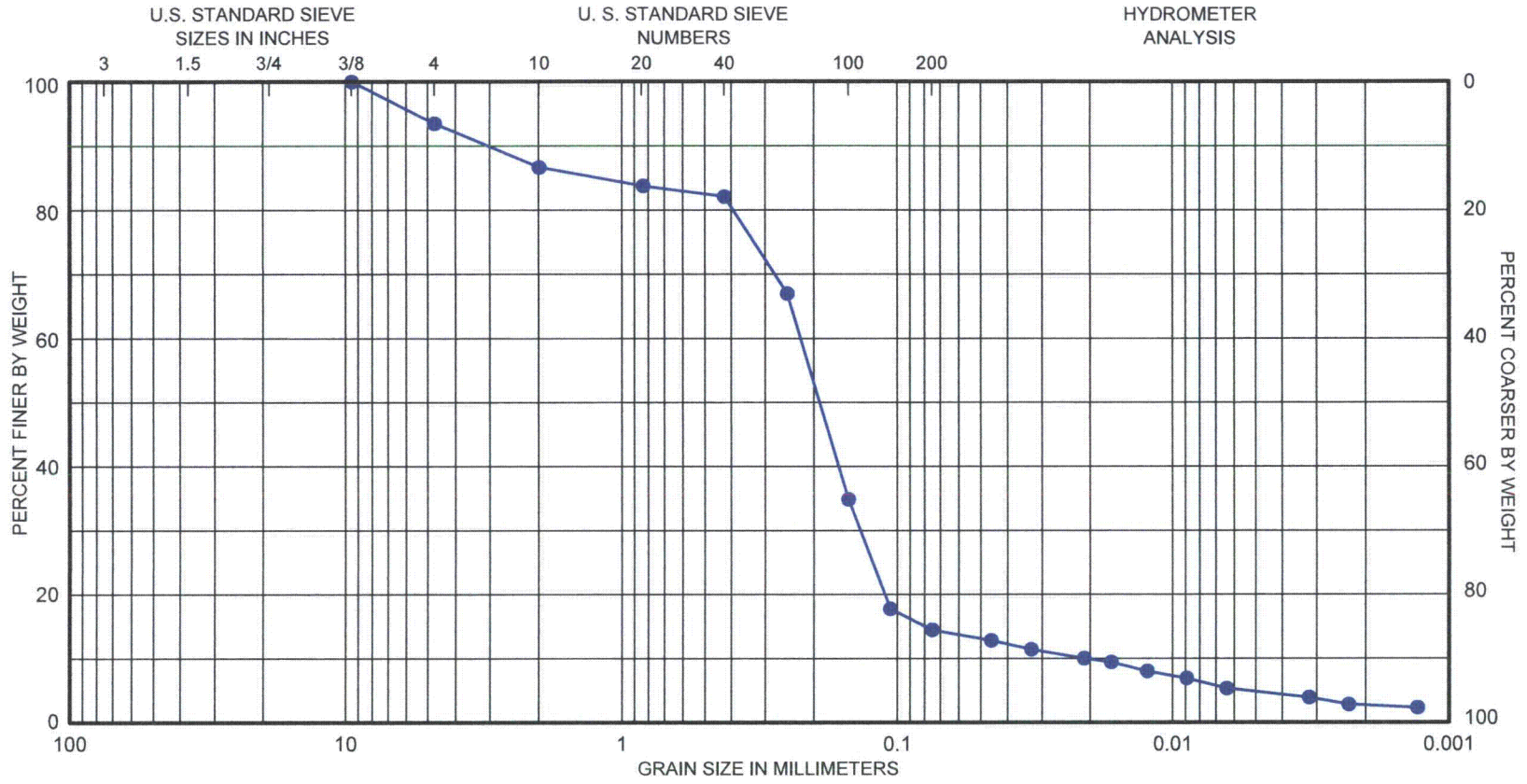
Peak Shearing Strain, %	Shear Modulus, G, ksf	Normalized Shear Modulus, G/G_{max}	Average ⁺ Shearing Strain, %	Material Damping Ratio ^x , D, %
1.76E-04	3056	1.00	1.76E-04	0.85
3.39E-04	3035	0.99	3.39E-04	0.86
6.54E-04	2993	0.98	6.54E-04	0.92
1.21E-03	2930	0.96	1.21E-03	0.94
2.17E-03	2848	0.93	2.00E-03	0.98
3.77E-03	2741	0.90	3.43E-03	1.26
6.29E-03	2590	0.85	5.54E-03	1.87
1.05E-02	2355	0.77	8.72E-03	2.68
1.83E-02	2049	0.67	1.43E-02	3.90
3.21E-02	1759	0.58	2.34E-02	5.11
4.62E-02	1605	0.53	3.24E-02	5.84

⁺ Average Shearing Strain from the First Three Cycles of the Free Vibration Decay Curve

^x Average Damping Ratio from the First Three Cycles of the Free Vibration Decay Curve

Table A.5 Variation in Shear Modulus, Normalized Shear Modulus and Material Damping Ratio with Shearing Strain from TS Tests of Specimen B-773B-2; Isotropic Confining Pressure, $\sigma_o = 4262$ psf

First Cycle				Tenth Cycle			
Peak Shearing Strain, %	Shear Modulus, G, ksf	Normalized Shear Modulus, G/G_{max}	Material Damping Ratio, D, %	Peak Shearing Strain, %	Shear Modulus, G, ksf	Normalized Shear Modulus, G/G_{max}	Material Damping Ratio, D, %
5.18E-04	3090	1.00	0.66	5.32E-04	3067	1.00	0.57
1.05E-03	3090	1.00	0.57	1.05E-03	3067	1.00	0.81
2.08E-03	3090	1.00	0.84	2.08E-03	3067	1.00	1.04
4.32E-03	2982	0.97	1.40	4.34E-03	2971	0.97	1.11
9.31E-03	2771	0.90	2.85	9.29E-03	2779	0.91	2.51



GRAVEL		SAND			SILT or CLAY		
Coarse	Fine	Coarse	Medium	Fine			
<u>SYMBOL</u>	<u>BORING</u>	<u>DEPTH, FT</u>	<u>C_c</u>	<u>C_u</u>	<u>D₅₀</u>	<u>D₉₀</u>	<u>CLASSIFICATION</u>
●	B-773B-2	15.9	3.91	10.61	0.19	3.07	Silty Sand (SM), olive gray, with shell fragments

GRAIN SIZE CURVE

APPENDIX B

Specimen B-773B_3

Borehole B-773B

Sample 3

Depth = 27 ft (8.2 m)

Total Unit Weight = 111.6 lb/ft³

Water Content = 35.0 %

FUGRO JOB #: 0411-09-1734
Testing Station: RC6



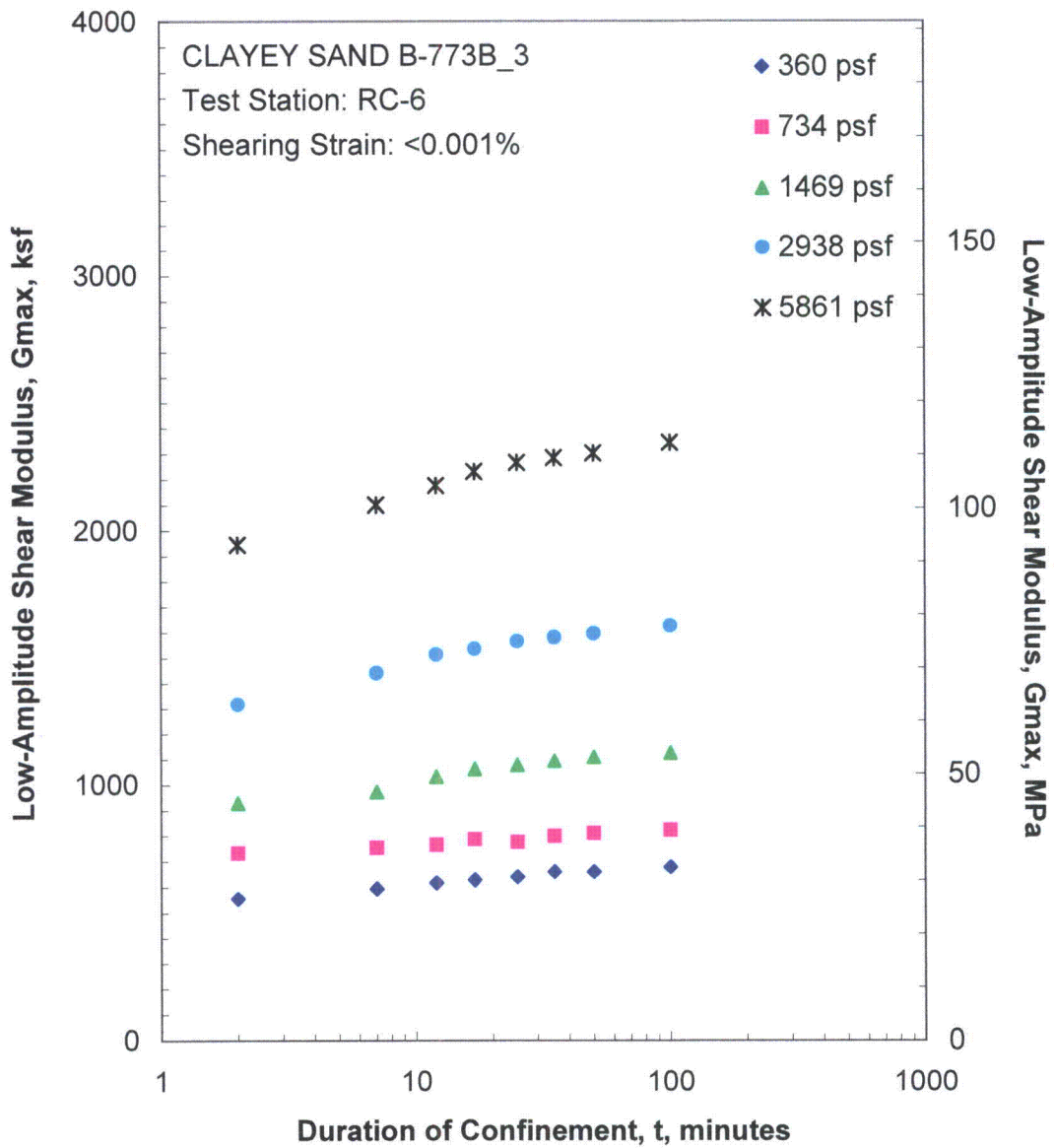


Figure B.1 Variation in Low-Amplitude Shear Modulus with Magnitude and Duration of Isotropic Confining Pressure from Resonant Column Tests

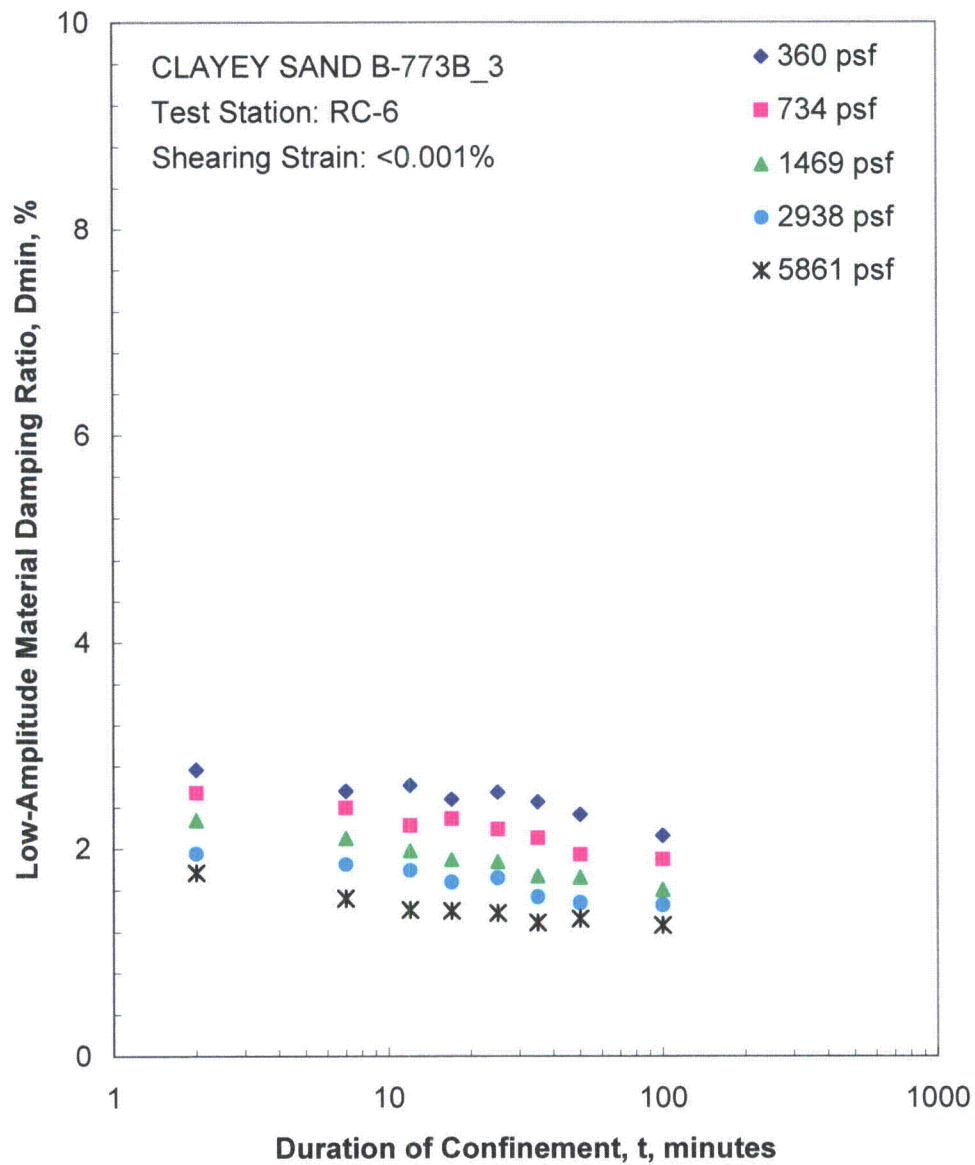


Figure B.2 Variation in Low-Amplitude Material Damping Ratio with Magnitude and Duration of Isotropic Confining Pressure from Resonant Column Tests

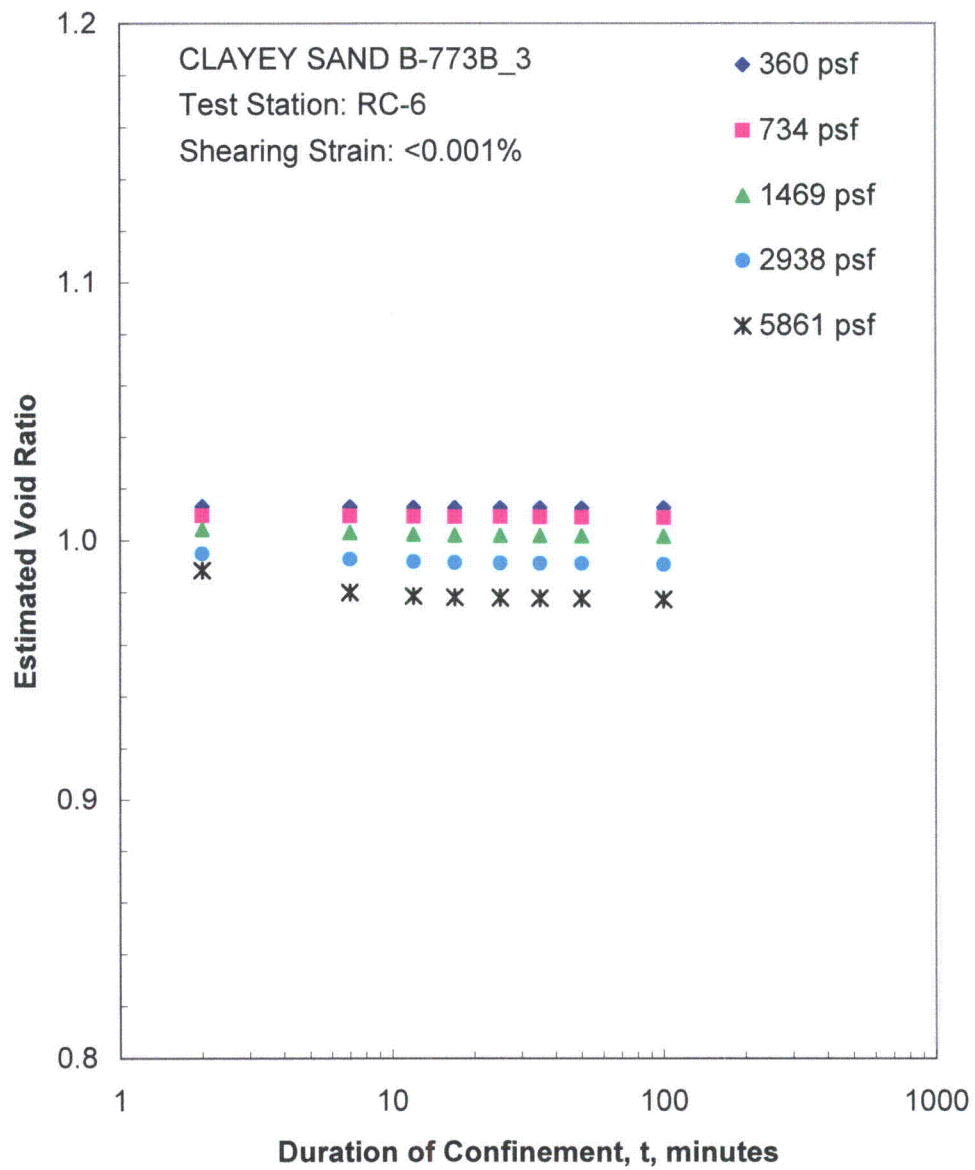


Figure B.3 Variation in Estimated Void Ratio with Magnitude and Duration of Isotropic Confining Pressure from Resonant Column Tests

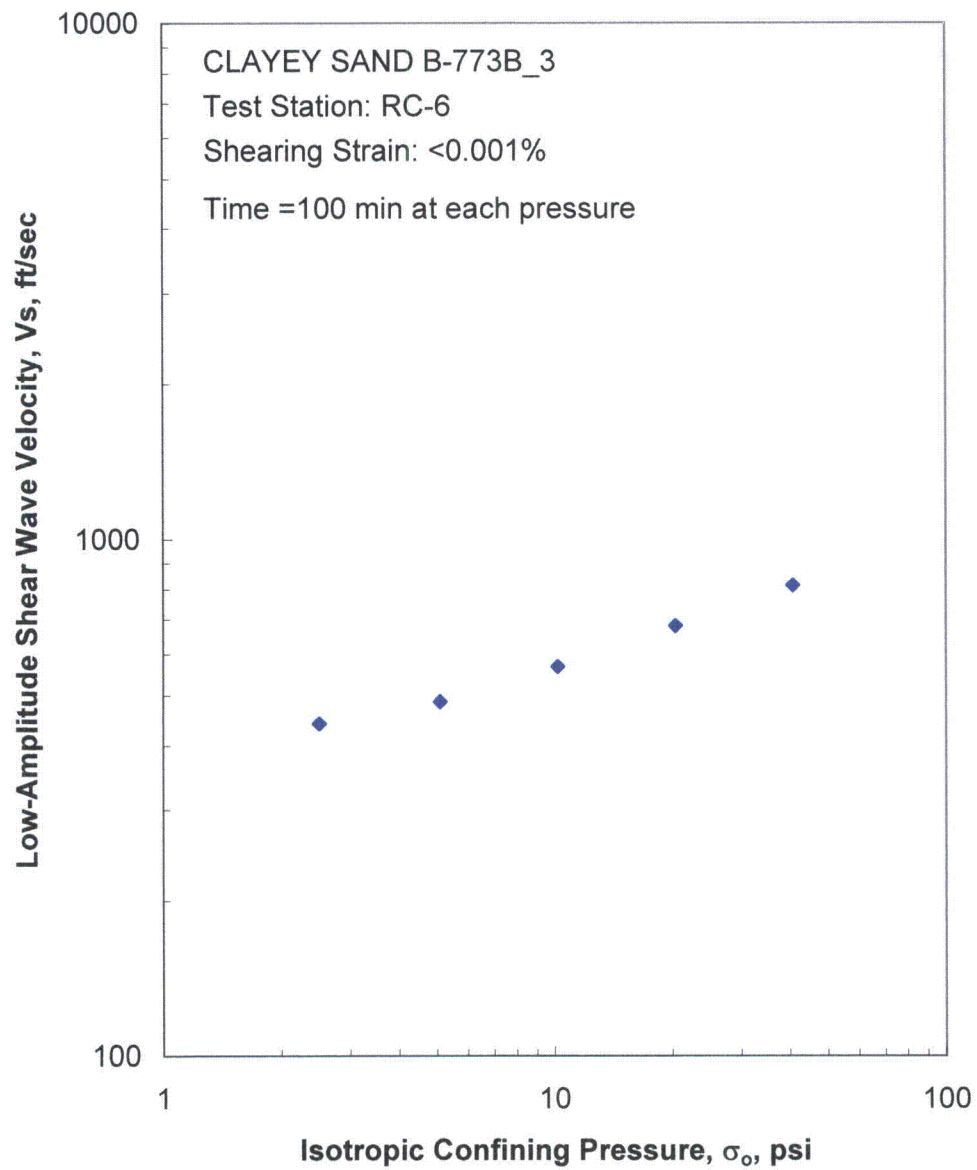


Figure B.4 Variation in Low-Amplitude Shear Wave Velocity with Isotropic Confining Pressure from Resonant Column Tests

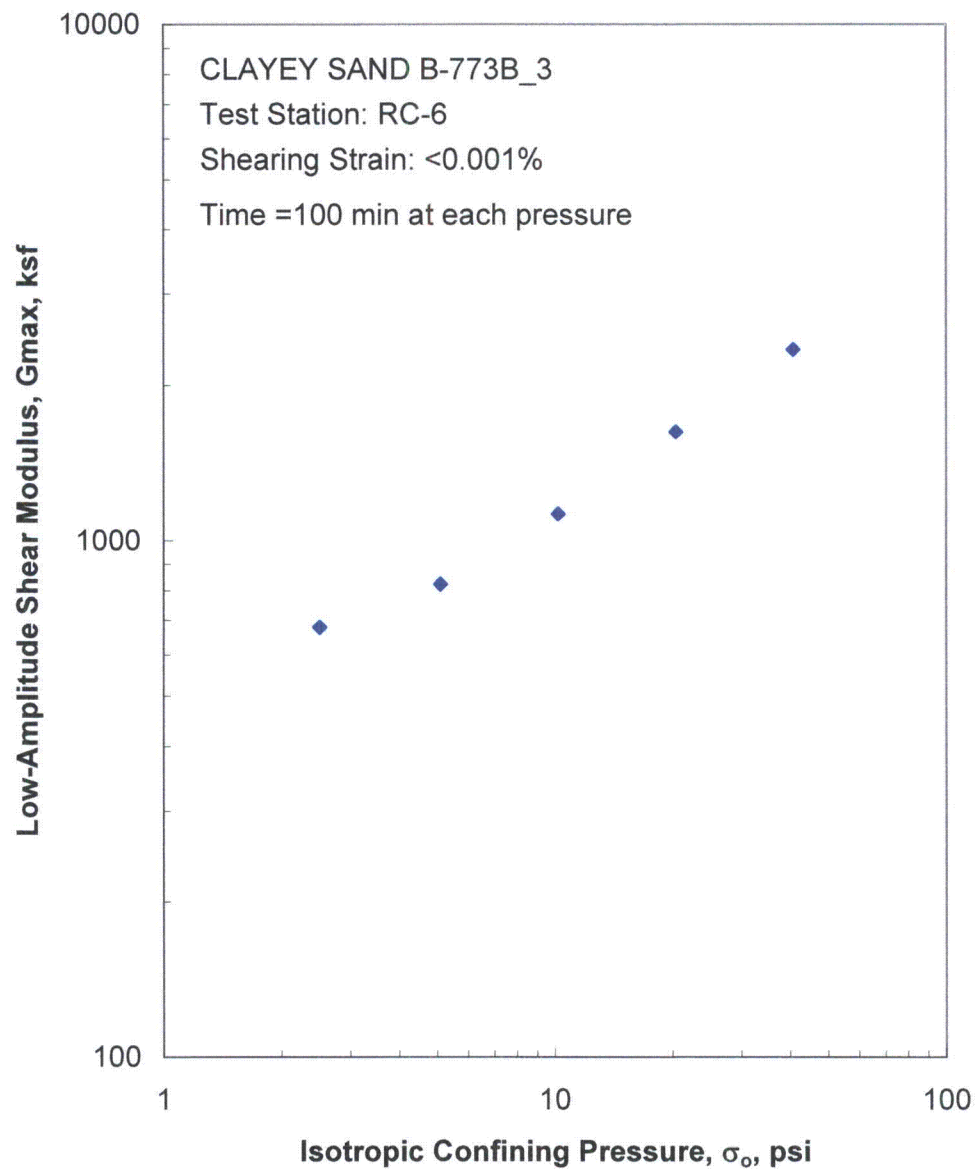


Figure B.5 Variation in Low-Amplitude Shear Modulus with Isotropic Confining Pressure from Resonant Column Tests

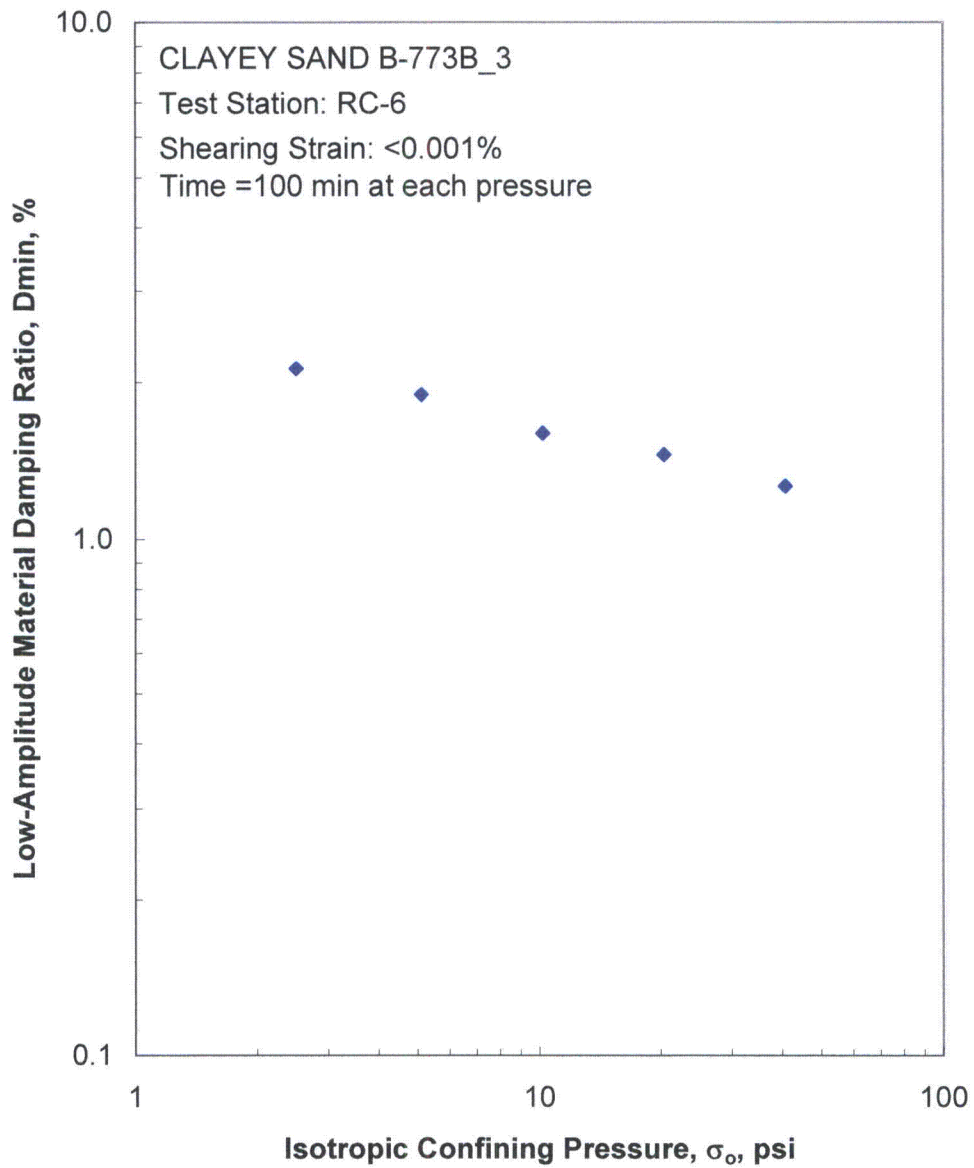


Figure B.6 Variation in Low-Amplitude Material Damping Ratio with Isotropic Confining Pressure from Resonant Column Tests

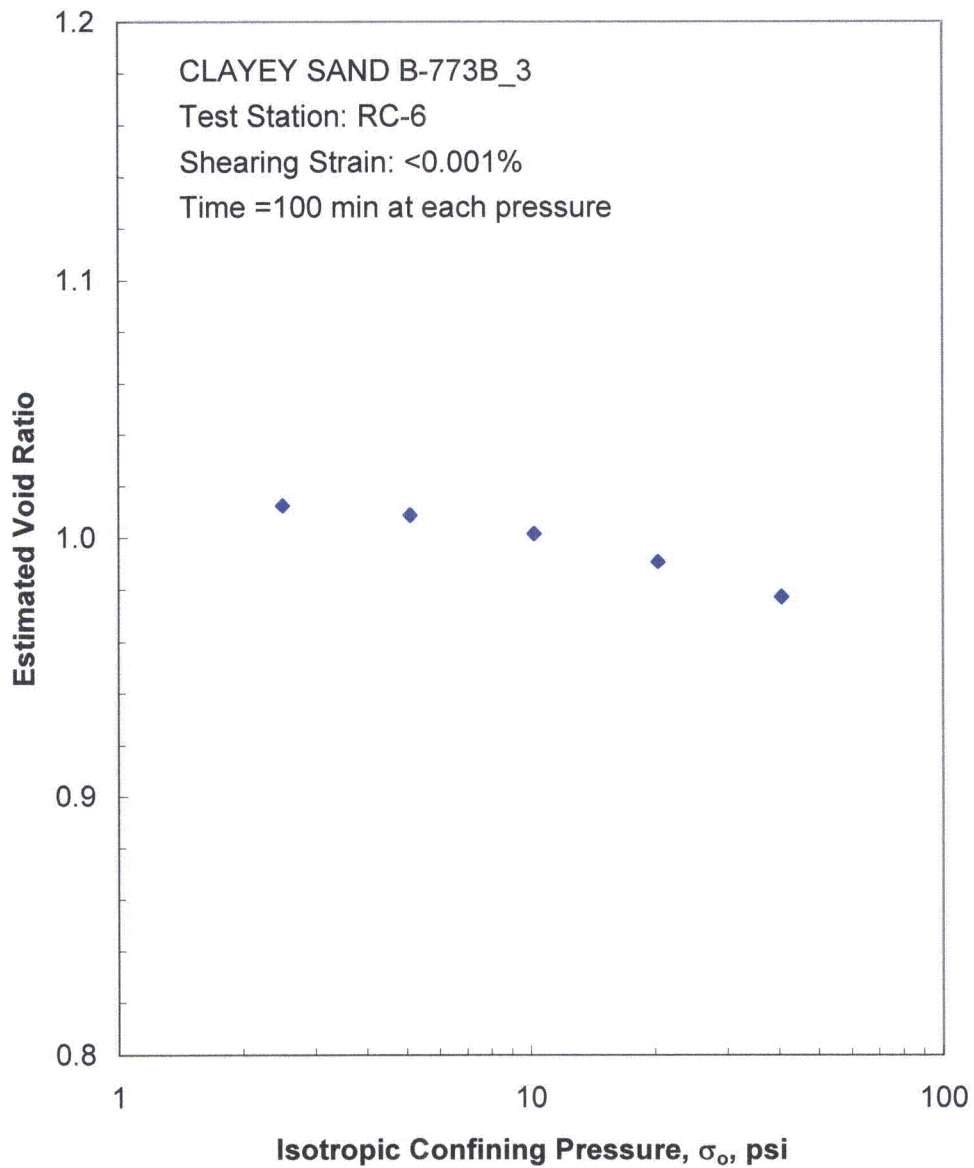


Figure B.7 Variation in Estimated Void Ratio with Isotropic Confining Pressure from Resonant Column Tests

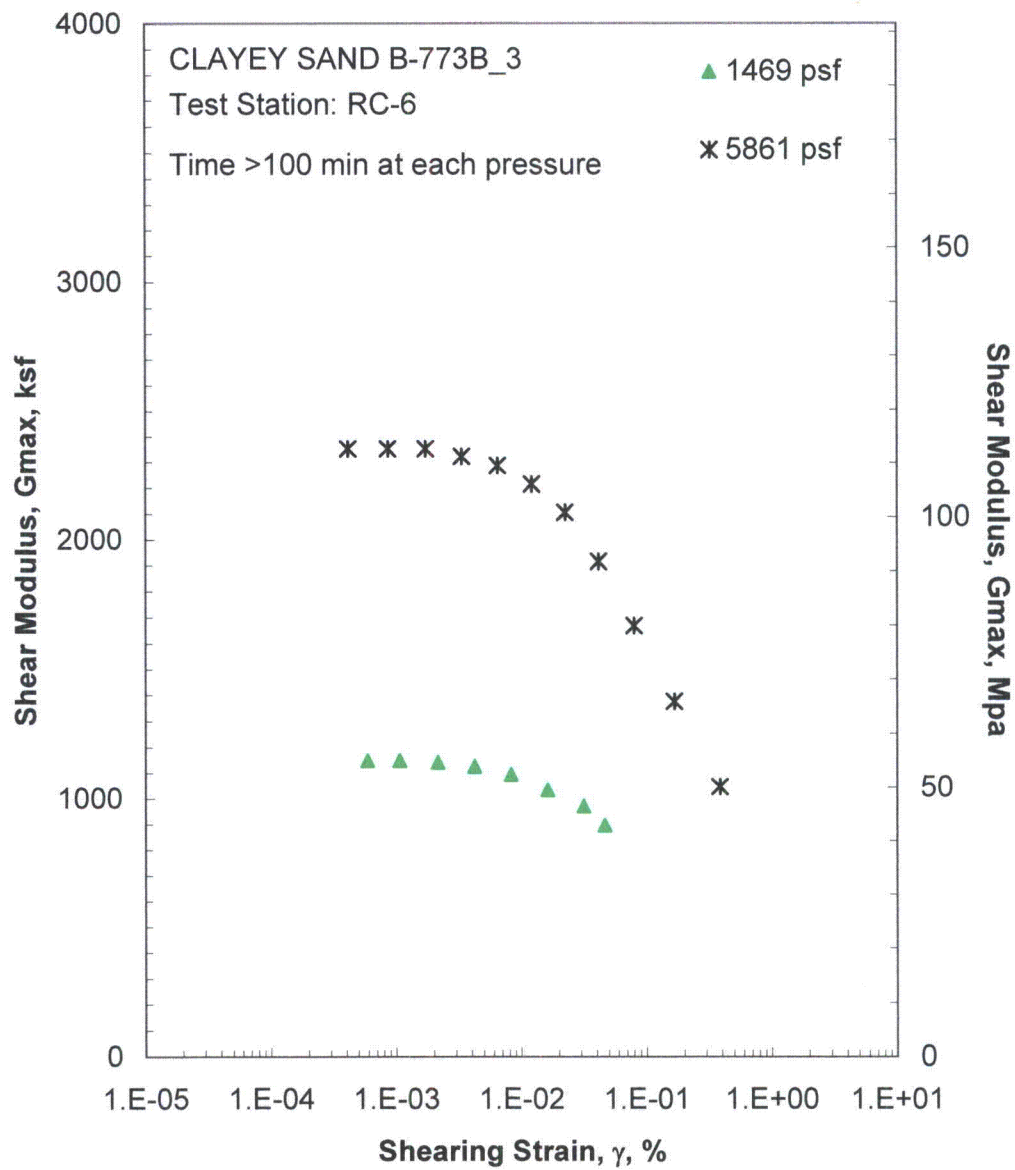


Figure B.8 Comparison of the Variation in Shear Modulus with Shearing Strain and Isotropic Confining Pressure from the Resonant Column Tests

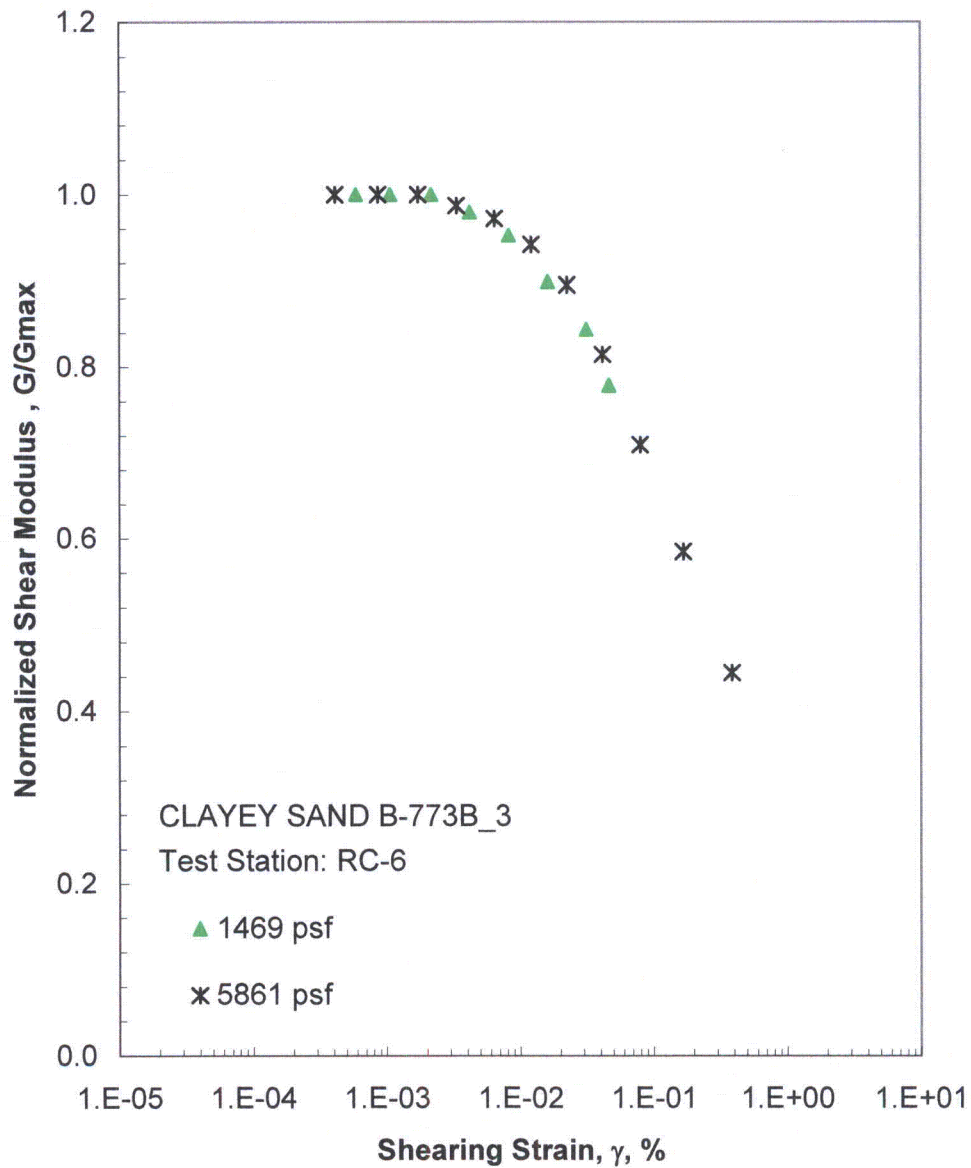


Figure B.9 Comparison of the Variation in Normalized Shear Modulus with Shearing Strain and Isotropic Confining Pressure from the Resonant Column Tests

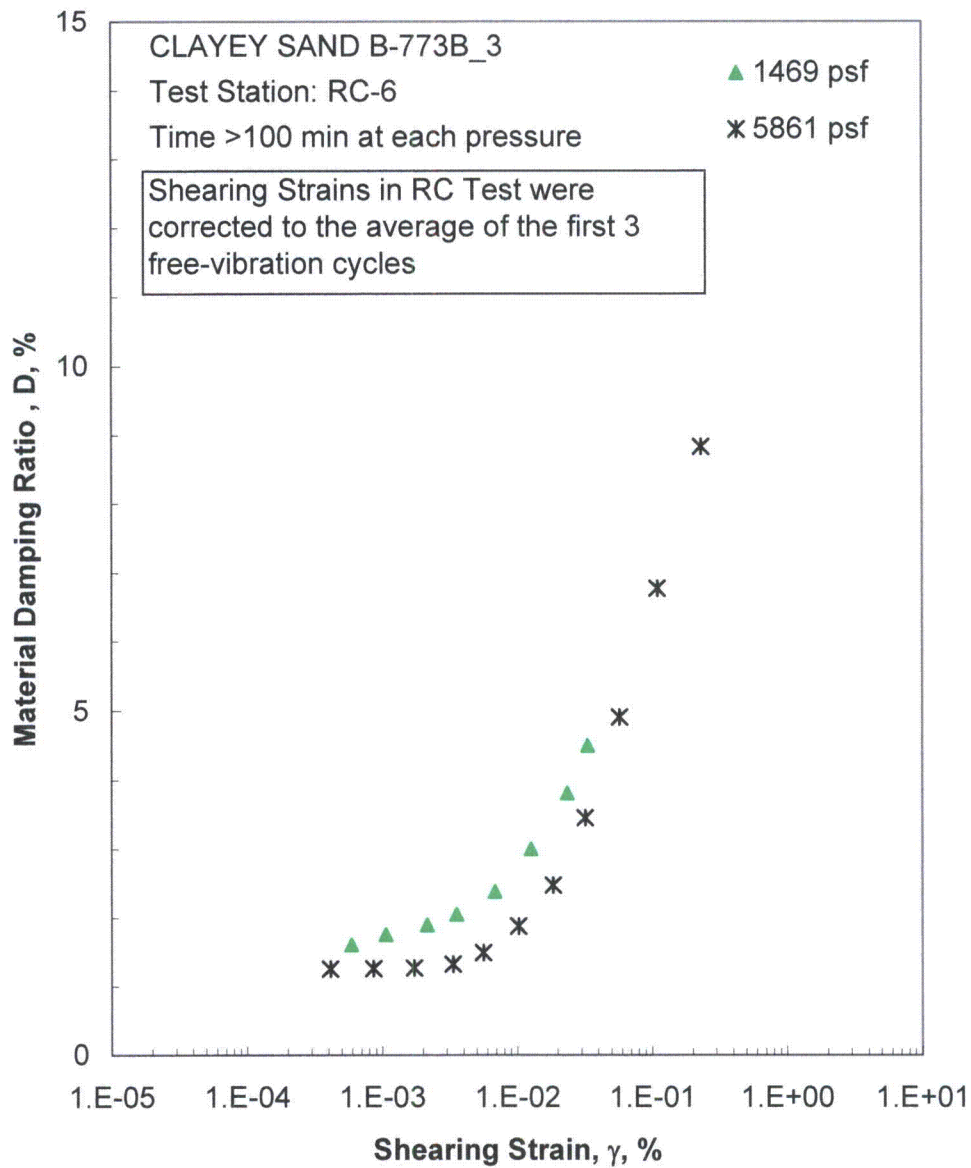


Figure B.10 Comparison of the Variation in Material Damping Ratio with Shearing Strain and Isotropic Confining Pressure from the Resonant Column Tests

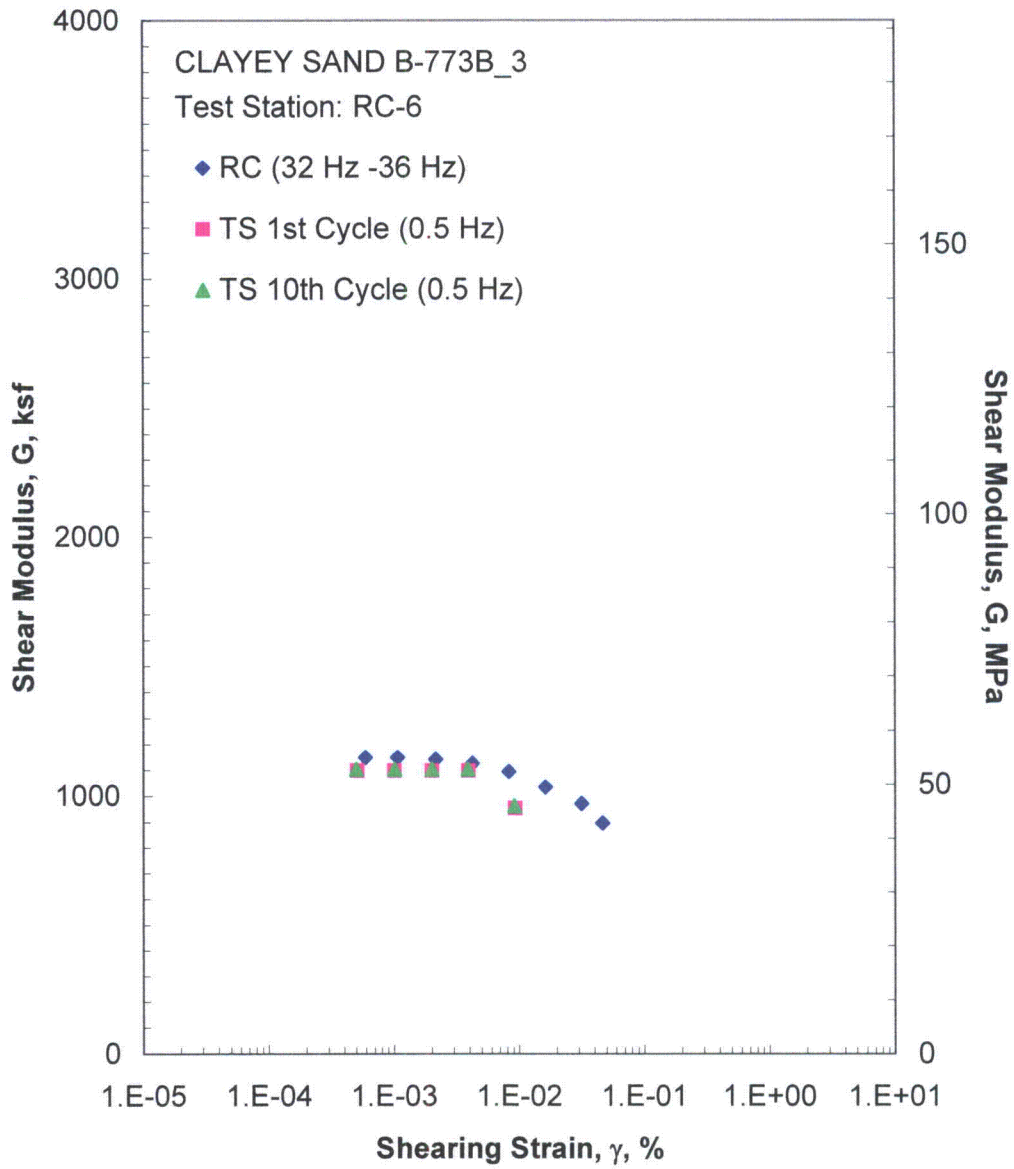


Figure B.11 Comparison of the Variation in Shear Modulus with Shearing Strain at an Isotropic Confining Pressure of 1469 psf from the Combined RCTS Tests

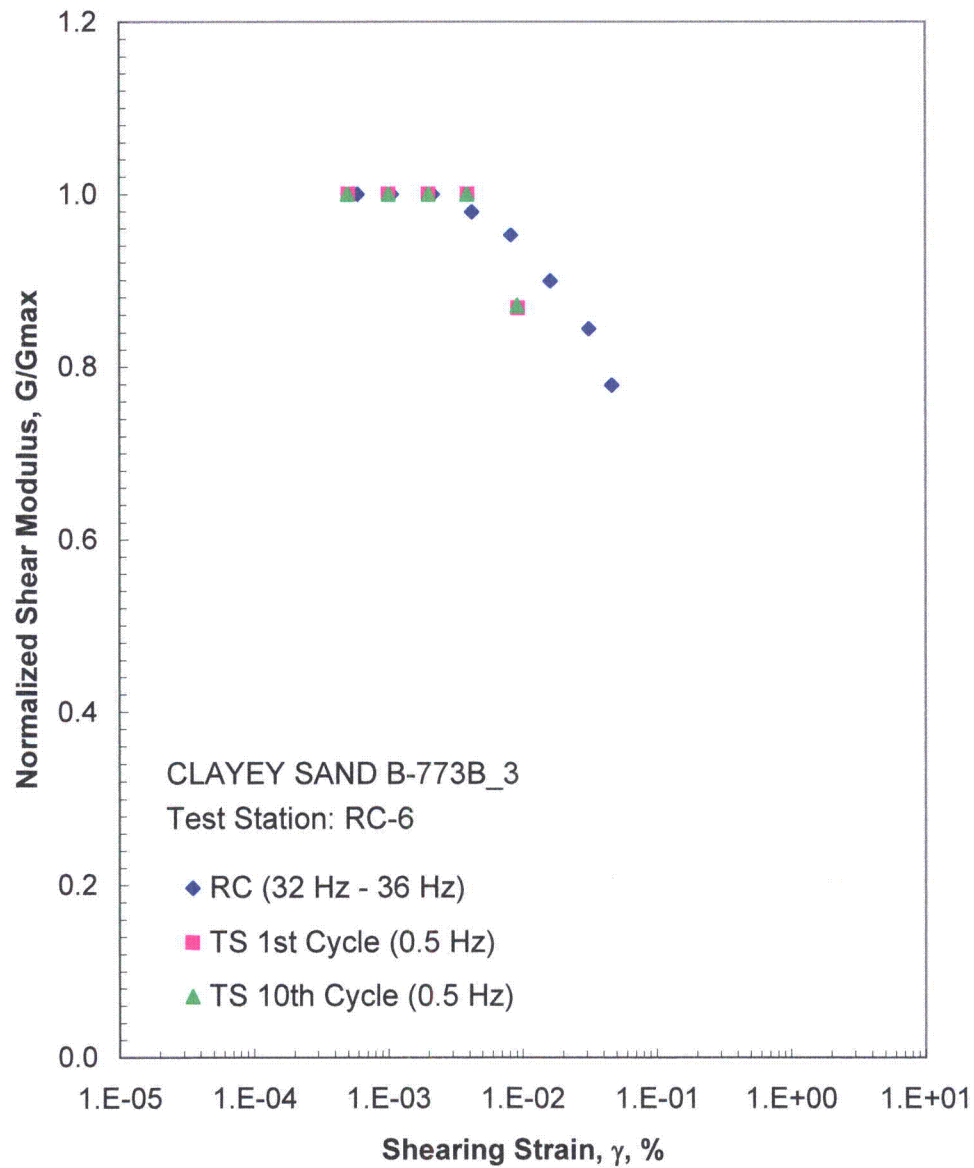


Figure B.12 Comparison of the Variation in Normalized Shear Modulus with Shearing Strain at an Isotropic Confining Pressure of 1469 psf from the Combined RCTS Tests

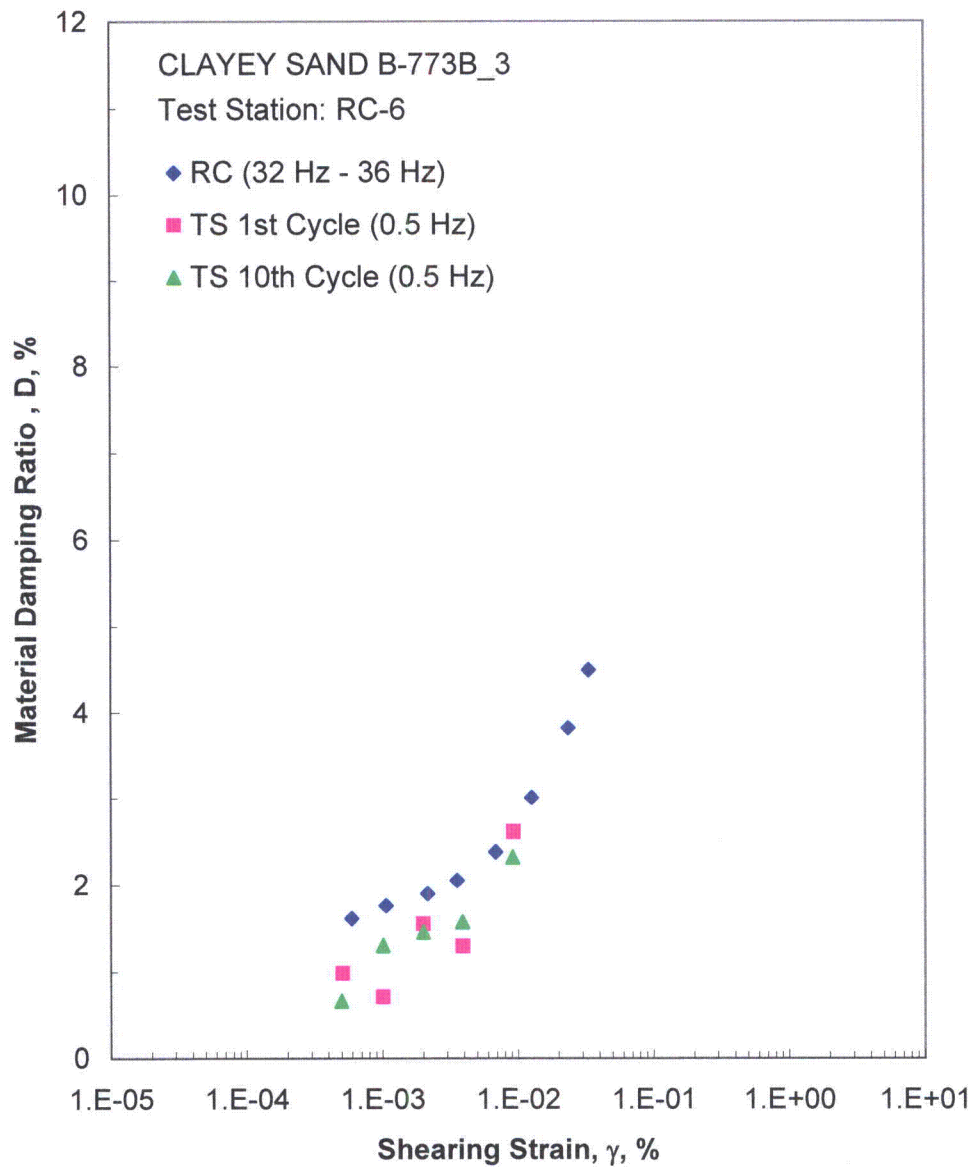


Figure B.13 Comparison of the Variation in Material Damping Ratio with Shearing Strain at an Isotropic Confining Pressure of 1469 psf from the Combined RCTS Tests

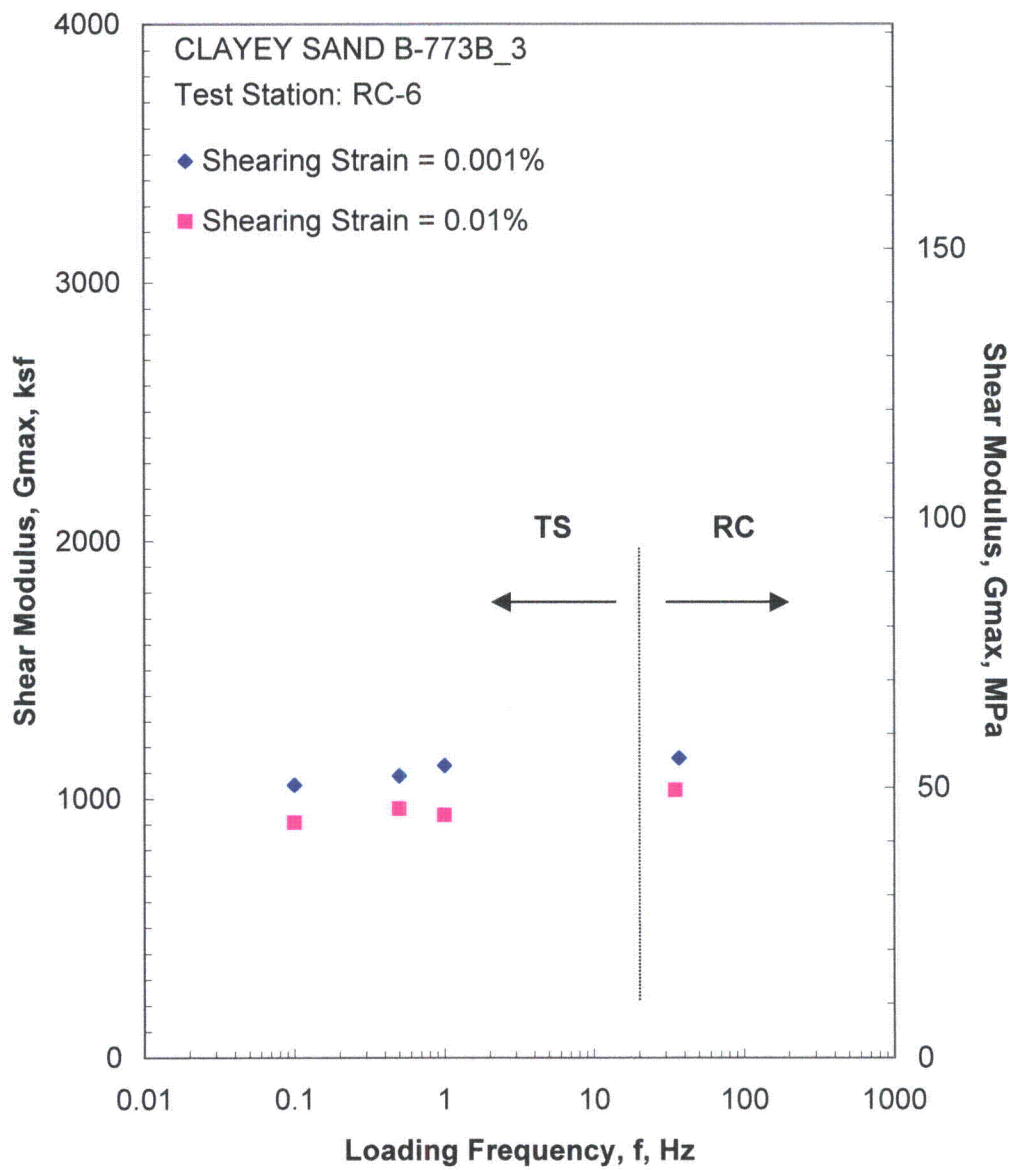


Figure B.14 Comparison of the Variation in Shear Modulus with Loading Frequency at an Isotropic Confining Pressure of 1469 psf from the Combined RCTS Tests

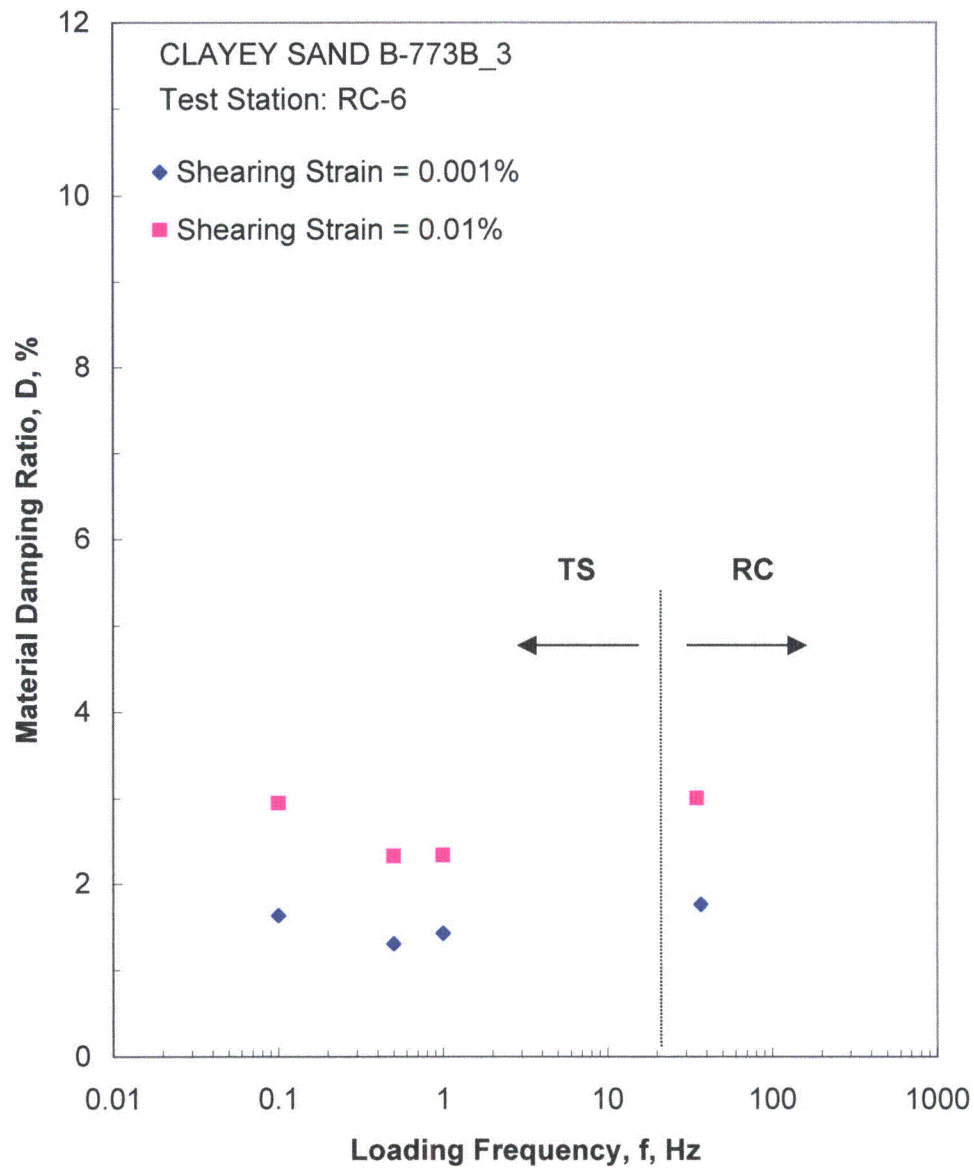


Figure B.15 Comparison of the Variation in Material Damping Ratio with Loading Frequency at an Isotropic Confining Pressure of 1469 psf from the Combined RCTS Tests

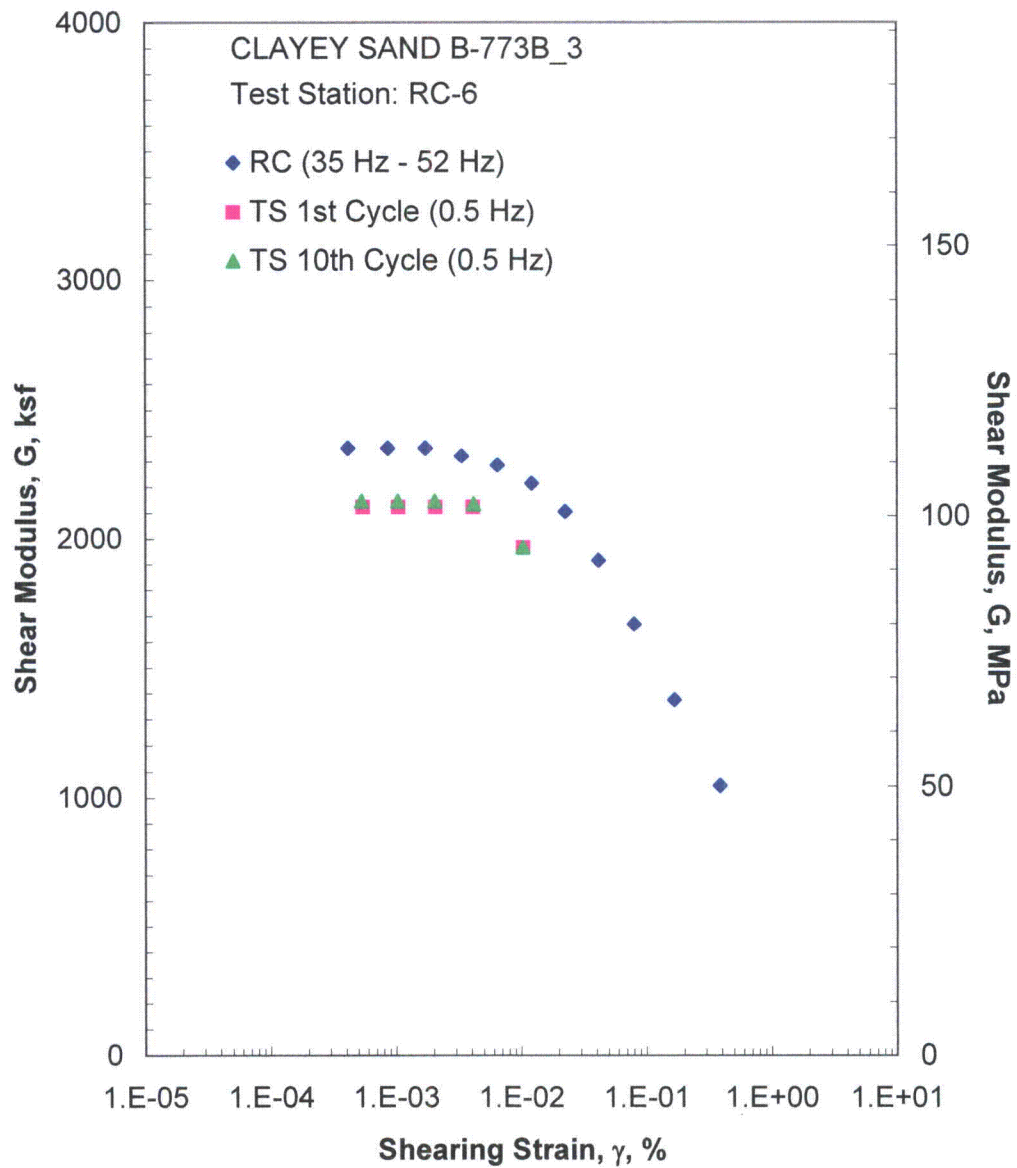


Figure B.16 Comparison of the Variation in Shear Modulus with Shearing Strain at an Isotropic Confining Pressure of 5861 psf from the Combined RCTS Tests

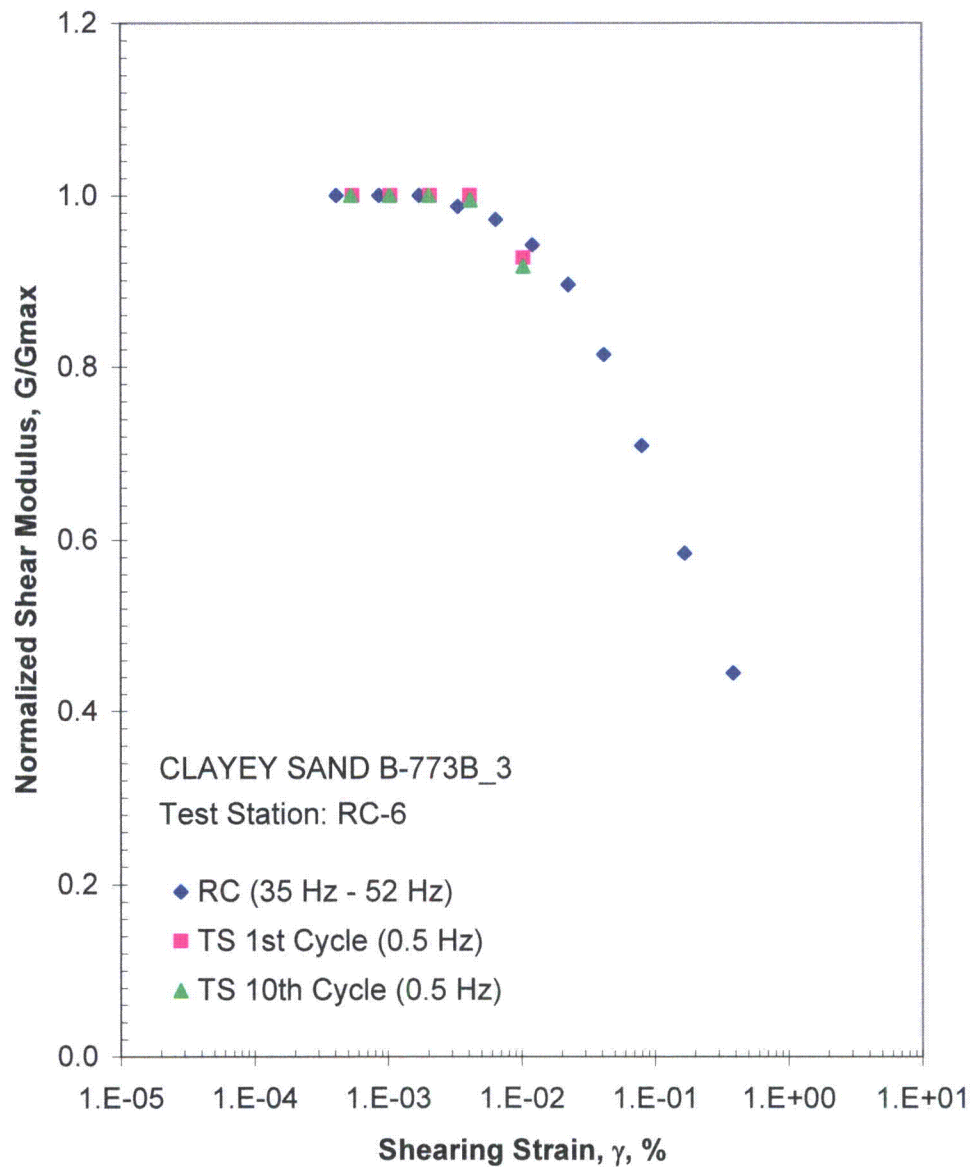


Figure B.17 Comparison of the Variation in Normalized Shear Modulus with Shearing Strain at an Isotropic Confining Pressure of 5861 psf from the Combined RCTS Tests

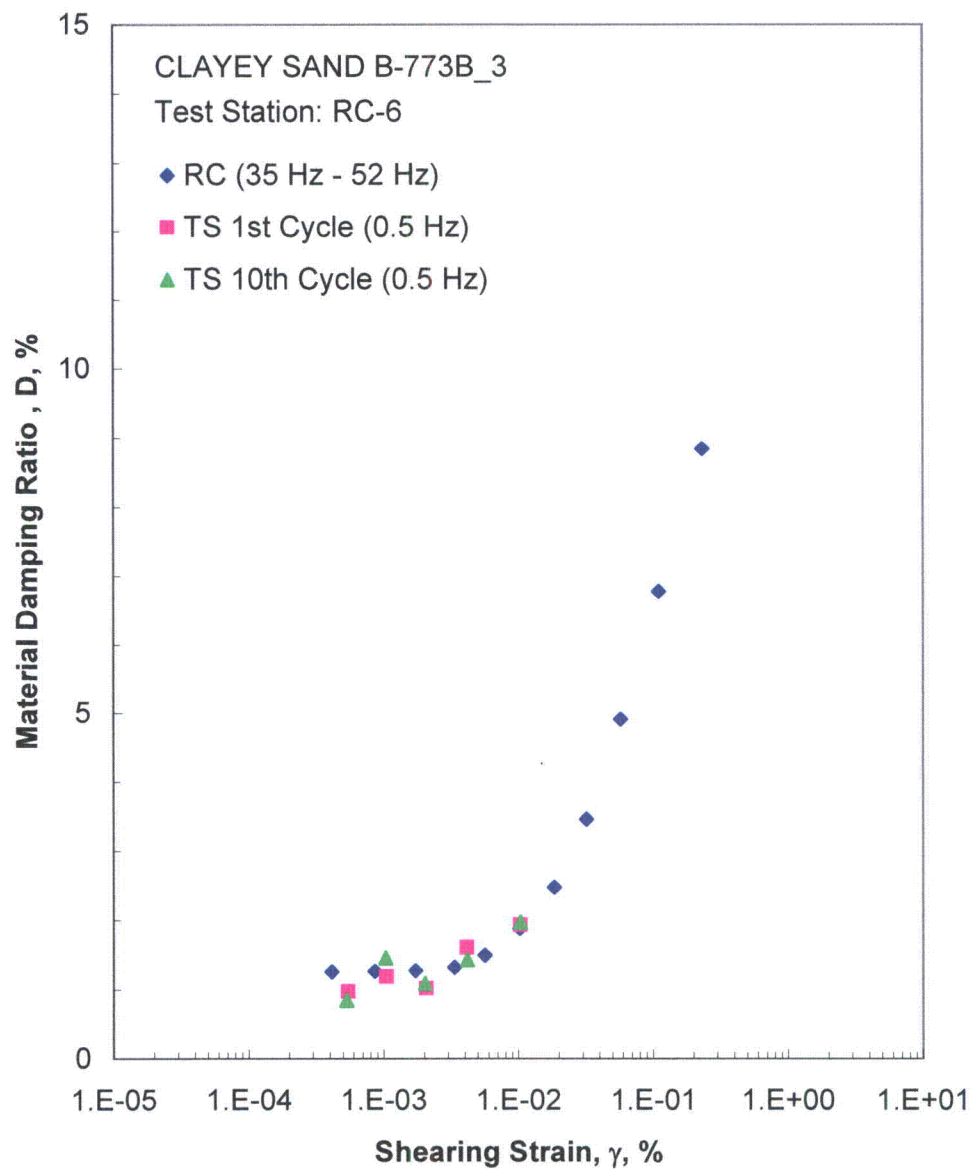


Figure B.18 Comparison of the Variation in Material Damping Ratio with Shearing Strain at an Isotropic Confining Pressure of 5861 psf from the Combined RCTS Tests

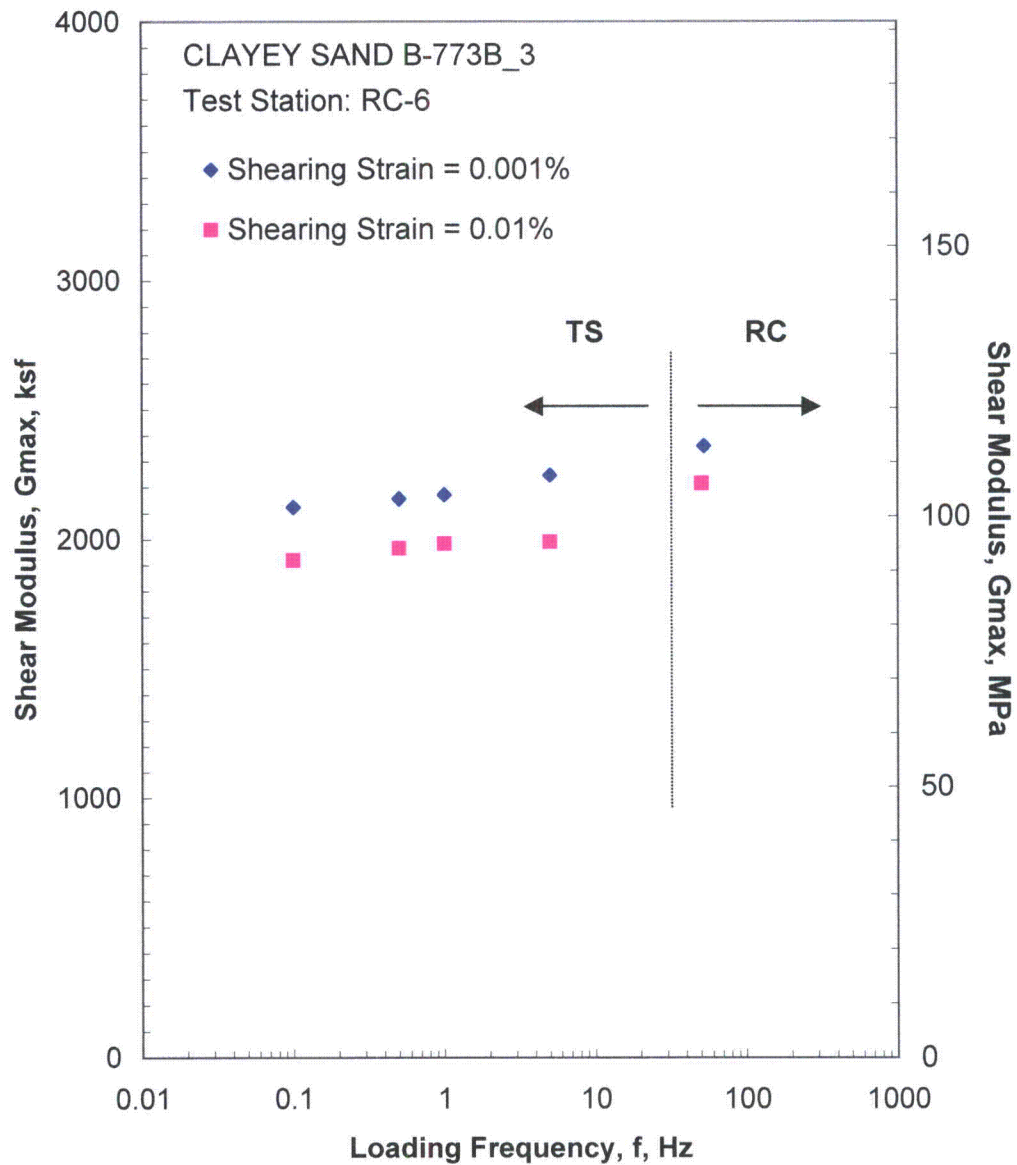


Figure B.19 Comparison of the Variation in Shear Modulus with Loading Frequency at an Isotropic Confining Pressure of 5861 psf from the Combined RCTS Tests

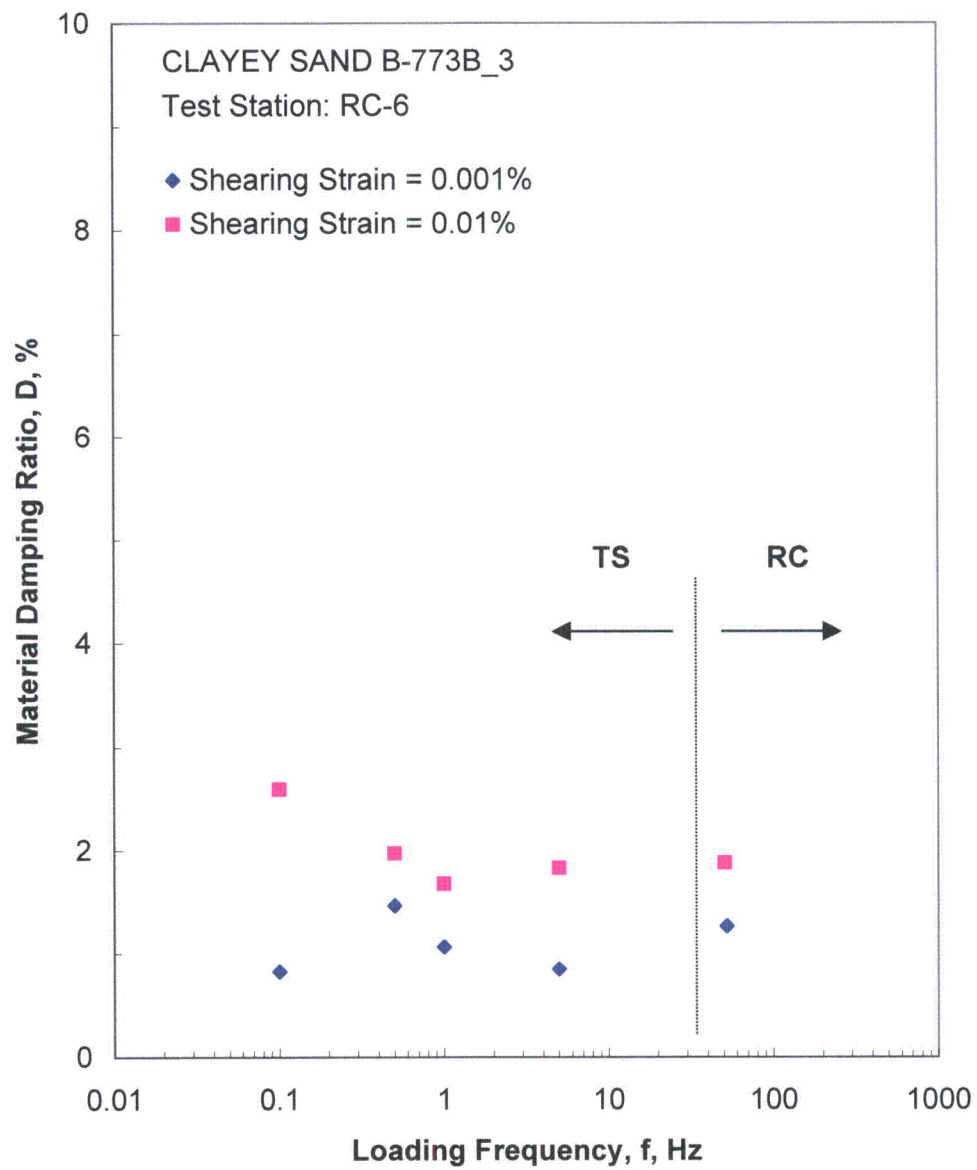


Figure B.20 Comparison of the Variation in Material Damping Ratio 5861 psf from the Combined RCTS Tests

Table B.1 Variation in Low-Amplitude Shear Wave Velocity, Low-Amplitude Shear Modulus, Low-Amplitude Material Damping Ratio and Estimated Void Ratio with Isotropic Confining Pressure from RC Tests of Specimen B-773B-3

Isotropic Confining Pressure, σ_o			Low-Amplitude Shear Modulus, G_{max}		Low-Amplitude Shear Wave Velocity, V_s	Low-Amplitude Material Damping Ratio, D_{min}	Estimated Void Ratio, e
(psi)	(psf)	(kPa)	(ksf)	(MPa)	(fps)	(%)	
3	360	17	678	33	442	2.13	1.01
5	734	35	823	40	486	1.89	1.01
10	1469	70	1125	54	567	1.60	1.00
20	2938	141	1627	78	680	1.46	0.99
41	5861	280	2345	113	814	1.27	0.98

Table B.2 Variation in Shear Modulus and Material Damping Ratio with Shearing Strain from RC Tests of Specimen B-773B-3; Isotropic Confining Pressure, $\sigma_o = 1469$ psf

Peak Shearing Strain, %	Shear Modulus, G, ksf	Normalized Shear Modulus, G/G_{max}	Average ⁺ Shearing Strain, %	Material Damping Ratio ^x , D, %
5.91E-04	1149	1.00	5.91E-04	1.61
1.06E-03	1149	1.00	1.06E-03	1.76
2.15E-03	1141	1.00	2.15E-03	1.90
4.22E-03	1126	0.98	3.54E-03	2.05
8.23E-03	1094	0.95	6.83E-03	2.38
1.62E-02	1033	0.90	1.26E-02	3.00
3.14E-02	970	0.84	2.35E-02	3.82
4.63E-02	895	0.78	3.34E-02	4.50

⁺ Average Shearing Strain from the First Three Cycles of the Free Vibration Decay Curve

^x Average Damping Ratio from the First Three Cycles of the Free Vibration Decay Curve

Table B.3 Variation in Shear Modulus, Normalized Shear Modulus and Material Damping Ratio with Shearing Strain from TS Tests of Specimen B-773B-3; Isotropic Confining Pressure, $\sigma_0 = 1469$ psf

First Cycle				Tenth Cycle			
Peak Shearing Strain, %	Shear Modulus, G, ksf	Normalized Shear Modulus, G/G_{max}	Material Damping Ratio, D, %	Peak Shearing Strain, %	Shear Modulus, G, ksf	Normalized Shear Modulus, G/G_{max}	Material Damping Ratio, D, %
5.09E-04	1097	1.00	0.98	4.99E-04	1104	1.00	0.66
1.01E-03	1097	1.00	0.71	1.01E-03	1104	1.00	1.30
2.00E-03	1097	1.00	1.55	2.01E-03	1104	1.00	1.45
3.91E-03	1097	1.00	1.29	3.89E-03	1104	1.00	1.57
9.24E-03	952	0.87	2.61	9.15E-03	961	0.87	2.32

Table B.4 Variation in Shear Modulus and Material Damping Ratio with Shearing Strain from RC Tests of Specimen B-773B-3; Isotropic Confining Pressure, $\sigma_o = 5861$ psf

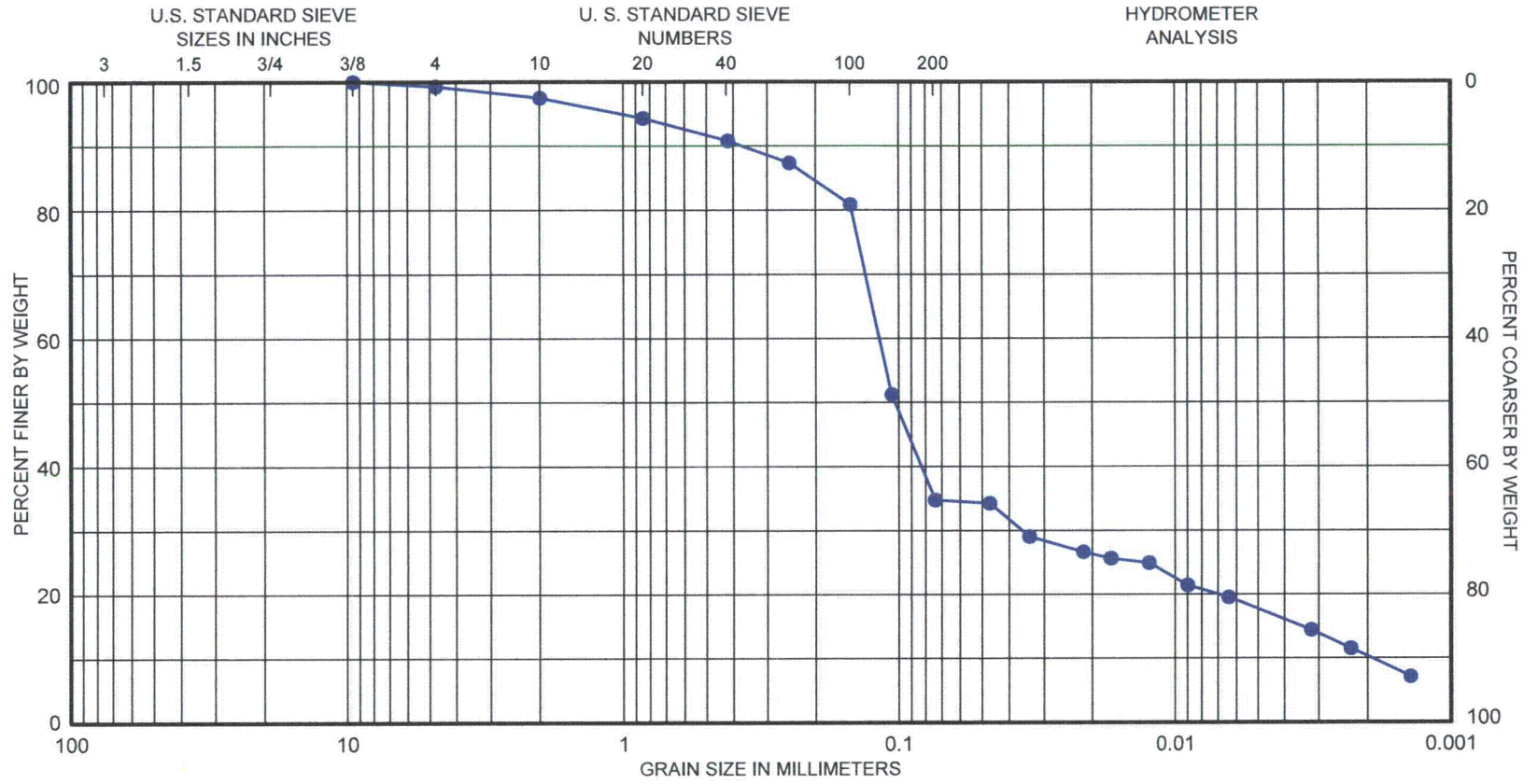
Peak Shearing Strain, %	Shear Modulus, G, ksf	Normalized Shear Modulus, G/G_{max}	Average ⁺ Shearing Strain, %	Material Damping Ratio ^x , D, %
4.13E-04	2352	1.00	4.13E-04	1.26
8.61E-04	2352	1.00	8.61E-04	1.27
1.72E-03	2352	1.00	1.72E-03	1.27
3.35E-03	2322	0.99	3.35E-03	1.33
6.45E-03	2286	0.97	5.61E-03	1.50
1.22E-02	2214	0.94	1.02E-02	1.88
2.25E-02	2105	0.89	1.85E-02	2.48
4.16E-02	1915	0.81	3.21E-02	3.46
7.99E-02	1669	0.71	5.75E-02	4.91
1.66E-01	1375	0.58	1.10E-01	6.78
3.85E-01	1047	0.44	2.31E-01	8.84

⁺ Average Shearing Strain from the First Three Cycles of the Free Vibration Decay Curve

^x Average Damping Ratio from the First Three Cycles of the Free Vibration Decay Curve

Table B.5 Variation in Shear Modulus, Normalized Shear Modulus and Material Damping Ratio with Shearing Strain from TS Tests of Specimen B-773B-3; Isotropic Confining Pressure, $\sigma_o = 5861$ psf

First Cycle				Tenth Cycle			
Peak Shearing Strain, %	Shear Modulus, G, ksf	Normalized Shear Modulus, G/G_{max}	Material Damping Ratio, D, %	Peak Shearing Strain, %	Shear Modulus, G, ksf	Normalized Shear Modulus, G/G_{max}	Material Damping Ratio, D, %
5.44E-04	2123	1.00	0.97	5.30E-04	2147	1.00	0.84
1.04E-03	2123	1.00	1.19	1.03E-03	2147	1.00	1.46
2.06E-03	2123	1.00	1.02	2.03E-03	2147	1.00	1.09
4.13E-03	2123	1.00	1.61	4.17E-03	2136	0.99	1.43
1.03E-02	1967	0.93	1.93	1.03E-02	1966	0.92	1.97



GRAVEL		SAND			SILT or CLAY		
Coarse	Fine	Coarse	Medium	Fine			
<u>SYMBOL</u>	<u>BORING</u>	<u>DEPTH, FT</u>	<u>C_c</u>	<u>C_u</u>	<u>D₅₀</u>	<u>D₉₀</u>	<u>CLASSIFICATION</u>
●	B-773B-3	27	5.71	60.51	0.1	0.37	Clayey Sand (SC), gray, with shell fragments

GRAIN SIZE CURVE

APPENDIX C

Specimen B-773B_4

Borehole B-773B

Sample 4

Depth = 37 ft (11.3 m)

Total Unit Weight = 103.0 lb/ft³

Water Content = 53.6 %

FUGRO JOB #: 0411-09-1734

Testing Station: RC5



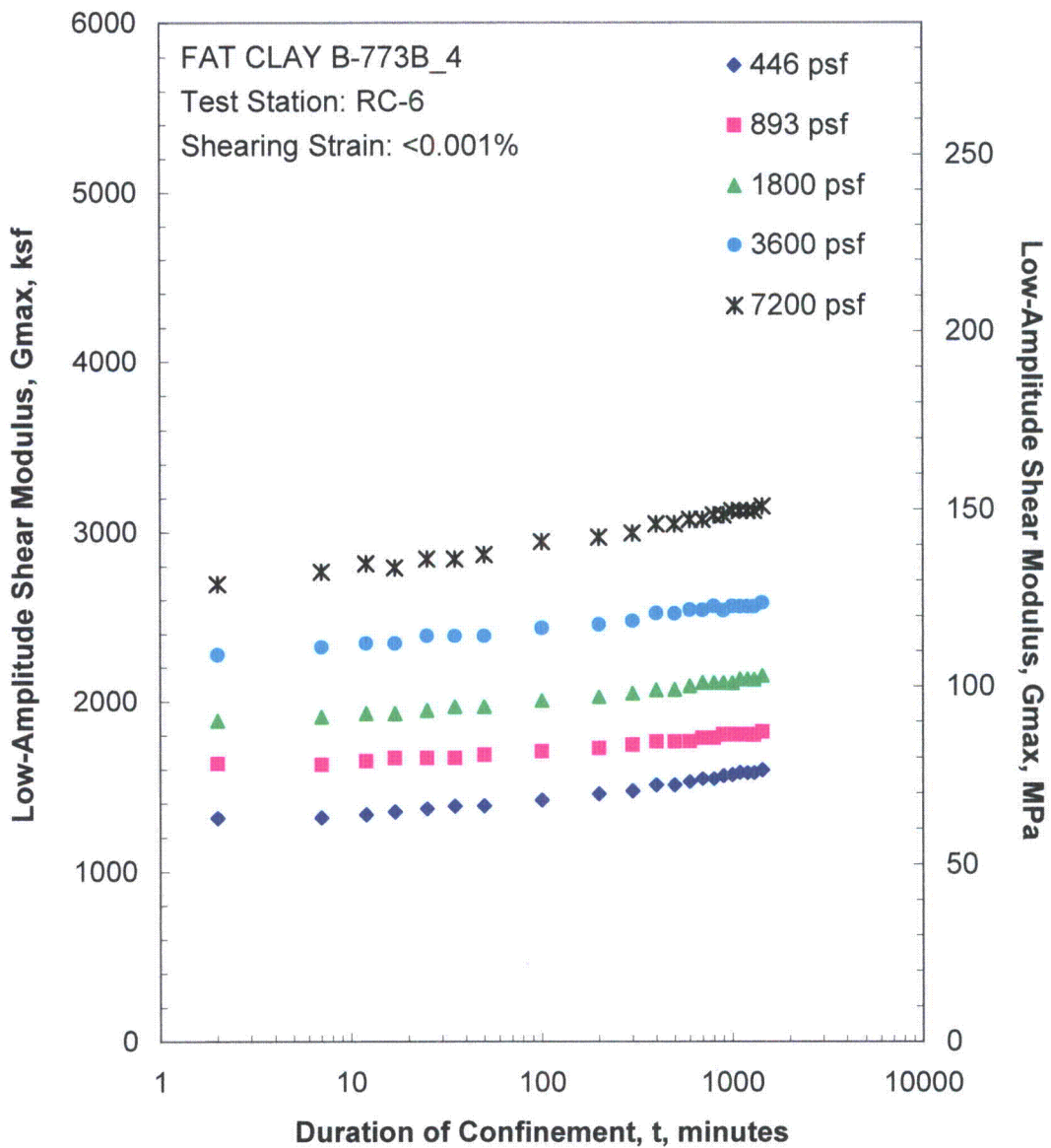


Figure C.1 Variation in Low-Amplitude Shear Modulus with Magnitude and Duration of Isotropic Confining Pressure from Resonant Column Tests

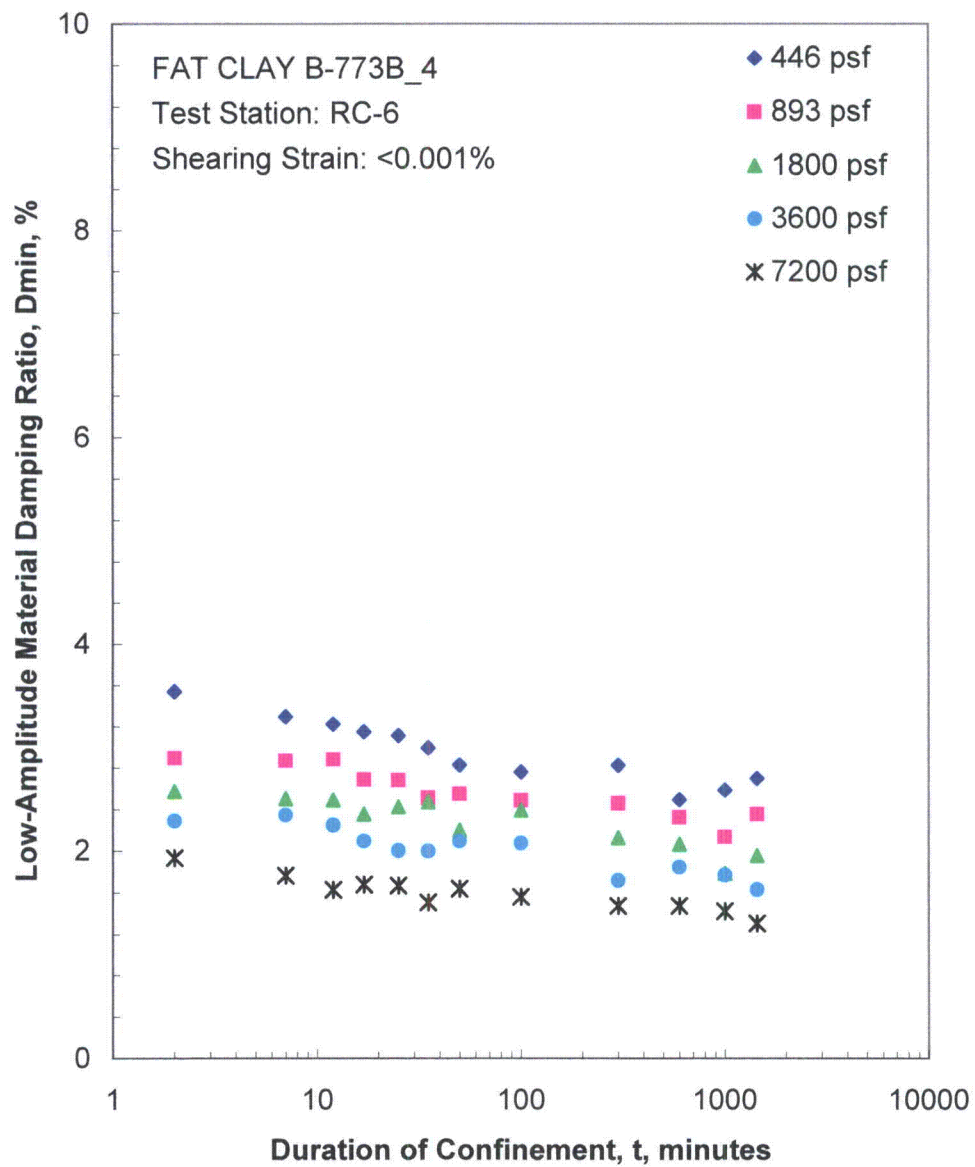


Figure C.2 Variation in Low-Amplitude Material Damping Ratio with Magnitude and Duration of Isotropic Confining Pressure from Resonant Column Tests

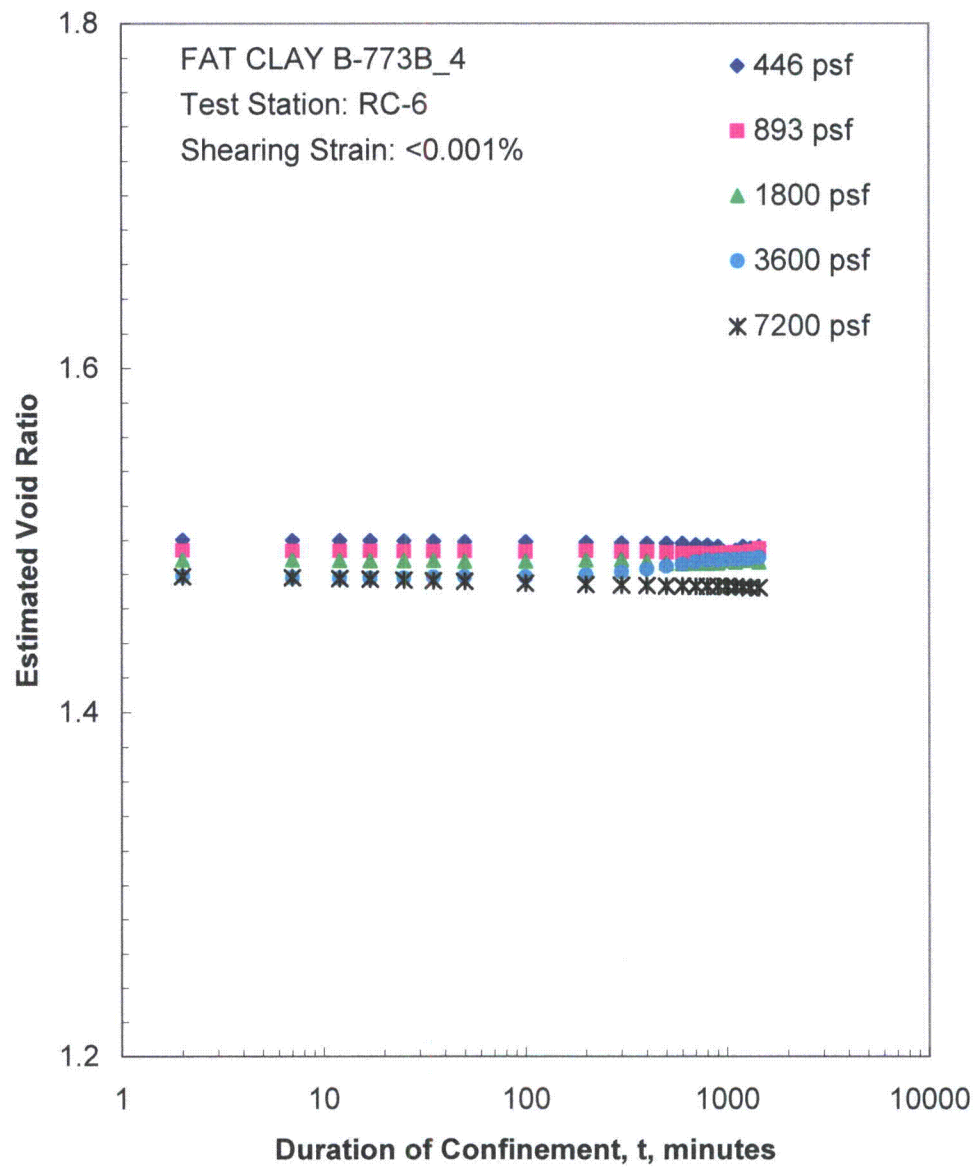


Figure C.3 Variation in Estimated Void Ratio with Magnitude and Duration of Isotropic Confining Pressure from Resonant Column Tests

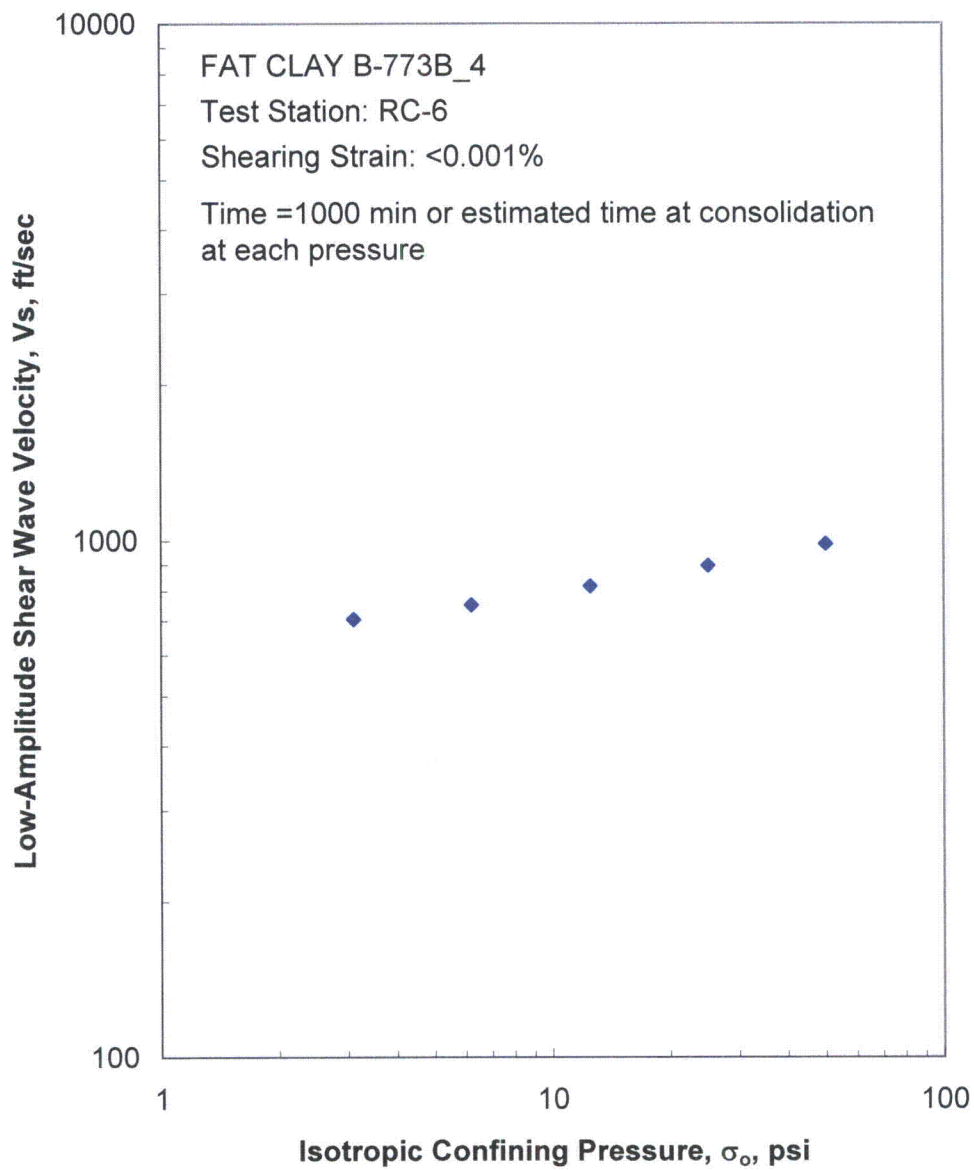


Figure C.4 Variation in Low-Amplitude Shear Wave Velocity with Isotropic Confining Pressure from Resonant Column Tests

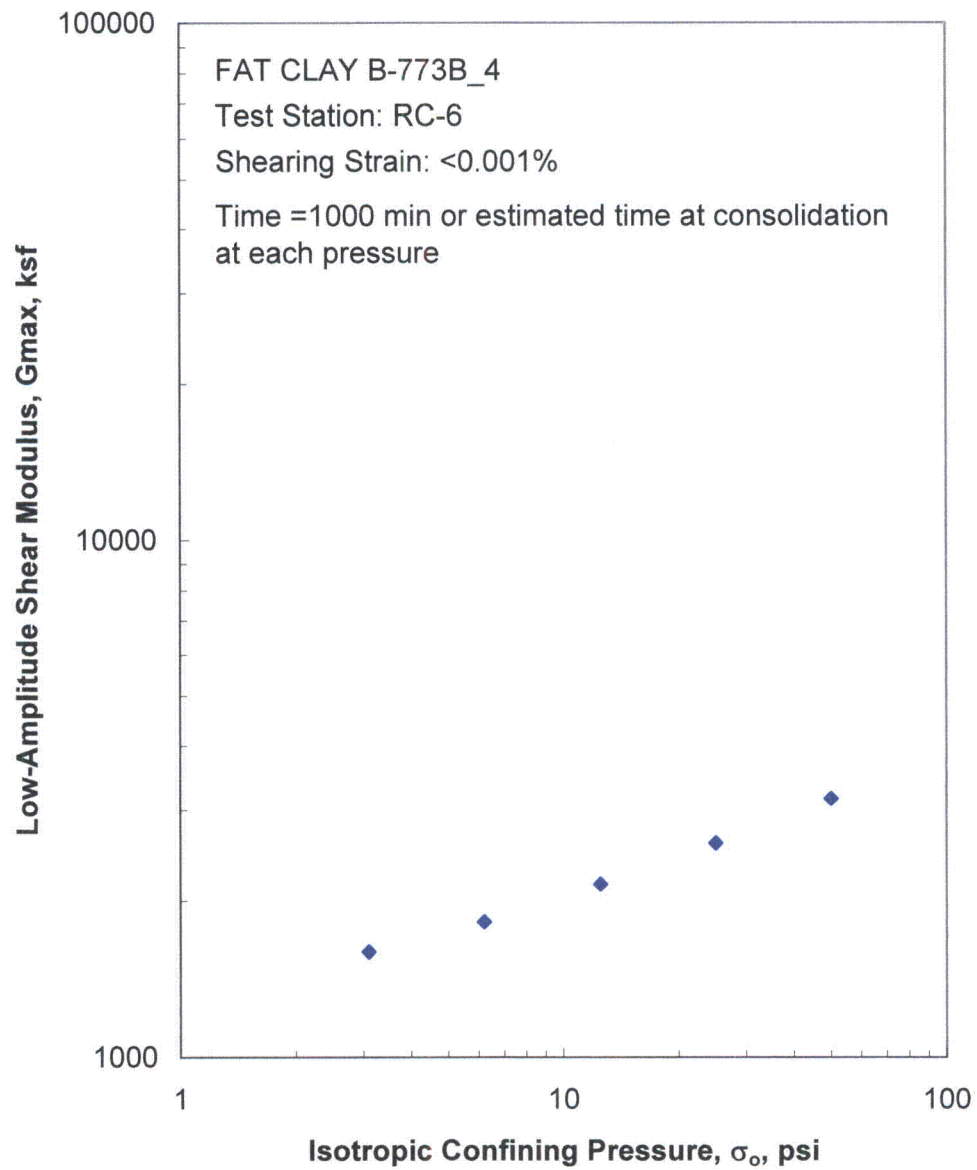


Figure C.5 Variation in Low-Amplitude Shear Modulus with Isotropic Confining Pressure from Resonant Column Tests

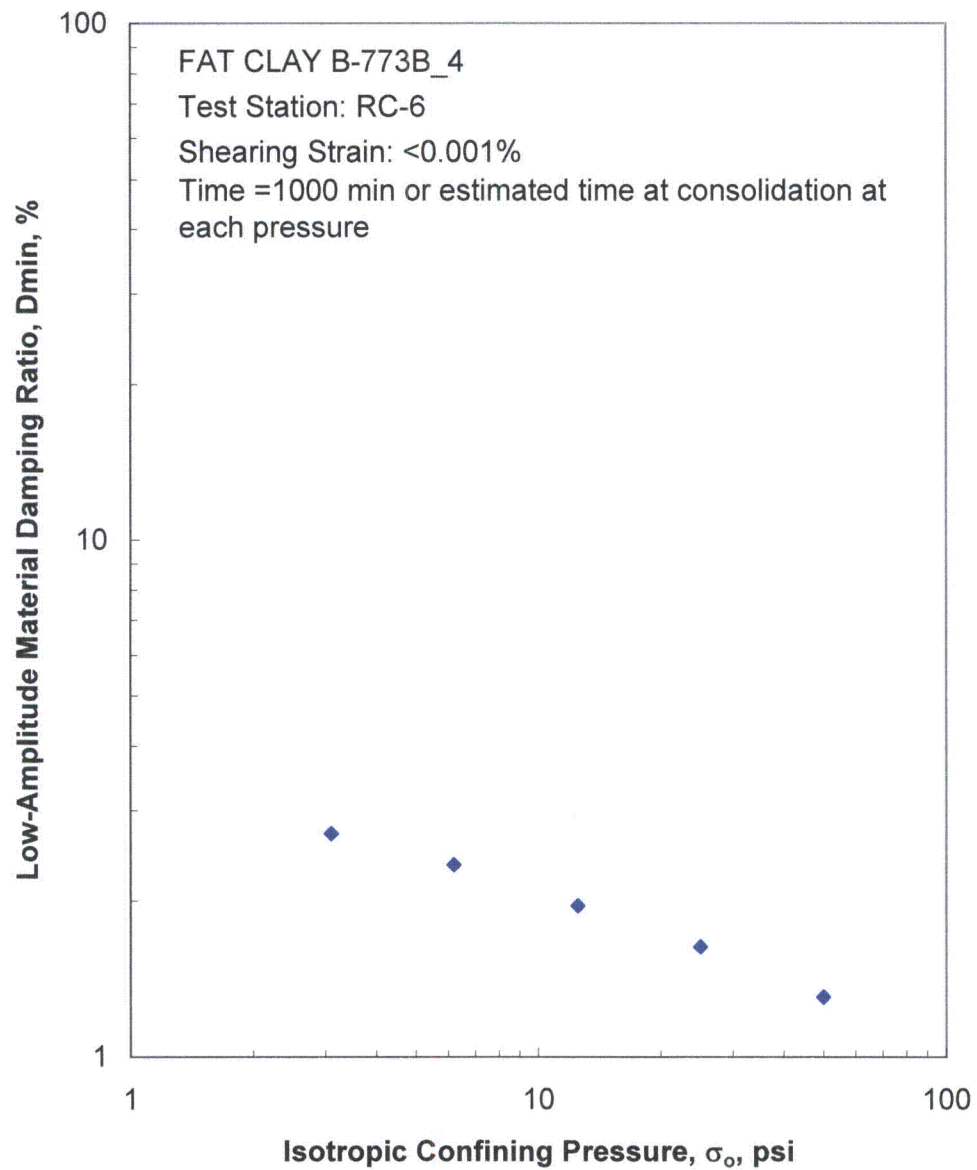


Figure C.6 Variation in Low-Amplitude Material Damping Ratio with Isotropic Confining Pressure from Resonant Column Tests

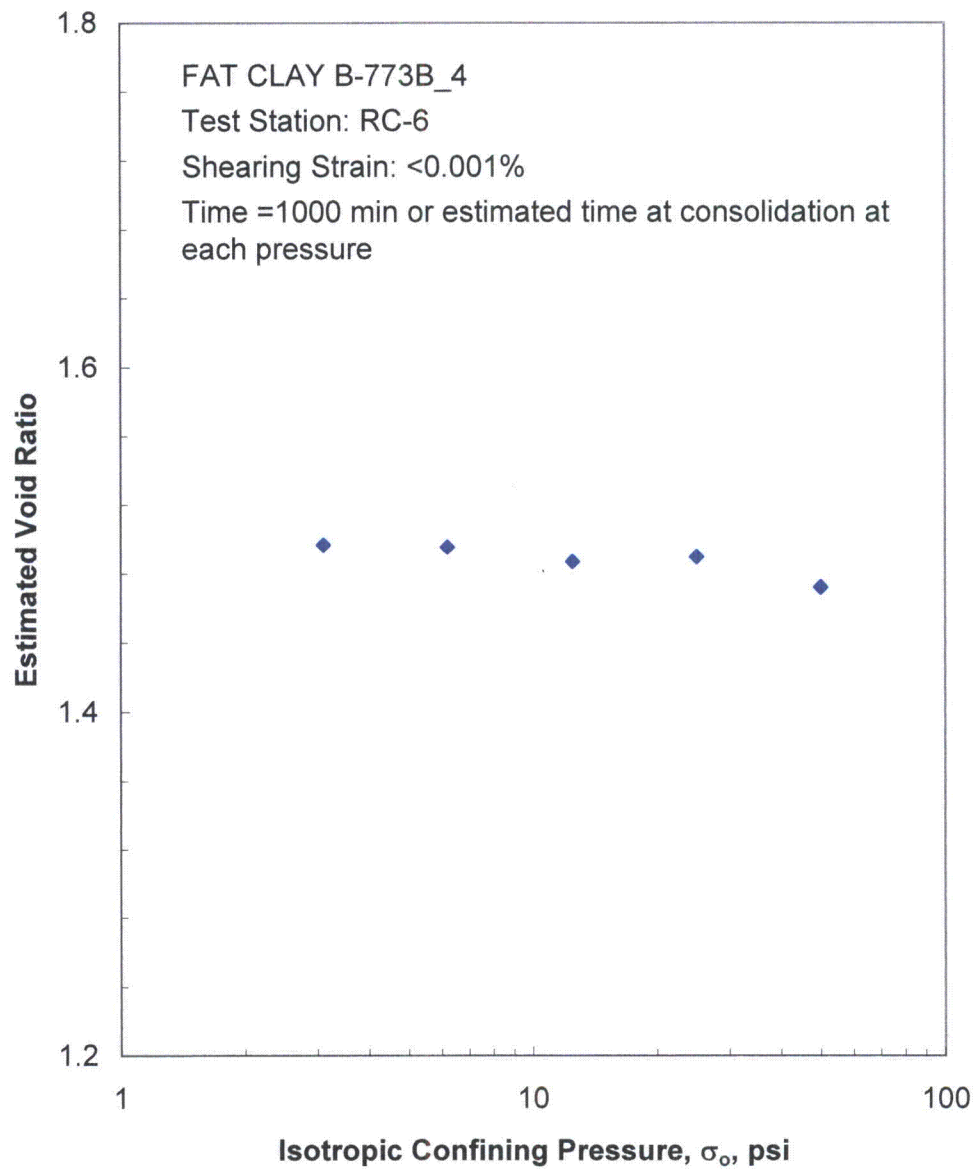


Figure C.7 Variation in Estimated Void Ratio with Isotropic Confining Pressure from Resonant Column Tests

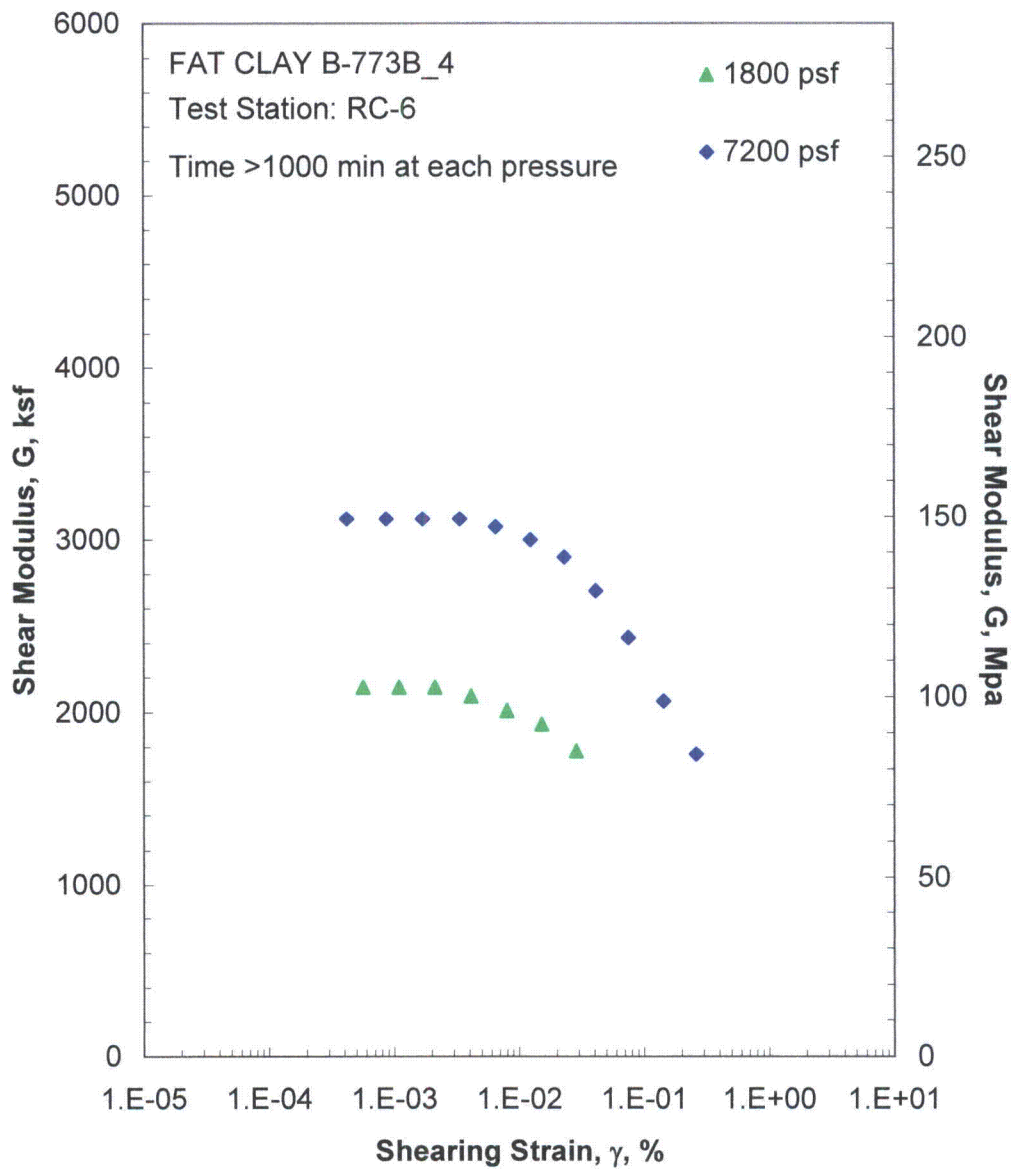


Figure C.8 Comparison of the Variation in Shear Modulus with Shearing Strain and Isotropic Confining Pressure from the Resonant Column Tests

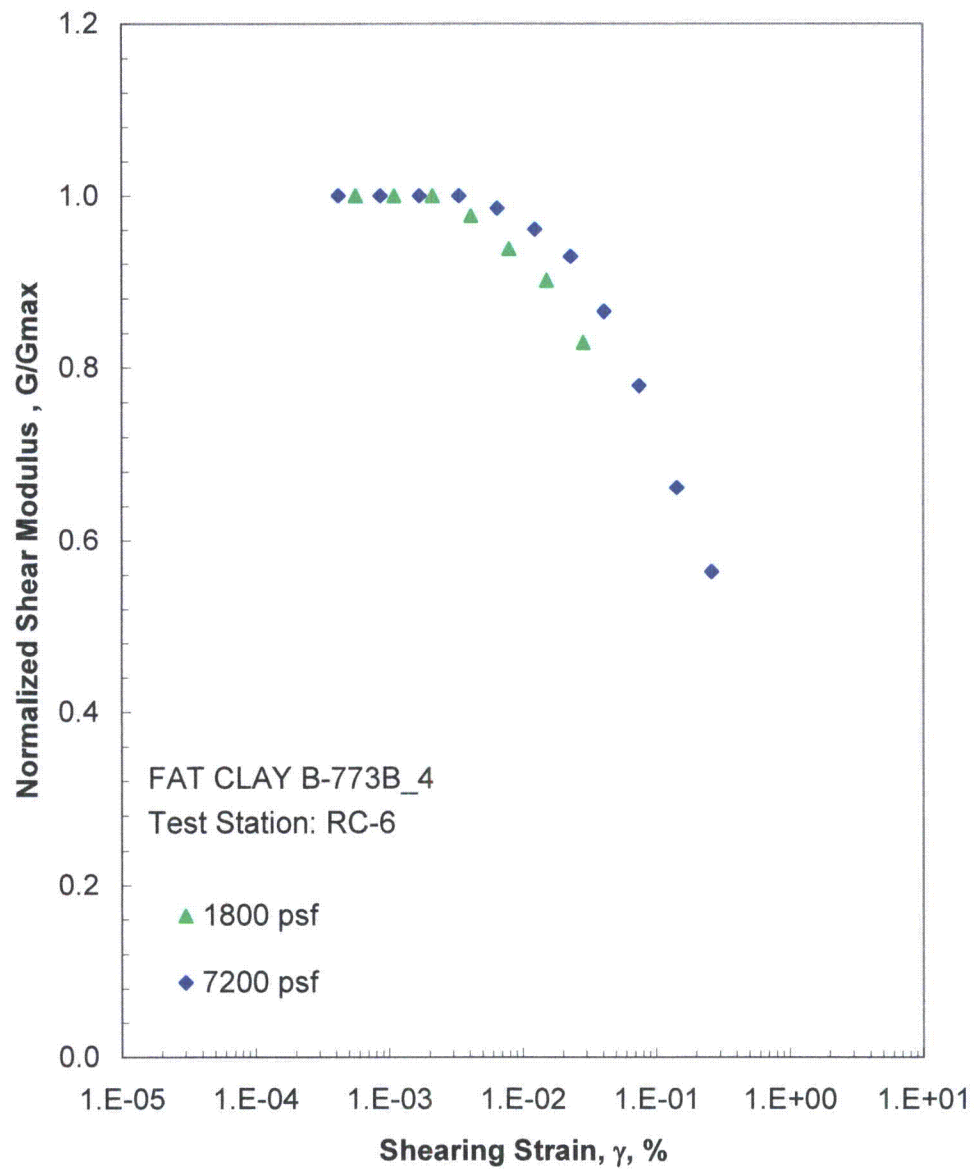


Figure C.9 Comparison of the Variation in Normalized Shear Modulus with Shearing Strain and Isotropic Confining Pressure from the Resonant Column Tests

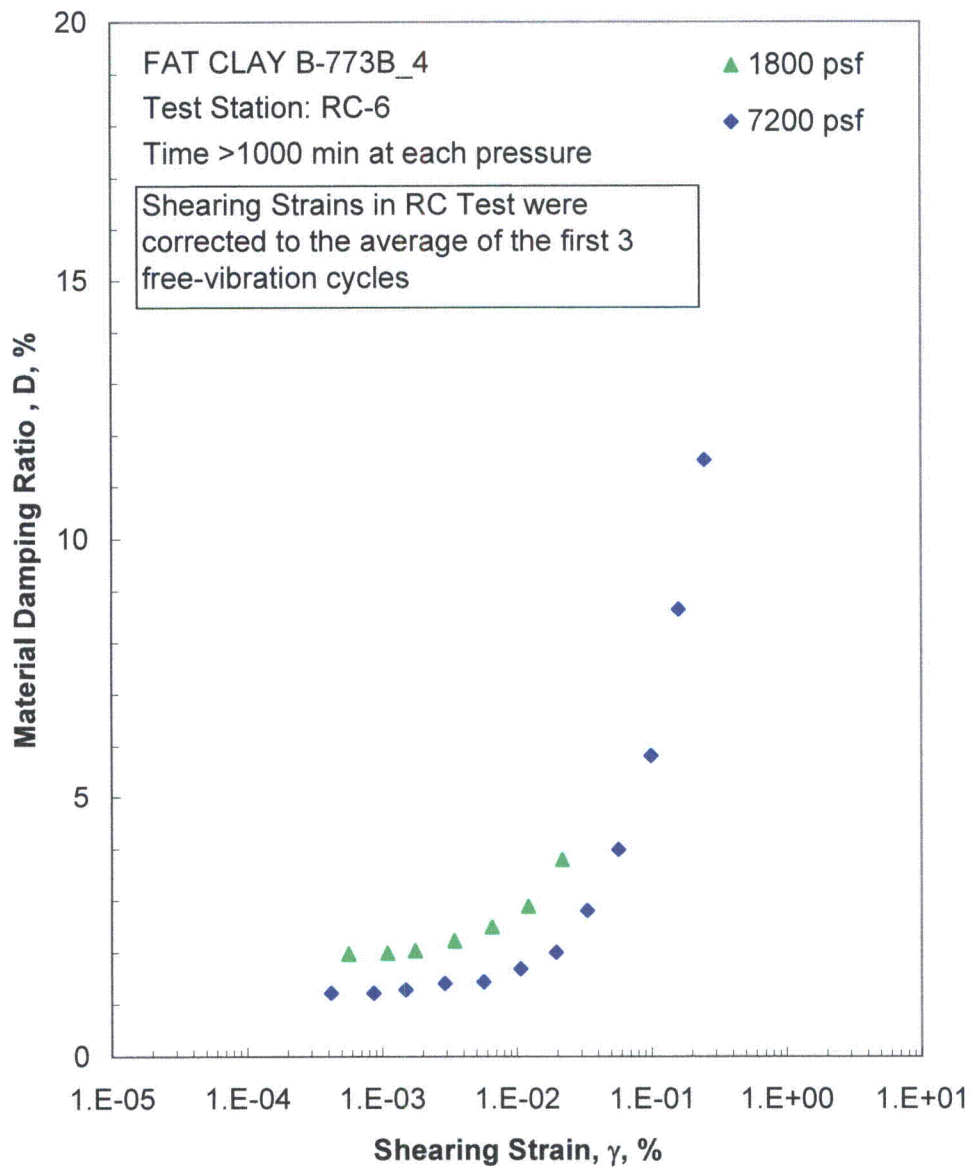


Figure C.10 Comparison of the Variation in Material Damping Ratio with Shearing Strain and Isotropic Confining Pressure from the Resonant Column Tests

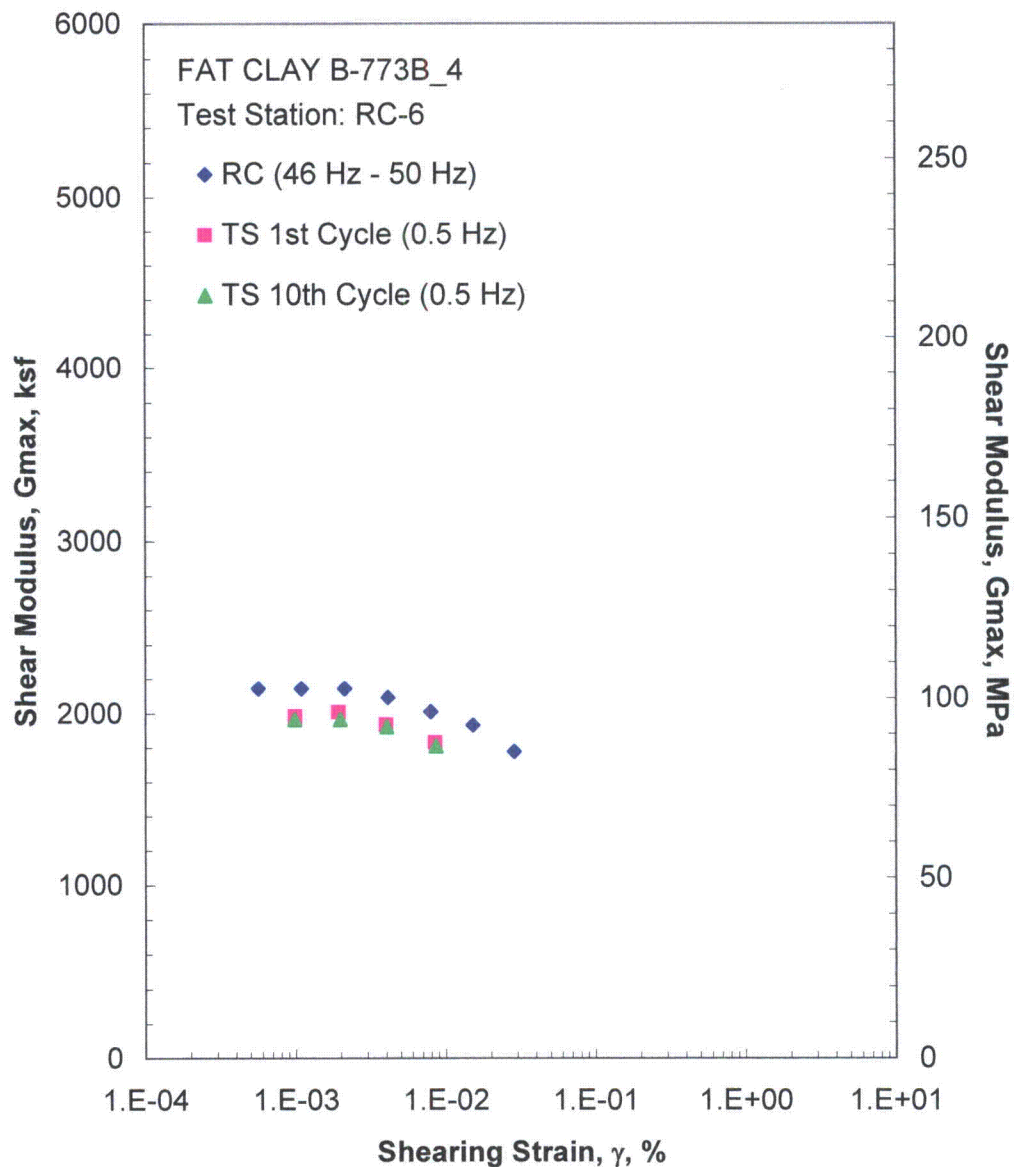


Figure C.11 Comparison of the Variation in Shear Modulus with Shearing Strain at an Isotropic Confining Pressure of 1800 psf from the Combined RCTS Tests

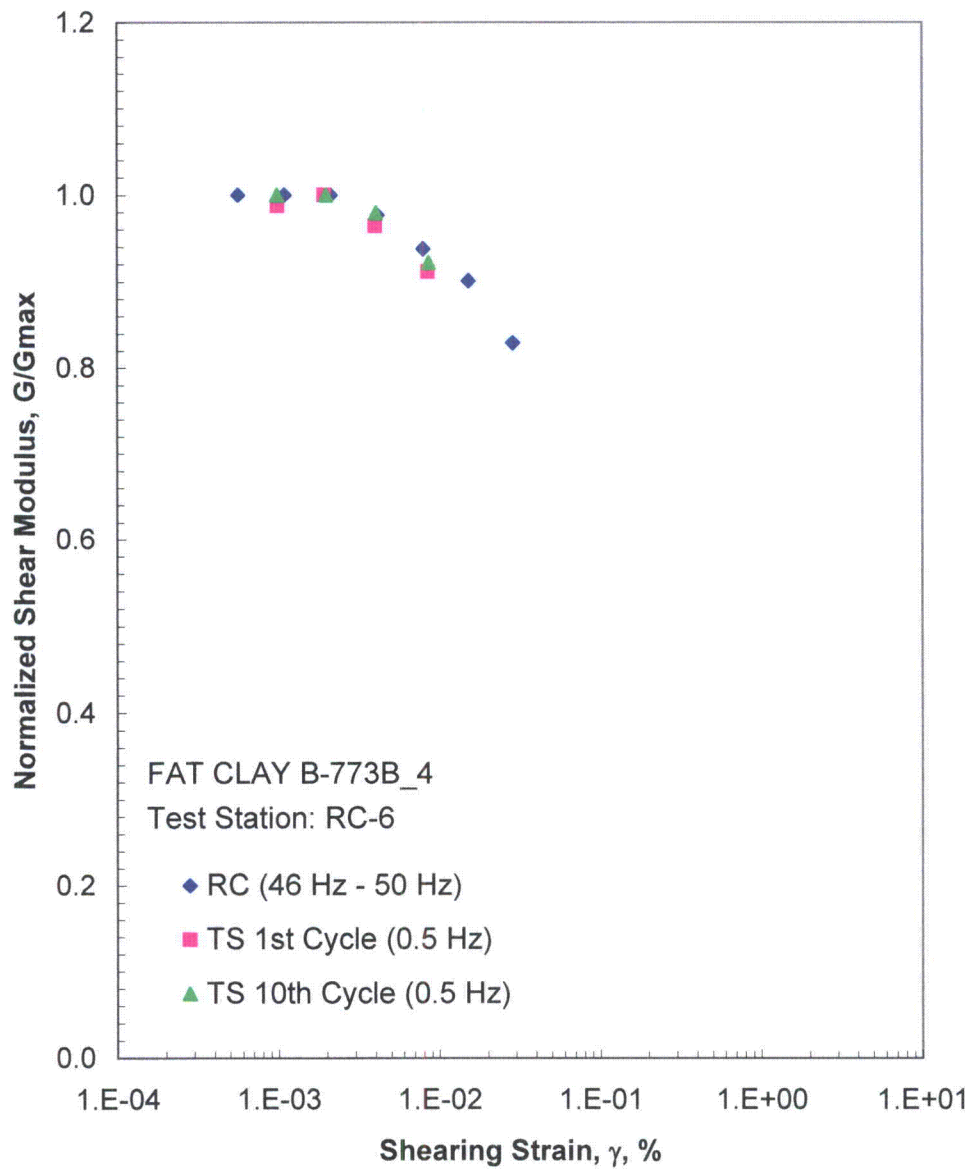


Figure C.12 Comparison of the Variation in Normalized Shear Modulus with Shearing Strain at an Isotropic Confining Pressure of 1800 psf from the Combined RCTS Tests

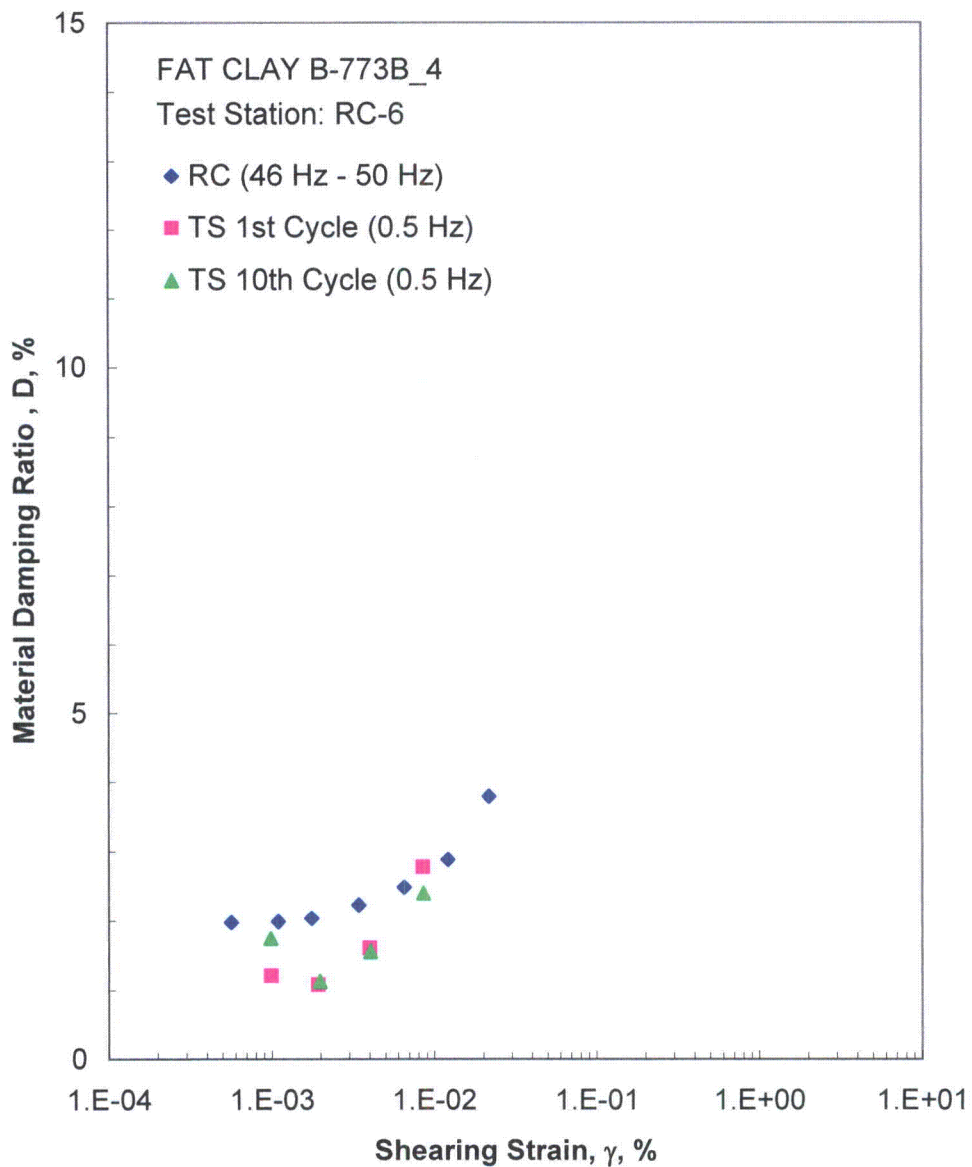


Figure C.13 Comparison of the Variation in Material Damping Ratio with Shearing Strain at an Isotropic Confining Pressure of 1800 psf from the Combined RCTS Tests

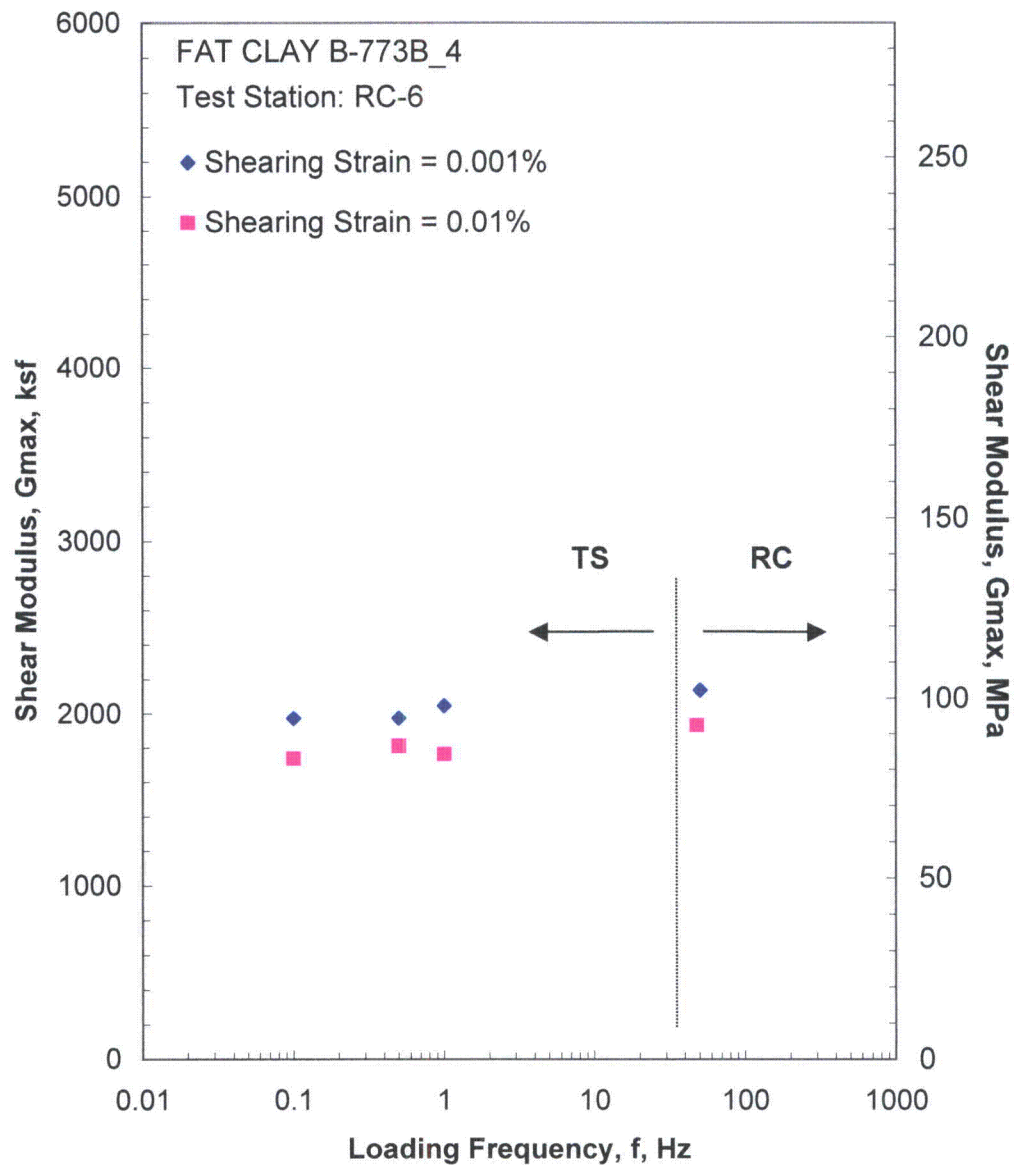


Figure C.14 Comparison of the Variation in Shear Modulus with Loading Frequency at an Isotropic Confining Pressure of 1800 psf from the Combined RCTS Tests

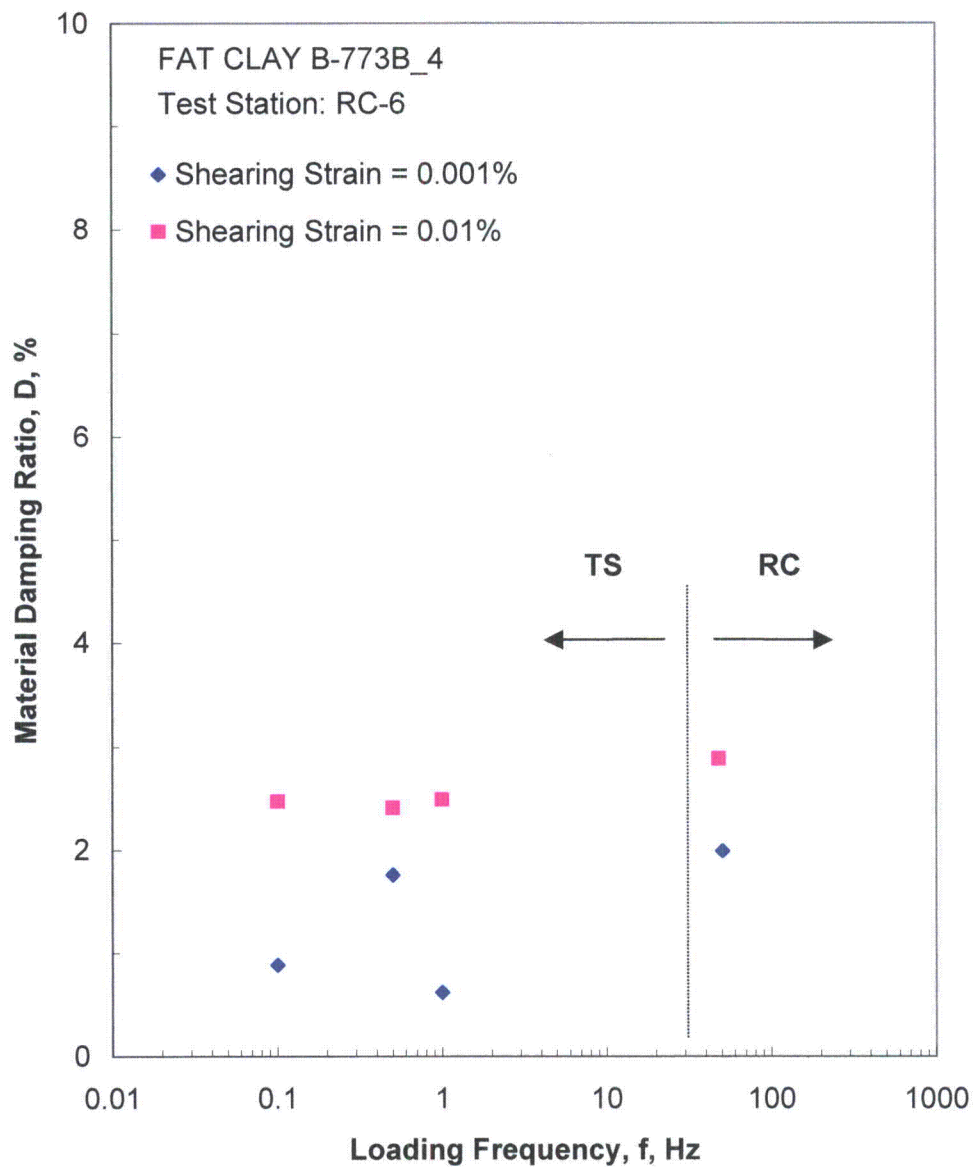


Figure C.15 Comparison of the Variation in Material Damping Ratio with Loading Frequency at an Isotropic Confining Pressure of 1800 psf from the Combined RCTS Tests

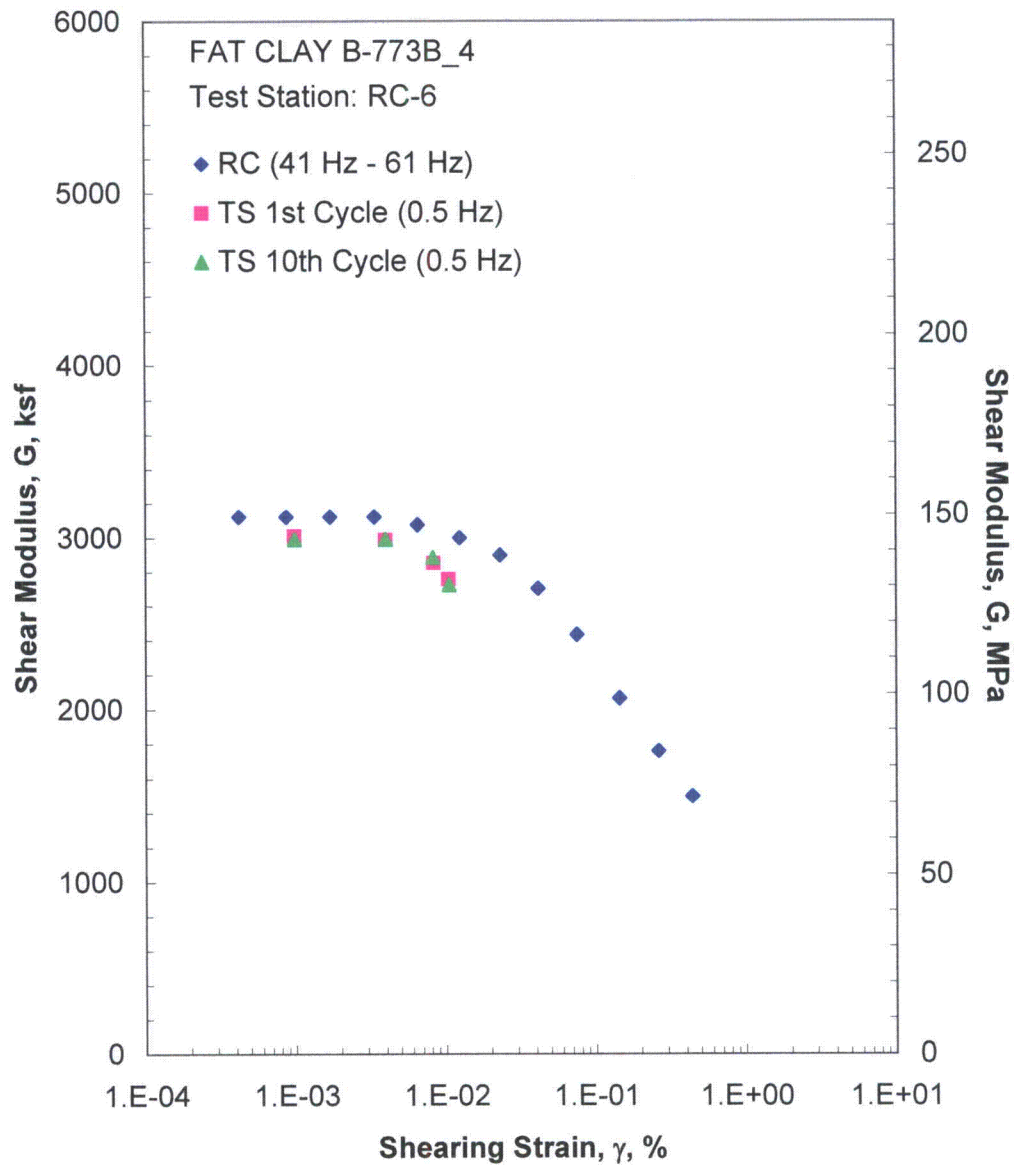


Figure C.16 Comparison of the Variation in Shear Modulus with Shearing Strain at an Isotropic Confining Pressure of 7200 psf from the Combined RCTS Tests

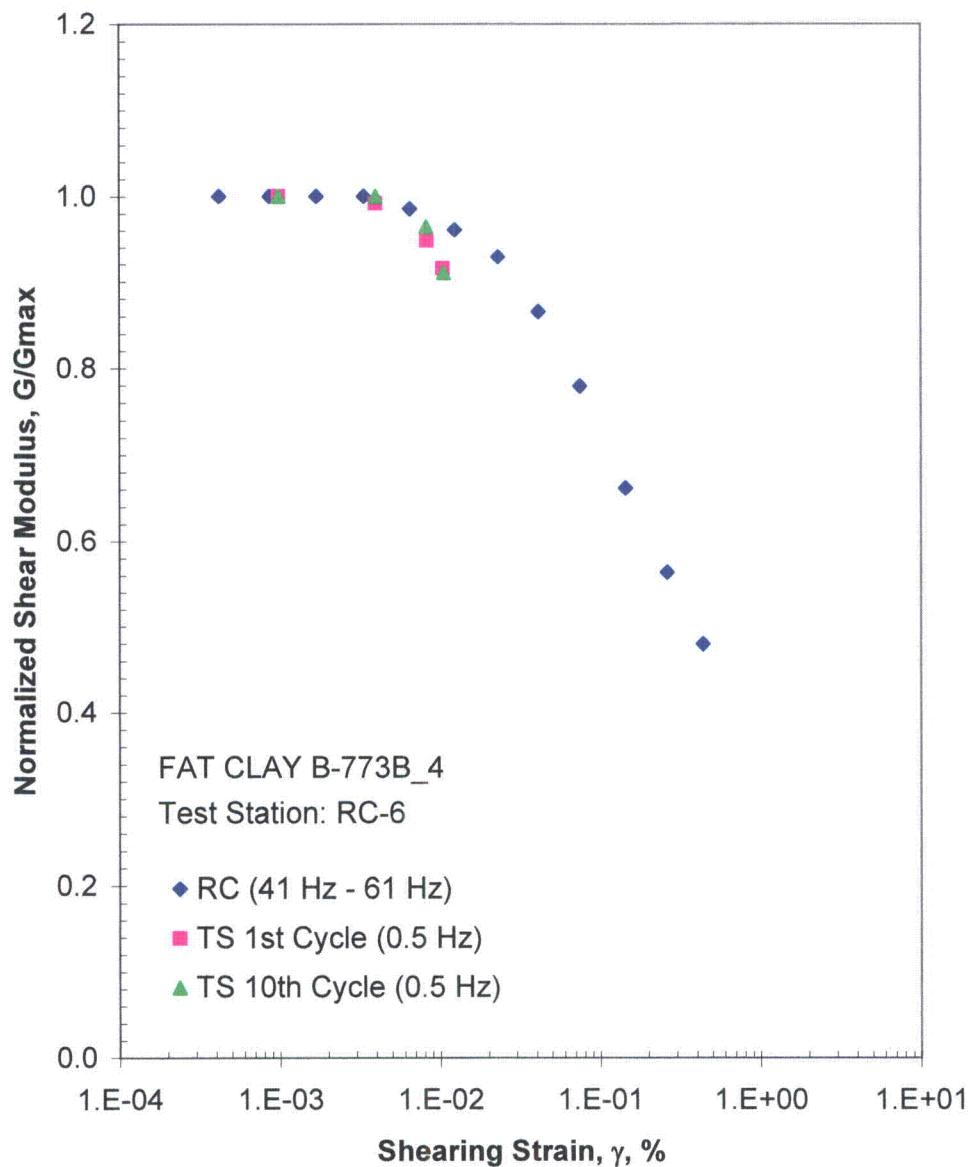


Figure C.17 Comparison of the Variation in Normalized Shear Modulus with Shearing Strain at an Isotropic Confining Pressure of 7200 psi from the Combined RCTS Tests

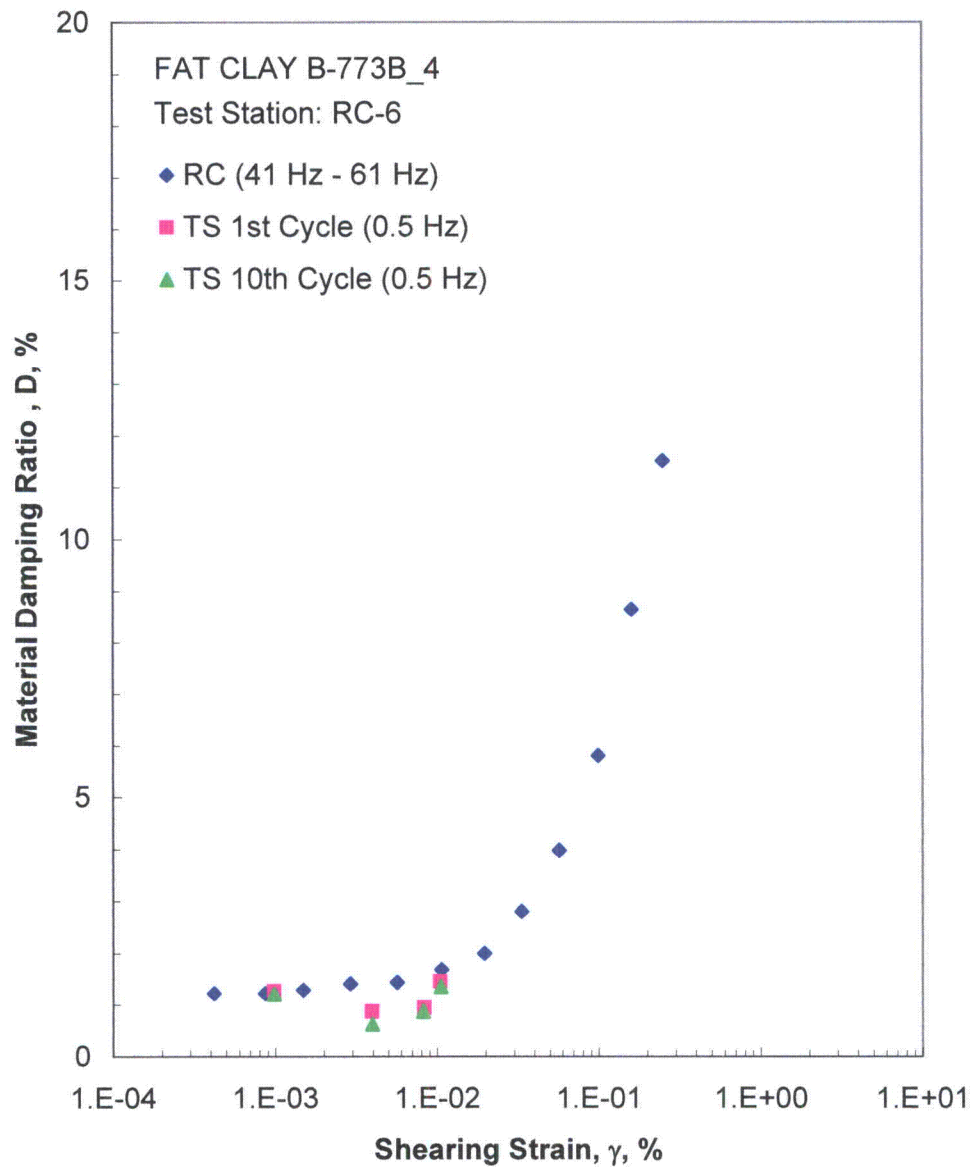


Figure C.18 Comparison of the Variation in Material Damping Ratio with Shearing Strain at an Isotropic Confining Pressure of 7200 psf from the Combined RCTS Tests

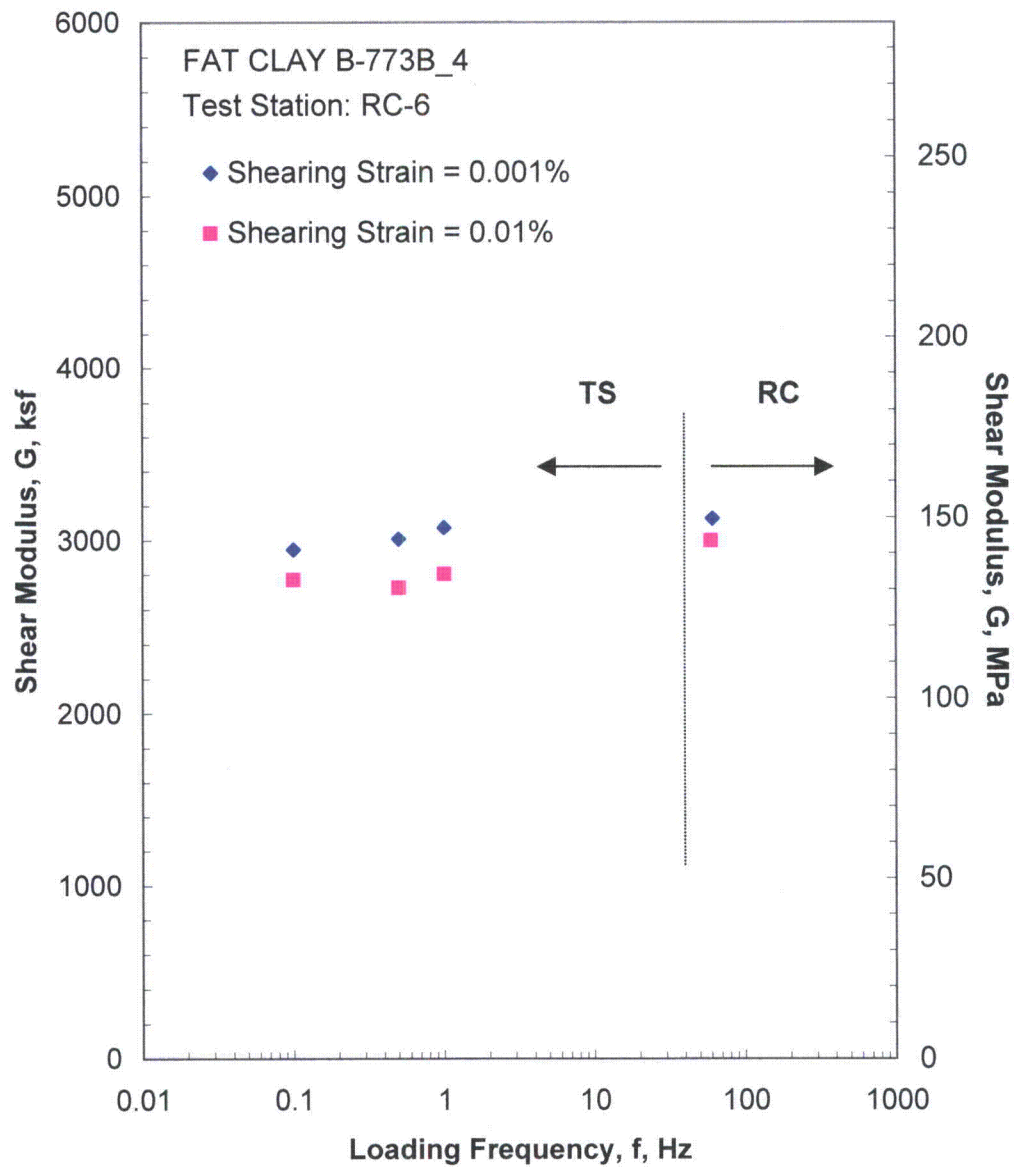


Figure C.19 Comparison of the Variation in Shear Modulus with Loading Frequency at an Isotropic Confining Pressure of 7200 psf from the Combined RCTS Tests

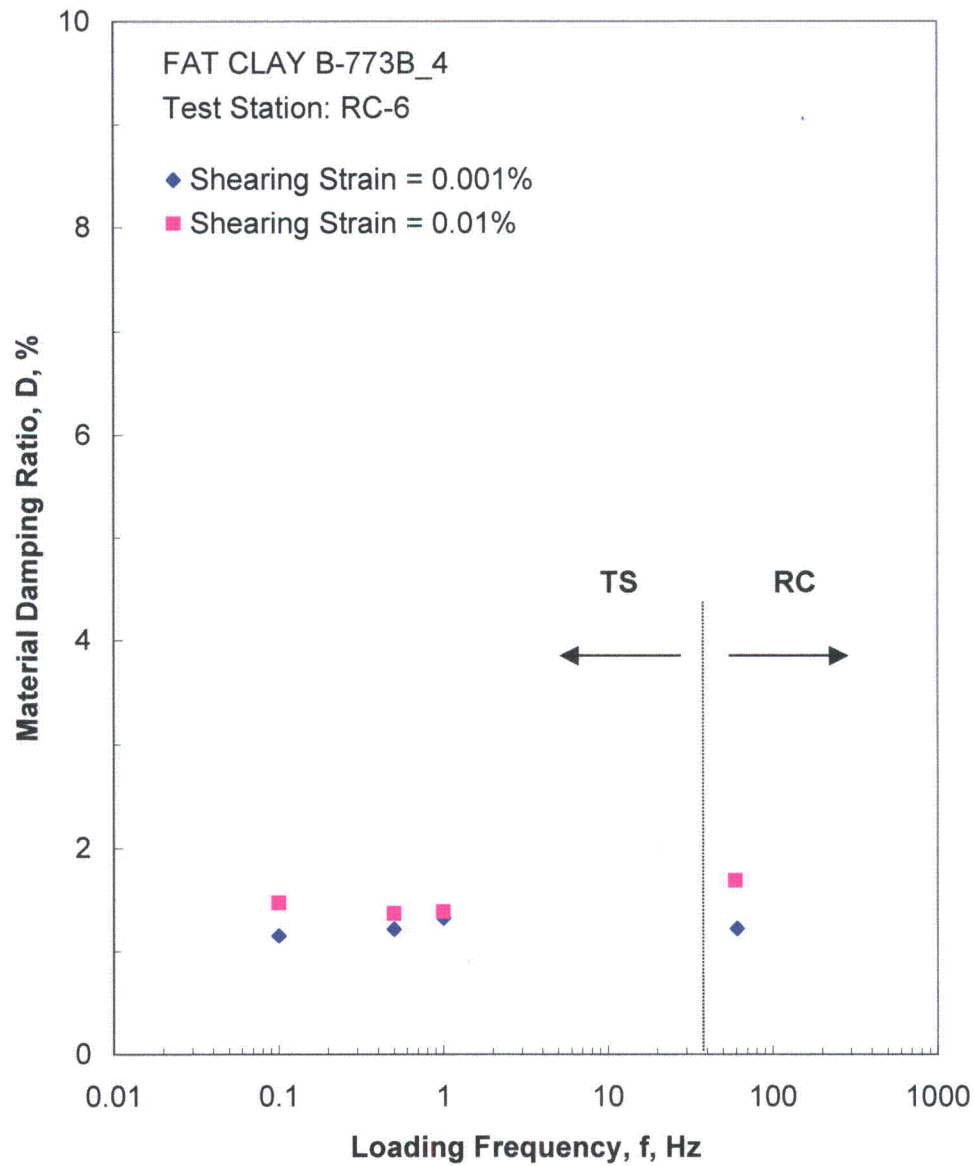


Figure C.20 Comparison of the Variation in Material Damping Ratio with Loading Frequency at an Isotropic Confining Pressure of 7200 psf from the Combined RCTS Tests

Table C.1 Variation in Low-Amplitude Shear Wave Velocity, Low-Amplitude Shear Modulus, Low-Amplitude Material Damping Ratio and Estimated Void Ratio with Isotropic Confining Pressure from RC Tests of Specimen B-773B-4

Isotropic Confining Pressure, σ_o			Low-Amplitude Shear Modulus, G_{max}		Low-Amplitude Shear Wave Velocity, V_s	Low-Amplitude Material Damping Ratio, D_{min}	Estimated Void Ratio, e
(psi)	(psf)	(kPa)	(ksf)	(MPa)	(fps)	(%)	
3	446	21	1597	77	704	2.70	1.50
6	893	43	1821	87	751	2.35	1.50
13	1800	86	2154	103	816	1.96	1.49
25	3600	172	2586	124	894	1.63	1.49
50	7200	345	3153	151	984	1.30	1.47

Table C.2 Variation in Shear Modulus and Material Damping Ratio with Shearing Strain from RC Tests of Specimen B-773B-4; Isotropic Confining Pressure, $\sigma_0 = 1800$ psf

Peak Shearing Strain, %	Shear Modulus, G, ksf	Normalized Shear Modulus, G/G_{max}	Average ⁺ Shearing Strain, %	Material Damping Ratio ^x , D, %
5.64E-04	2144	1.00	5.64E-04	1.98
1.09E-03	2144	1.00	1.09E-03	1.99
2.12E-03	2144	1.00	1.76E-03	2.04
4.12E-03	2095	0.98	3.42E-03	2.23
7.95E-03	2010	0.94	6.52E-03	2.48
1.52E-02	1932	0.90	1.21E-02	2.88
2.86E-02	1778	0.83	2.18E-02	3.79

⁺ Average Shearing Strain from the First Three Cycles of the Free Vibration Decay Curve

^x Average Damping Ratio from the First Three Cycles of the Free Vibration Decay Curve

Table C.3 Variation in Shear Modulus, Normalized Shear Modulus and Material Damping Ratio with Shearing Strain from TS Tests of Specimen B-773B-4; Isotropic Confining Pressure, $\sigma_0 = 1800$ psf

First Cycle				Tenth Cycle			
Peak Shearing Strain, %	Shear Modulus, G, ksf	Normalized Shear Modulus, G/G_{max}	Material Damping Ratio, D, %	Peak Shearing Strain, %	Shear Modulus, G, ksf	Normalized Shear Modulus, G/G_{max}	Material Damping Ratio, D, %
9.91E-04	1982	0.99	1.21	9.84E-04	1964	1.00	1.75
1.93E-03	2007	1.00	1.08	1.98E-03	1964	1.00	1.13
4.01E-03	1935	0.96	1.61	4.04E-03	1923	0.98	1.56
8.48E-03	1829	0.91	2.78	8.57E-03	1810	0.92	2.40

Table C.4 Variation in Shear Modulus and Material Damping Ratio with Shearing Strain from RC Tests of Specimen B-773B-4; Isotropic Confining Pressure, $\sigma_0 = 7200$ psf

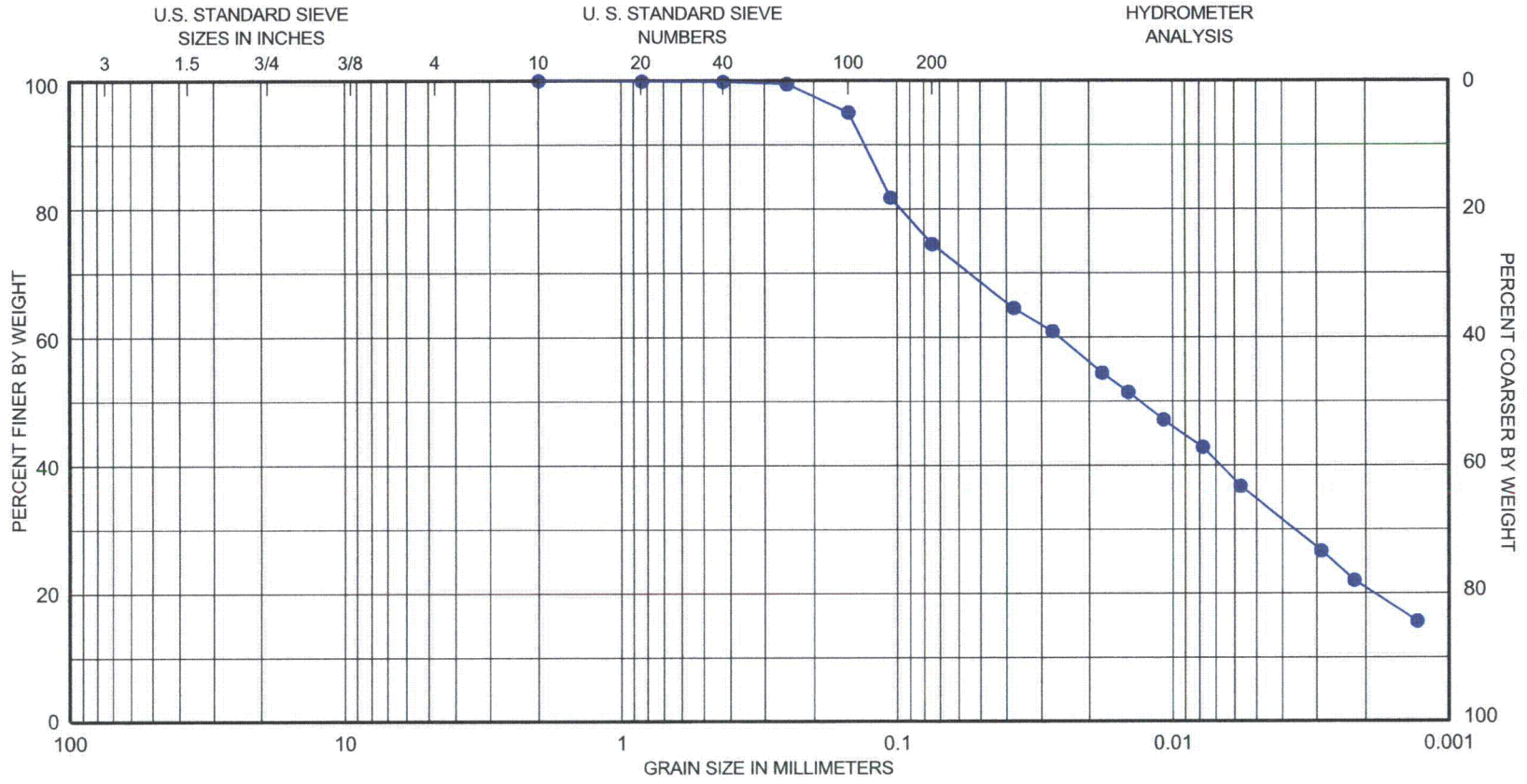
Peak Shearing Strain, %	Shear Modulus, G, ksf	Normalized Shear Modulus, G/G_{max}	Average ⁺ Shearing Strain, %	Material Damping Ratio ^x , D, %
4.19E-04	3121	1.00	4.19E-04	1.22
8.65E-04	3121	1.00	8.65E-04	1.22
1.69E-03	3121	1.00	1.49E-03	1.29
3.35E-03	3121	1.00	2.91E-03	1.41
6.49E-03	3075	0.99	5.64E-03	1.44
1.24E-02	2998	0.96	1.06E-02	1.69
2.30E-02	2897	0.93	1.95E-02	2.00
4.11E-02	2700	0.87	3.33E-02	2.80
7.48E-02	2431	0.78	5.68E-02	3.98
1.43E-01	2064	0.66	9.90E-02	5.81
2.61E-01	1759	0.56	1.59E-01	8.65
4.36E-01	1497	0.48	2.49E-01	11.52

⁺ Average Shearing Strain from the First Three Cycles of the Free Vibration Decay Curve

^x Average Damping Ratio from the First Three Cycles of the Free Vibration Decay Curve

Table C.5 Variation in Shear Modulus, Normalized Shear Modulus and Material Damping Ratio with Shearing Strain from TS Tests of Specimen B-773B-4; Isotropic Confining Pressure, $\sigma_o = 7200$ psf

First Cycle				Tenth Cycle			
Peak Shearing Strain, %	Shear Modulus, G, ksf	Normalized Shear Modulus, G/G_{max}	Material Damping Ratio, D, %	Peak Shearing Strain, %	Shear Modulus, G, ksf	Normalized Shear Modulus, G/G_{max}	Material Damping Ratio, D, %
9.82E-04	3010	1.00	1.27	9.84E-04	2993	1.00	1.21
3.96E-03	2987	0.99	0.88	3.97E-03	2993	1.00	0.63
8.29E-03	2853	0.95	0.95	8.19E-03	2886	0.96	0.88
1.04E-02	2755	0.92	1.46	1.05E-02	2723	0.91	1.36



GRAVEL		SAND			SILT or CLAY		
Coarse	Fine	Coarse	Medium	Fine			
<u>SYMBOL</u>	<u>BORING</u>	<u>DEPTH, FT</u>	<u>C_c</u>	<u>C_u</u>	<u>D₅₀</u>	<u>D₉₀</u>	<u>CLASSIFICATION</u>
●	B-773B-4	37	NA	NA	0.01	0.13	Fat Clay with sand(CH), gray

GRAIN SIZE CURVE

APPENDIX D

Specimen B-773B_5

Borehole B-773B

Sample 5

Depth = 47 ft (14.3 m)

Total Unit Weight = 110.9 lb/ft³

Water Content = 34.1%

FUGRO JOB #: 0411-09-1734
Testing Station: RC6



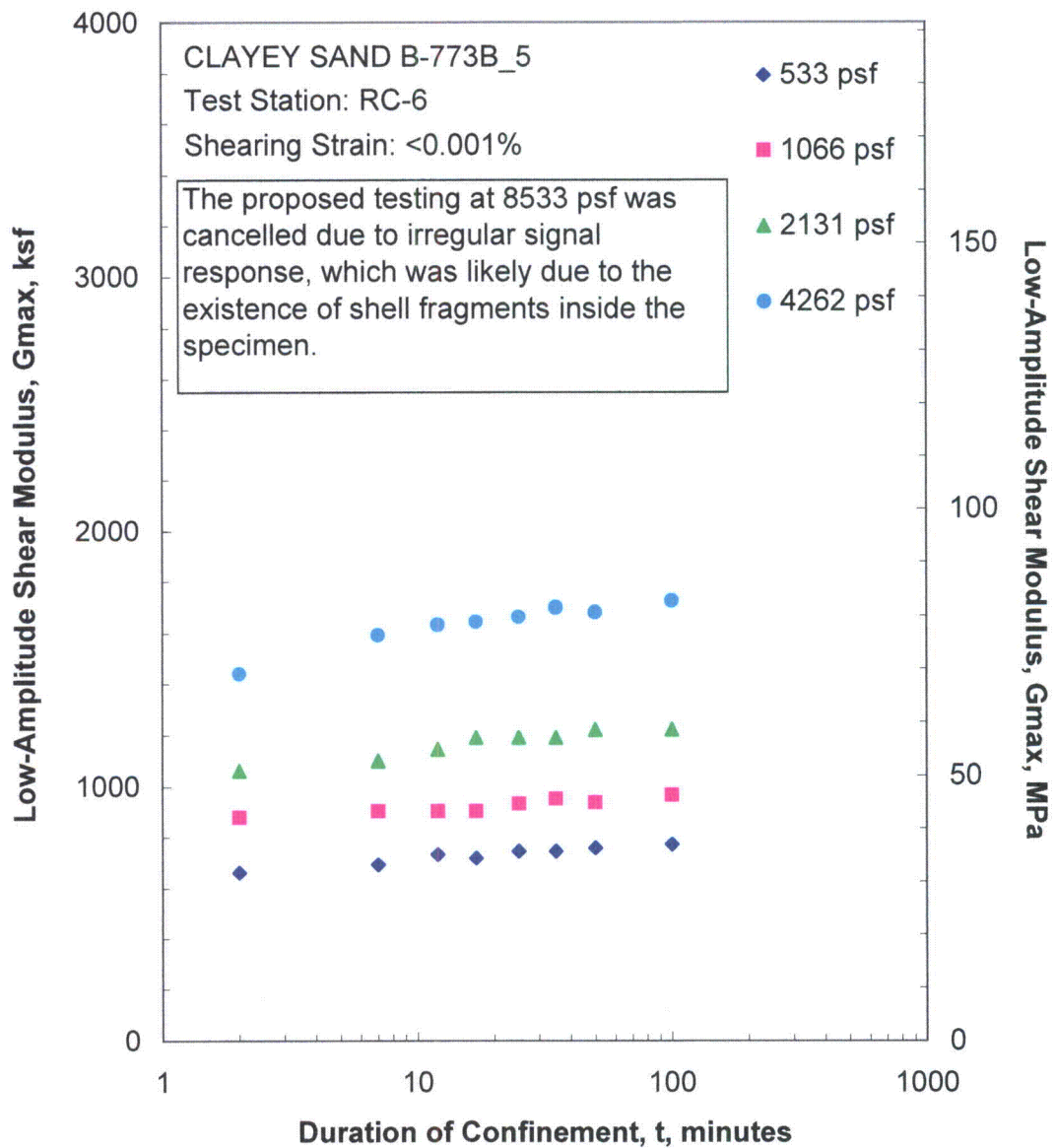


Figure D.1 Variation in Low-Amplitude Shear Modulus with Magnitude and Duration of Isotropic Confining Pressure from Resonant Column Tests

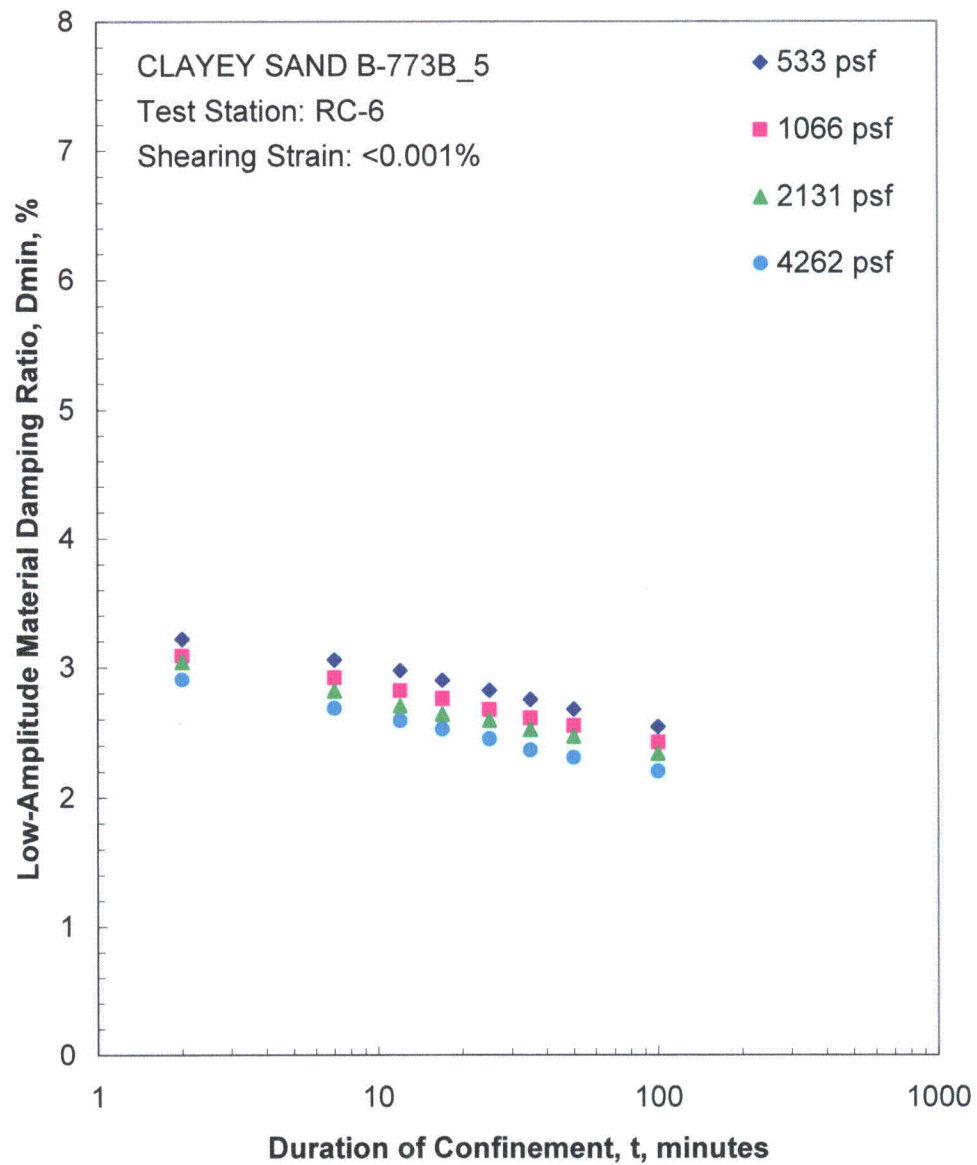


Figure D.2 Variation in Low-Amplitude Material Damping Ratio with Magnitude and Duration of Isotropic Confining Pressure from Resonant Column Tests

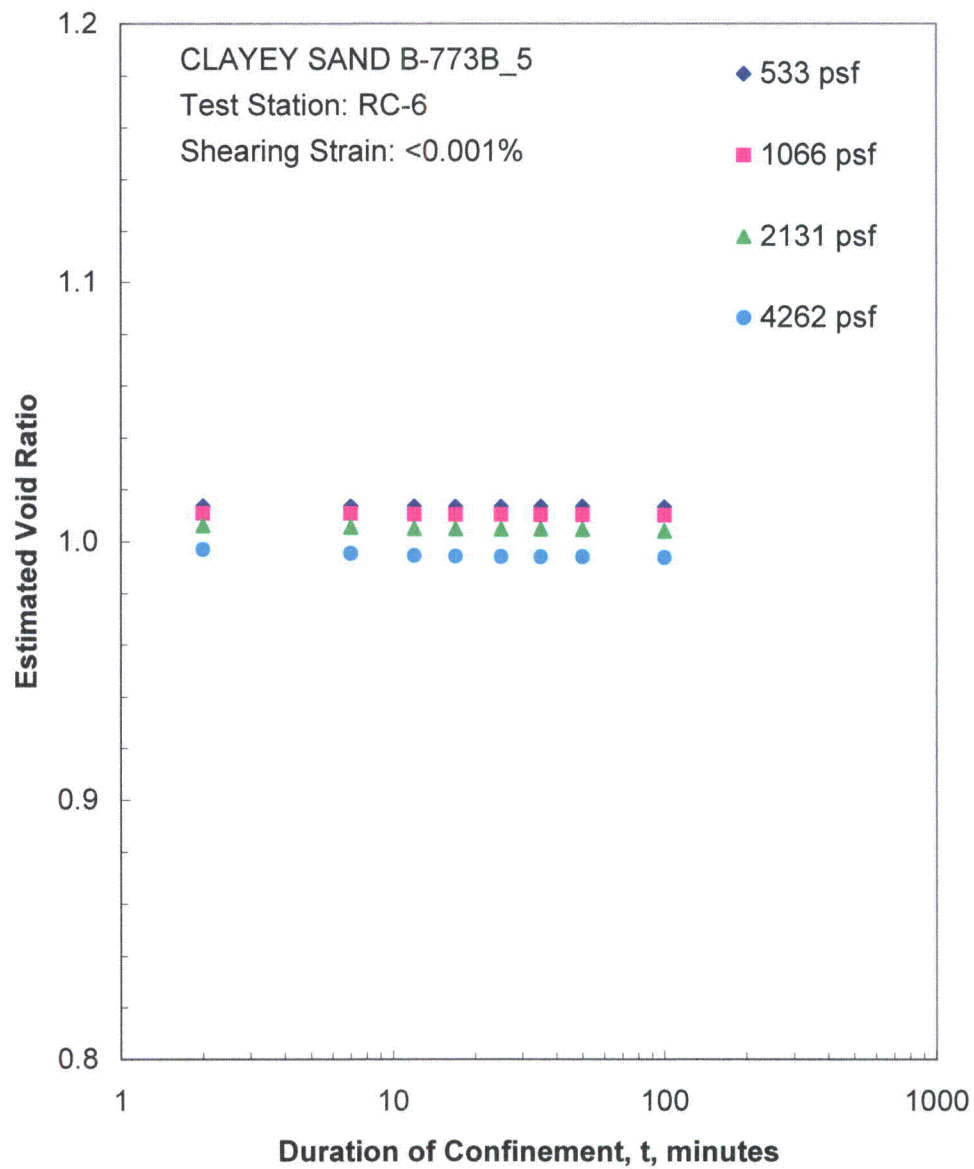


Figure D.3 Variation in Estimated Void Ratio with Magnitude and Duration of Isotropic Confining Pressure from Resonant Column Tests

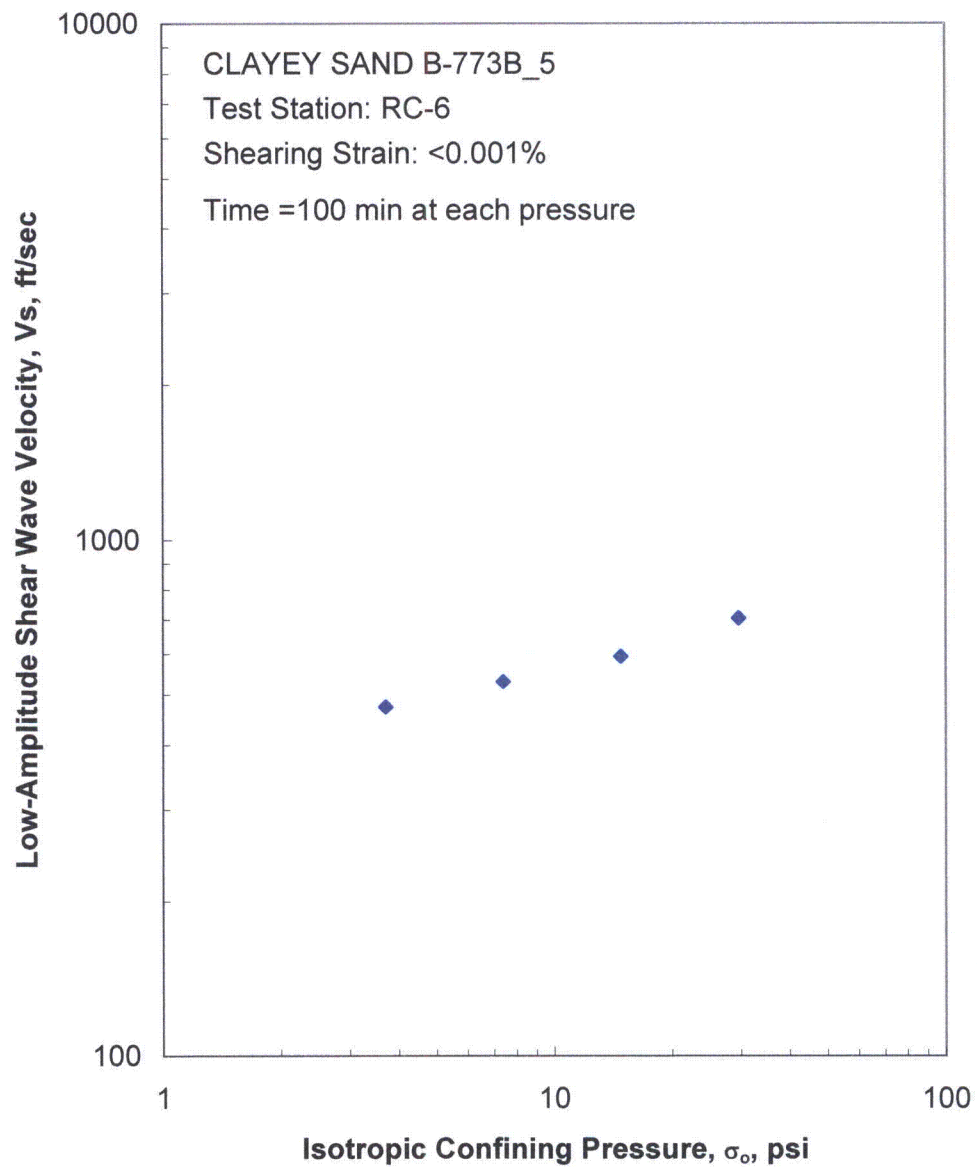


Figure D.4 Variation in Low-Amplitude Shear Wave Velocity with Isotropic Confining Pressure from Resonant Column Tests

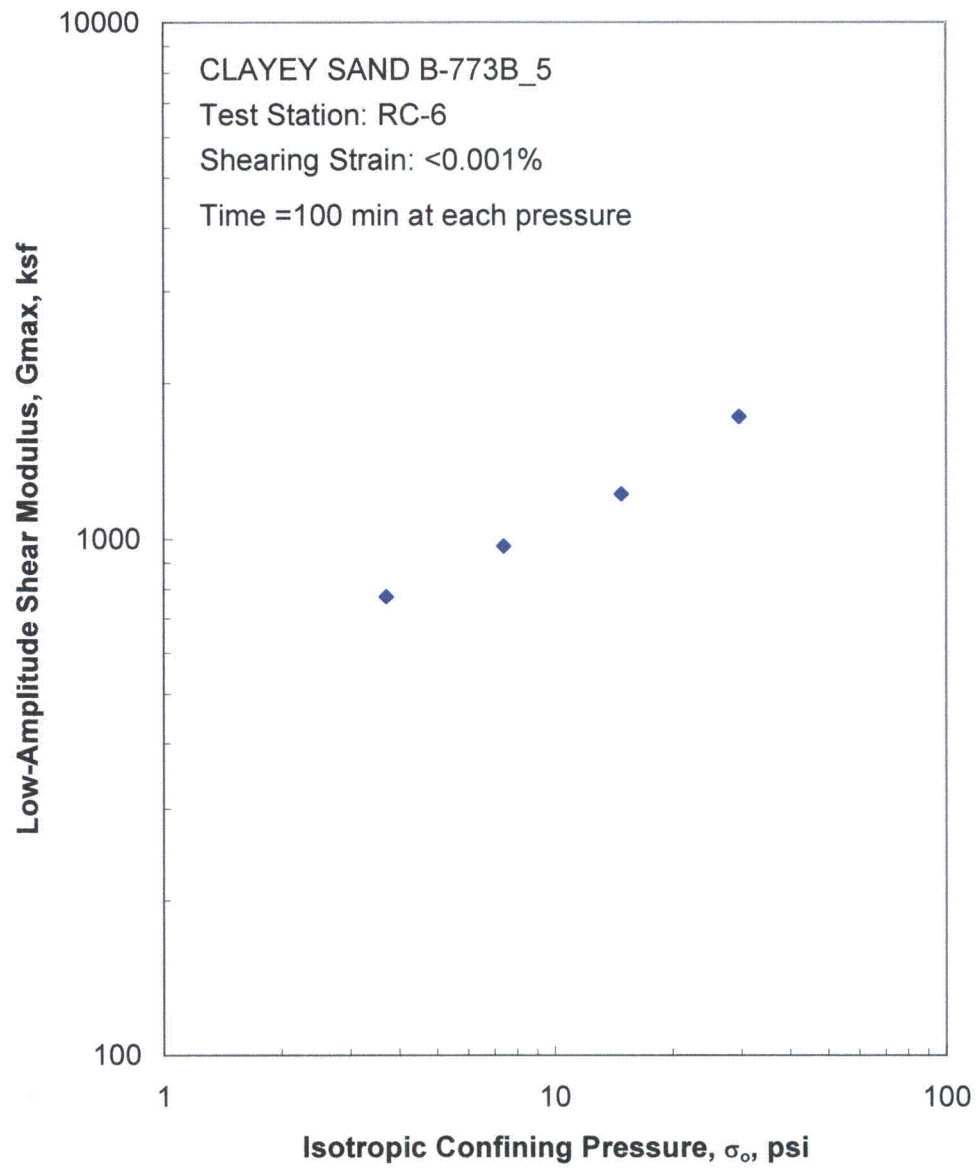


Figure D.5 Variation in Low-Amplitude Shear Modulus with Isotropic Confining Pressure from Resonant Column Tests

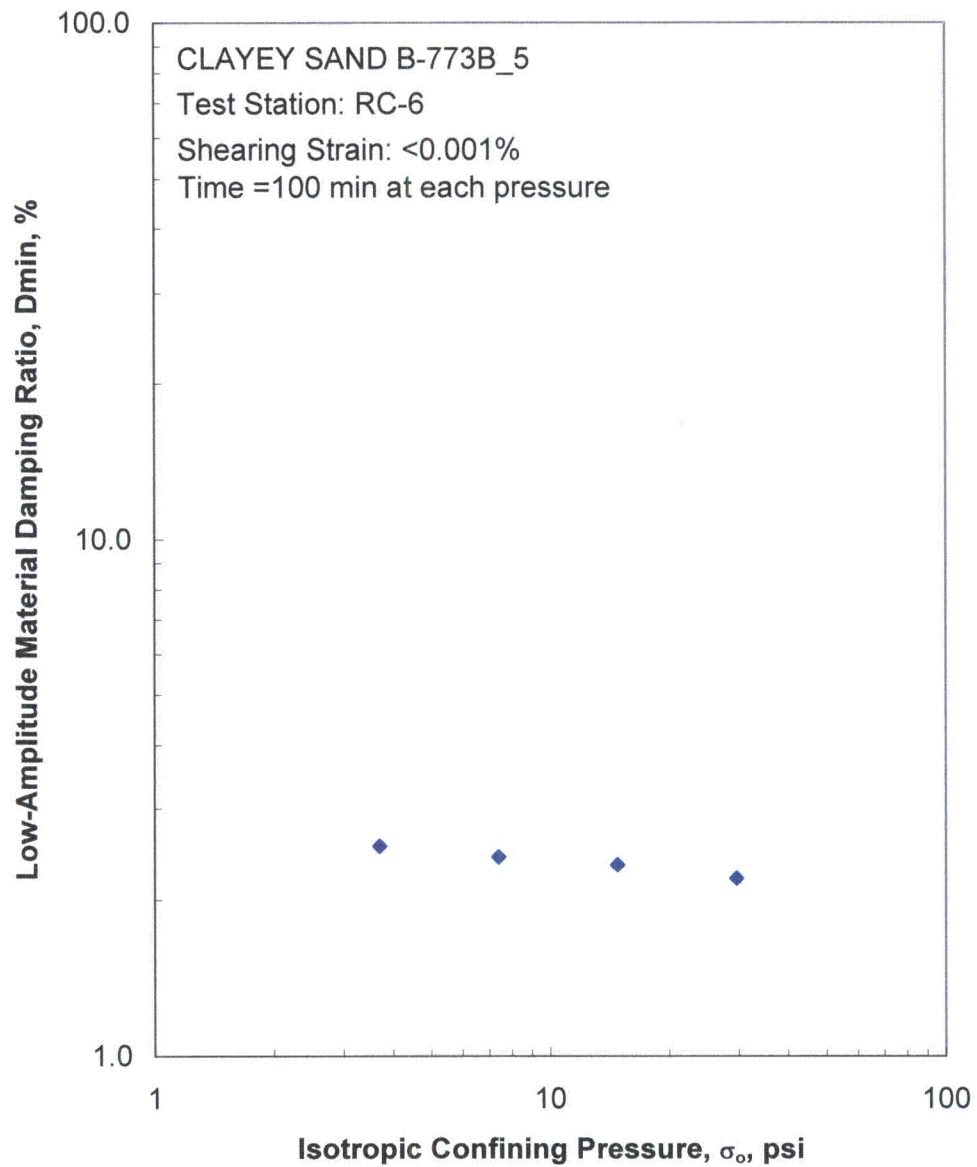


Figure D.6 Variation in Low-Amplitude Material Damping Ratio with Isotropic Confining Pressure from Resonant Column Tests

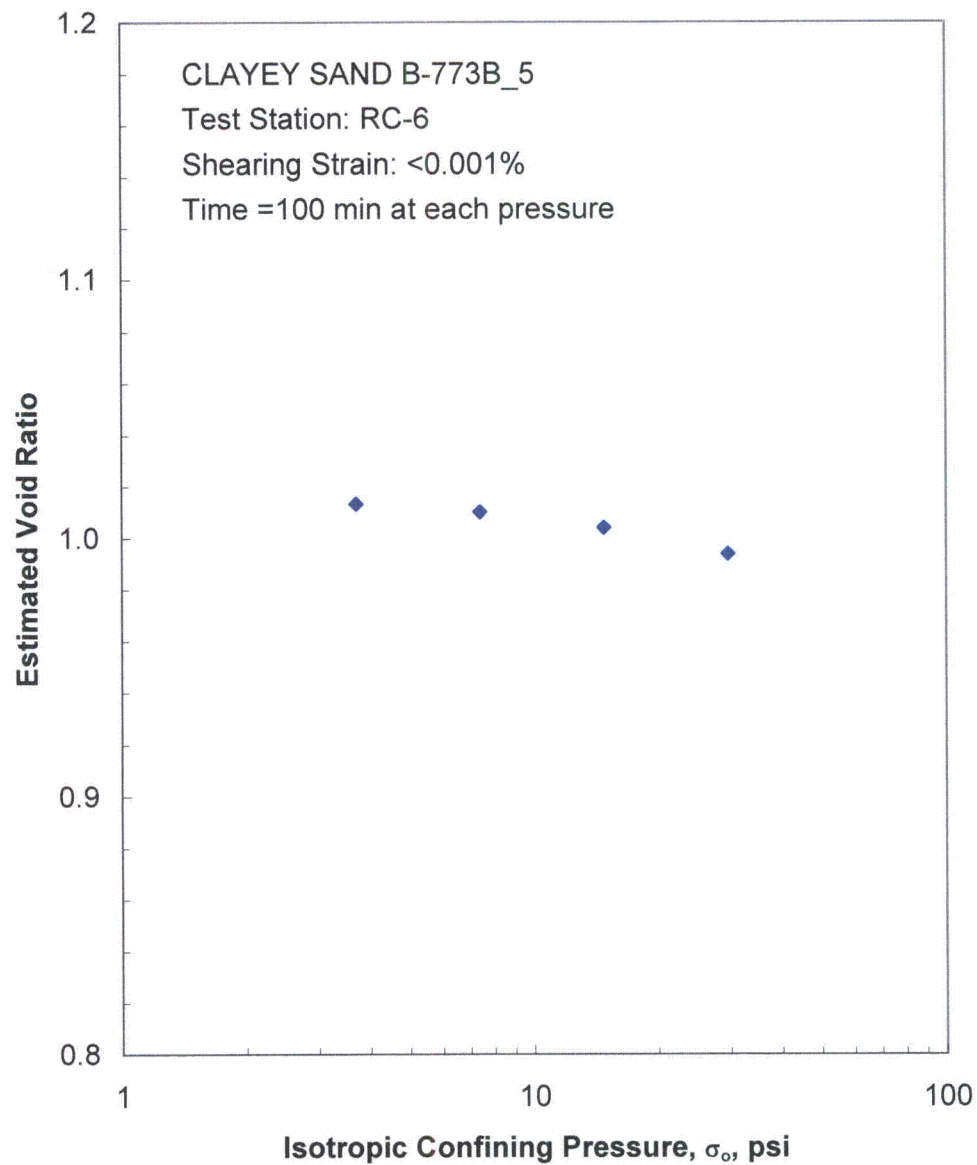


Figure D.7 Variation in Estimated Void Ratio with Isotropic Confining Pressure from Resonant Column Tests

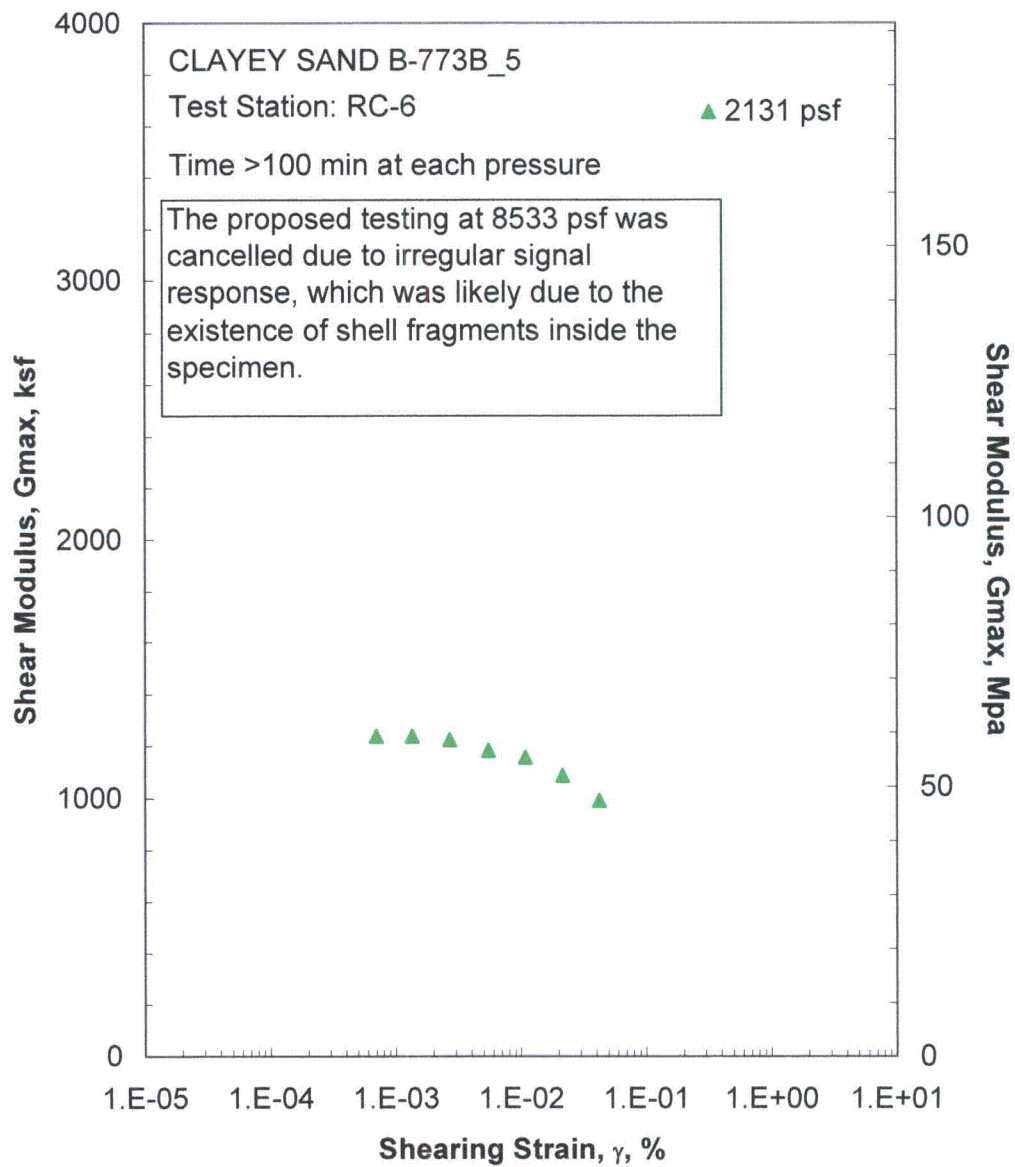


Figure D.8 The Variation in Shear Modulus with Shearing Strain from the Resonant Column Tests

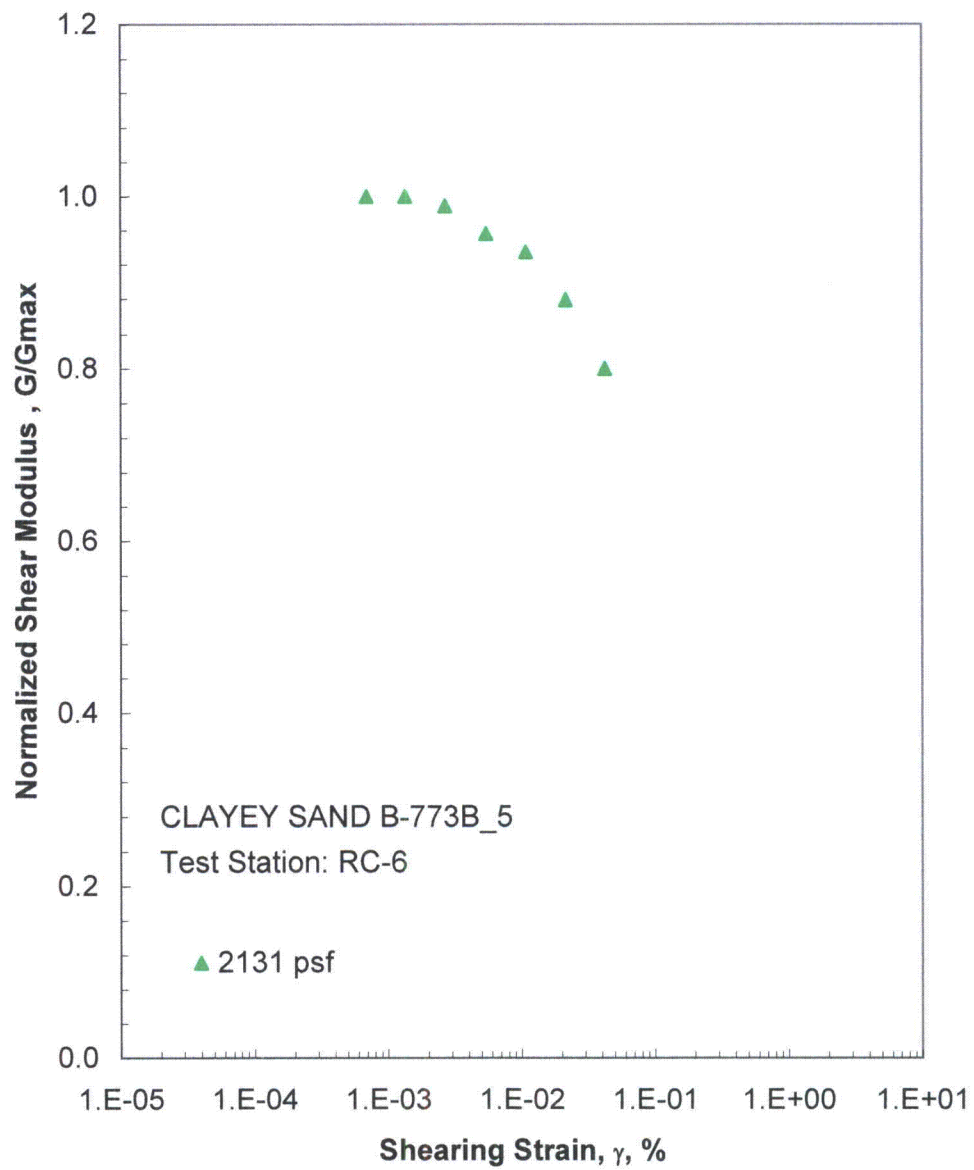


Figure D.9 The Variation in Normalized Shear Modulus with Shearing Strain from the Resonant Column Tests

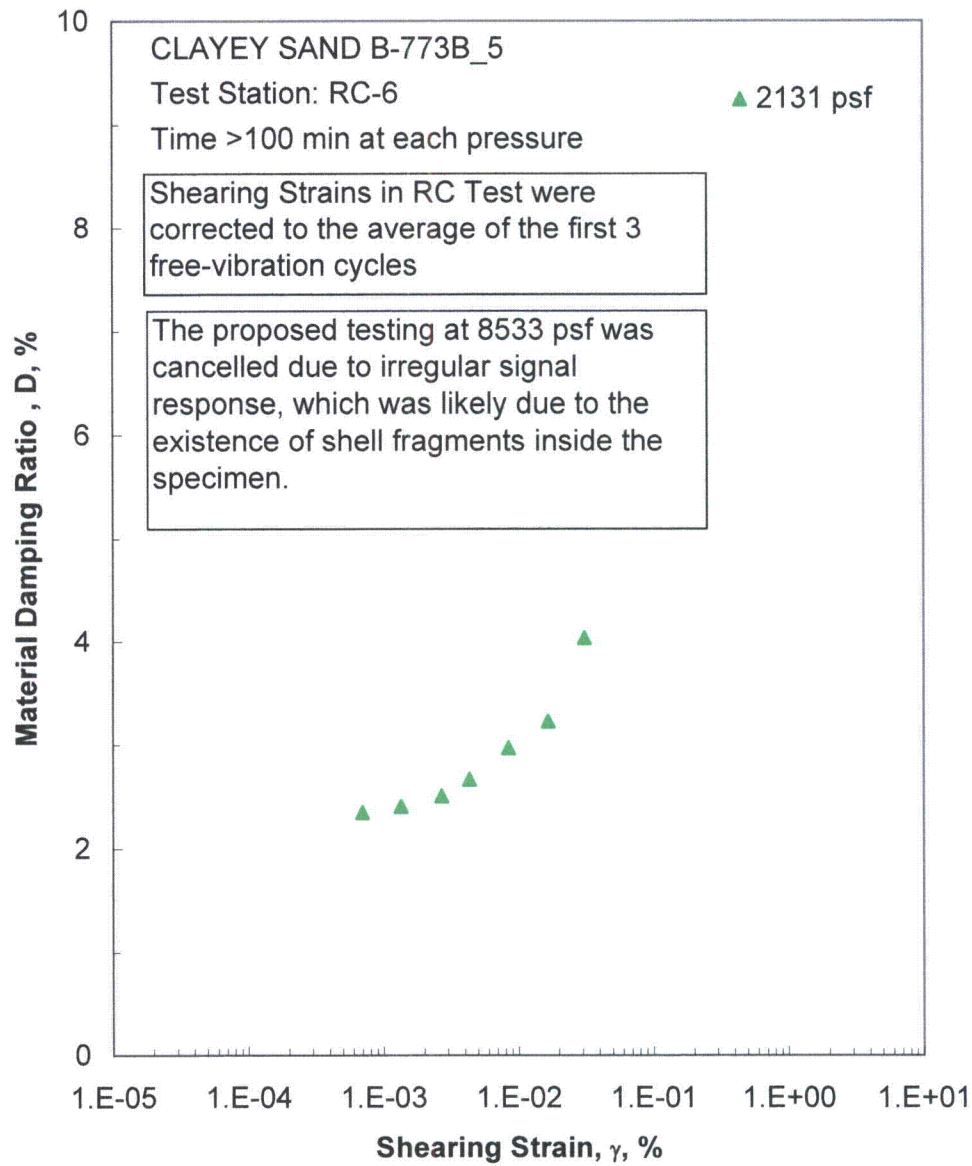


Figure D.10 The Variation in Material Damping Ratio with Shearing Strain from the Resonant Column Tests

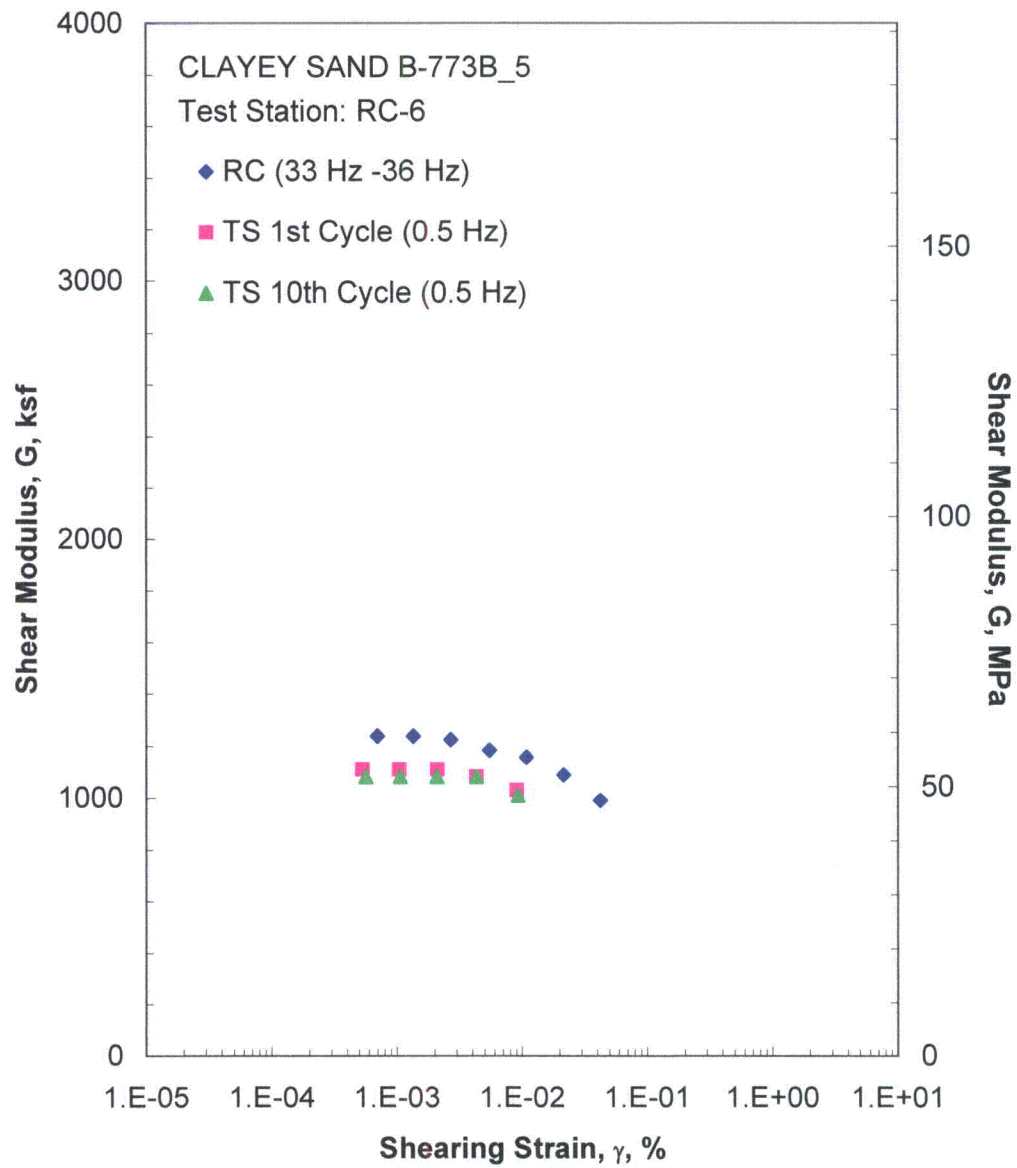


Figure D.11 Comparison of the Variation in Shear Modulus with Shearing Strain at an Isotropic Confining Pressure of 2131 psf from the Combined RCTS Tests

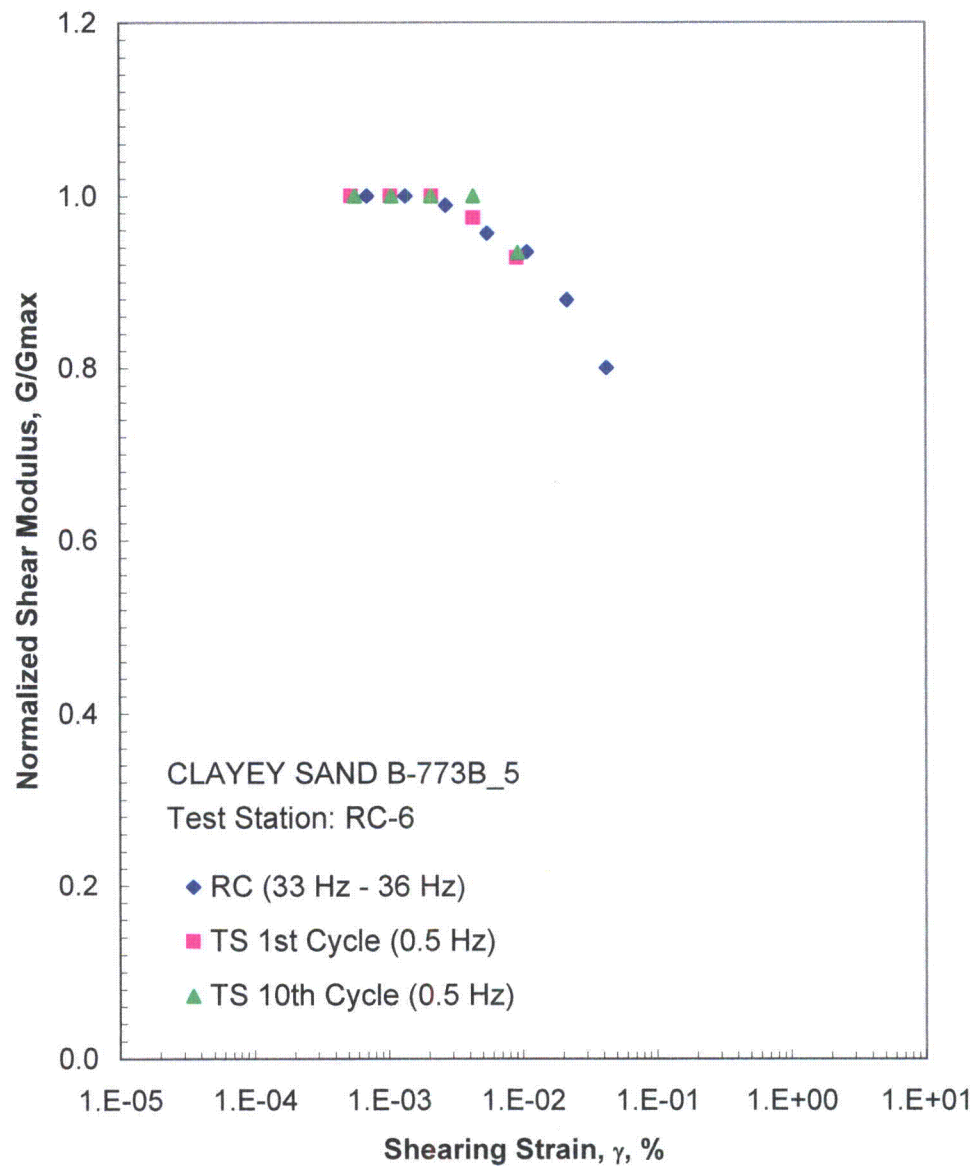


Figure D.12 Comparison of the Variation in Normalized Shear Modulus with Shearing Strain at an Isotropic Confining Pressure of 2131 psf from the Combined RCTS Tests

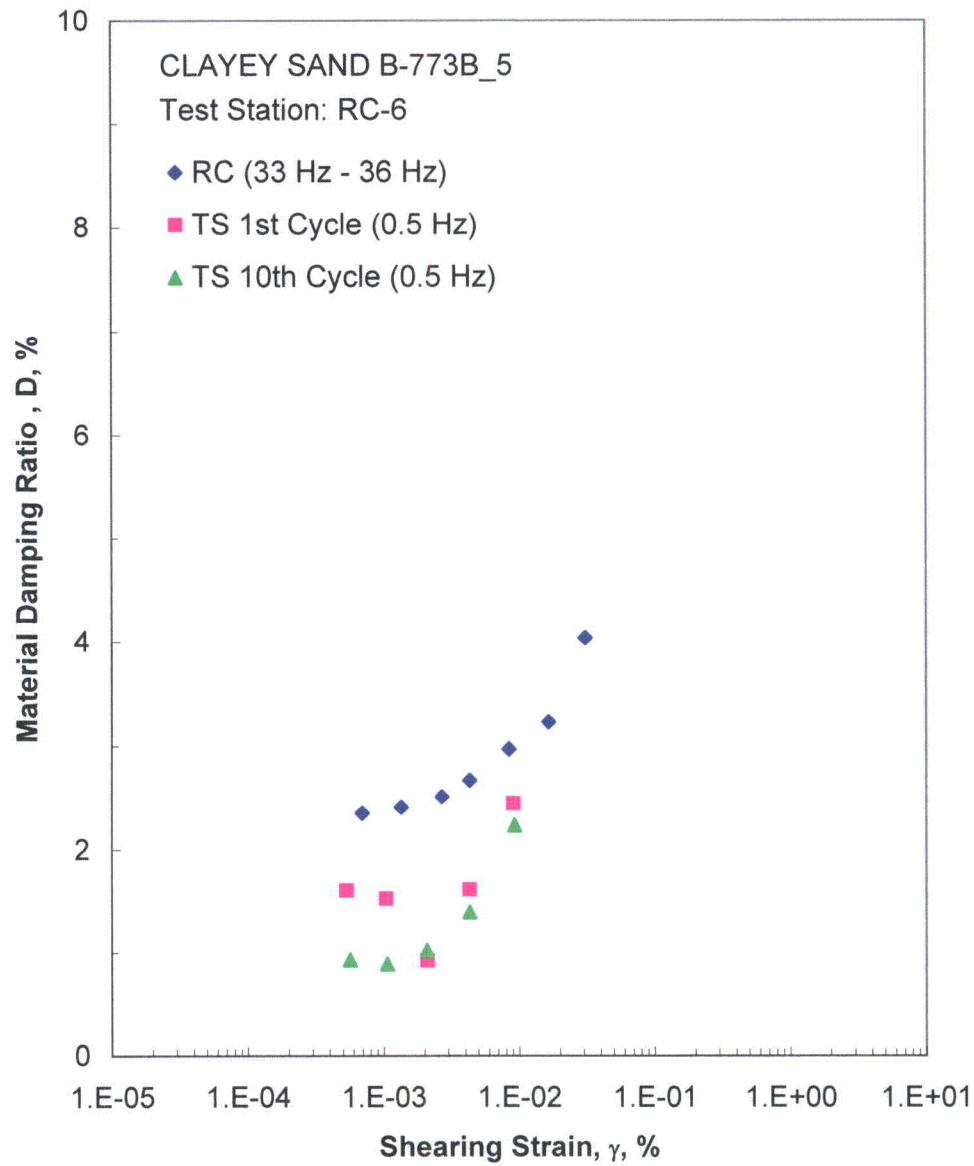


Figure D.13 Comparison of the Variation in Material Damping Ratio with Shearing Strain at an Isotropic Confining Pressure of 2131 psf from the Combined RCTS Tests

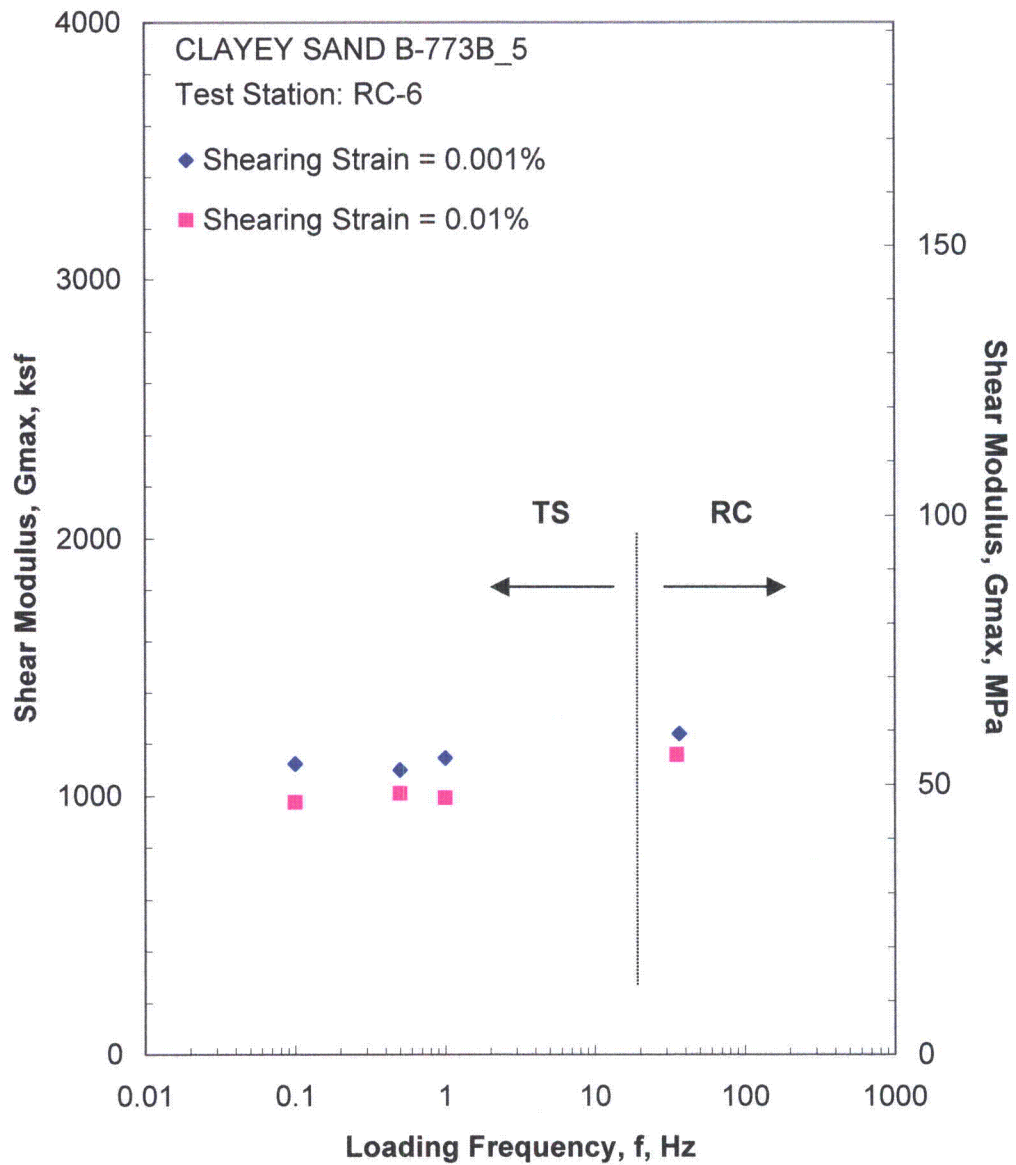


Figure D.14 Comparison of the Variation in Shear Modulus with Loading Frequency at an Isotropic Confining Pressure of 2131 psf from the Combined RCTS Tests

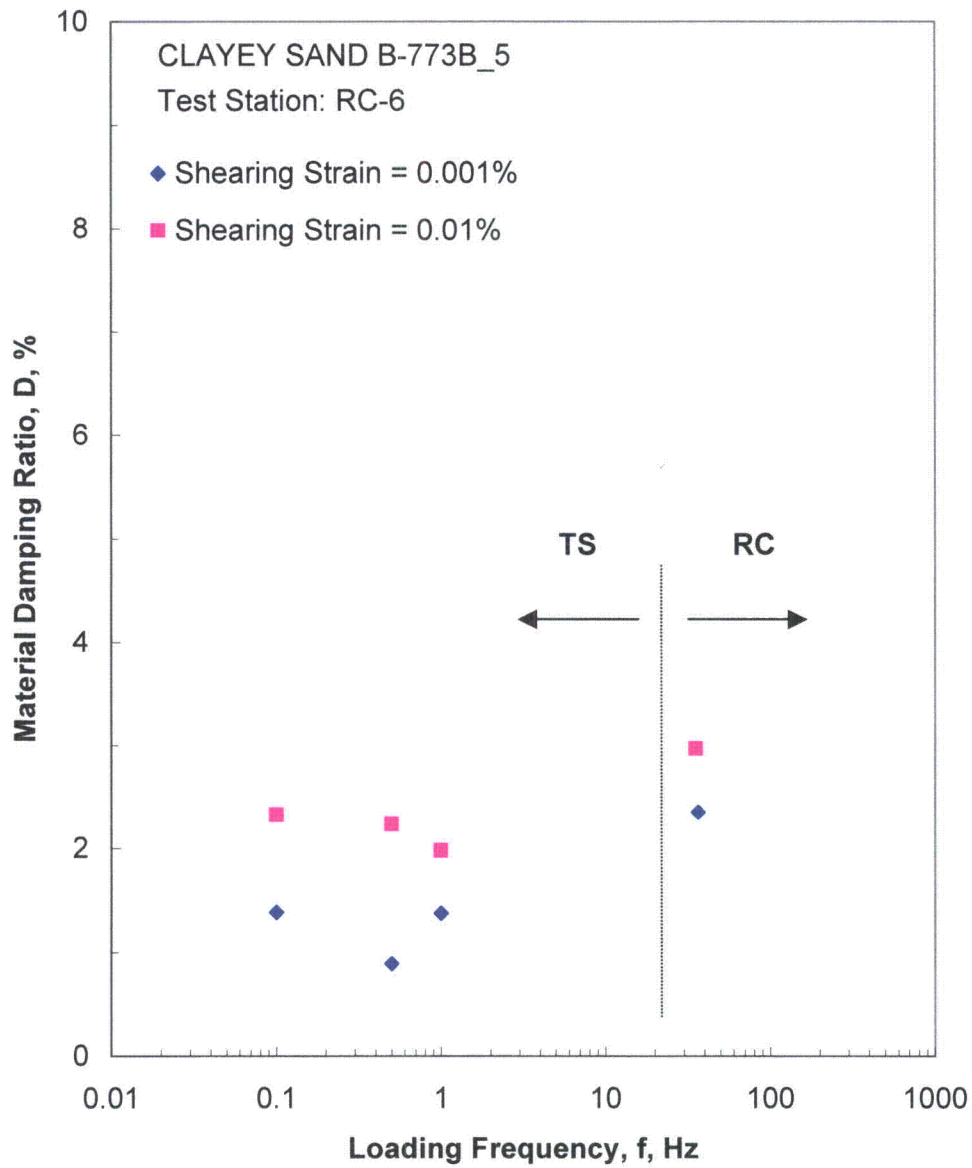


Figure D.15 Comparison of the Variation in Material Damping Ratio with Loading Frequency at an Isotropic Confining Pressure of 2131 psf from the Combined RCTS Tests

Table D.1 Variation in Low-Amplitude Shear Wave Velocity, Low-Amplitude Shear Modulus, Low-Amplitude Material Damping Ratio and Estimated Void Ratio with Isotropic Confining Pressure from RC Tests of Specimen B-773B-5

Isotropic Confining Pressure, σ_o			Low-Amplitude Shear Modulus, G_{max}		Low-Amplitude Shear Wave Velocity, V_s	Low-Amplitude Material Damping Ratio, D_{min}	Estimated Void Ratio, e
(psi)	(psf)	(kPa)	(ksf)	(MPa)	(fps)	(%)	
4	533	25	773	37	473	2.54	1.01
7	1066	51	969	46	529	2.42	1.01
15	2131	102	1223	59	594	2.34	1.00
30	4262	204	1726	83	704	2.20	0.99

Table D.2 Variation in Shear Modulus and Material Damping Ratio with Shearing Strain from RC Tests of Specimen B-773B-5; Isotropic Confining Pressure, $\sigma_o = 2131$ psf

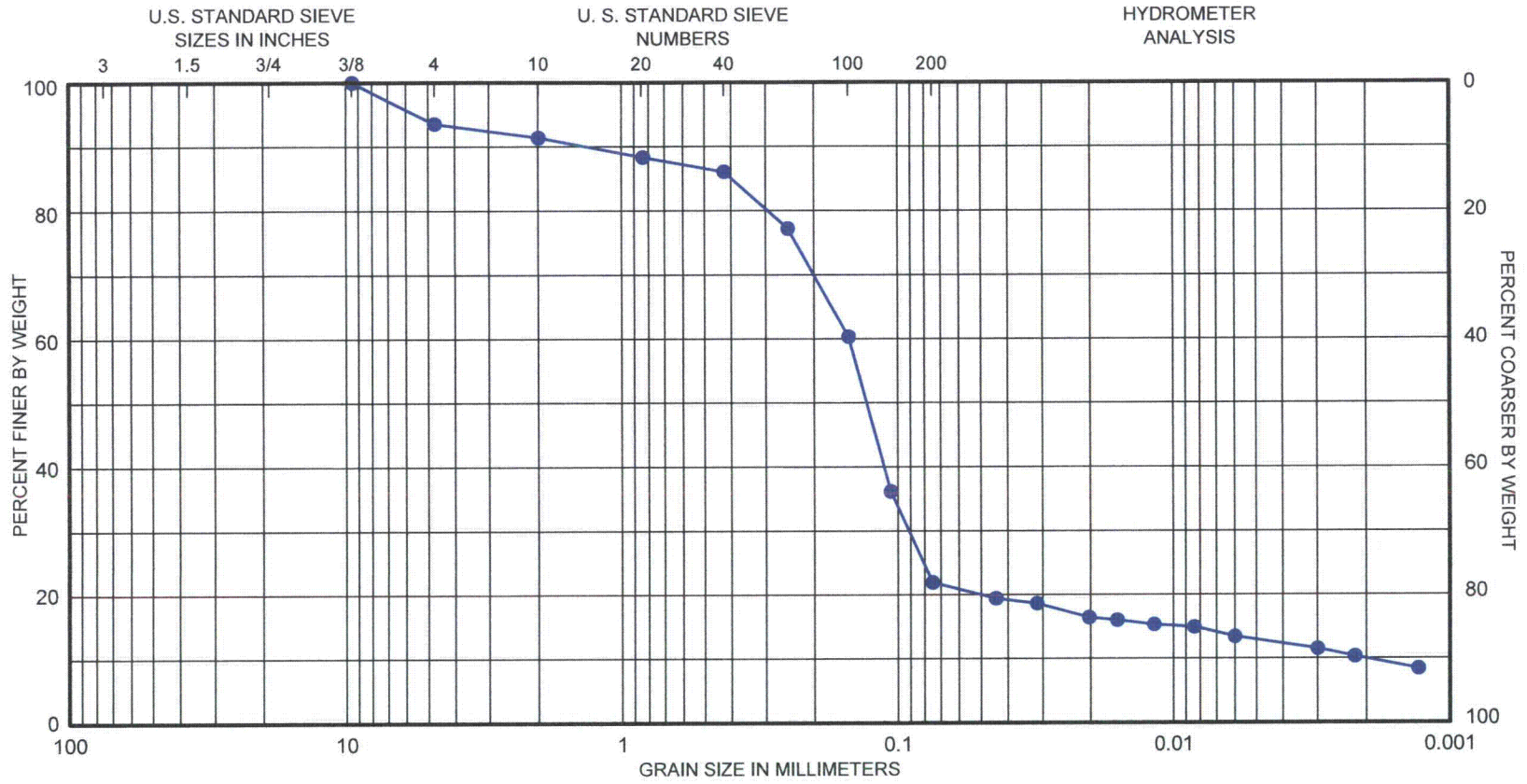
Peak Shearing Strain, %	Shear Modulus, G, ksf	Normalized Shear Modulus, G/G_{max}	Average ⁺ Shearing Strain, %	Material Damping Ratio ^x , D, %
6.95E-04	1238	1.00	6.95E-04	2.35
1.35E-03	1238	1.00	1.35E-03	2.41
2.69E-03	1225	0.99	2.69E-03	2.51
5.47E-03	1184	0.96	4.32E-03	2.67
1.08E-02	1157	0.93	8.43E-03	2.97
2.15E-02	1088	0.88	1.66E-02	3.23
4.22E-02	991	0.80	3.08E-02	4.04

⁺ Average Shearing Strain from the First Three Cycles of the Free Vibration Decay Curve

^x Average Damping Ratio from the First Three Cycles of the Free Vibration Decay Curve

Table D.3 Variation in Shear Modulus, Normalized Shear Modulus and Material Damping Ratio with Shearing Strain from TS Tests of Specimen B-773B-5; Isotropic Confining Pressure, $\sigma_0 = 2131$ psf

First Cycle				Tenth Cycle			
Peak Shearing Strain, %	Shear Modulus, G, ksf	Normalized Shear Modulus, G/G_{max}	Material Damping Ratio, D, %	Peak Shearing Strain, %	Shear Modulus, G, ksf	Normalized Shear Modulus, G/G_{max}	Material Damping Ratio, D, %
5.31E-04	1110	1.00	1.60	5.65E-04	1083	1.00	0.93
1.04E-03	1110	1.00	1.52	1.06E-03	1083	1.00	0.89
2.10E-03	1110	1.00	0.92	2.09E-03	1083	1.00	1.02
4.31E-03	1082	0.97	1.61	4.31E-03	1083	1.00	1.39
9.06E-03	1030	0.93	2.44	9.23E-03	1011	0.93	2.23



GRAVEL		SAND			SILT or CLAY		
Coarse	Fine	Coarse	Medium	Fine			
<u>SYMBOL</u>	<u>BORING</u>	<u>DEPTH, FT</u>	<u>C_c</u>	<u>C_u</u>	<u>D₅₀</u>	<u>D₉₀</u>	<u>CLASSIFICATION</u>
●	B-773B-5	47	27.57	73.77	0.13	1.35	Clayey Sand (SC), olive gray, with shell fragments

GRAIN SIZE CURVE

APPENDIX E

Specimen B-773B_6

Borehole B-773B

Sample 6

Depth = 57.0 ft (17.4 m)

Total Unit Weight = 106.4 lb/ft³

Water Content = 44.5 %

FUGRO JOB #: 0411-09-1734

Testing Station: RC6



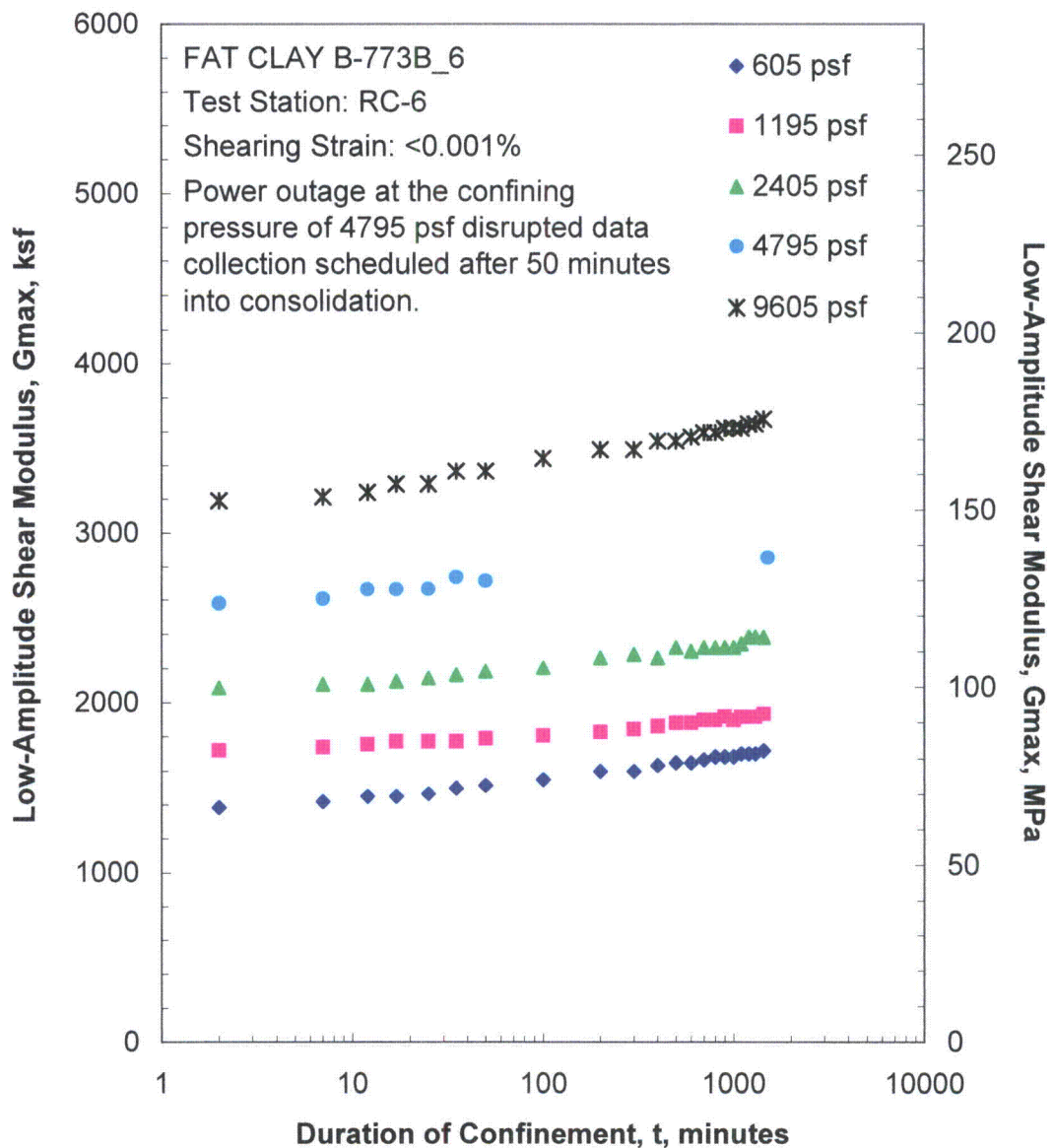


Figure E.1 Variation in Low-Amplitude Shear Modulus with Magnitude and Duration of Isotropic Confining Pressure from Resonant Column Tests

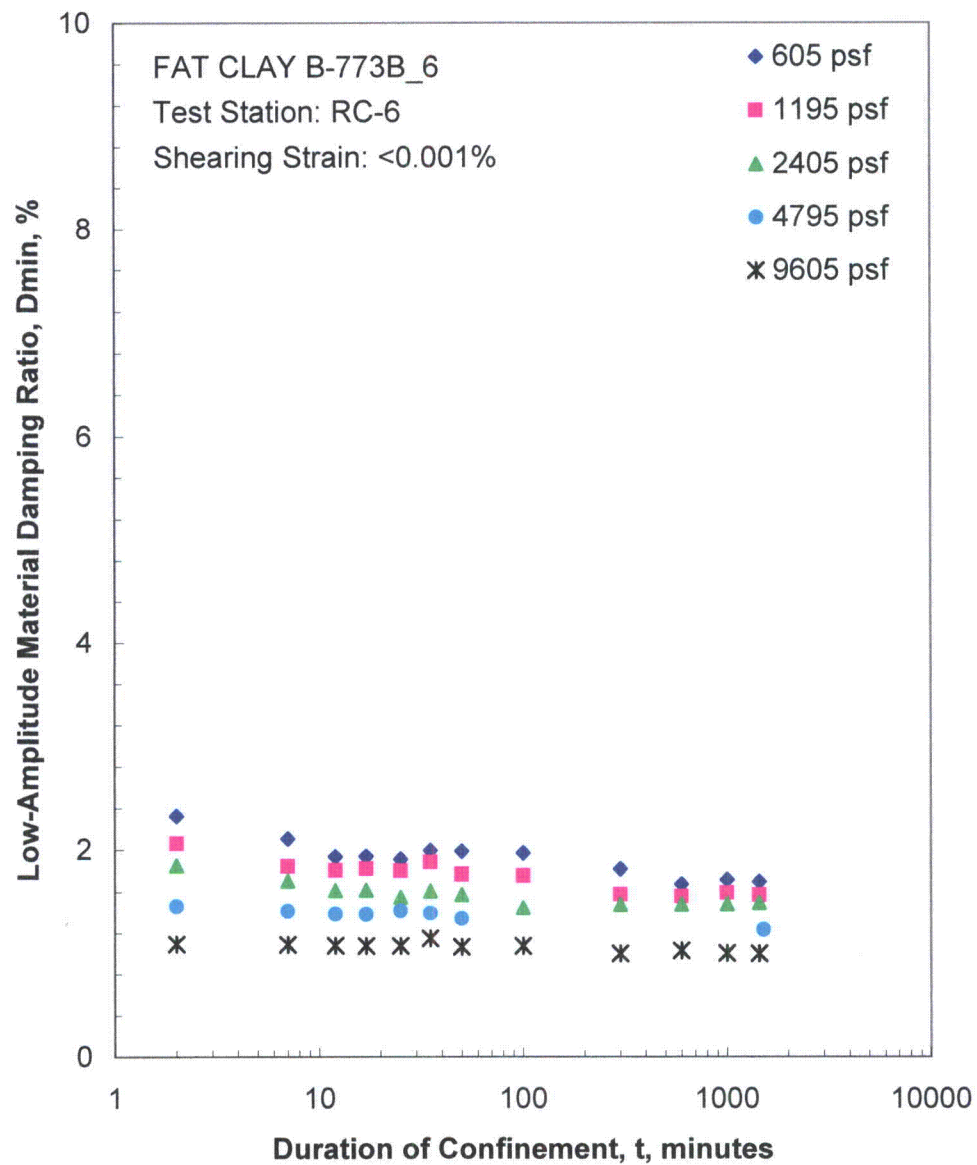


Figure E.2 Variation in Low-Amplitude Material Damping Ratio with Magnitude and Duration of Isotropic Confining Pressure from Resonant Column Tests

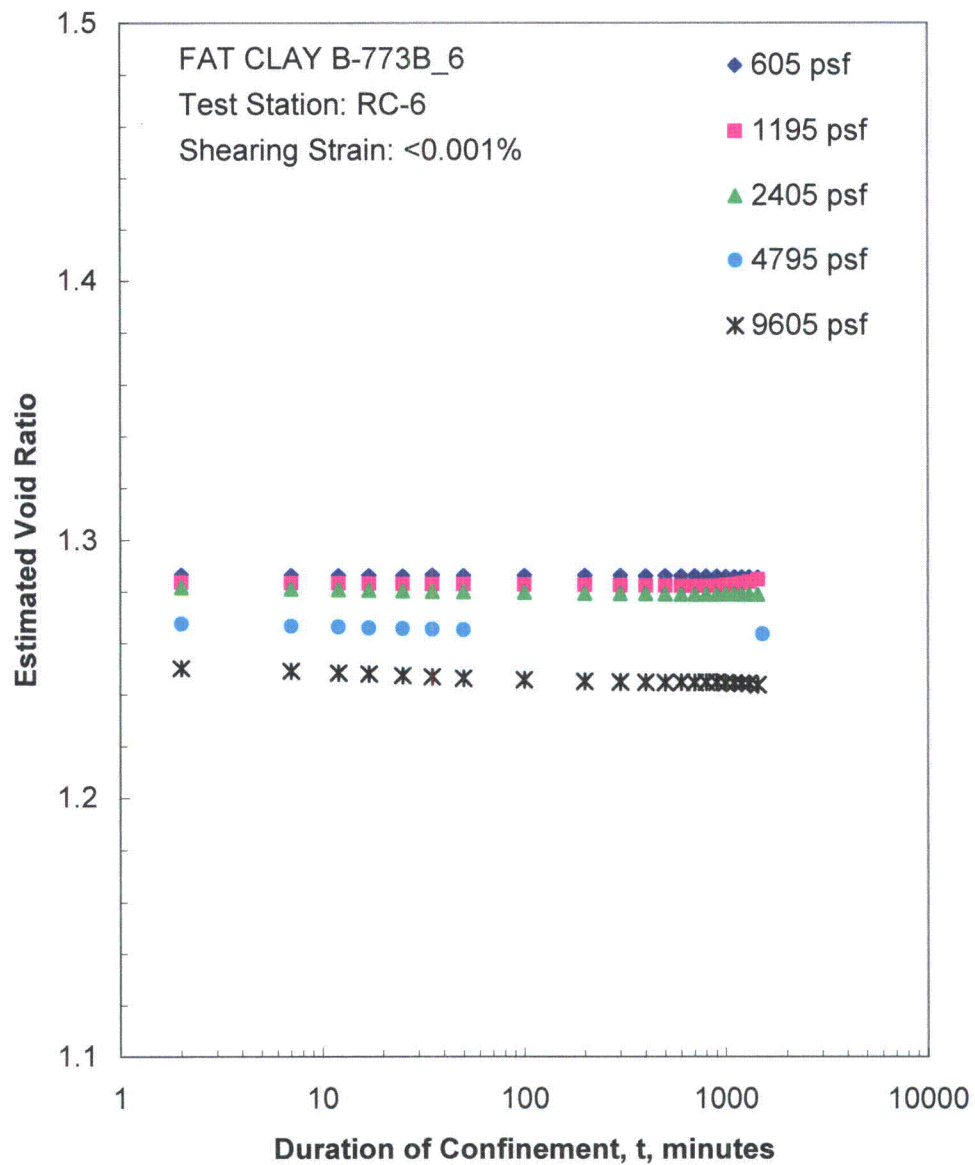


Figure E.3 Variation in Estimated Void Ratio with Magnitude and Duration of Isotropic Confining Pressure from Resonant Column Tests

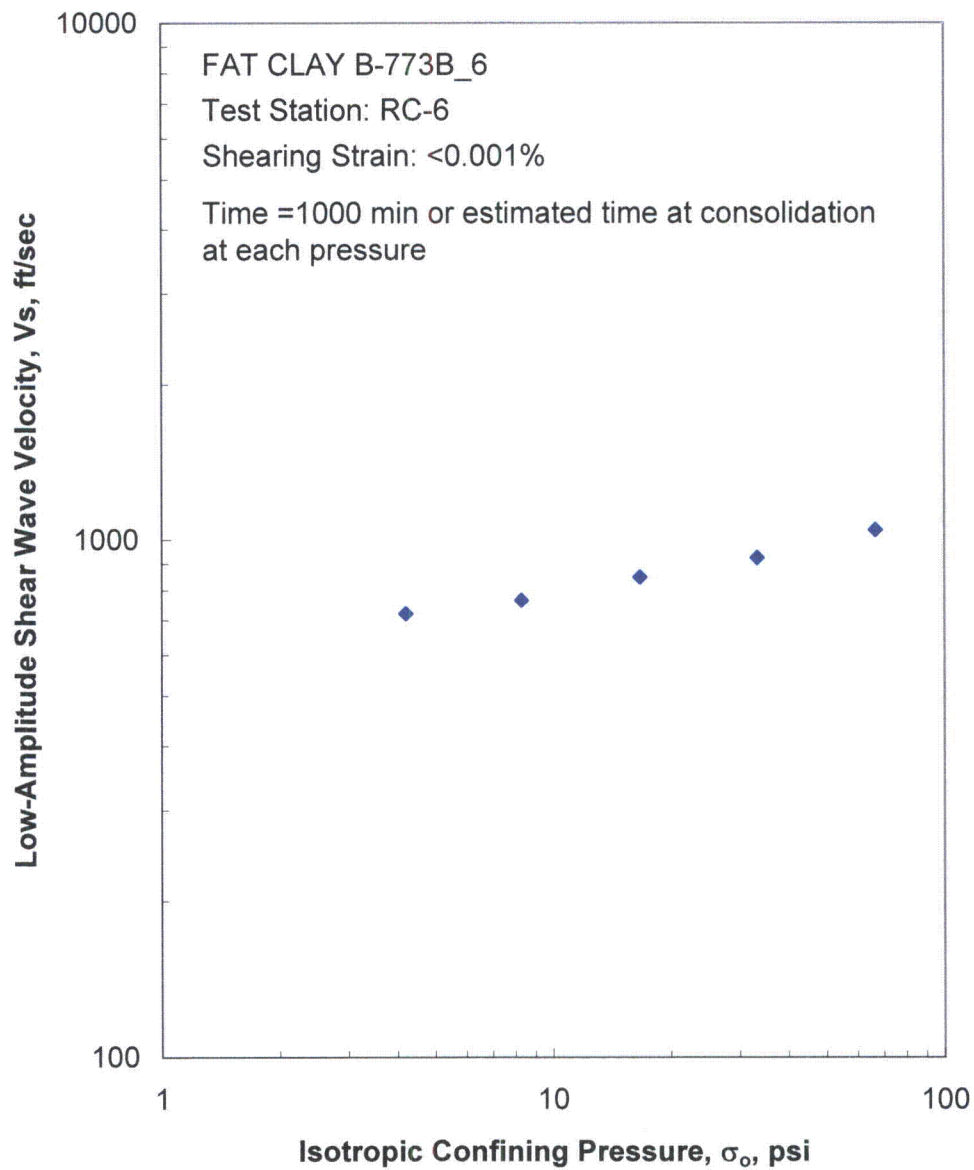


Figure E.4 Variation in Low-Amplitude Shear Wave Velocity with Isotropic Confining Pressure from Resonant Column Tests

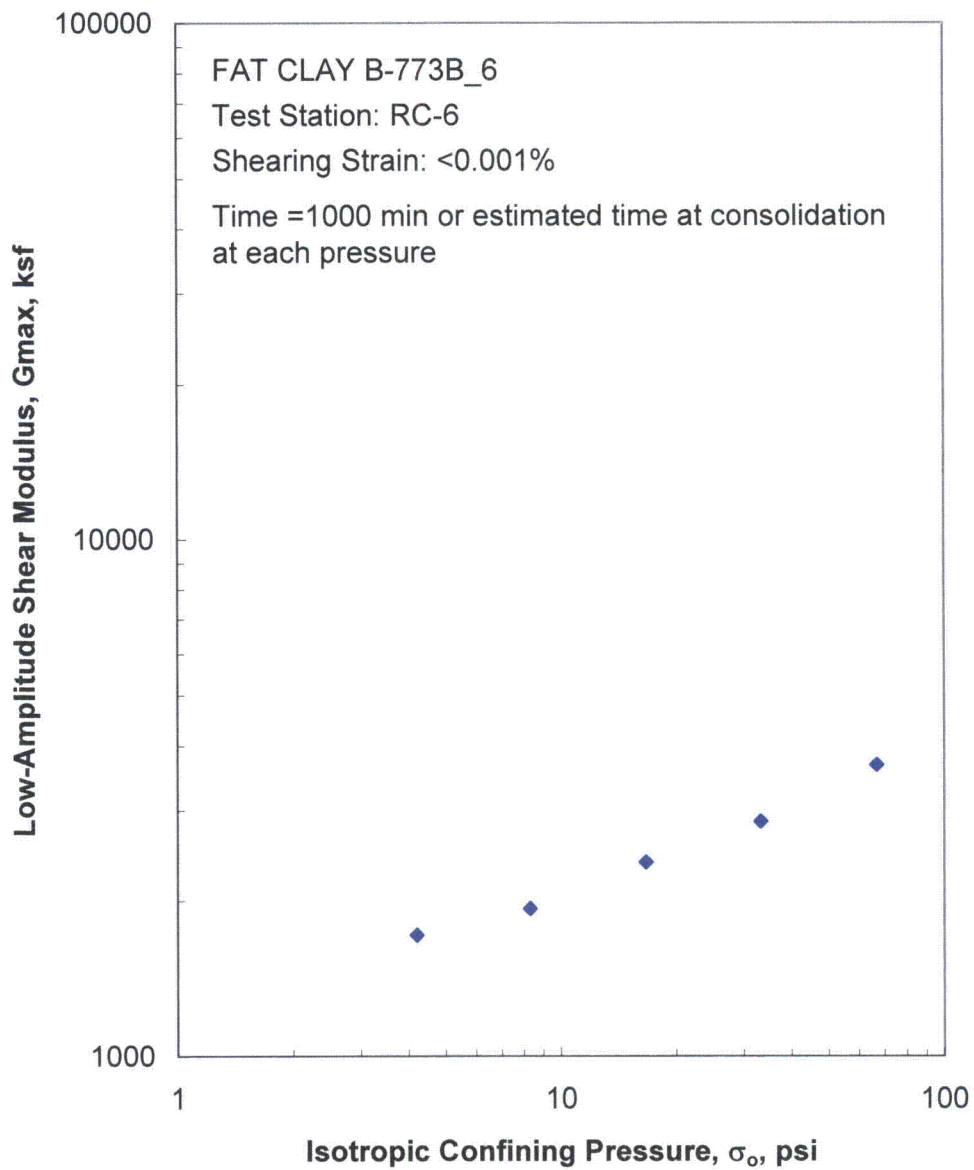


Figure E.5 Variation in Low-Amplitude Shear Modulus with Isotropic Confining Pressure from Resonant Column Tests

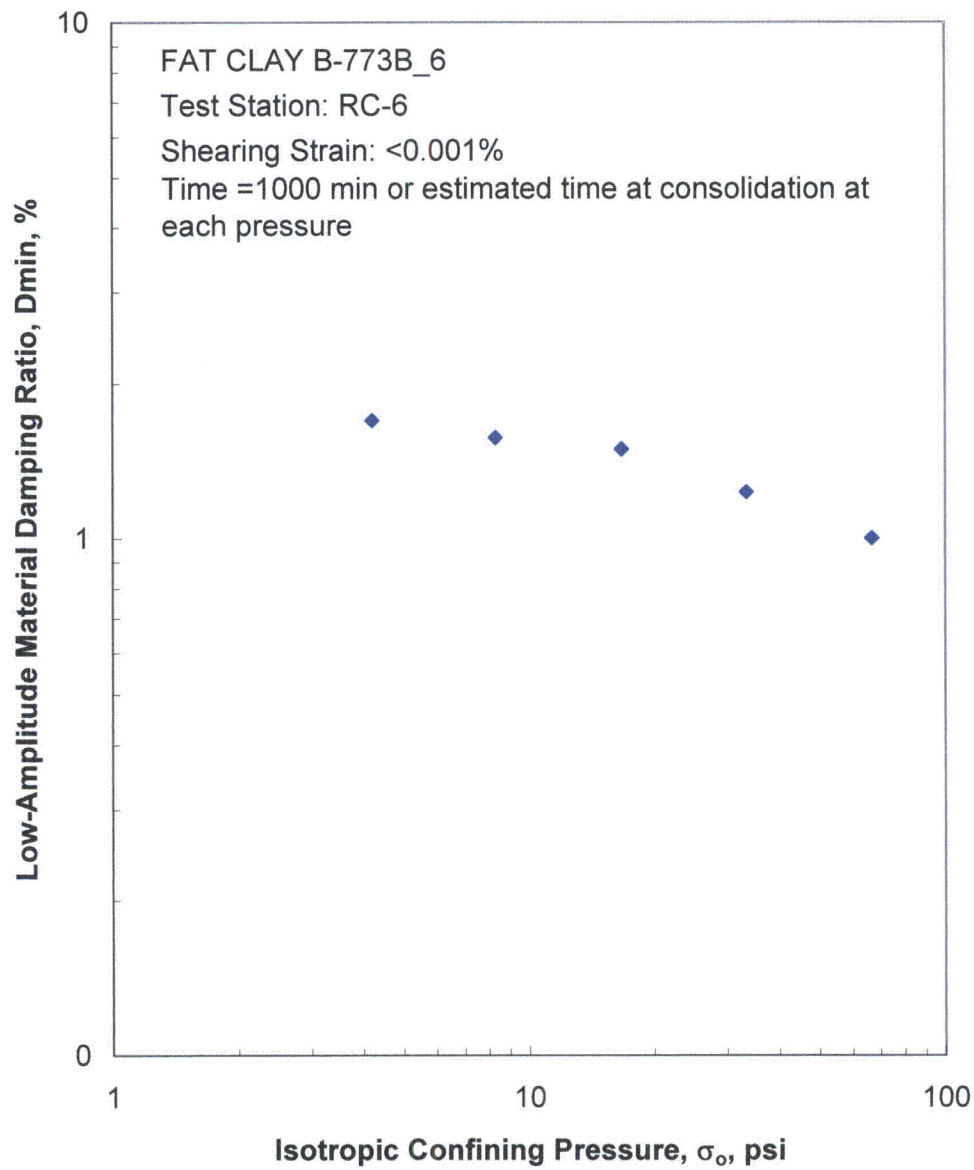


Figure E.6 Variation in Low-Amplitude Material Damping Ratio with Isotropic Confining Pressure from Resonant Column Tests

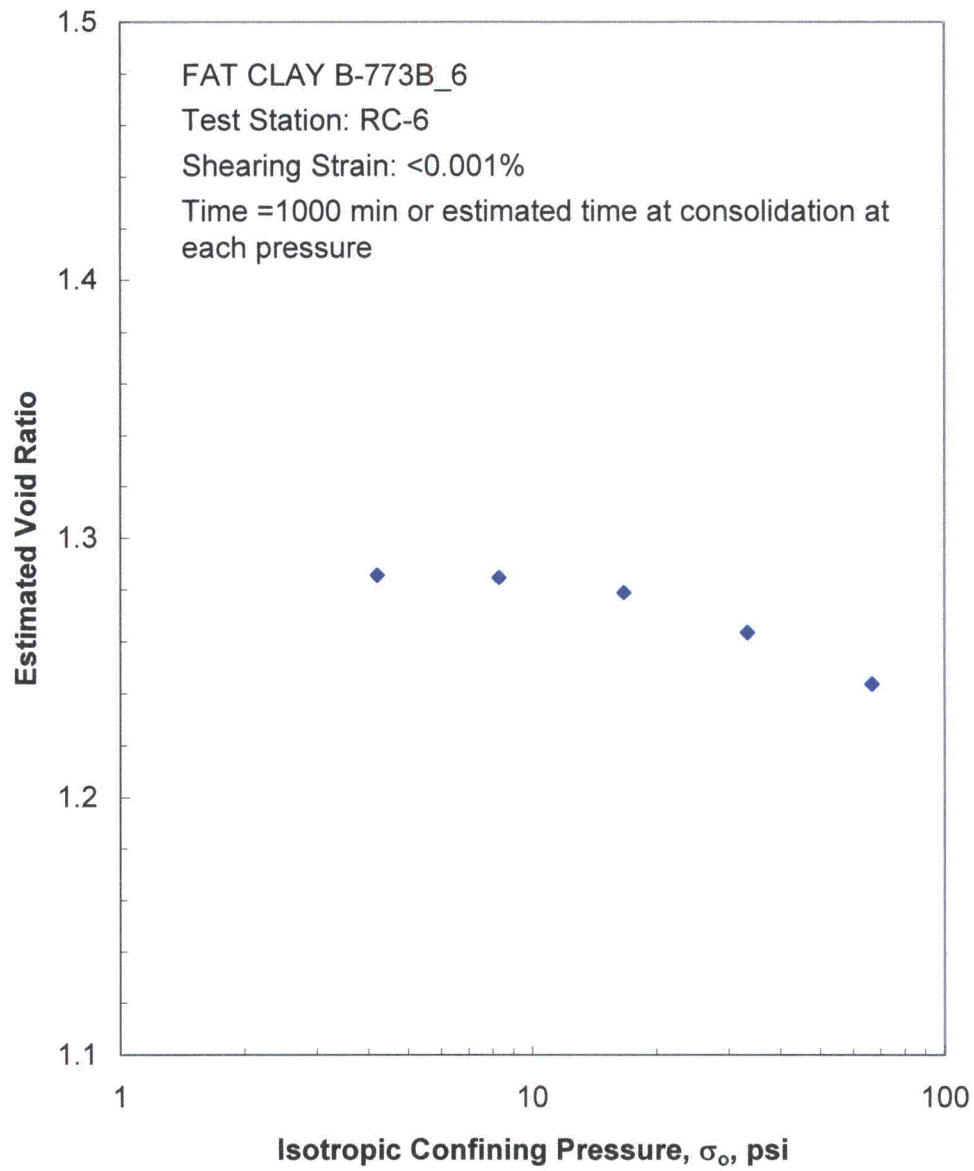


Figure E.7 Variation in Estimated Void Ratio with Isotropic Confining Pressure from Resonant Column Tests

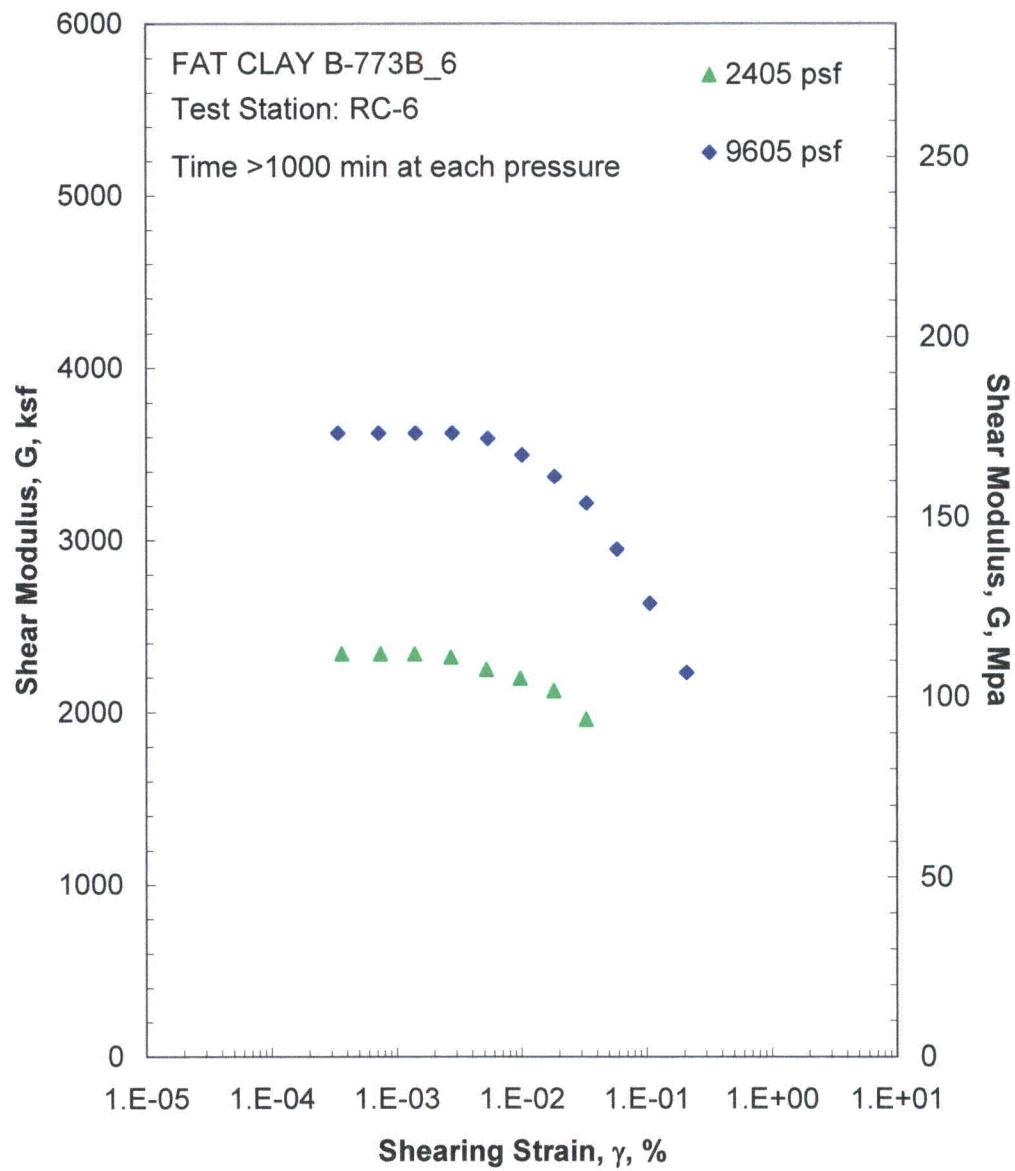


Figure E.8 Comparison of the Variation in Shear Modulus with Shearing Strain and Isotropic Confining Pressure from the Resonant Column Tests

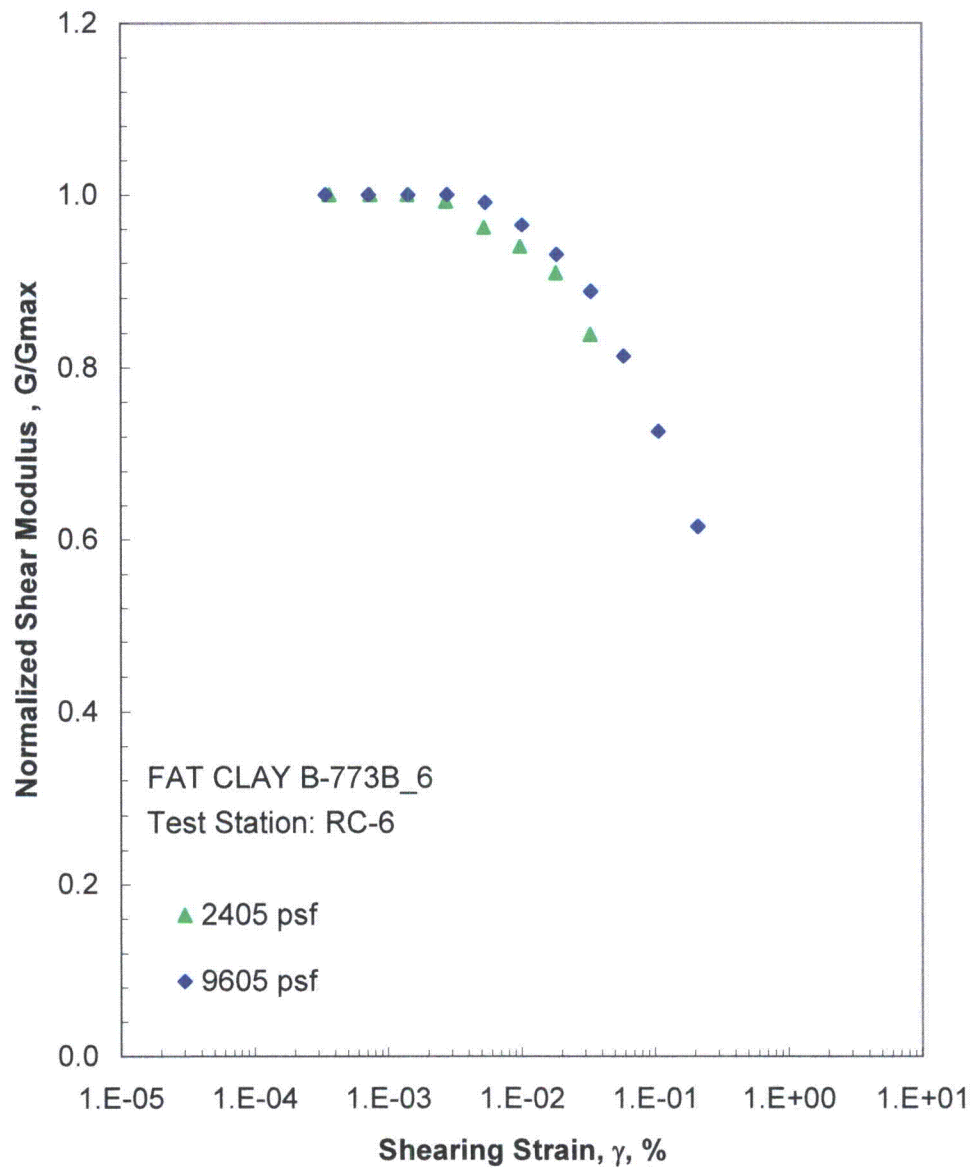


Figure E.9 Comparison of the Variation in Normalized Shear Modulus with Shearing Strain and Isotropic Confining Pressure from the Resonant Column Tests

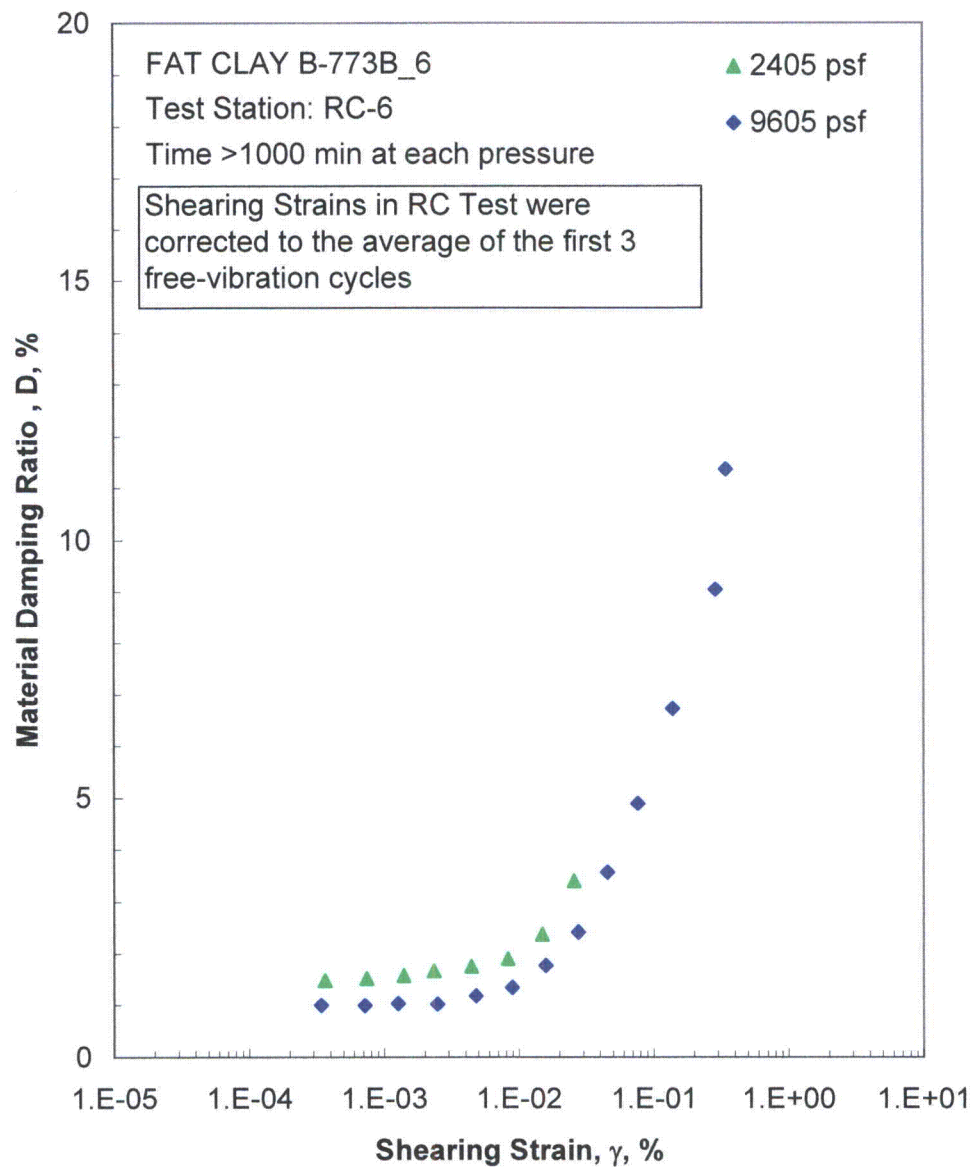


Figure E.10 Comparison of the Variation in Material Damping Ratio with Shearing Strain and Isotropic Confining Pressure from the Resonant Column Tests

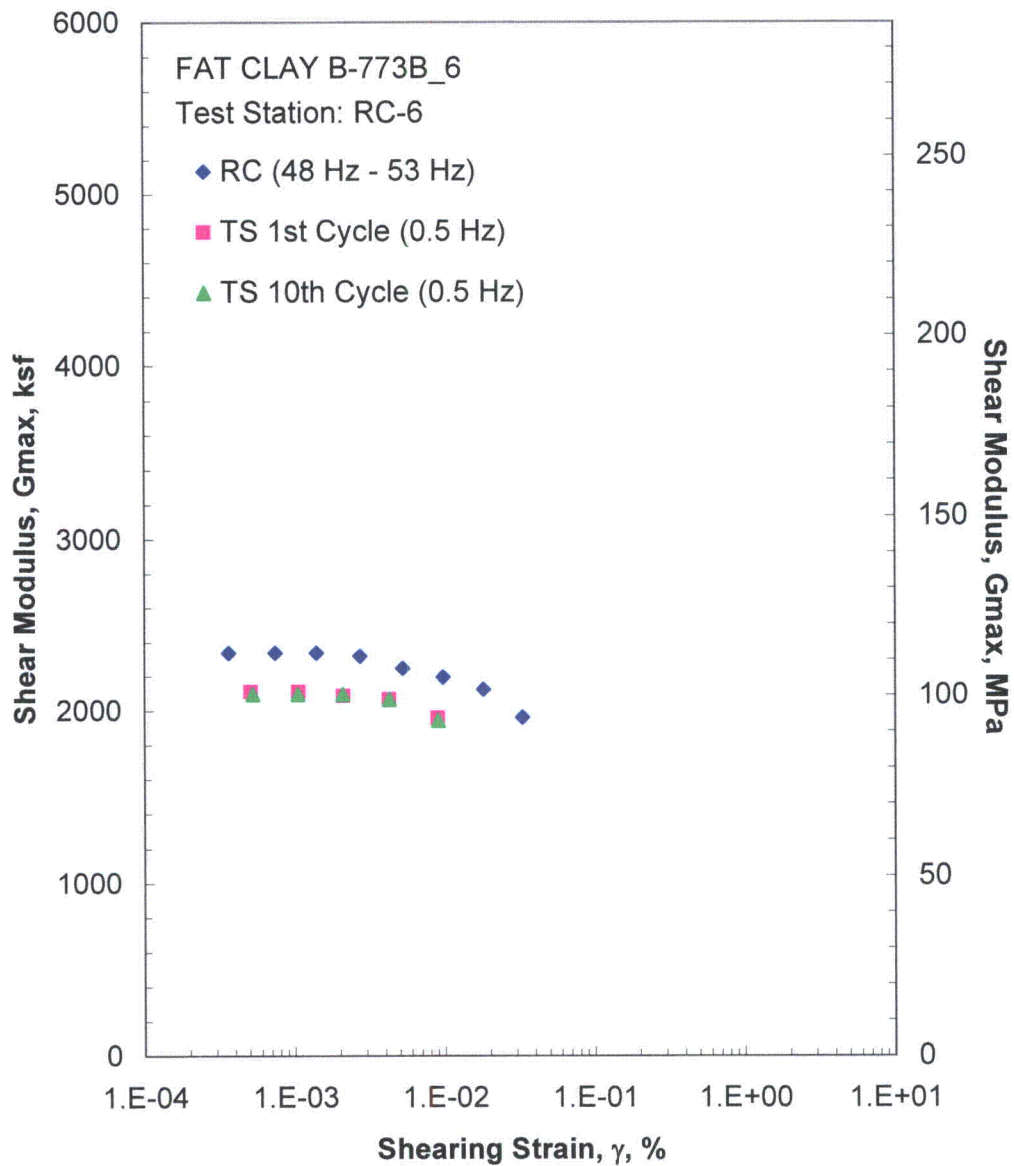


Figure E.11 Comparison of the Variation in Shear Modulus with Shearing Strain at an Isotropic Confining Pressure of 2405 psf from the Combined RCTS Tests

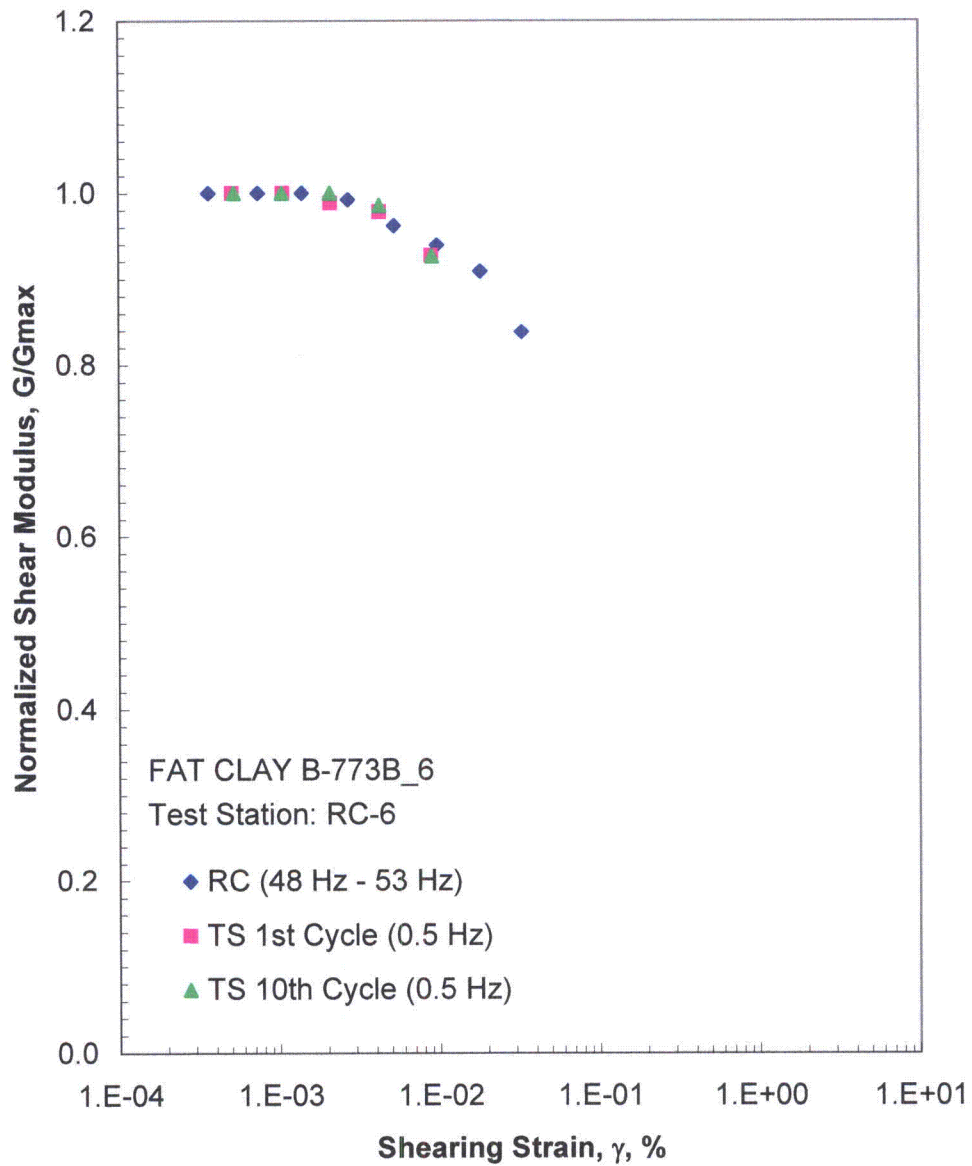


Figure E.12 Comparison of the Variation in Normalized Shear Modulus with Shearing Strain at an Isotropic Confining Pressure of 2405 psf from the Combined RCTS Tests

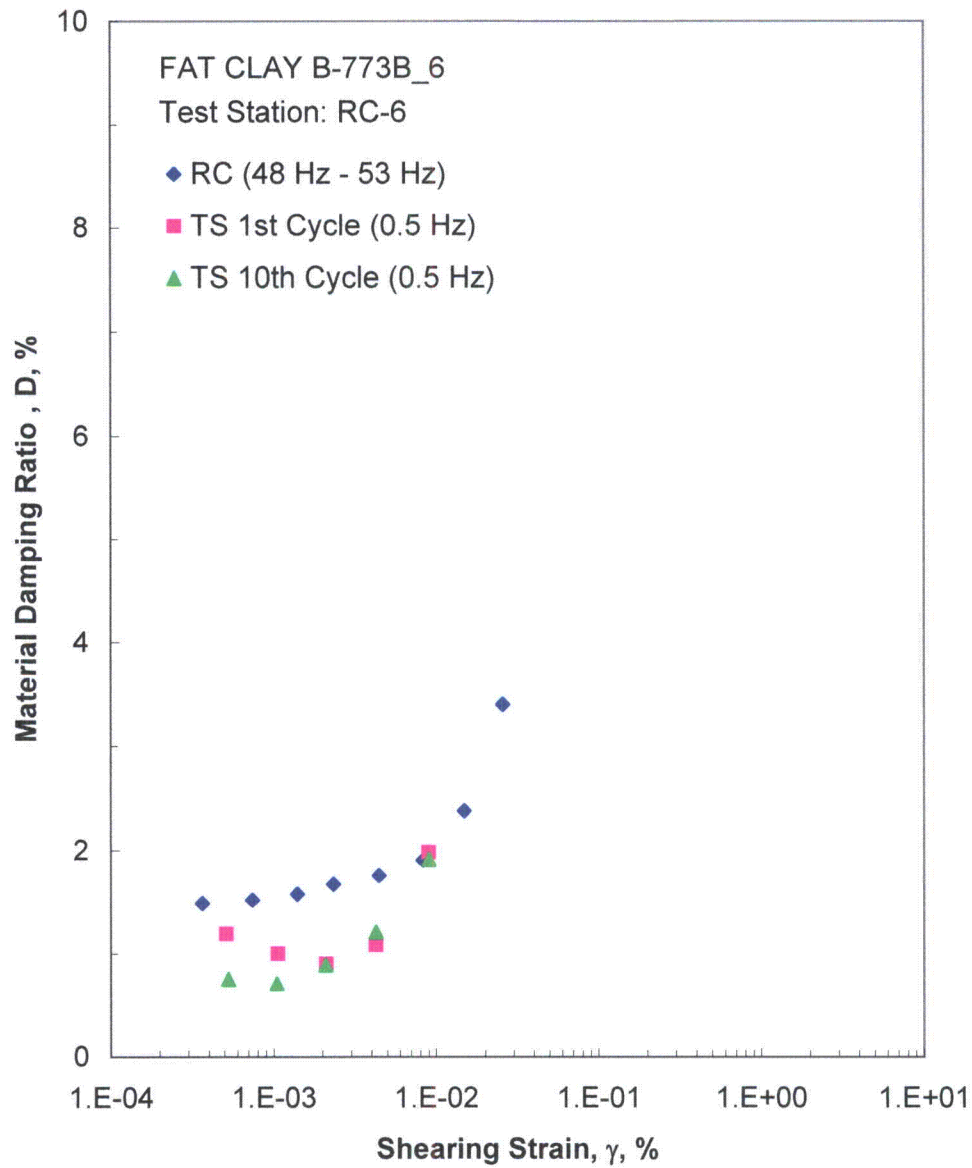


Figure E.13 Comparison of the Variation in Material Damping Ratio with Shearing Strain at an Isotropic Confining Pressure of 2405 psf from the Combined RCTS Tests

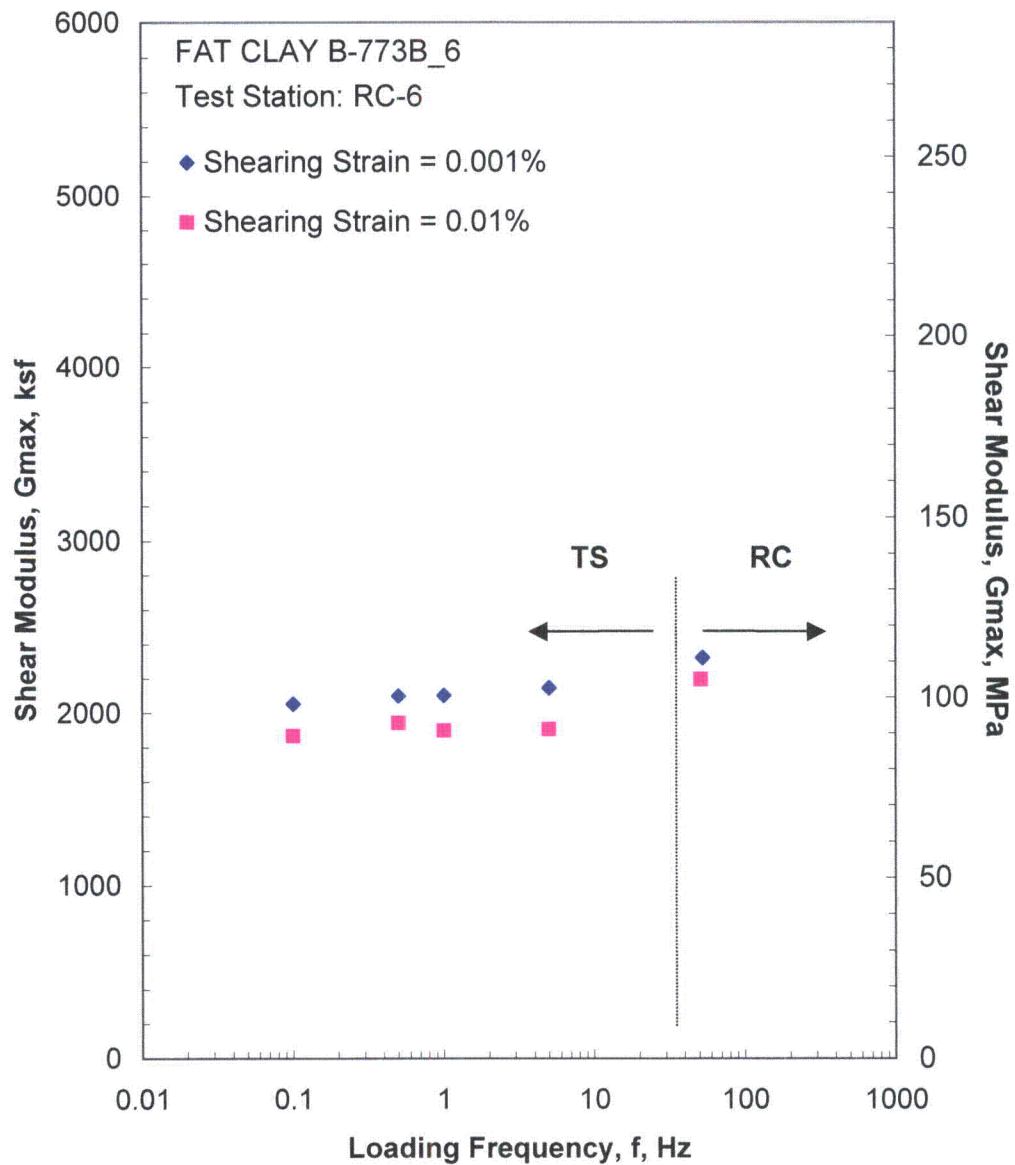


Figure E.14 Comparison of the Variation in Shear Modulus with Loading Frequency at an Isotropic Confining Pressure of 2405 psf from the Combined RCTS Tests

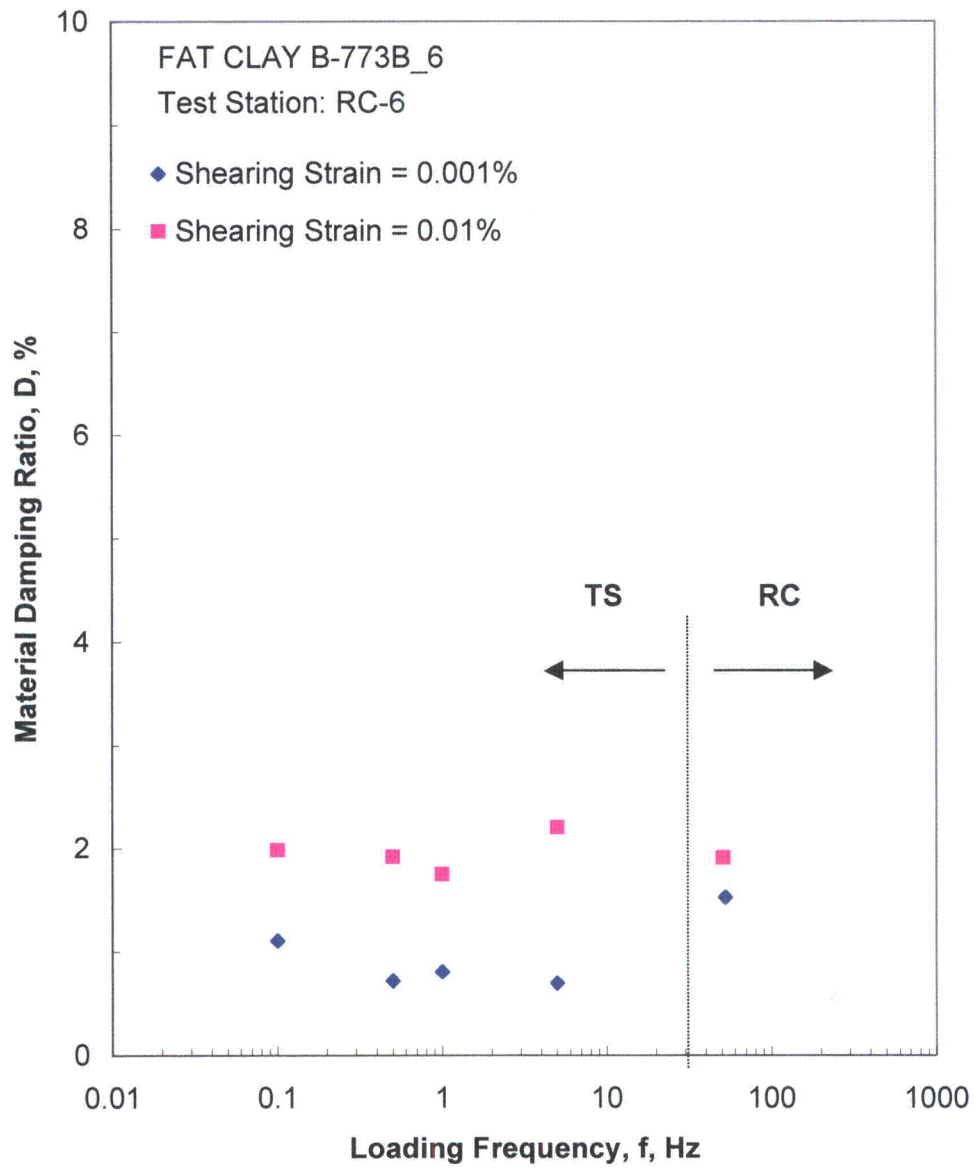


Figure E.15 Comparison of the Variation in Material Damping Ratio with Loading Frequency at an Isotropic Confining Pressure of 2405 psf from the Combined RCTS Tests

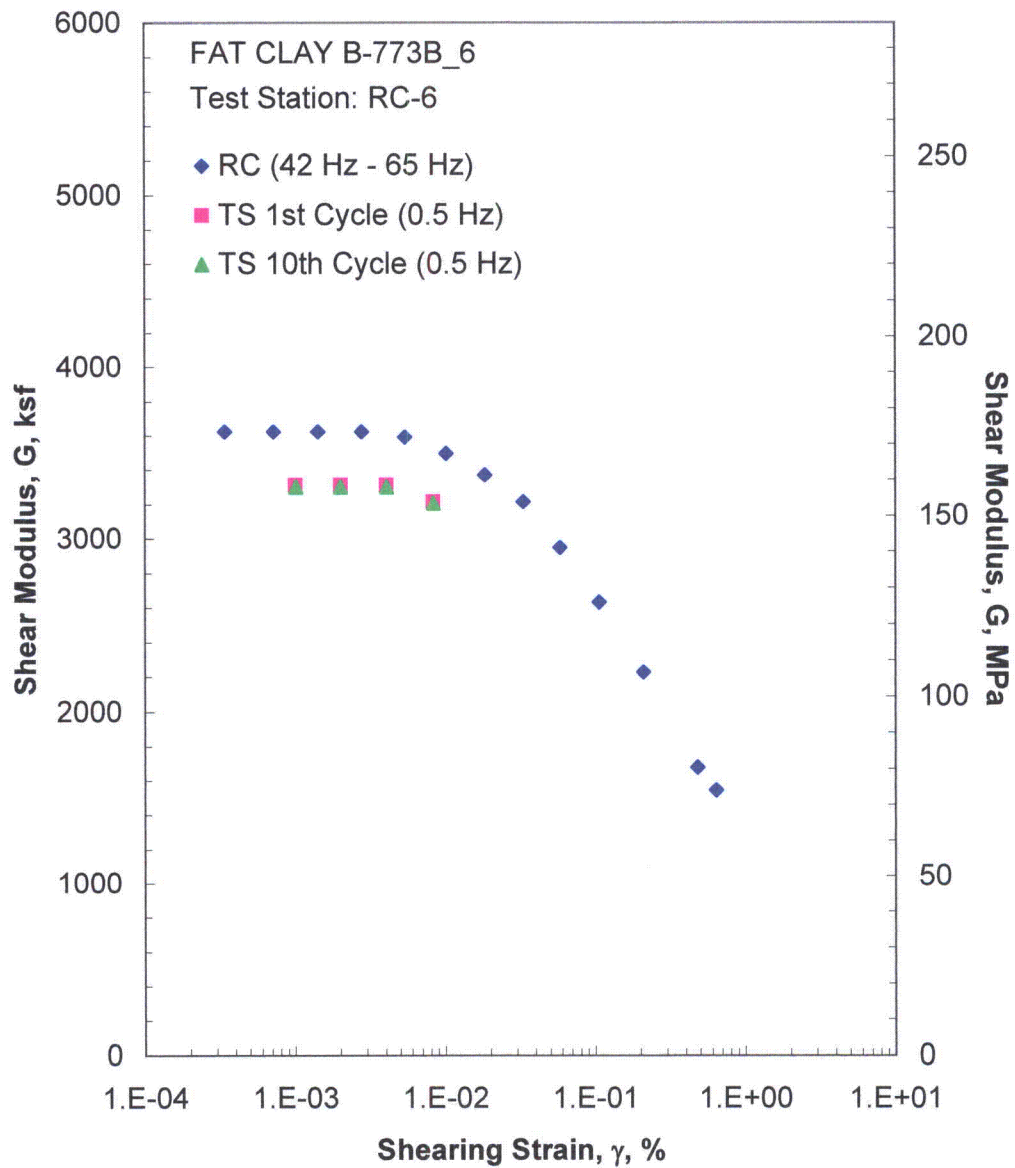


Figure E.16 Comparison of the Variation in Shear Modulus with Shearing Strain at an Isotropic Confining Pressure of 9605 psf from the Combined RCTS Tests

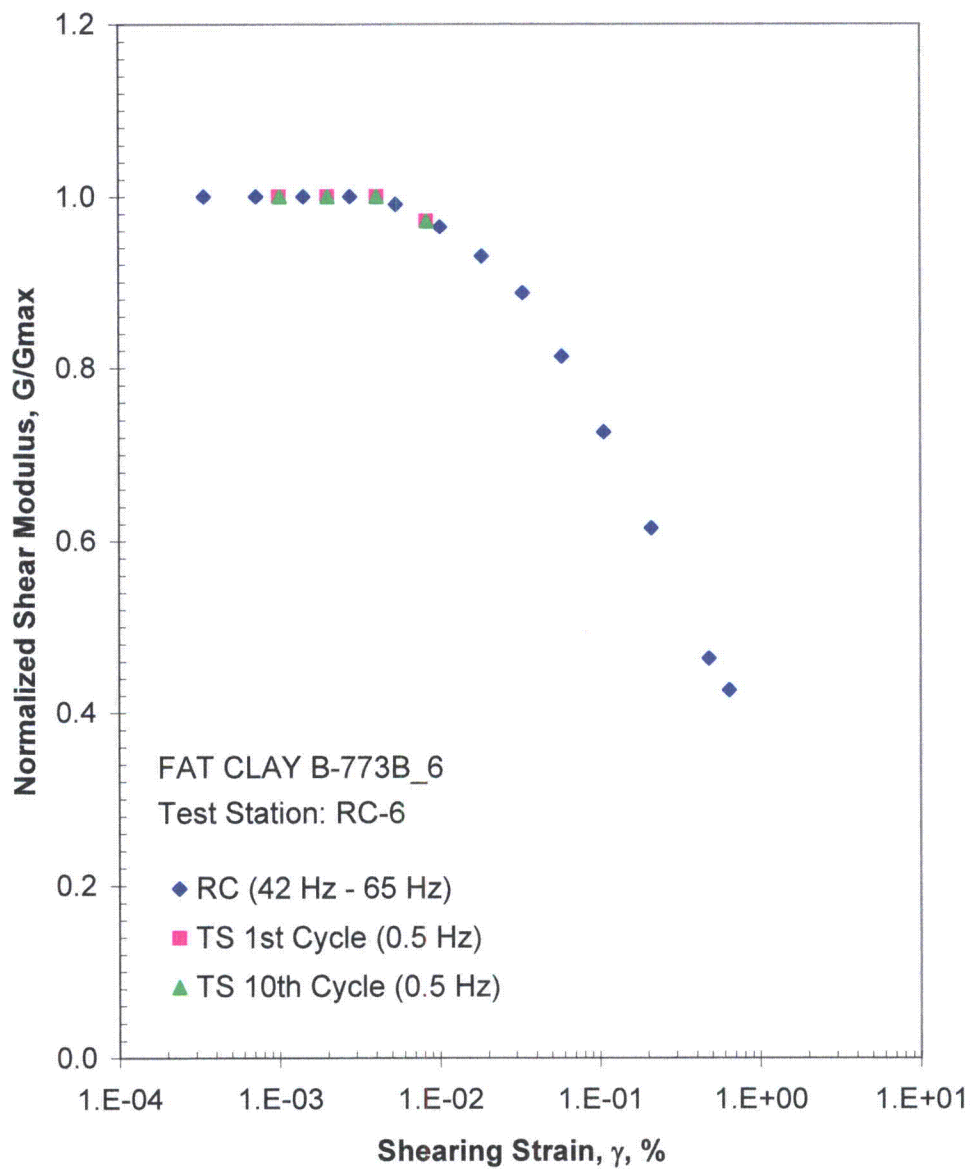


Figure E.17 Comparison of the Variation in Normalized Shear Modulus with Shearing Strain at an Isotropic Confining Pressure of 9605 psi from the Combined RCTS Tests

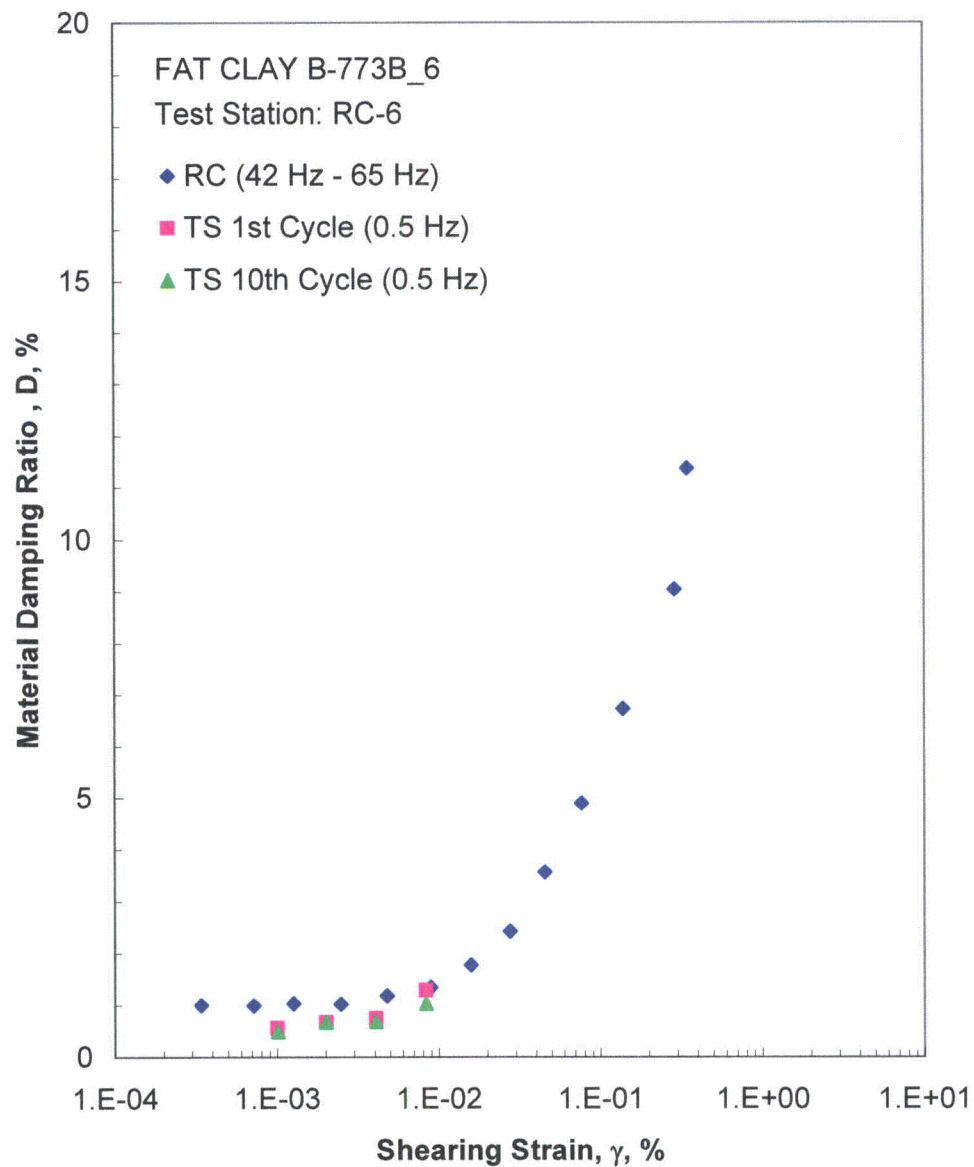


Figure E.18 Comparison of the Variation in Material Damping Ratio with Shearing Strain at an Isotropic Confining Pressure of 9605 psf from the Combined RCTS Tests

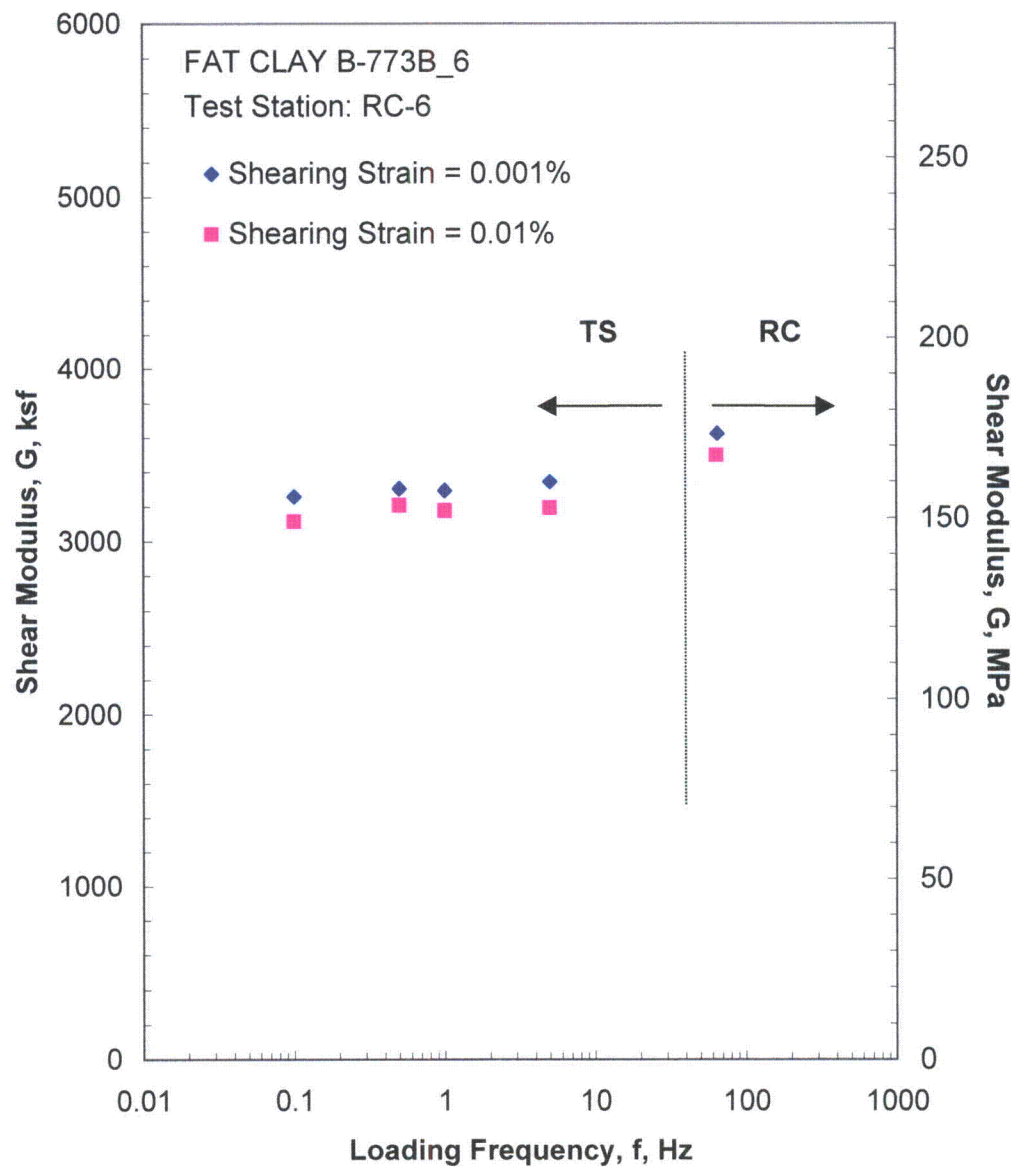


Figure E.19 Comparison of the Variation in Shear Modulus with Loading Frequency at an Isotropic Confining Pressure of 9605 psf from the Combined RCTS Tests

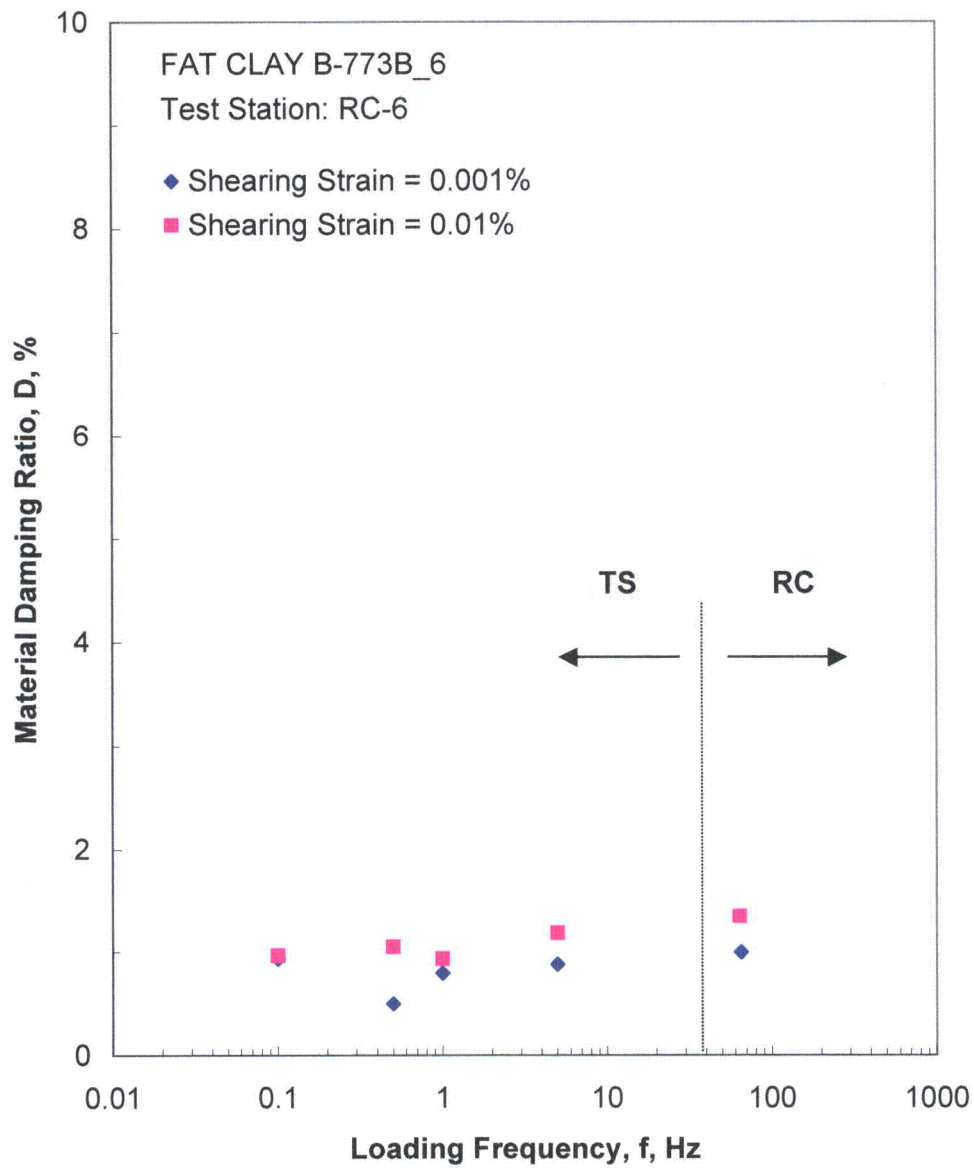


Figure E.20 Comparison of the Variation in Material Damping Ratio with Loading Frequency at an Isotropic Confining Pressure of 9605 psf from the Combined RCTS Tests

Table E.1 Variation in Low-Amplitude Shear Wave Velocity, Low-Amplitude Shear Modulus, Low-Amplitude Material Damping Ratio and Estimated Void Ratio with Isotropic Confining Pressure from RC Tests of Specimen B-773B-6

Isotropic Confining Pressure, σ_o			Low-Amplitude Shear Modulus, G_{max}		Low-Amplitude Shear Wave Velocity, V_s	Low-Amplitude Material Damping Ratio, D_{min}	Estimated Void Ratio, e
(psi)	(psf)	(kPa)	(ksf)	(MPa)	(fps)	(%)	
4	605	29	1718	82	720	1.70	1.29
8	1195	57	1933	93	764	1.57	1.28
17	2405	115	2383	114	847	1.49	1.28
33	4795	229	2854	137	924	1.23	1.26
67	9605	460	3675	176	1044	1.00	1.24

Table E.2 Variation in Shear Modulus and Material Damping Ratio with Shearing Strain from RC Tests of Specimen B-773B-6; Isotropic Confining Pressure, $\sigma_o = 2405$ psf

Peak Shearing Strain, %	Shear Modulus, G, ksf	Normalized Shear Modulus, G/G_{max}	Average ⁺ Shearing Strain, %	Material Damping Ratio ^x , D, %
3.64E-04	2338	1.00	3.64E-04	1.49
7.40E-04	2338	1.00	7.40E-04	1.52
1.40E-03	2338	1.00	1.40E-03	1.58
2.72E-03	2320	0.99	2.34E-03	1.67
5.23E-03	2248	0.96	4.45E-03	1.76
9.75E-03	2196	0.94	8.28E-03	1.91
1.81E-02	2124	0.91	1.49E-02	2.38
3.29E-02	1960	0.84	2.56E-02	3.40

⁺ Average Shearing Strain from the First Three Cycles of the Free Vibration Decay Curve

^x Average Damping Ratio from the First Three Cycles of the Free Vibration Decay Curve

Table E.3 Variation in Shear Modulus, Normalized Shear Modulus and Material Damping Ratio with Shearing Strain from TS Tests of Specimen B-773B-6; Isotropic Confining Pressure, $\sigma_o = 2405$ psf

First Cycle				Tenth Cycle			
Peak Shearing Strain, %	Shear Modulus, G, ksf	Normalized Shear Modulus, G/G_{max}	Material Damping Ratio, D, %	Peak Shearing Strain, %	Shear Modulus, G, ksf	Normalized Shear Modulus, G/G_{max}	Material Damping Ratio, D, %
5.10E-04	2111	1.00	1.19	5.25E-04	2096	1.00	0.75
1.06E-03	2111	1.00	1.00	1.05E-03	2096	1.00	0.71
2.10E-03	2087	0.99	0.90	2.09E-03	2096	1.00	0.89
4.25E-03	2065	0.98	1.08	4.25E-03	2066	0.99	1.21
8.97E-03	1957	0.93	1.98	9.04E-03	1942	0.93	1.91

Table E.4 Variation in Shear Modulus and Material Damping Ratio with Shearing Strain from RC Tests of Specimen B-773B-6; Isotropic Confining Pressure, $\sigma_0 = 9605$ psf

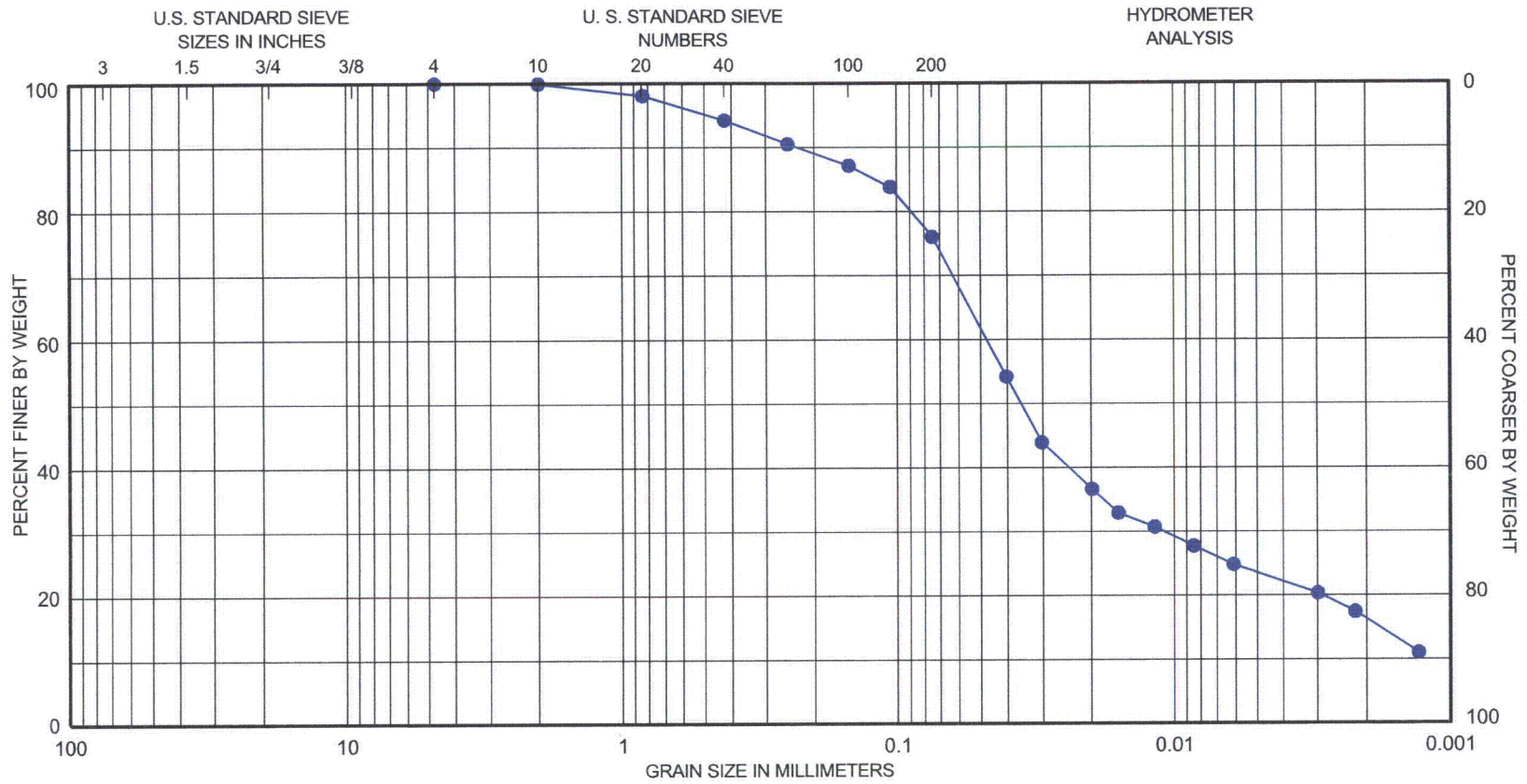
Peak Shearing Strain, %	Shear Modulus, G, ksf	Normalized Shear Modulus, G/G_{max}	Average ⁺ Shearing Strain, %	Material Damping Ratio ^x , D, %
3.41E-04	3624	1.00	3.41E-04	1.00
7.19E-04	3624	1.00	7.19E-04	1.00
1.42E-03	3624	1.00	1.26E-03	1.04
2.78E-03	3624	1.00	2.48E-03	1.03
5.38E-03	3591	0.99	4.79E-03	1.18
1.01E-02	3496	0.96	8.90E-03	1.34
1.84E-02	3370	0.93	1.58E-02	1.77
3.32E-02	3215	0.89	2.75E-02	2.42
5.82E-02	2947	0.81	4.54E-02	3.56
1.06E-01	2632	0.73	7.64E-02	4.89
2.09E-01	2228	0.61	1.38E-01	6.73
4.79E-01	1680	0.46	2.87E-01	9.05
6.39E-01	1545	0.43	3.45E-01	11.37

⁺ Average Shearing Strain from the First Three Cycles of the Free Vibration Decay Curve

^x Average Damping Ratio from the First Three Cycles of the Free Vibration Decay Curve

Table E.5 Variation in Shear Modulus, Normalized Shear Modulus and Material Damping Ratio with Shearing Strain from TS Tests of Specimen B-773B-6; Isotropic Confining Pressure, $\sigma_0 = 9605$ psf

First Cycle				Tenth Cycle			
Peak Shearing Strain, %	Shear Modulus, G, ksf	Normalized Shear Modulus, G/G_{max}	Material Damping Ratio, D, %	Peak Shearing Strain, %	Shear Modulus, G, ksf	Normalized Shear Modulus, G/G_{max}	Material Damping Ratio, D, %
1.00E-03	3311	1.00	0.56	1.01E-03	3301	1.00	0.49
2.01E-03	3311	1.00	0.68	2.01E-03	3301	1.00	0.68
4.07E-03	3311	1.00	0.75	4.08E-03	3301	1.00	0.69
8.31E-03	3217	0.97	1.29	8.33E-03	3207	0.97	1.04



GRAVEL		SAND			SILT or CLAY		
Coarse	Fine	Coarse	Medium	Fine			
<u>SYMBOL</u>	<u>BORING</u>	<u>DEPTH, FT</u>	<u>C_c</u>	<u>C_u</u>	<u>D₅₀</u>	<u>D₉₀</u>	<u>CLASSIFICATION</u>
●	B-773B-6	57	NA	NA	0.04	0.23	Fat Clay with sand (CH), olive gray

GRAIN SIZE CURVE

APPENDIX F

Specimen B-773B_7

Borehole B-773B

Sample 7

Depth = 66.1 ft (20.1 m)

Total Unit Weight = 110.1 lb/ft³

Water Content = 33.5 %

FUGRO JOB #: 0411-09-1734
Testing Station: RC7



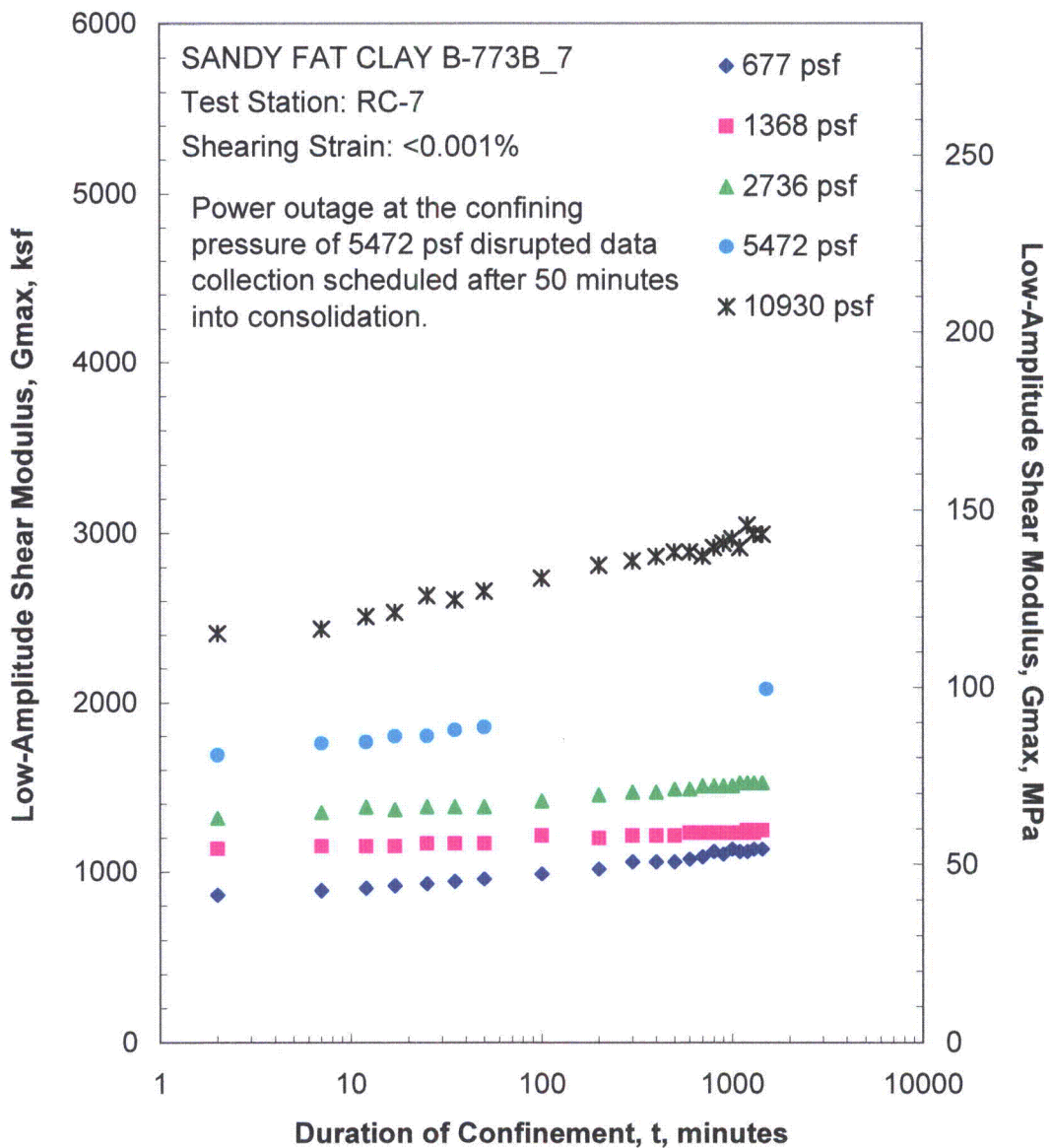


Figure F.1 Variation in Low-Amplitude Shear Modulus with Magnitude and Duration of Isotropic Confining Pressure from Resonant Column Tests

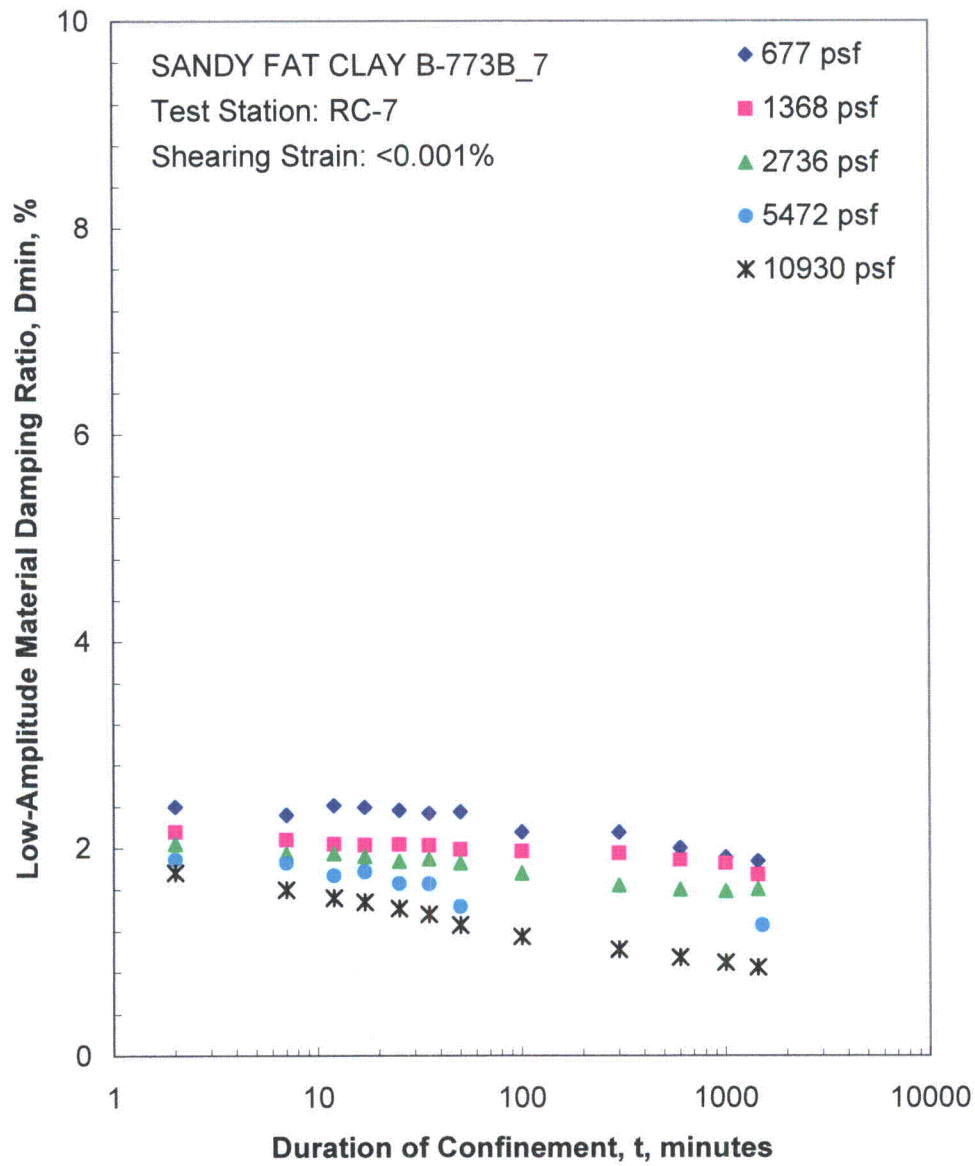


Figure F.2 Variation in Low-Amplitude Material Damping Ratio with Magnitude and Duration of Isotropic Confining Pressure from Resonant Column Tests

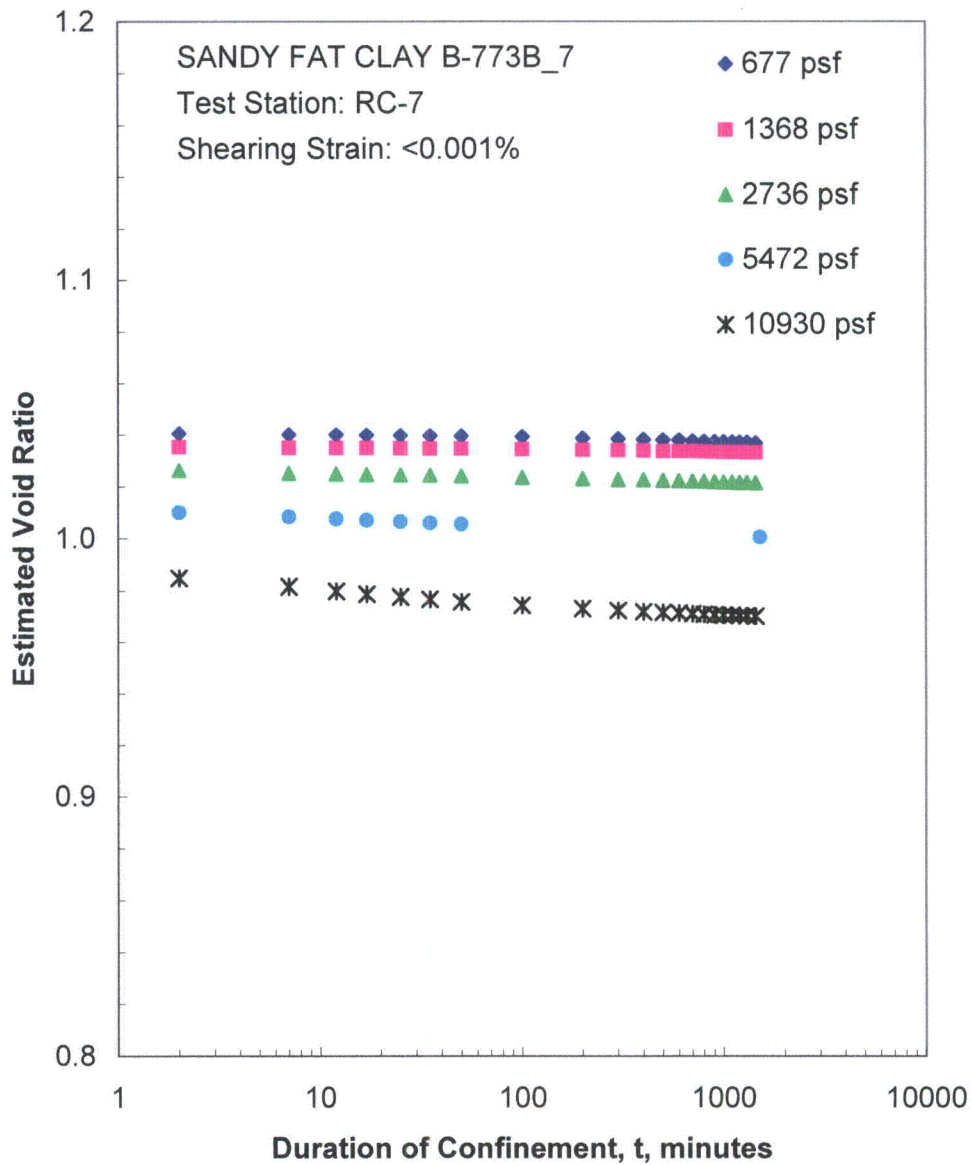


Figure F.3 Variation in Estimated Void Ratio with Magnitude and Duration of Isotropic Confining Pressure from Resonant Column Tests

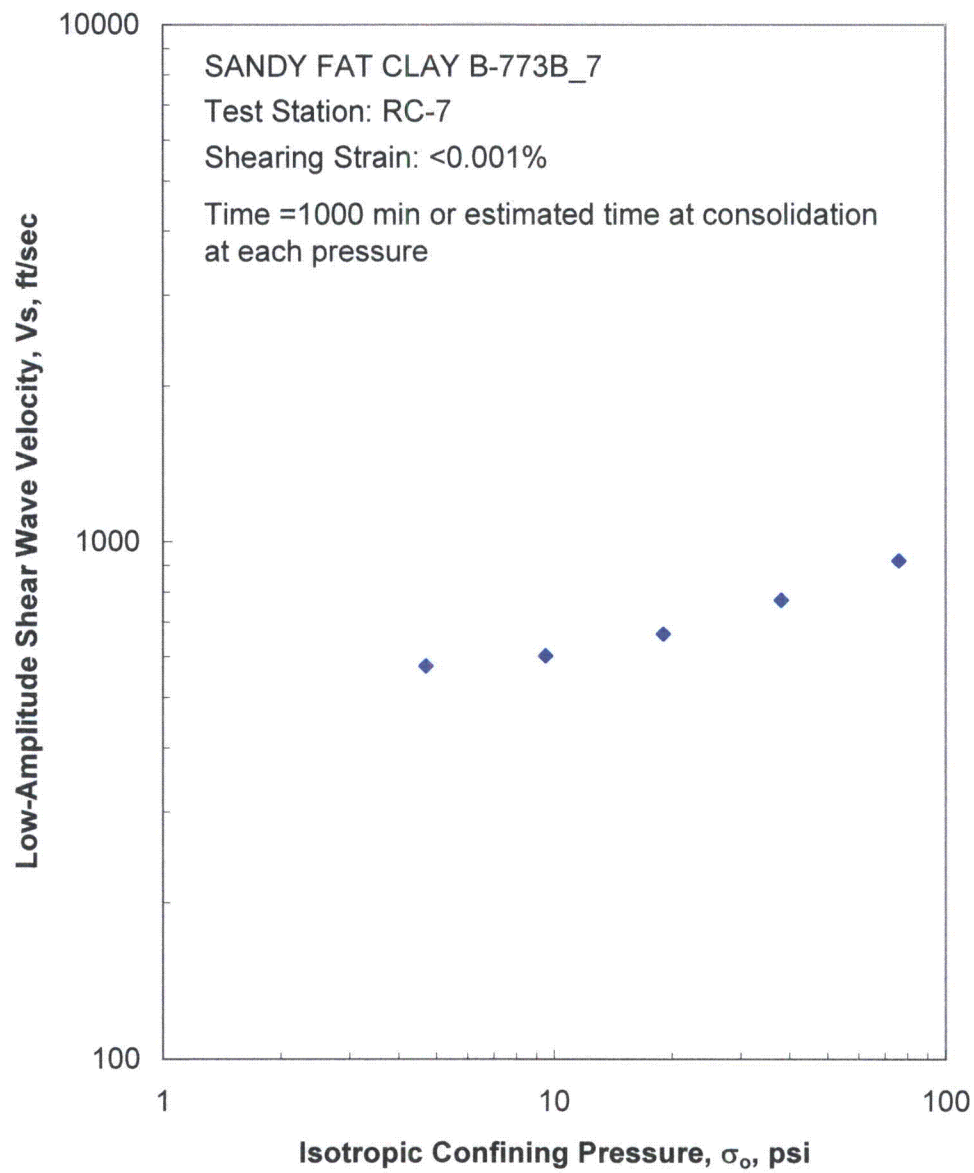


Figure F.4 Variation in Low-Amplitude Shear Wave Velocity with Isotropic Confining Pressure from Resonant Column Tests

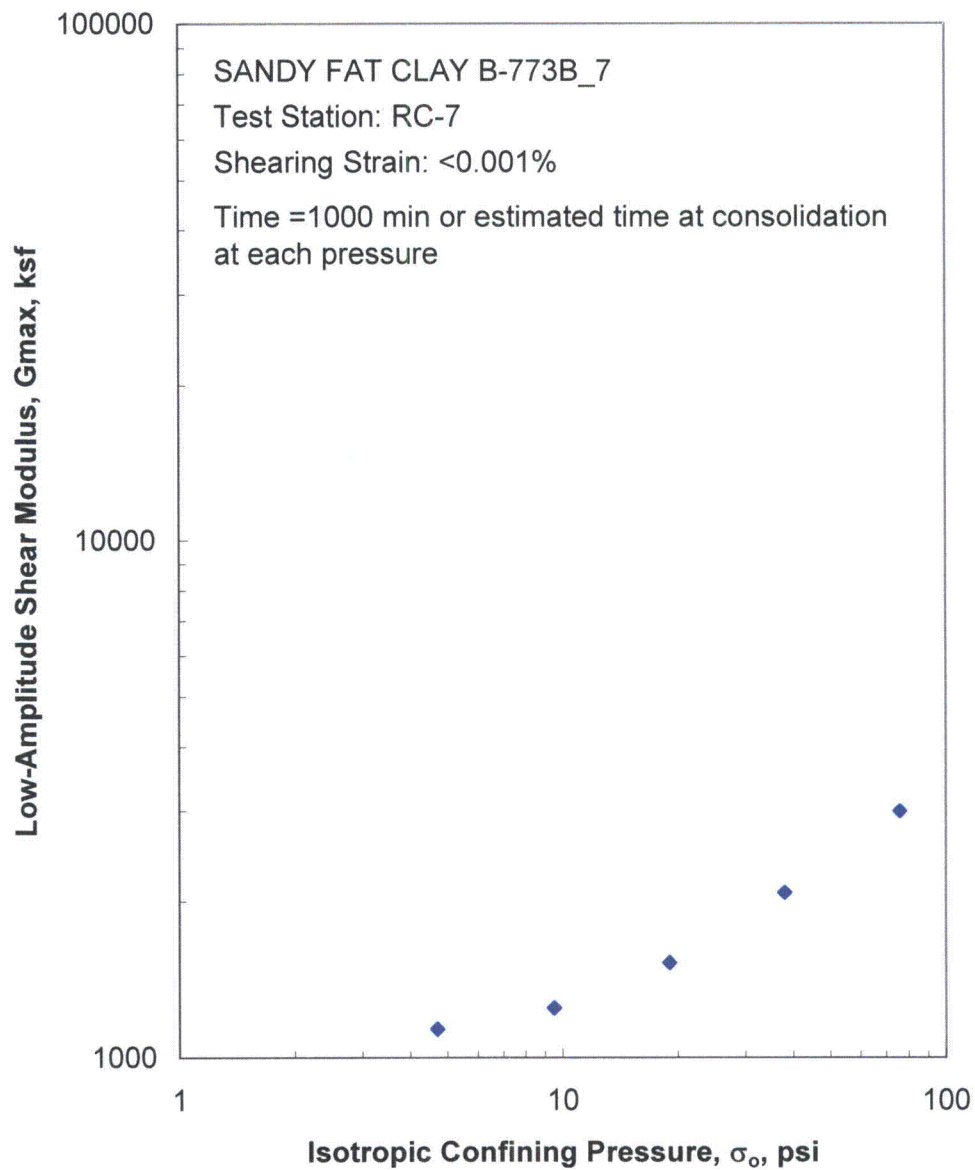


Figure F.5 Variation in Low-Amplitude Shear Modulus with Isotropic Confining Pressure from Resonant Column Tests

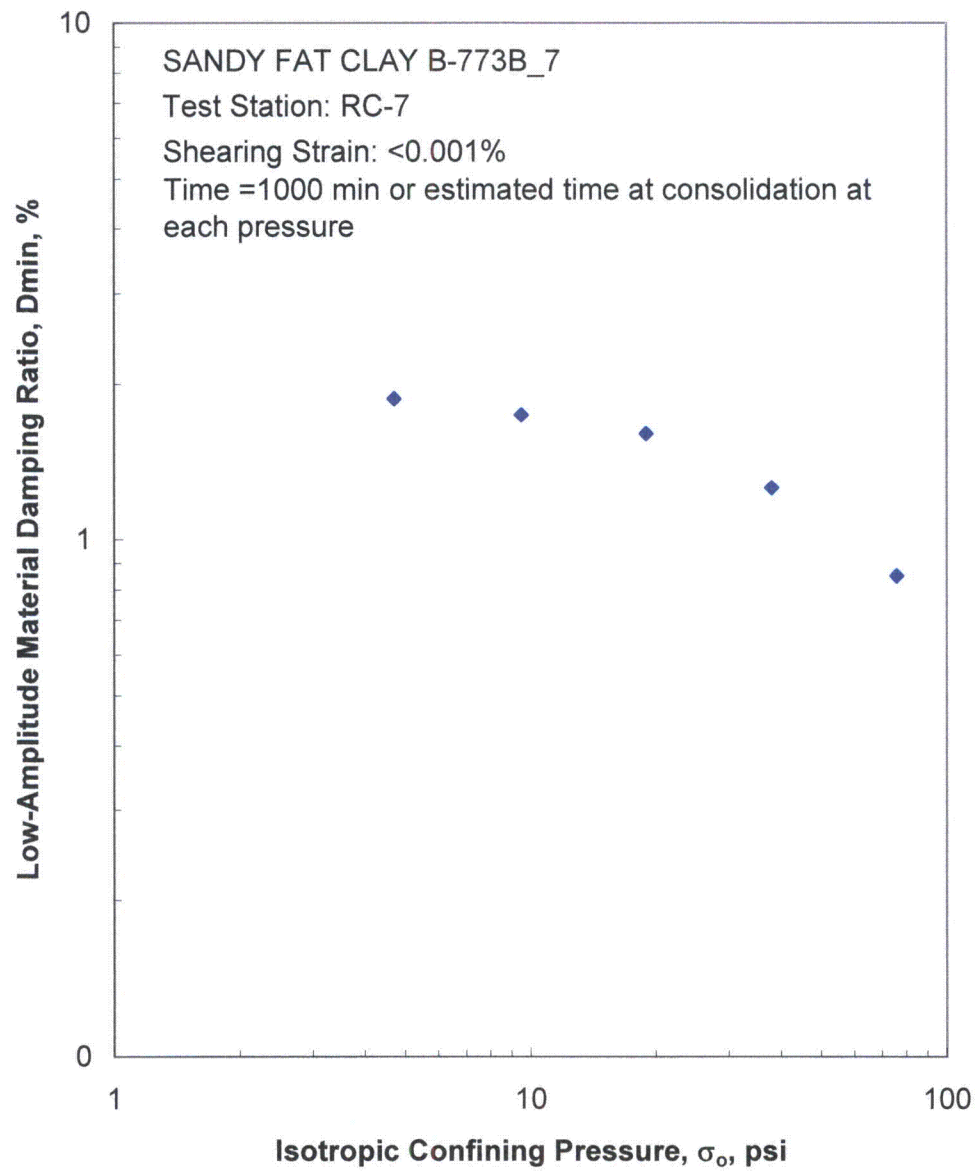


Figure F.6 Variation in Low-Amplitude Material Damping Ratio with Isotropic Confining Pressure from Resonant Column Tests

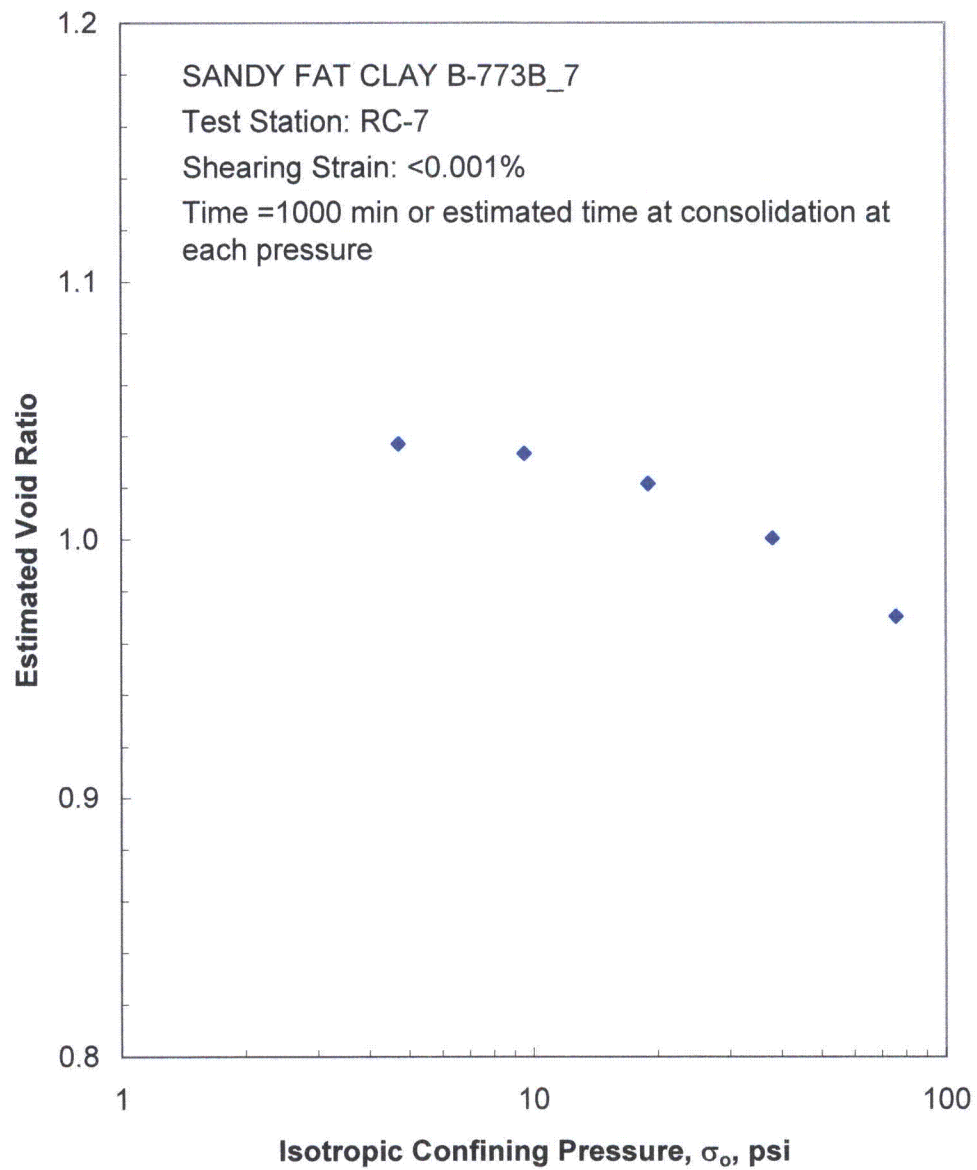


Figure F.7 Variation in Estimated Void Ratio with Isotropic Confining Pressure from Resonant Column Tests

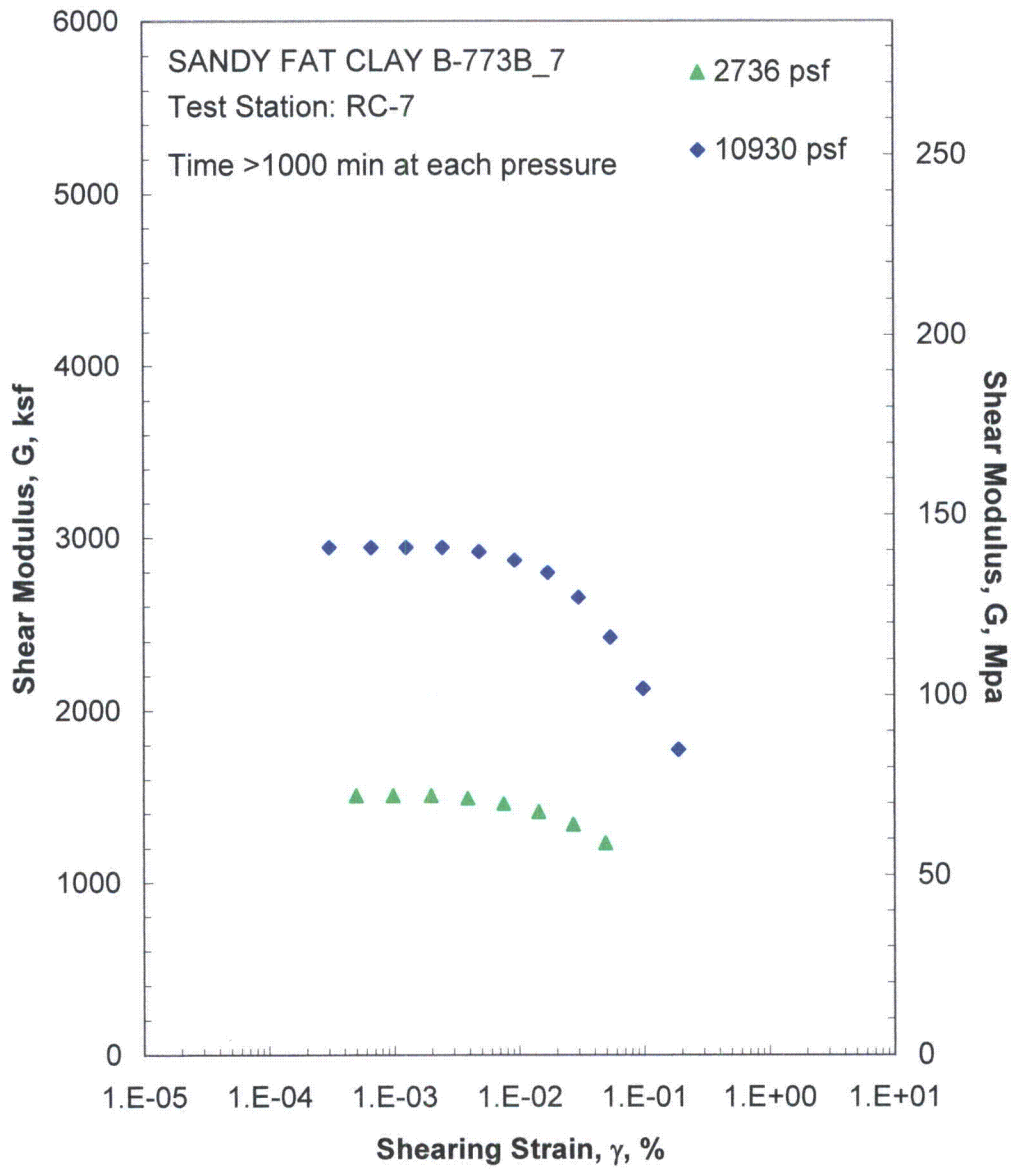


Figure F.8 Comparison of the Variation in Shear Modulus with Shearing Strain and Isotropic Confining Pressure from the Resonant Column Tests

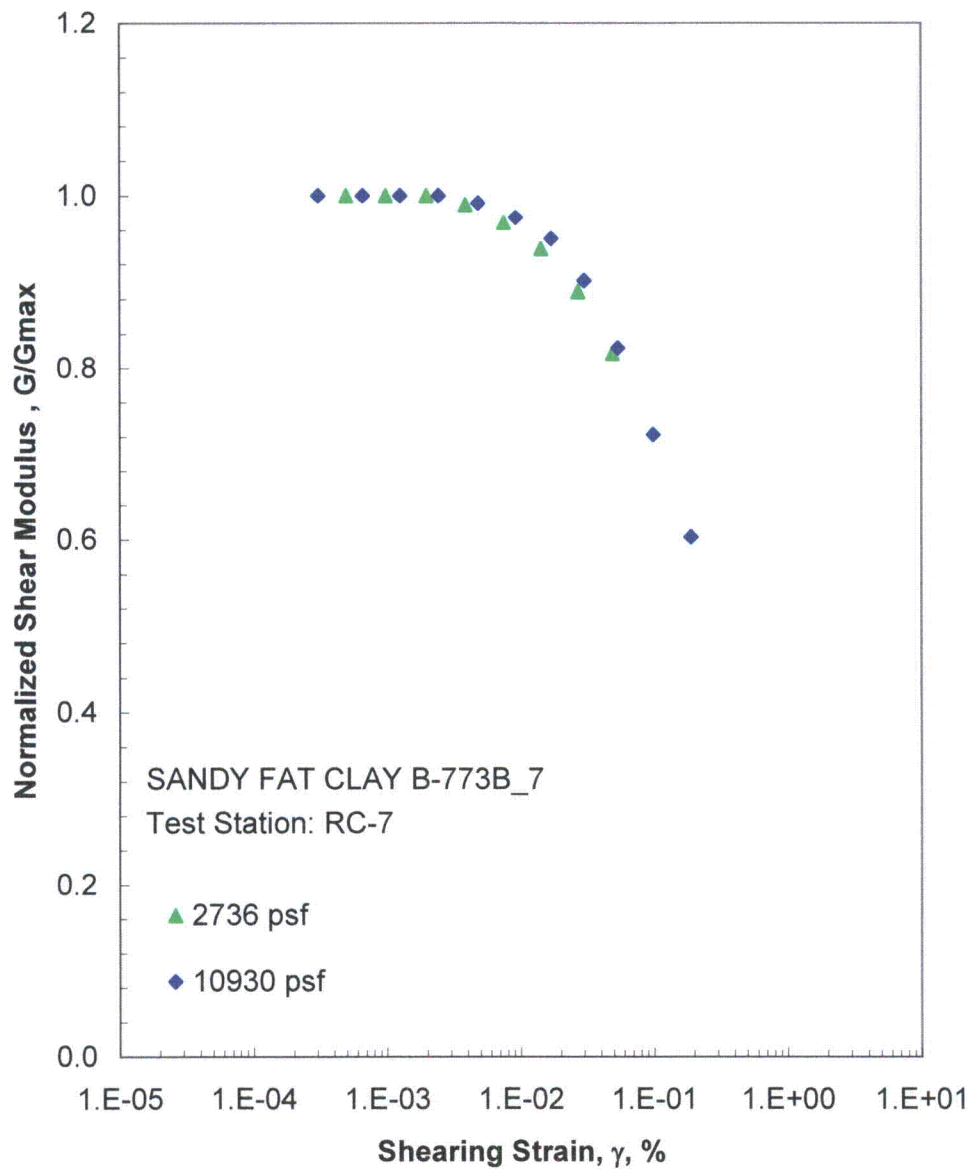


Figure F.9 Comparison of the Variation in Normalized Shear Modulus with Shearing Strain and Isotropic Confining Pressure from the Resonant Column Tests

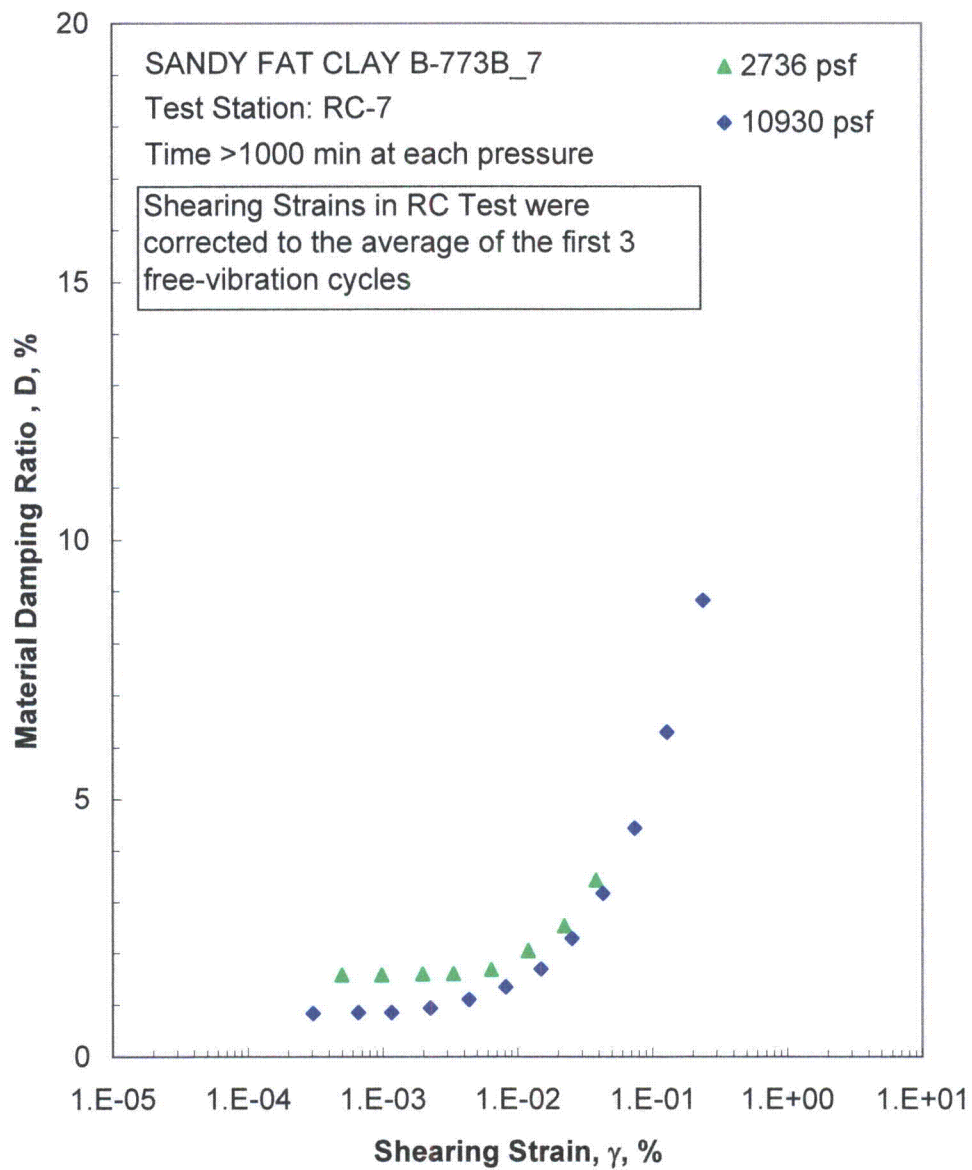


Figure F.10 Comparison of the Variation in Material Damping Ratio with Shearing Strain and Isotropic Confining Pressure from the Resonant Column Tests

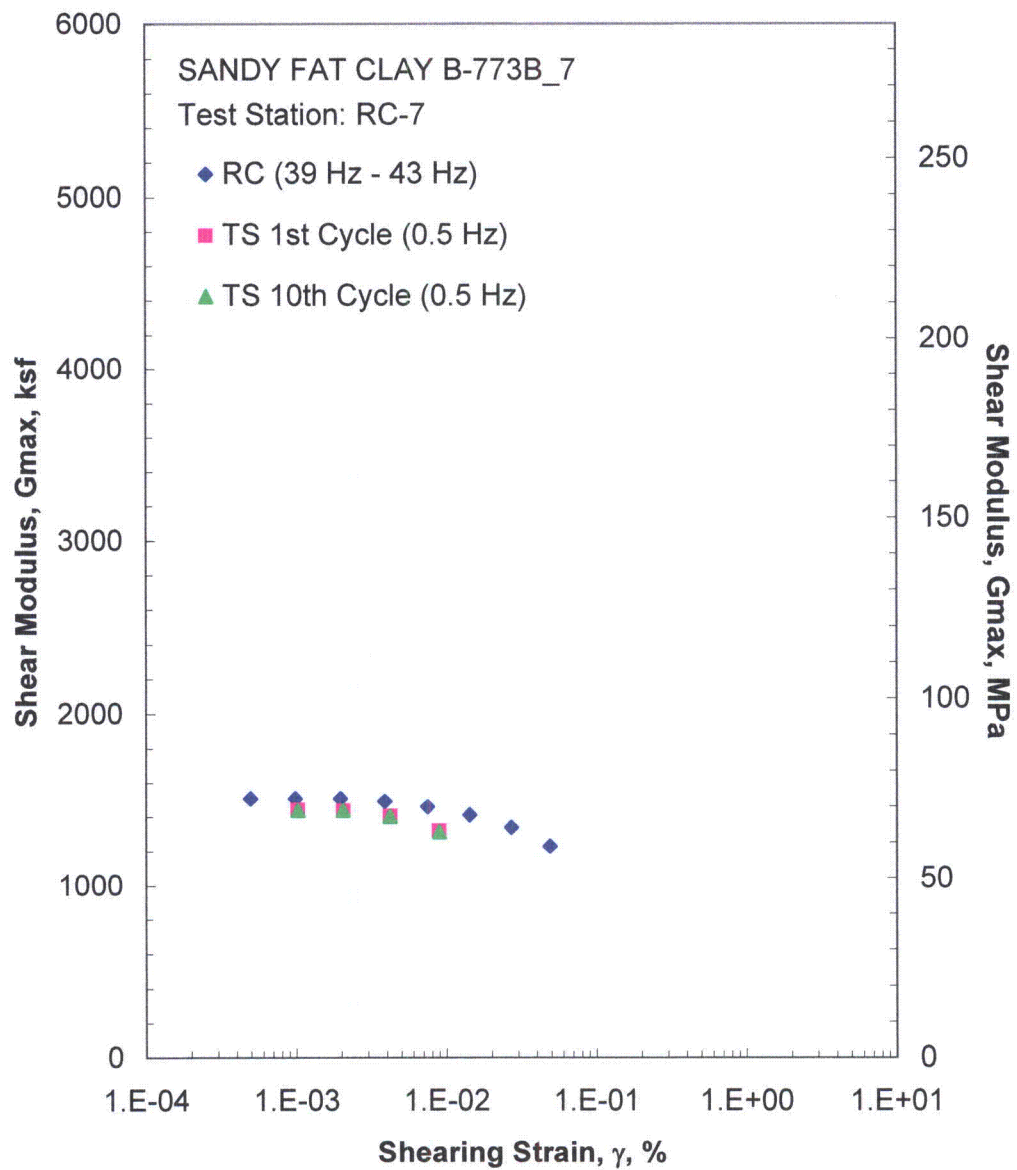


Figure F.11 Comparison of the Variation in Shear Modulus with Shearing Strain at an Isotropic Confining Pressure of 2736 psf from the Combined RCTS Tests

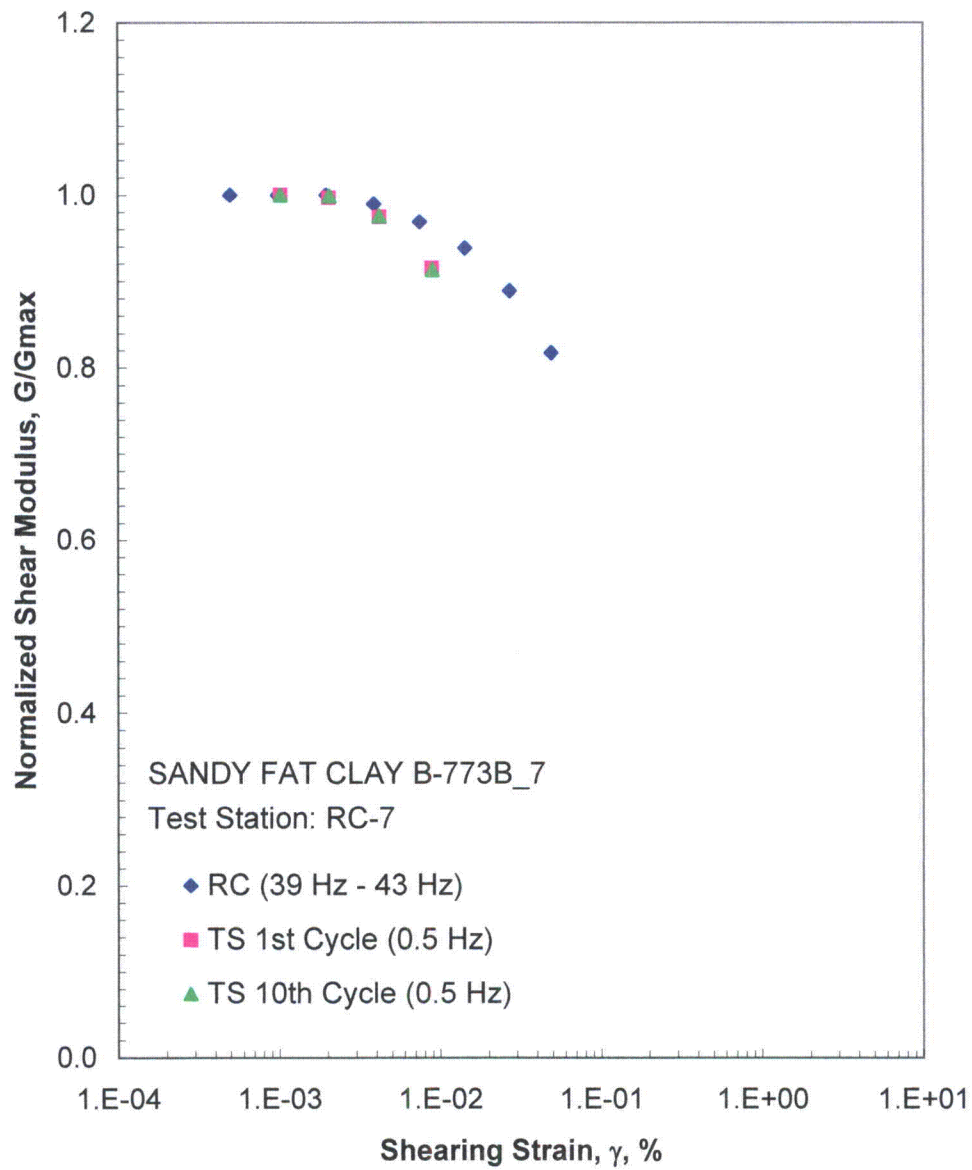


Figure F.12 Comparison of the Variation in Normalized Shear Modulus with Shearing Strain at an Isotropic Confining Pressure of 2736 psf from the Combined RCTS Tests

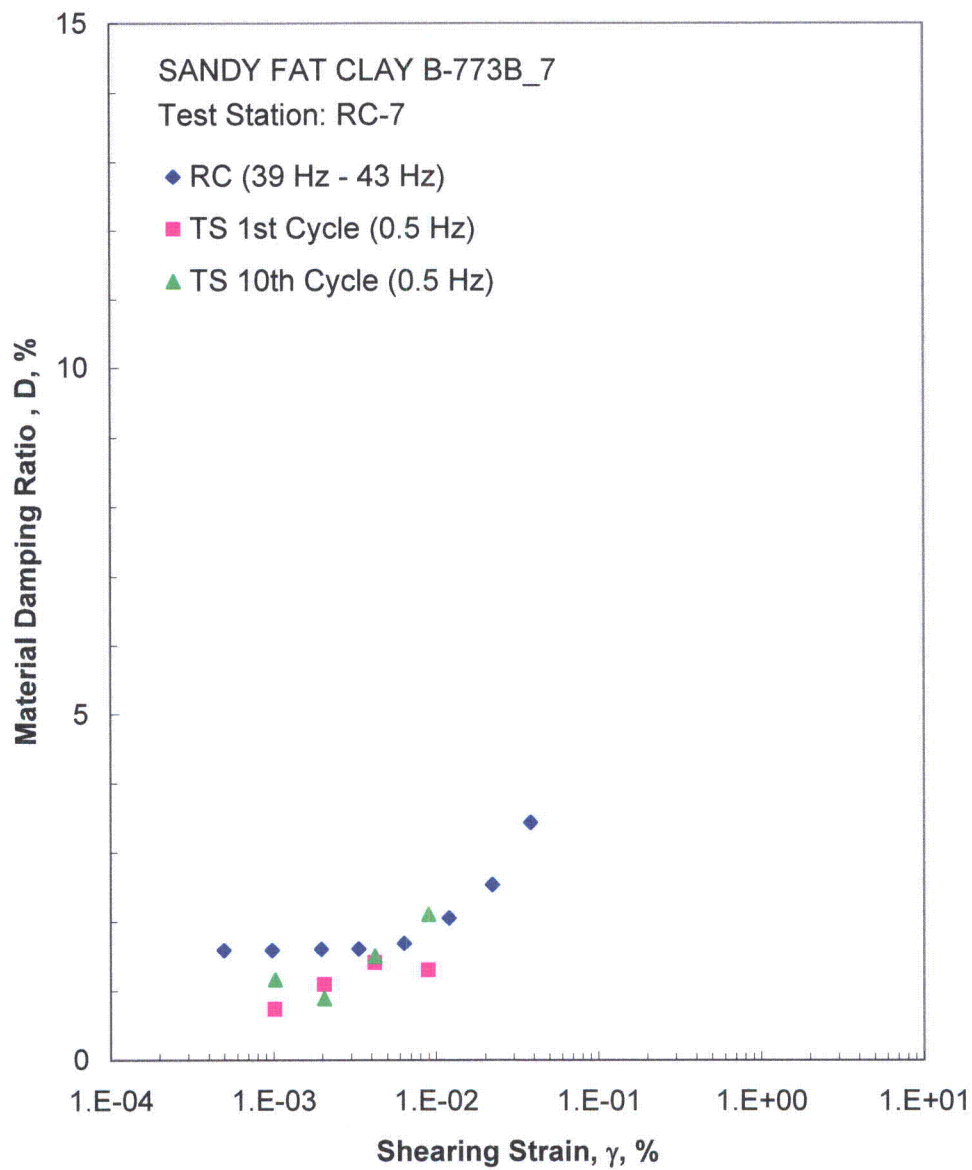


Figure F.13 Comparison of the Variation in Material Damping Ratio with Shearing Strain at an Isotropic Confining Pressure of 2736 psf from the Combined RCTS Tests

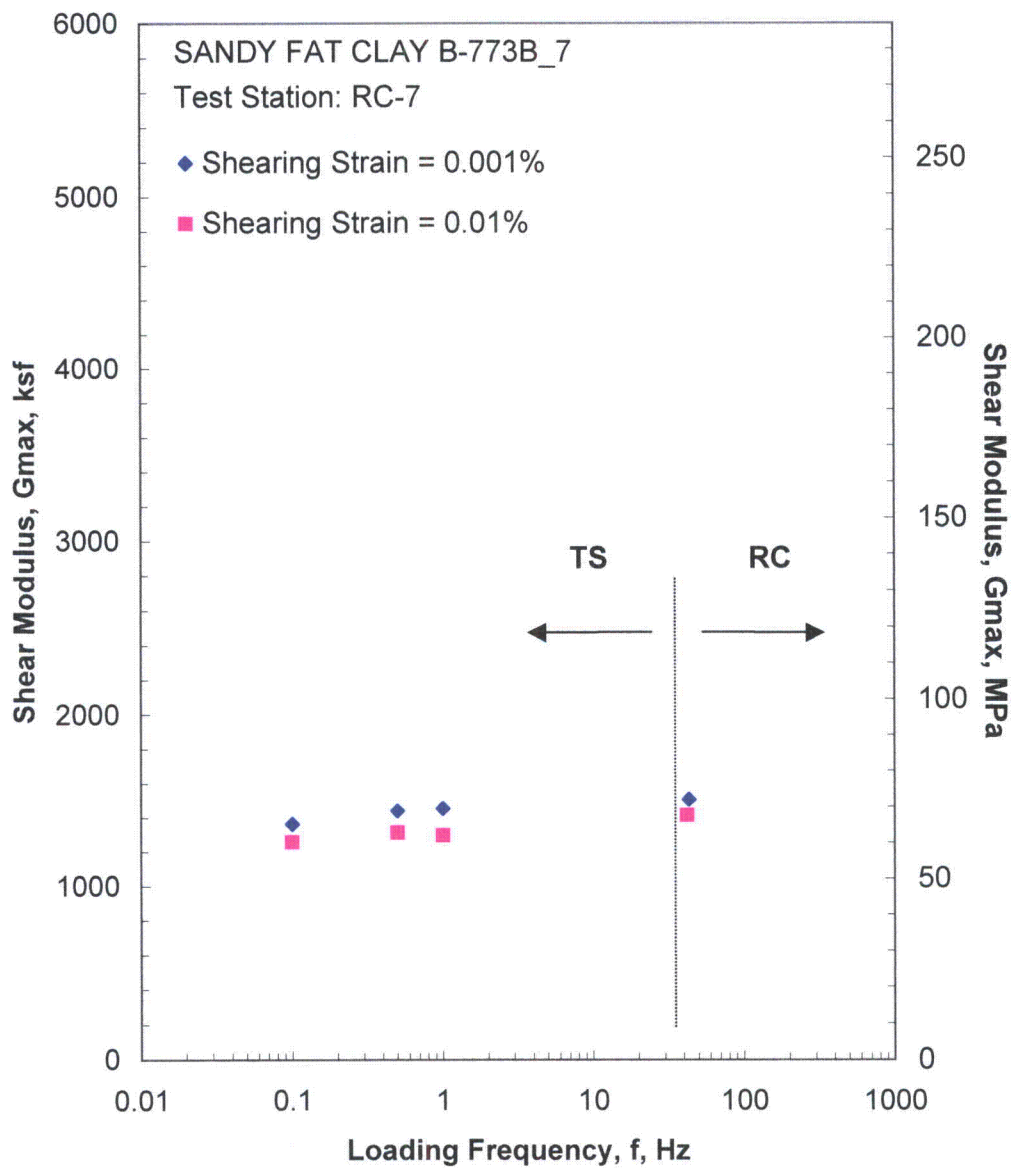


Figure F.14 Comparison of the Variation in Shear Modulus with Loading Frequency at an Isotropic Confining Pressure of 2736 psf from the Combined RCTS Tests

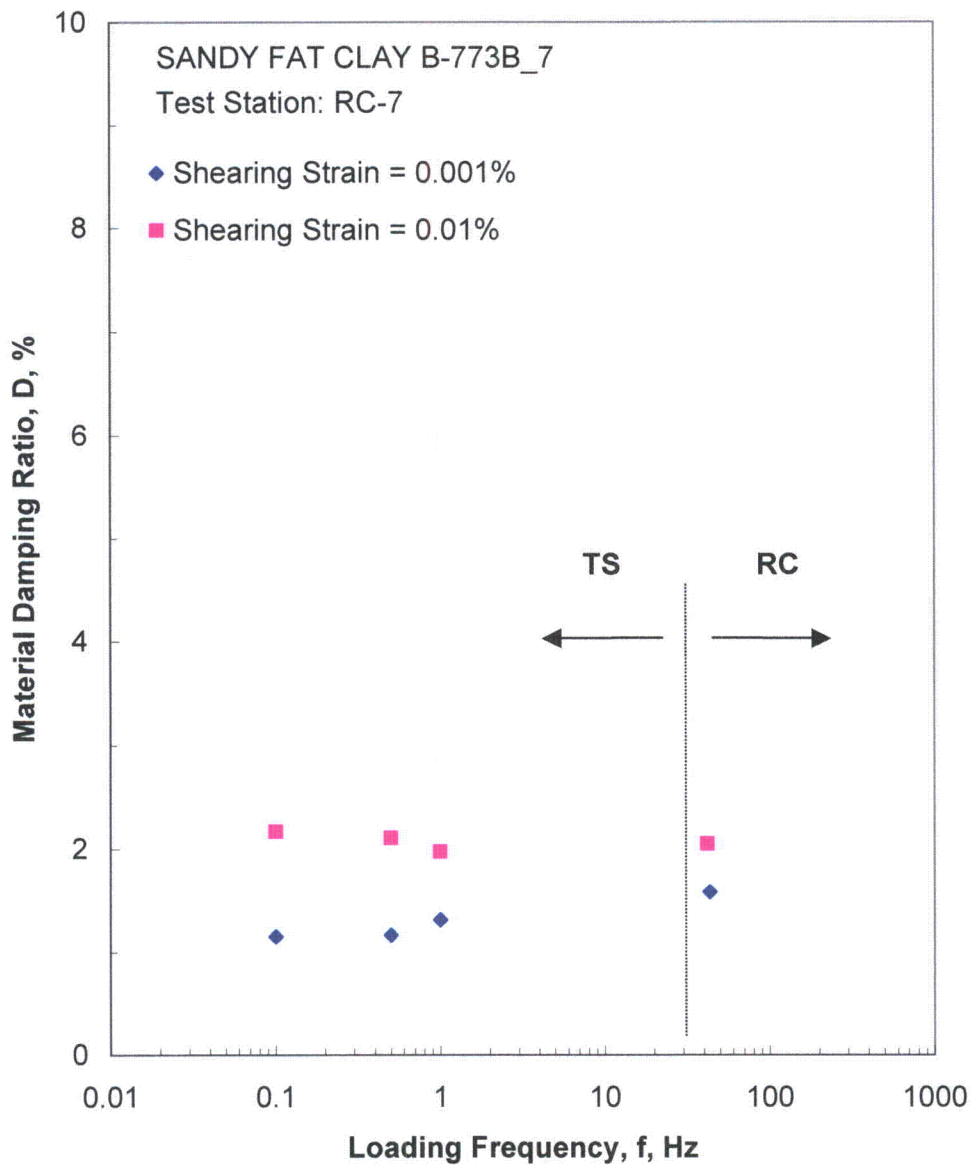


Figure F.15 Comparison of the Variation in Material Damping Ratio with Loading Frequency at an Isotropic Confining Pressure of 2736 psf from the Combined RCTS Tests

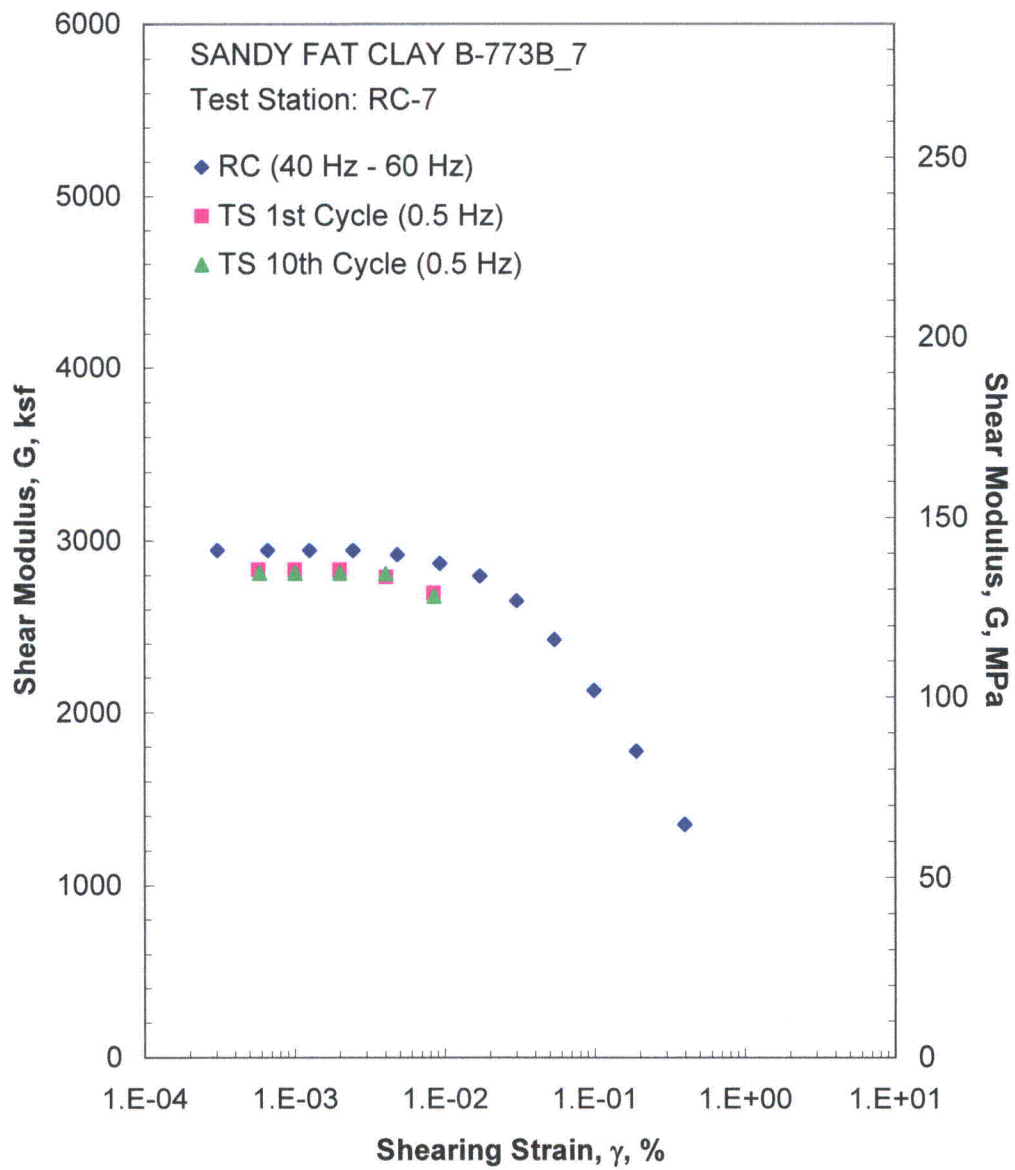


Figure F.16 Comparison of the Variation in Shear Modulus with Shearing Strain at an Isotropic Confining Pressure of 10930 psf from the Combined RCTS Tests

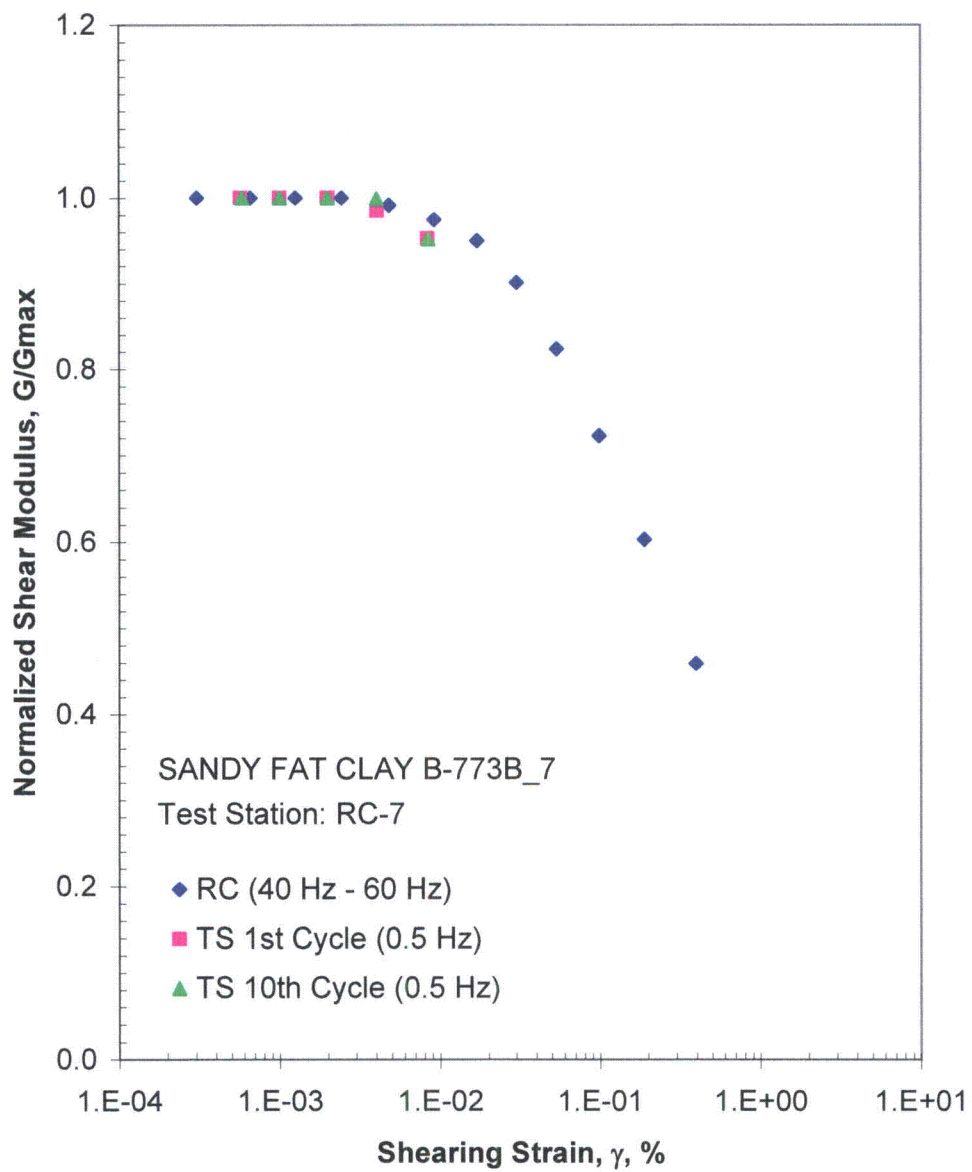


Figure F.17 Comparison of the Variation in Normalized Shear Modulus with Shearing Strain at an Isotropic Confining Pressure of 10930 psi from the Combined RCTS Tests

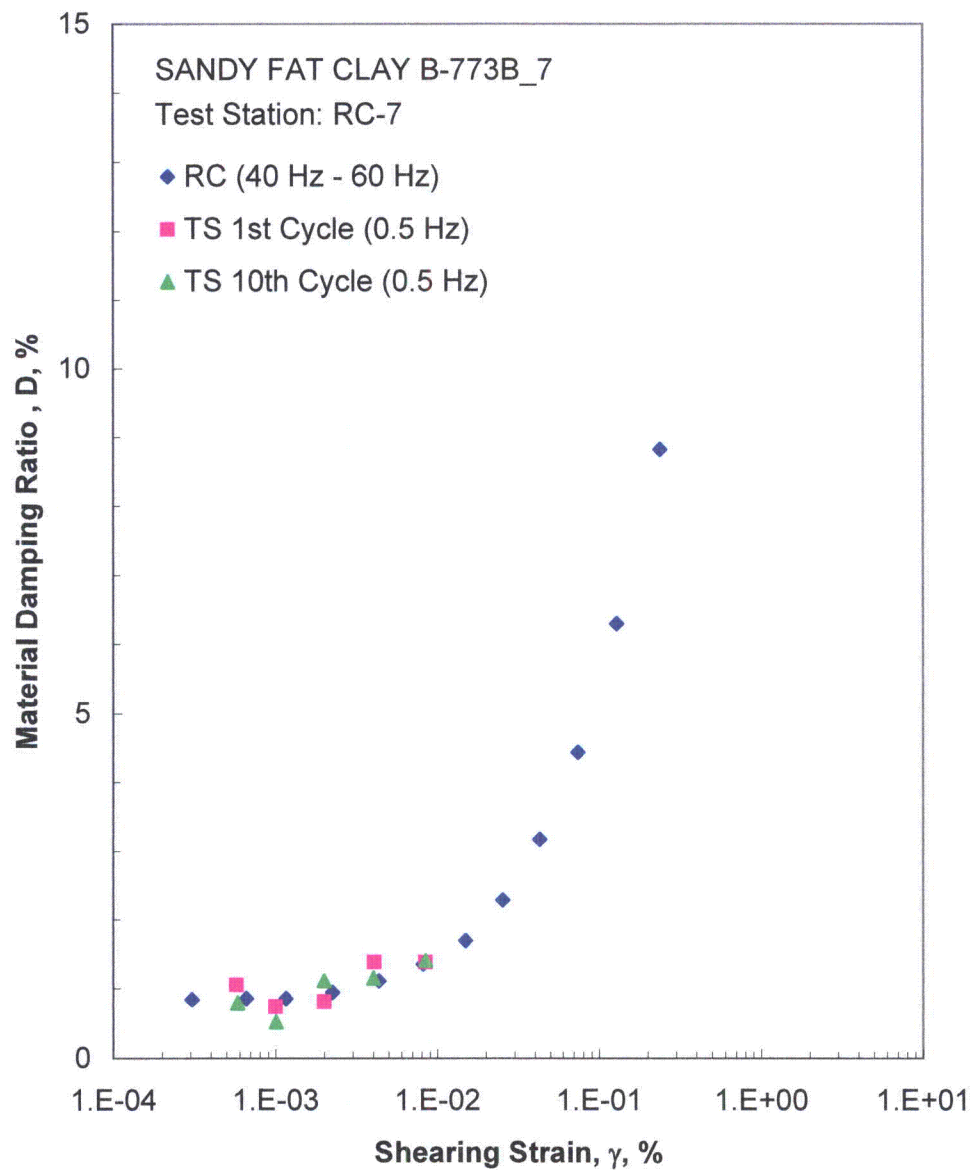


Figure F.18 Comparison of the Variation in Material Damping Ratio with Shearing Strain at an Isotropic Confining Pressure of 10930 psf from the Combined RCTS Tests

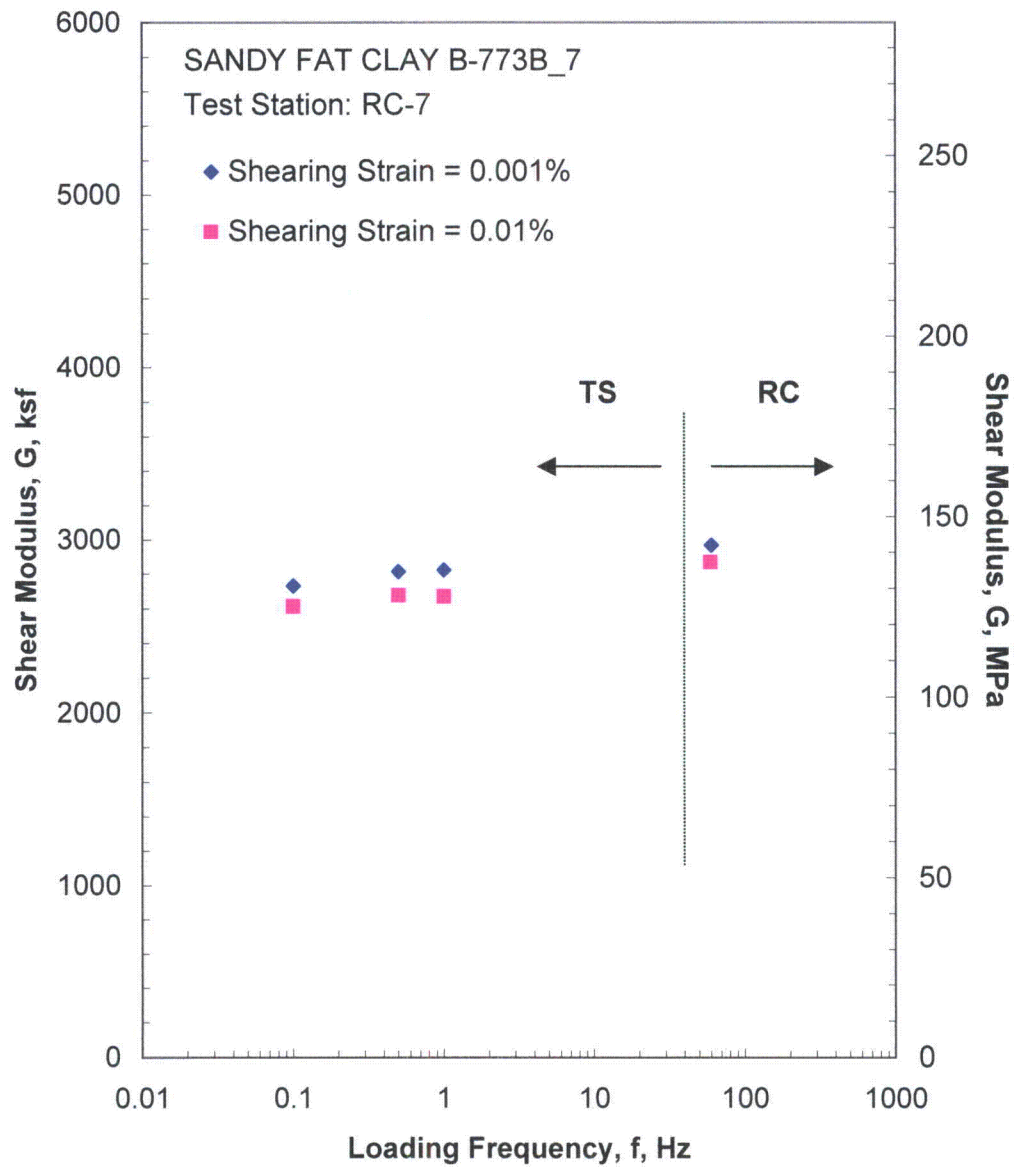


Figure F.19 Comparison of the Variation in Shear Modulus with Loading Frequency at an Isotropic Confining Pressure of 10930 psf from the Combined RCTS Tests

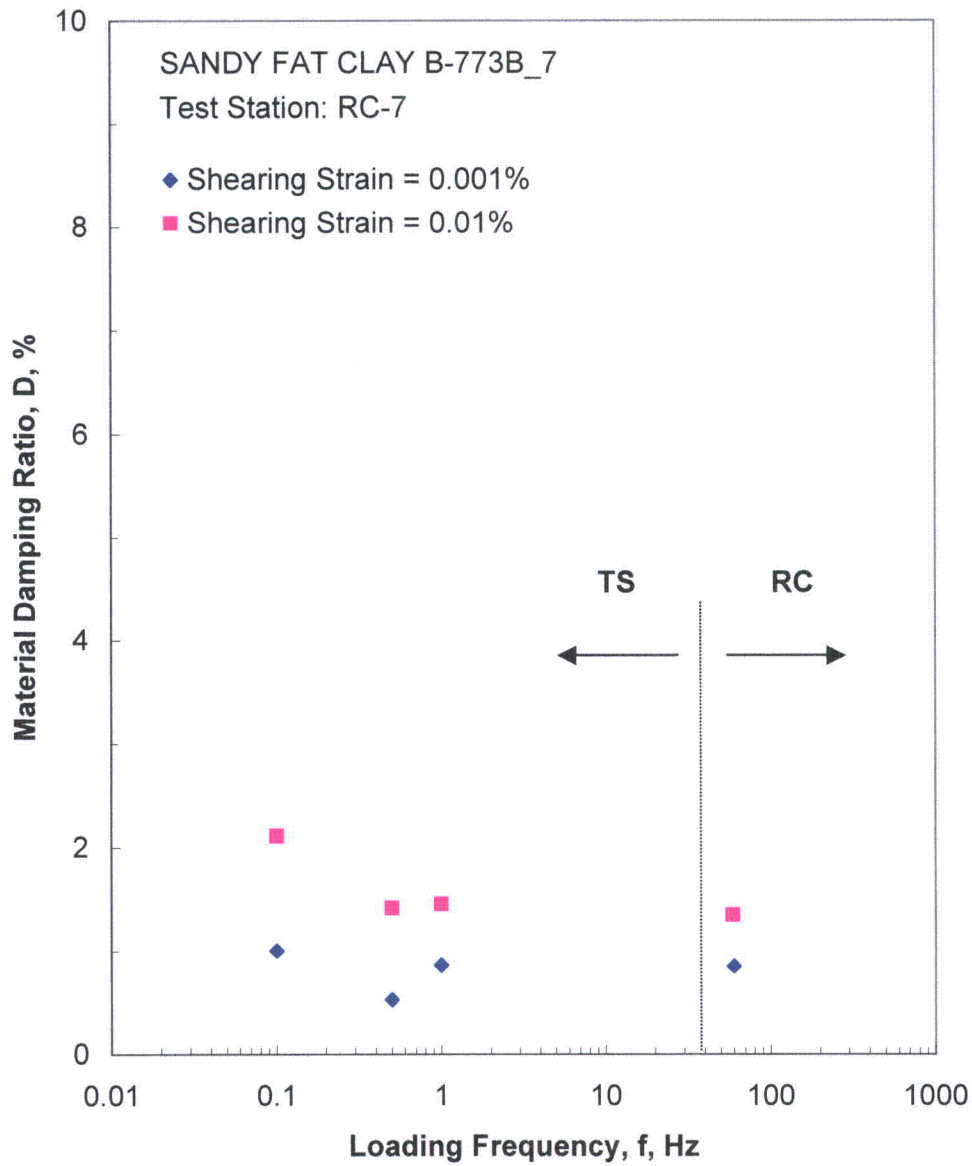


Figure F.20 Comparison of the Variation in Material Damping Ratio with Loading Frequency at an Isotropic Confining Pressure of 10930 psf from the Combined RCTS Tests

Table F.1 Variation in Low-Amplitude Shear Wave Velocity, Low-Amplitude Shear Modulus, Low-Amplitude Material Damping Ratio and Estimated Void Ratio with Isotropic Confining Pressure from RC Tests of Specimen B-773B-7

Isotropic Confining Pressure, σ_o			Low-Amplitude Shear Modulus, G_{max}		Low-Amplitude Shear Wave Velocity, V_s	Low-Amplitude Material Damping Ratio, D_{min}	Estimated Void Ratio, e
(psi)	(psf)	(kPa)	(ksf)	(MPa)	(fps)	(%)	
5	677	32	1135	54	575	1.87	1.04
10	1368	65	1247	60	602	1.74	1.03
19	2736	131	1524	73	664	1.60	1.02
38	5472	262	2080	100	771	1.26	1.00
76	10930	523	2994	144	918	0.85	0.97

Table F.2 Variation in Shear Modulus and Material Damping Ratio with Shearing Strain from RC Tests of Specimen B-773B-7; Isotropic Confining Pressure, $\sigma_o = 2736$ psf

Peak Shearing Strain, %	Shear Modulus, G, ksf	Normalized Shear Modulus, G/G_{max}	Average ⁺ Shearing Strain, %	Material Damping Ratio ^x , D, %
4.96E-04	1506	1.00	4.96E-04	1.59
9.80E-04	1506	1.00	9.80E-04	1.59
1.97E-03	1506	1.00	1.97E-03	1.60
3.88E-03	1491	0.99	3.33E-03	1.61
7.48E-03	1459	0.97	6.36E-03	1.69
1.43E-02	1413	0.94	1.20E-02	2.05
2.71E-02	1339	0.89	2.22E-02	2.53
4.89E-02	1231	0.82	3.81E-02	3.43

⁺ Average Shearing Strain from the First Three Cycles of the Free Vibration Decay Curve

^x Average Damping Ratio from the First Three Cycles of the Free Vibration Decay Curve

Table F.3 Variation in Shear Modulus, Normalized Shear Modulus and Material Damping Ratio with Shearing Strain from TS Tests of Specimen B-773B-7; Isotropic Confining Pressure, $\sigma_o = 2736$ psf

First Cycle				Tenth Cycle			
Peak Shearing Strain, %	Shear Modulus, G, ksf	Normalized Shear Modulus, G/G_{max}	Material Damping Ratio, D, %	Peak Shearing Strain, %	Shear Modulus, G, ksf	Normalized Shear Modulus, G/G_{max}	Material Damping Ratio, D, %
1.02E-03	1442	1.00	0.74	1.02E-03	1439	1.00	1.16
2.05E-03	1437	1.00	1.09	2.05E-03	1438	1.00	0.89
4.19E-03	1405	0.97	1.41	4.19E-03	1404	0.98	1.50
8.93E-03	1319	0.91	1.30	8.96E-03	1314	0.91	2.10

Table F.4 Variation in Shear Modulus and Material Damping Ratio with Shearing Strain from RC Tests of Specimen B-773B-7; Isotropic Confining Pressure, $\sigma_0 = 10930$ psf

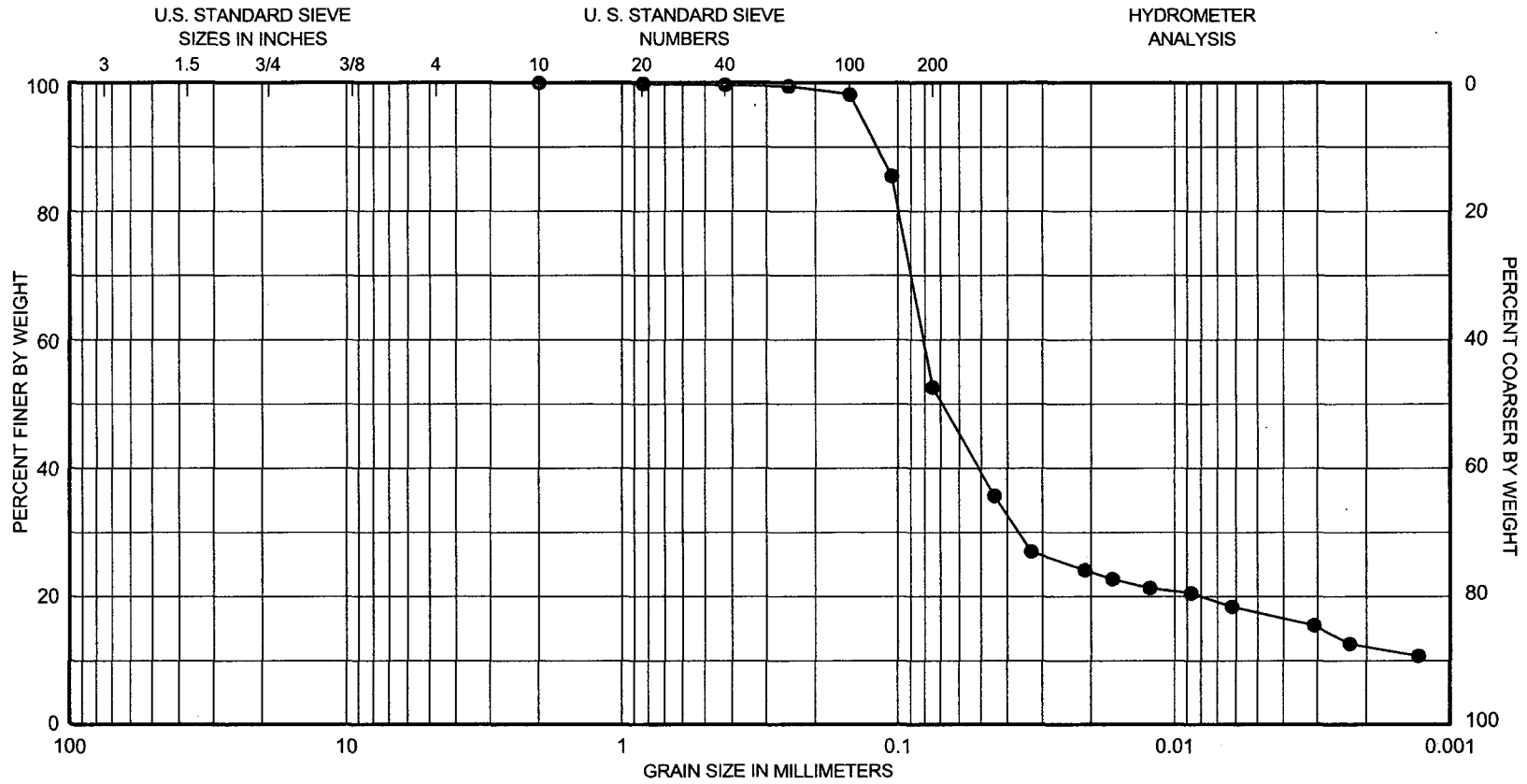
Peak Shearing Strain, %	Shear Modulus, G, ksf	Normalized Shear Modulus, G/G_{max}	Average ⁺ Shearing Strain, %	Material Damping Ratio ^x , D, %
3.05E-04	2943	1.00	3.05E-04	0.84
6.59E-04	2943	1.00	6.59E-04	0.86
1.26E-03	2943	1.00	1.16E-03	0.85
2.44E-03	2943	1.00	2.24E-03	0.94
4.82E-03	2918	0.99	4.34E-03	1.11
9.24E-03	2868	0.97	8.13E-03	1.35
1.71E-02	2795	0.95	1.48E-02	1.69
3.01E-02	2651	0.90	2.53E-02	2.28
5.36E-02	2424	0.82	4.29E-02	3.17
9.84E-02	2126	0.72	7.38E-02	4.44
1.89E-01	1775	0.60	1.28E-01	6.30
3.96E-01	1351	0.46	2.38E-01	8.82

⁺ Average Shearing Strain from the First Three Cycles of the Free Vibration Decay Curve

^x Average Damping Ratio from the First Three Cycles of the Free Vibration Decay Curve

Table F.5 Variation in Shear Modulus, Normalized Shear Modulus and Material Damping Ratio with Shearing Strain from TS Tests of Specimen B-773B-7; Isotropic Confining Pressure, $\sigma_o = 10930$ psf

First Cycle				Tenth Cycle			
Peak Shearing Strain, %	Shear Modulus, G, ksf	Normalized Shear Modulus, G/G_{max}	Material Damping Ratio, D, %	Peak Shearing Strain, %	Shear Modulus, G, ksf	Normalized Shear Modulus, G/G_{max}	Material Damping Ratio, D, %
5.72E-04	2831	1.00	1.05	5.82E-04	2812	1.00	0.79
1.00E-03	2831	1.00	0.74	1.01E-03	2812	1.00	0.52
2.00E-03	2831	1.00	0.81	1.99E-03	2812	1.00	1.11
4.06E-03	2790	0.99	1.38	4.03E-03	2809	1.00	1.15
8.40E-03	2697	0.95	1.38	8.46E-03	2677	0.95	1.41



APPENDIX G

Specimen B-773B_9

Borehole B-773B

Sample 9

Depth = 87 ft (26.5 m)

Total Unit Weight = 99.1 lb/ft³

Water Content = 59.2 %

FUGRO JOB #: 0411-09-1734

Testing Station: RC5



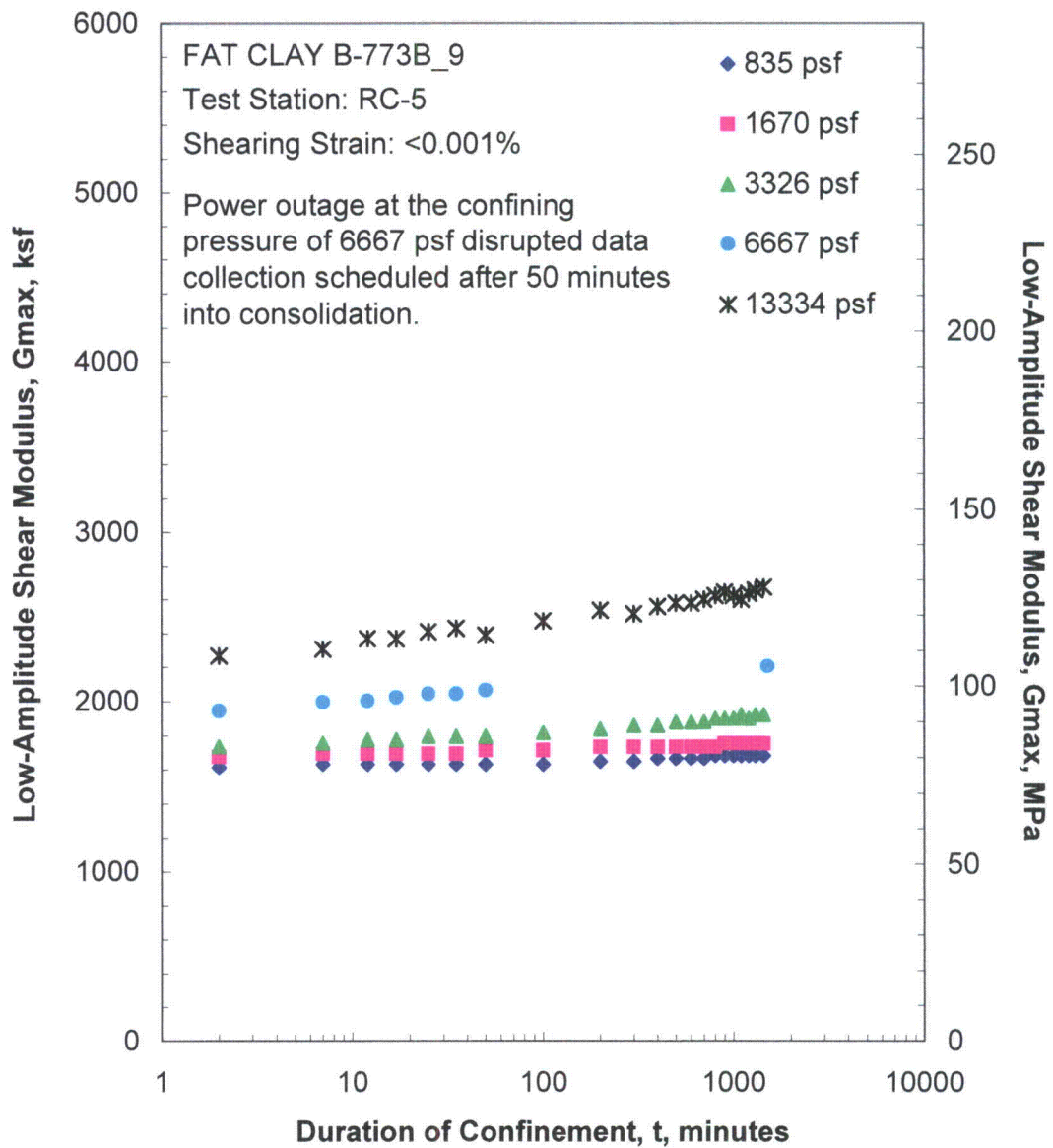


Figure G.1 Variation in Low-Amplitude Shear Modulus with Magnitude and Duration of Isotropic Confining Pressure from Resonant Column Tests

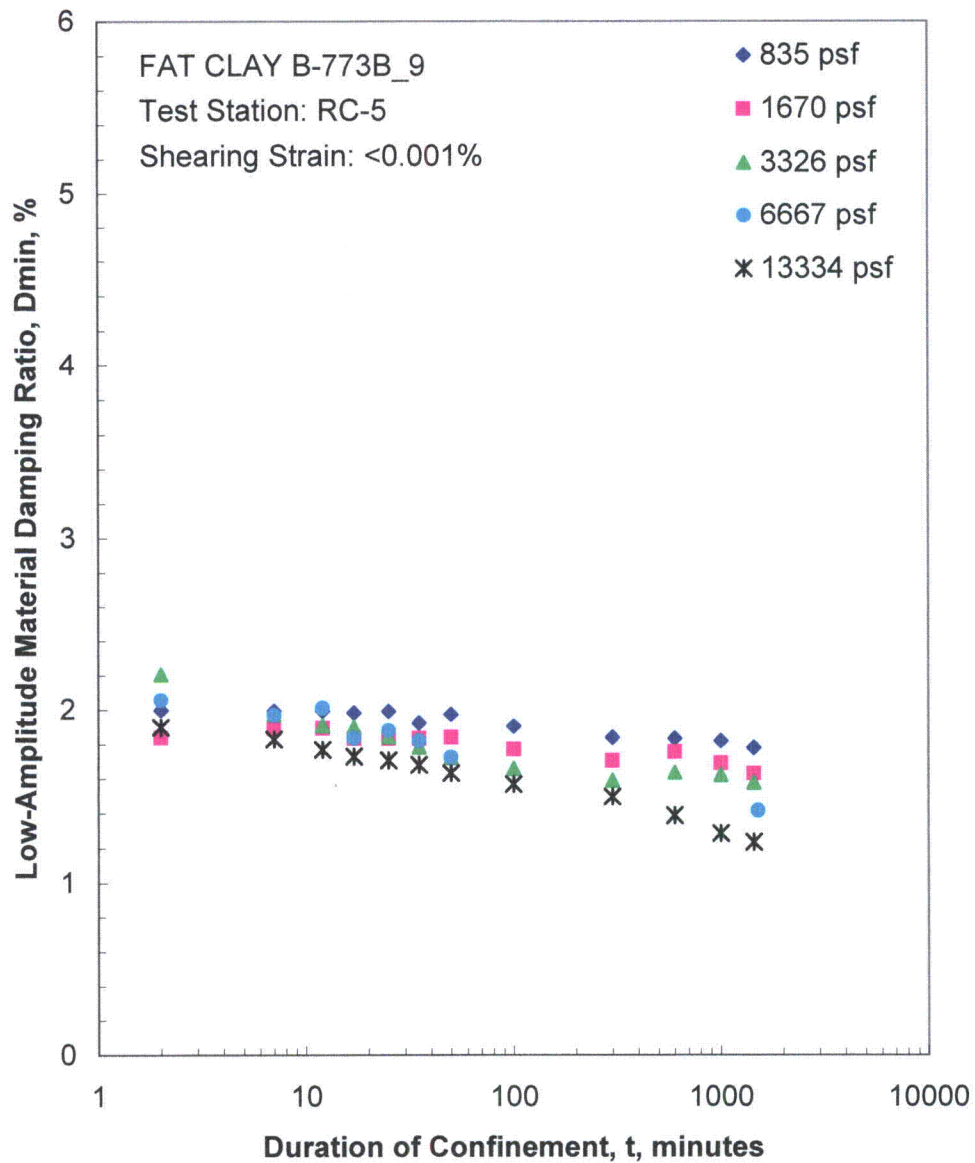


Figure G.2 Variation in Low-Amplitude Material Damping Ratio with Magnitude and Duration of Isotropic Confining Pressure from Resonant Column Tests

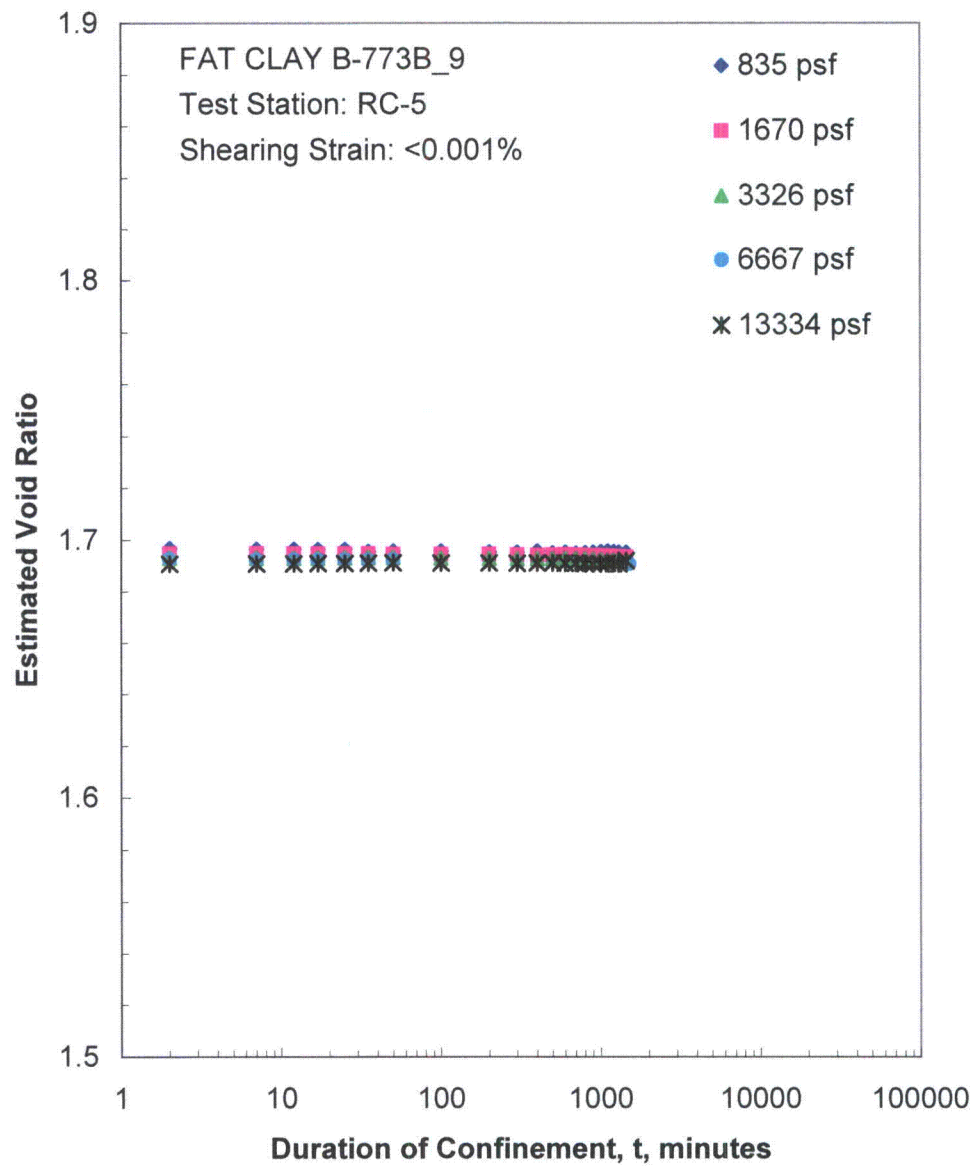


Figure G.3 Variation in Estimated Void Ratio with Magnitude and Duration of Isotropic Confining Pressure from Resonant Column Tests

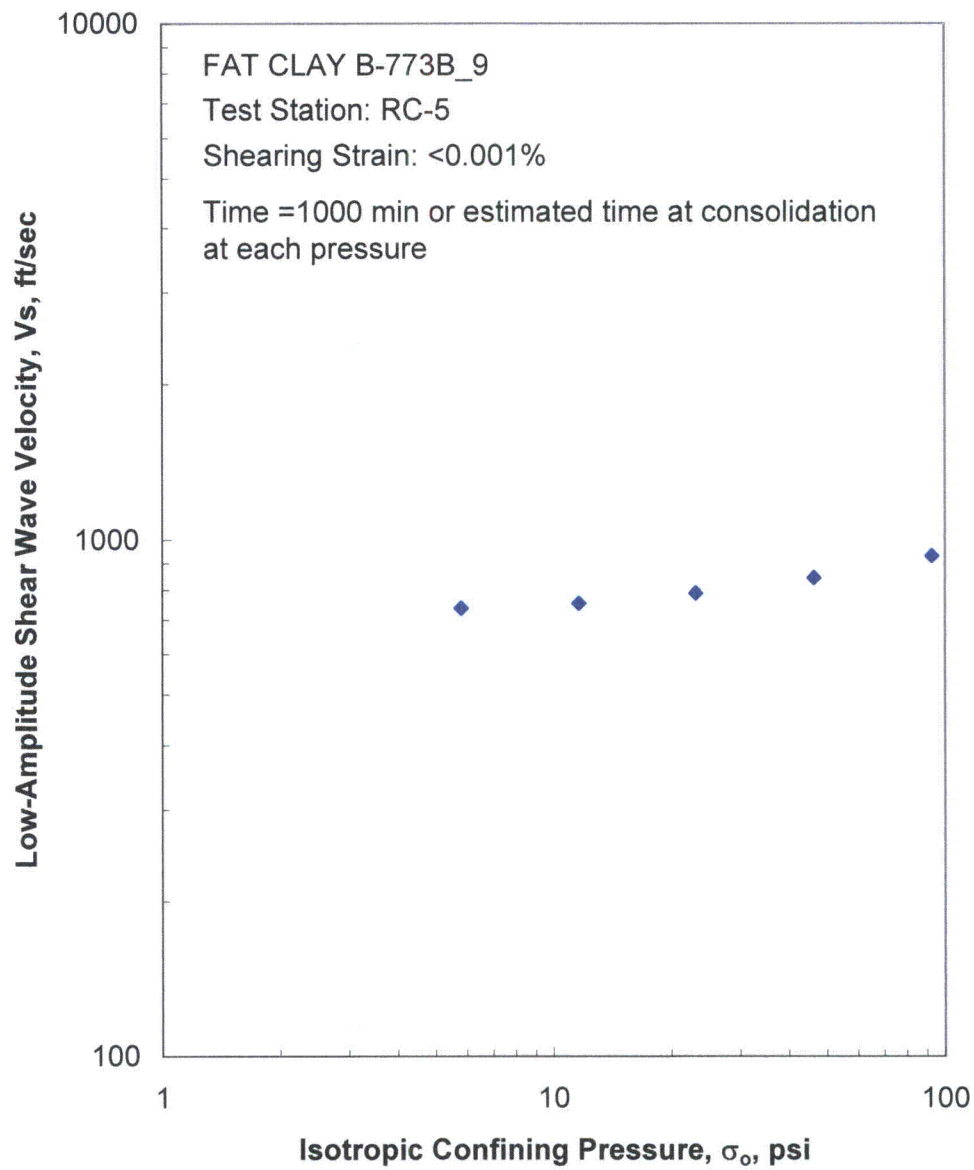


Figure G.4 Variation in Low-Amplitude Shear Wave Velocity with Isotropic Confining Pressure from Resonant Column Tests

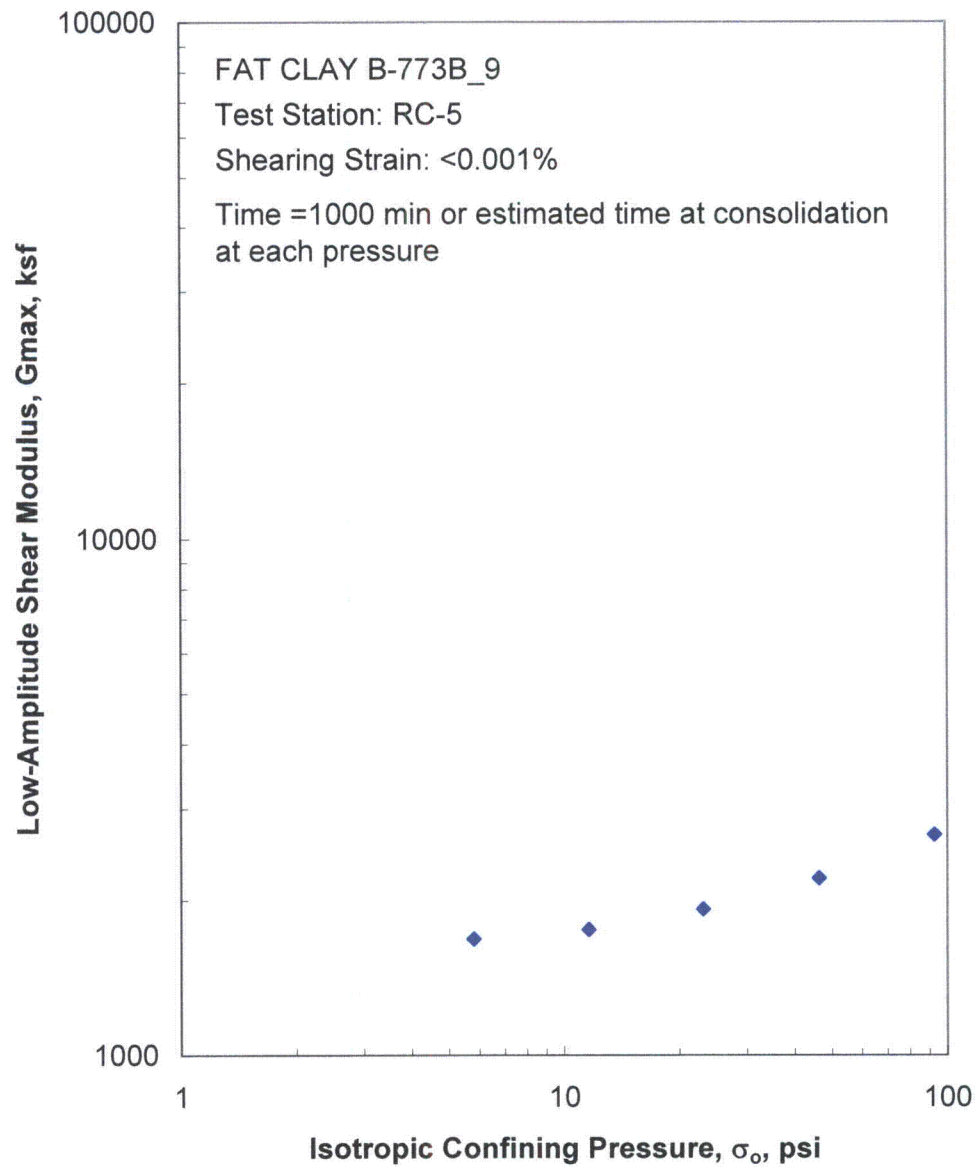


Figure G.5 Variation in Low-Amplitude Shear Modulus with Isotropic Confining Pressure from Resonant Column Tests

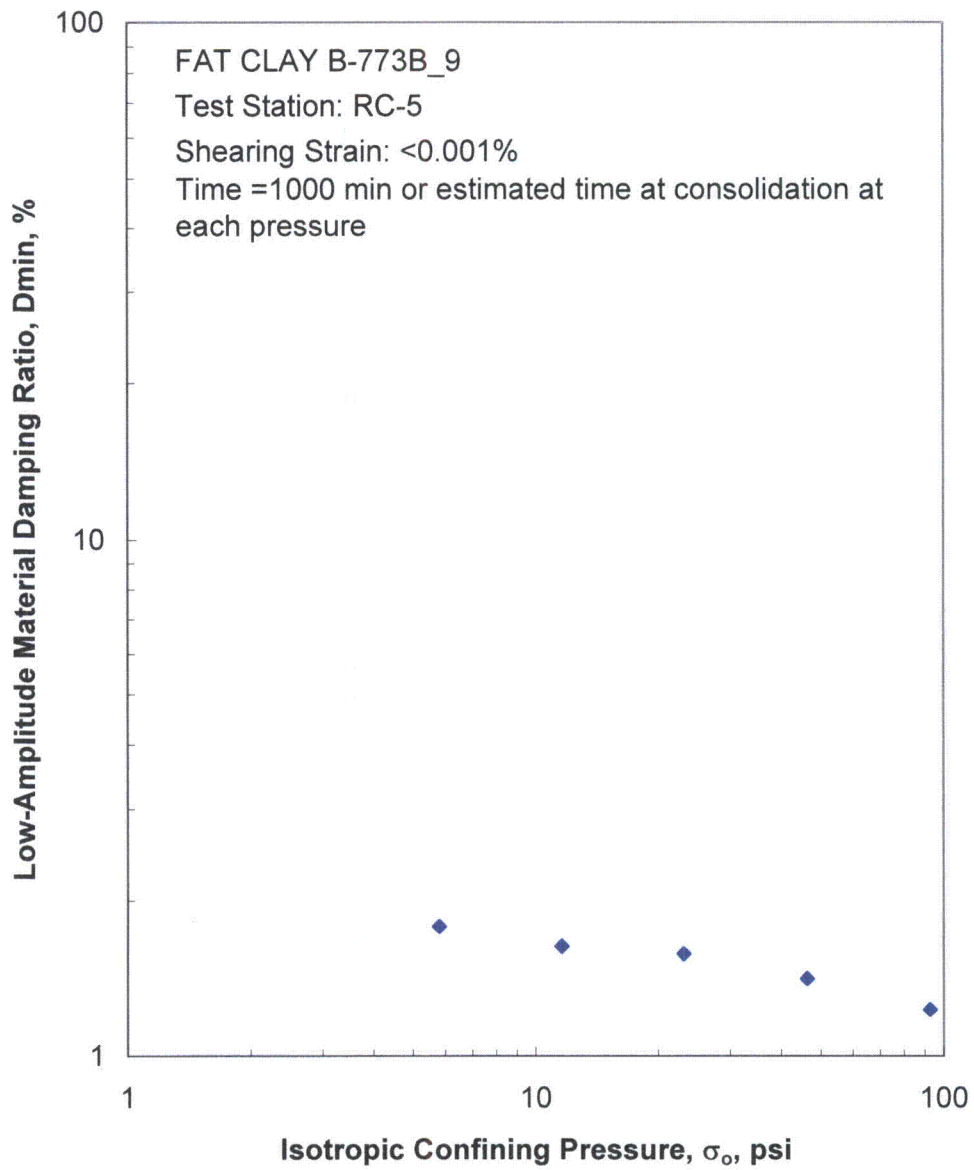


Figure G.6 Variation in Low-Amplitude Material Damping Ratio with Isotropic Confining Pressure from Resonant Column Tests

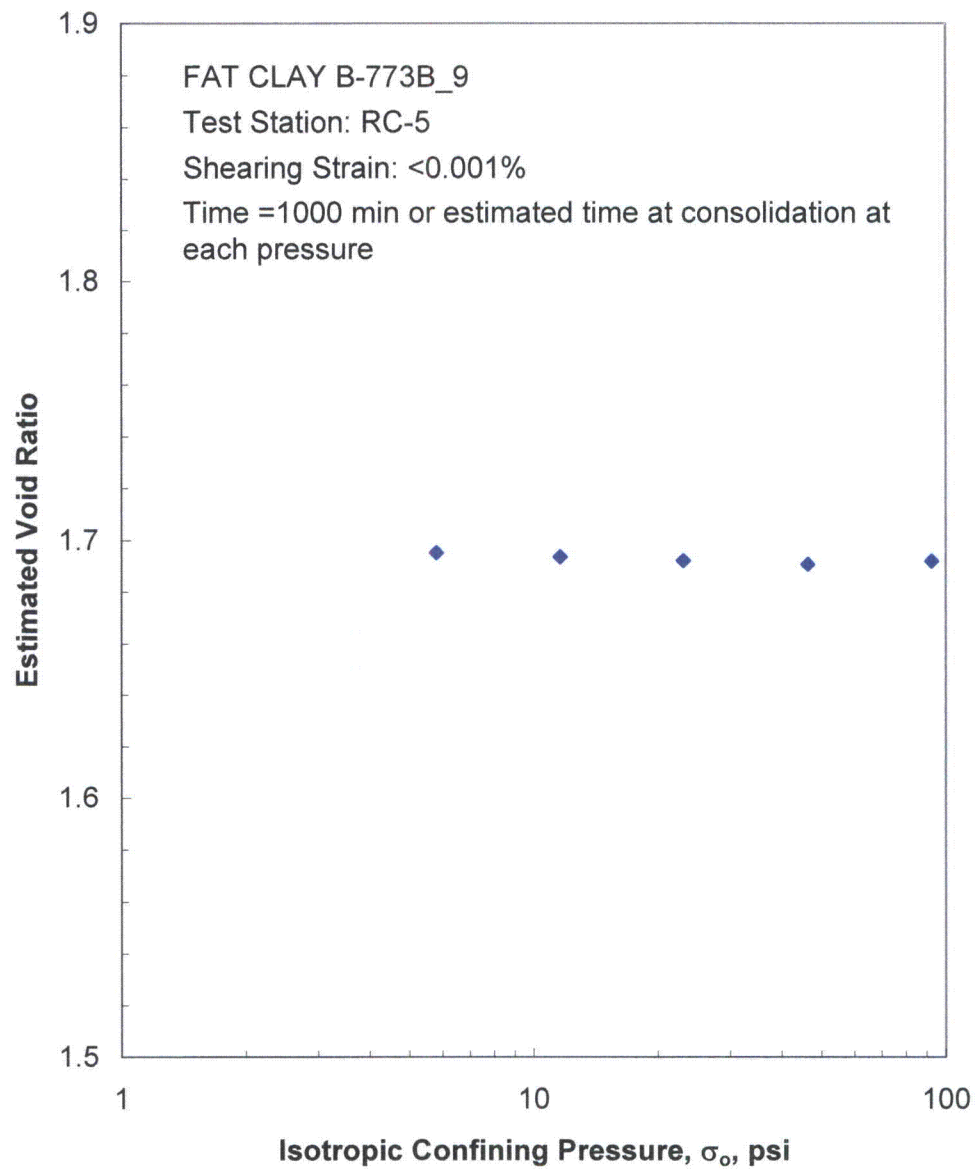


Figure G.7 Variation in Estimated Void Ratio with Isotropic Confining Pressure from Resonant Column Tests

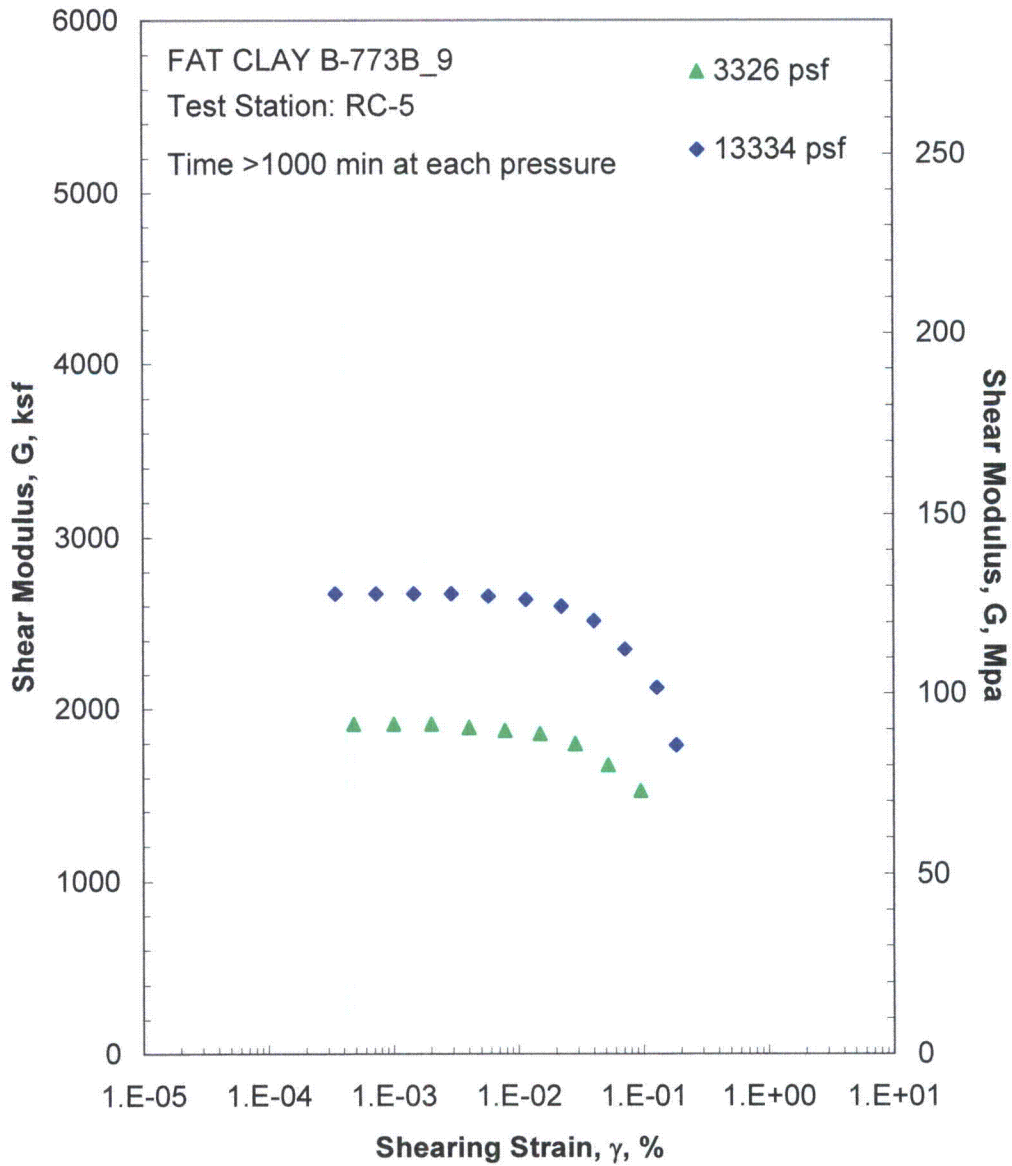


Figure G.8 Comparison of the Variation in Shear Modulus with Shearing Strain and Isotropic Confining Pressure from the Resonant Column Tests

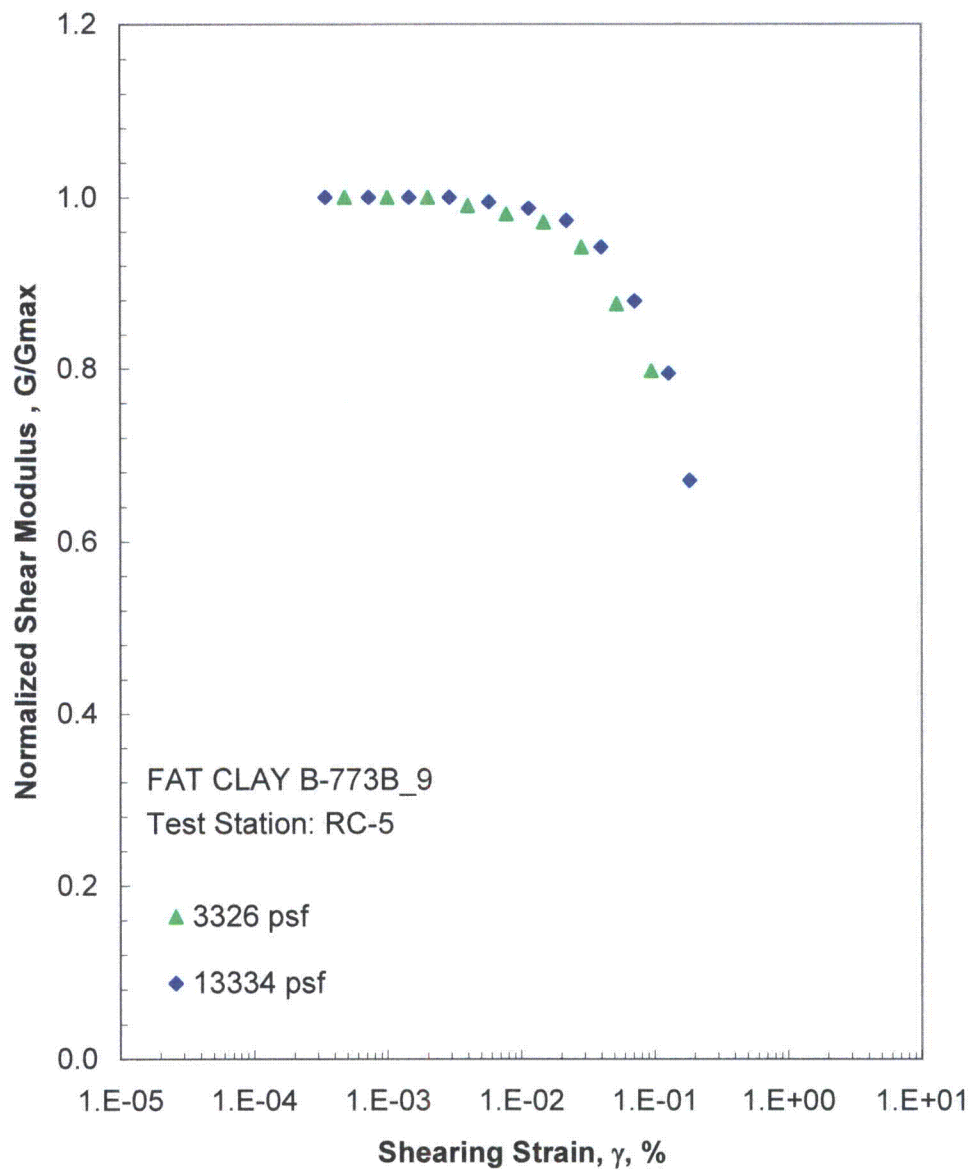


Figure G.9 Comparison of the Variation in Normalized Shear Modulus with Shearing Strain and Isotropic Confining Pressure from the Resonant Column Tests

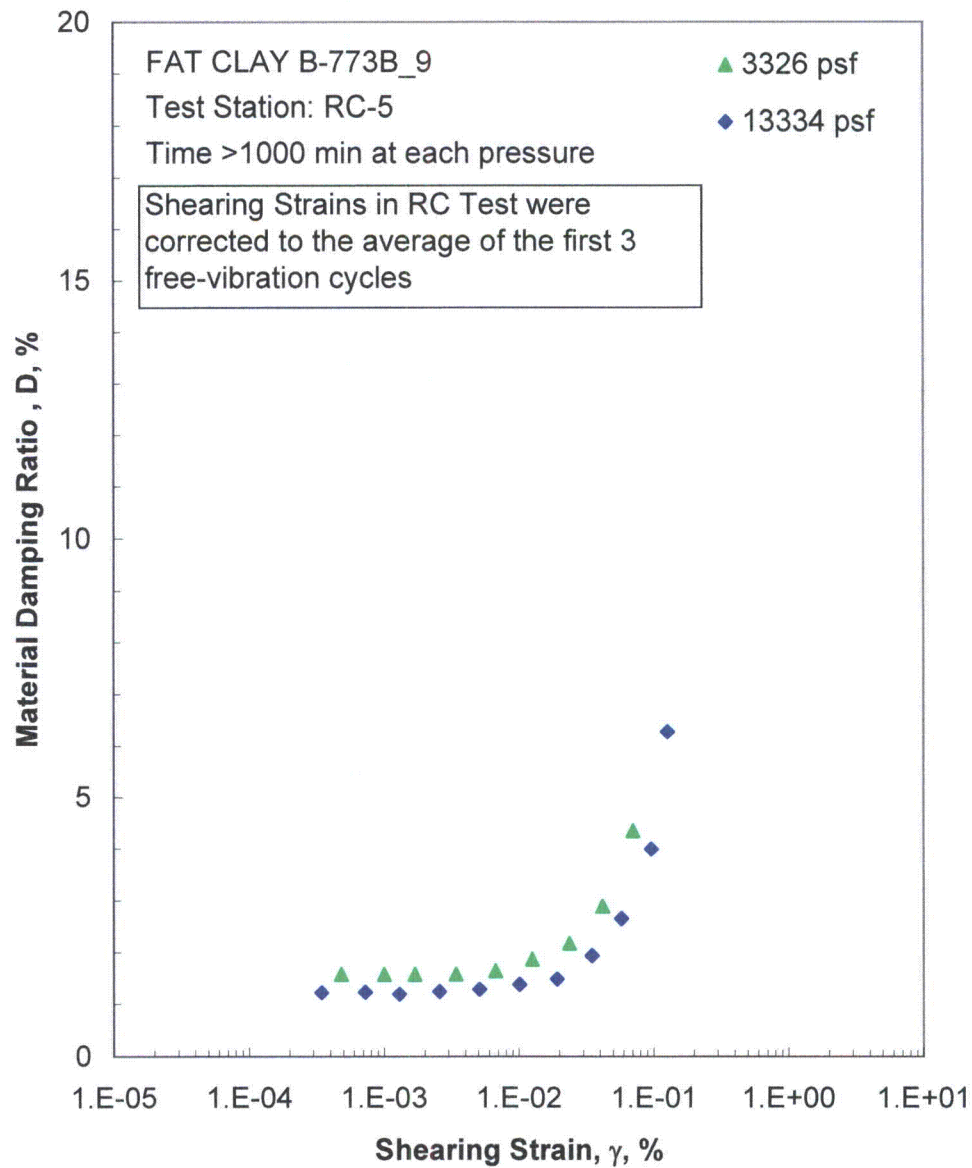


Figure G.10 Comparison of the Variation in Material Damping Ratio with Shearing Strain and Isotropic Confining Pressure from the Resonant Column Tests

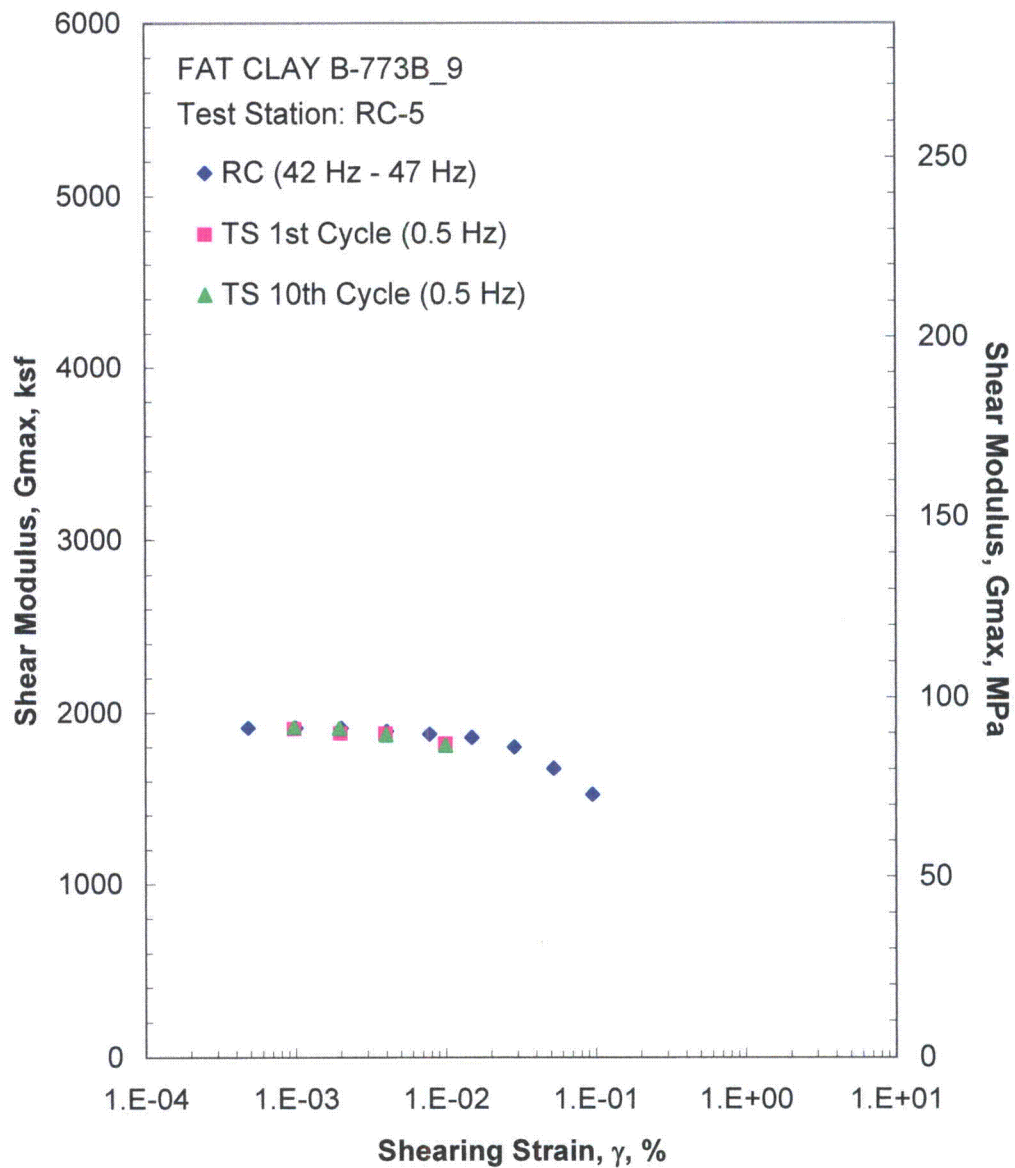


Figure G.11 Comparison of the Variation in Shear Modulus with Shearing Strain at an Isotropic Confining Pressure of 3326 psf from the Combined RCTS Tests

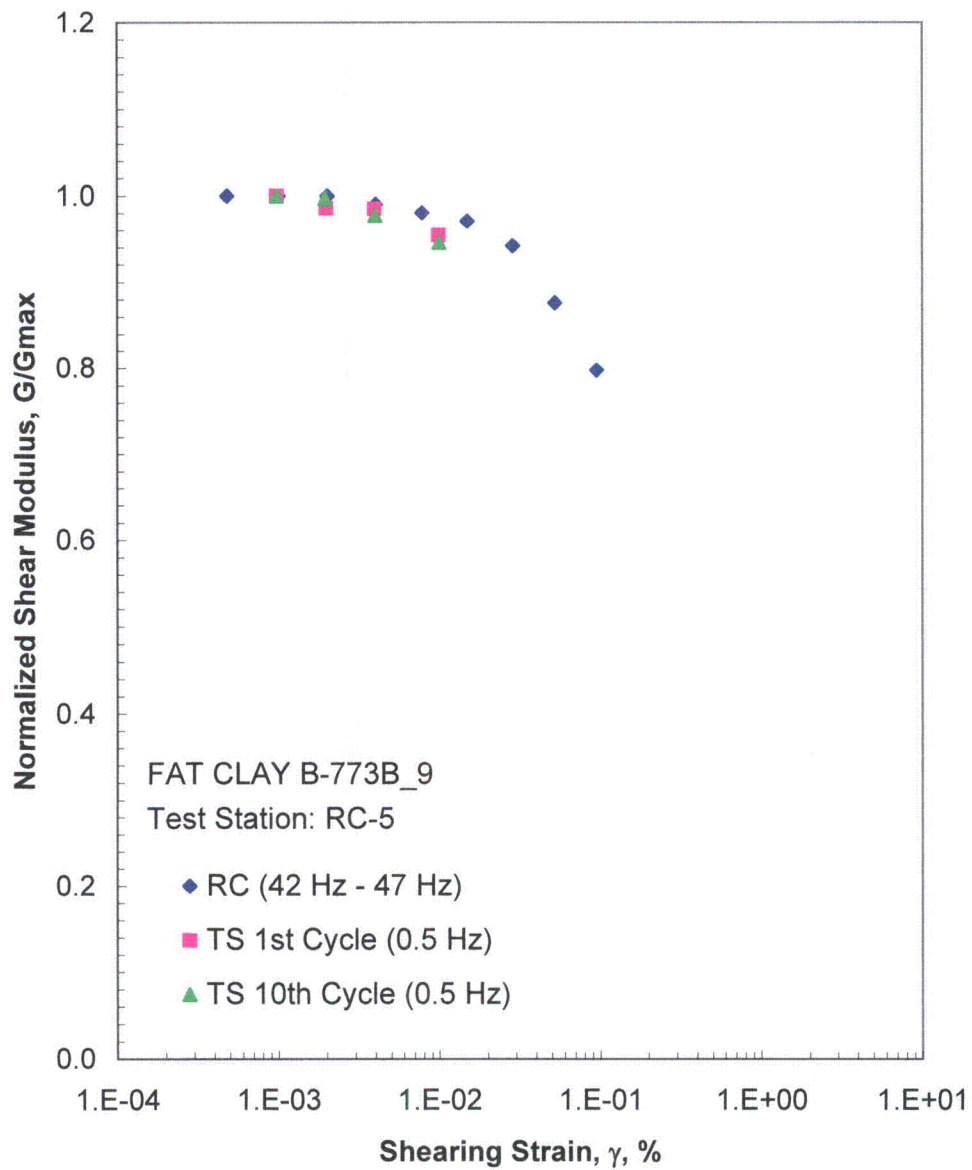


Figure G.12 Comparison of the Variation in Normalized Shear Modulus with Shearing Strain at an Isotropic Confining Pressure of 3326 psf from the Combined RCTS Tests

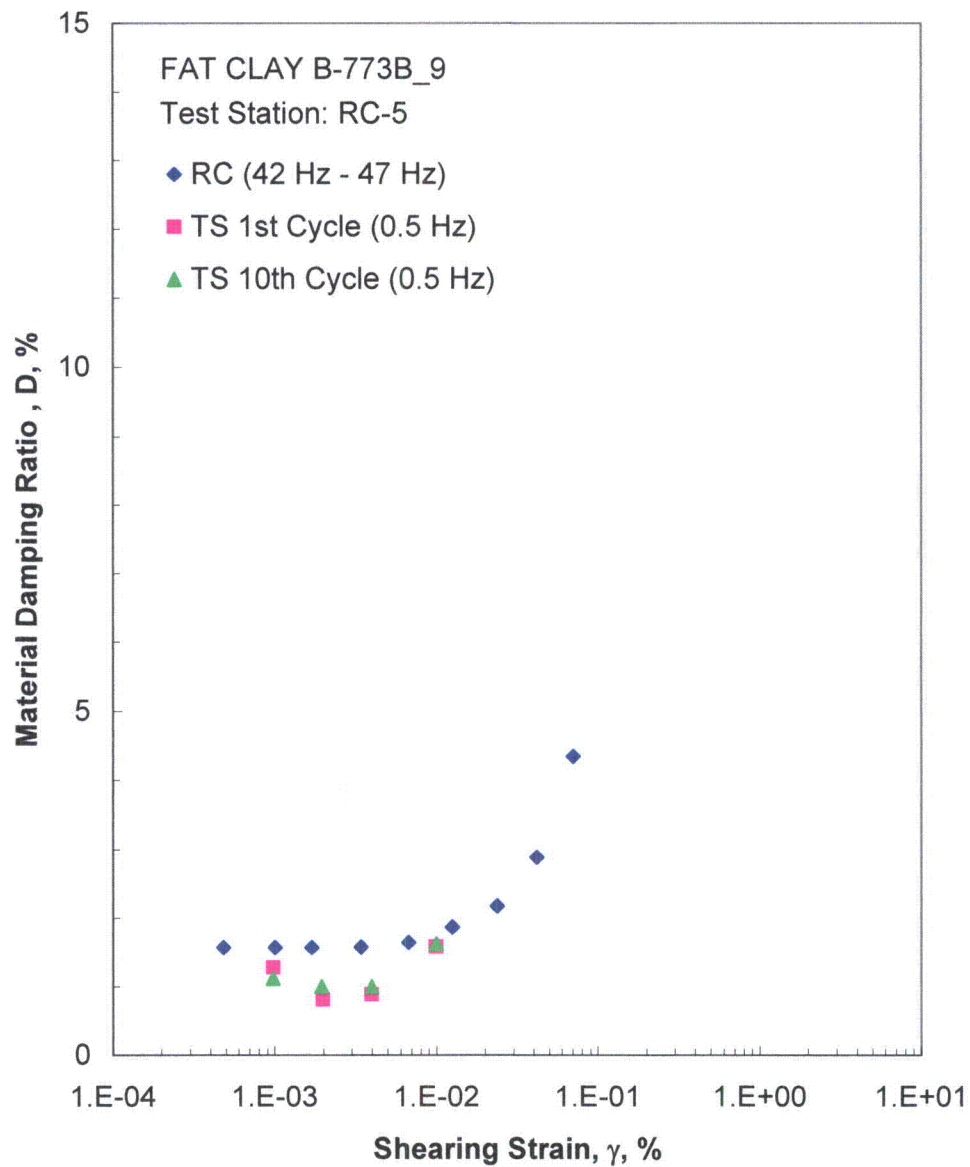


Figure G.13 Comparison of the Variation in Material Damping Ratio with Shearing Strain at an Isotropic Confining Pressure of 3326 psf from the Combined RCTS Tests

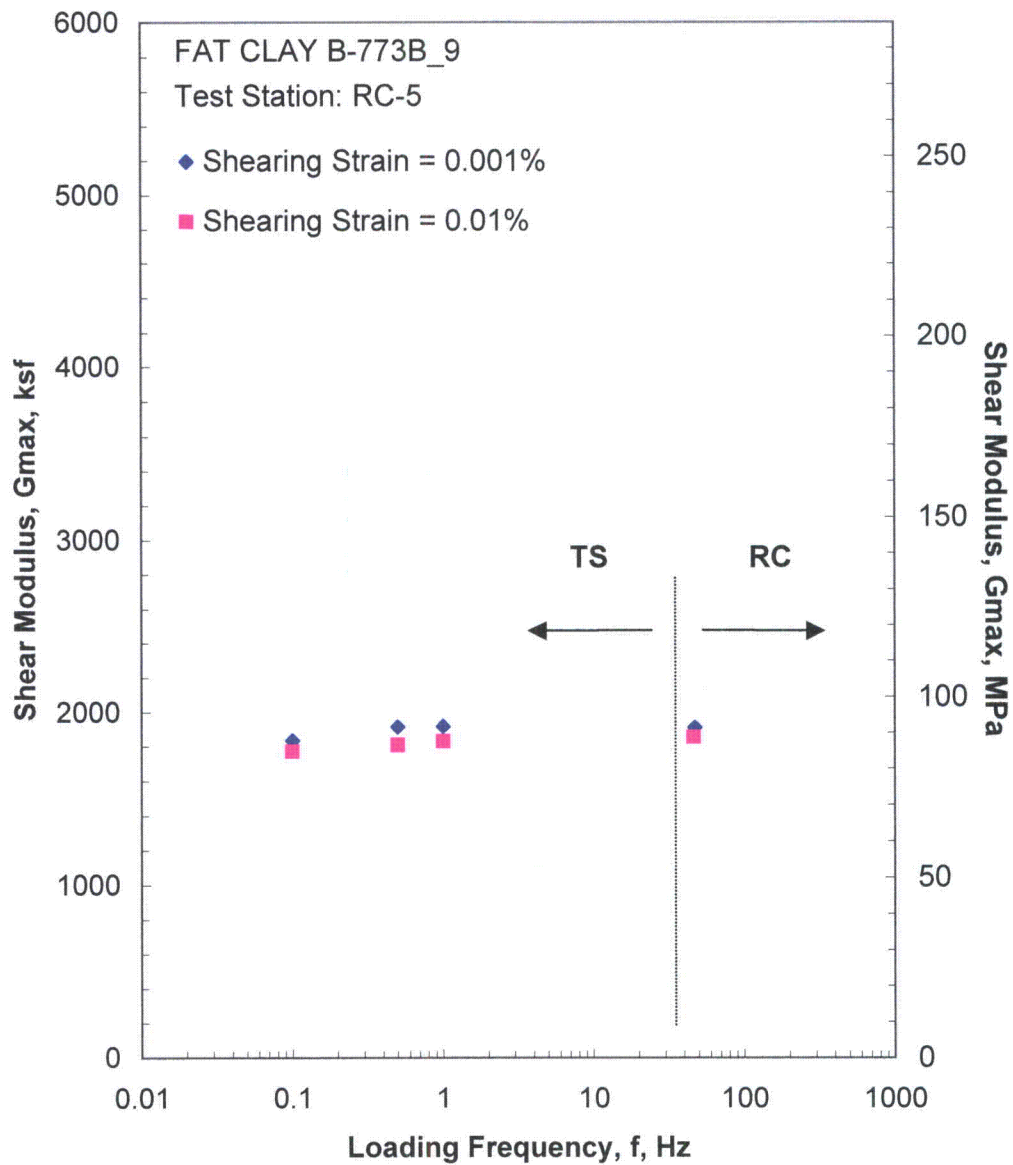


Figure G.14 Comparison of the Variation in Shear Modulus with Loading Frequency at an Isotropic Confining Pressure of 3326 psf from the Combined RCTS Tests

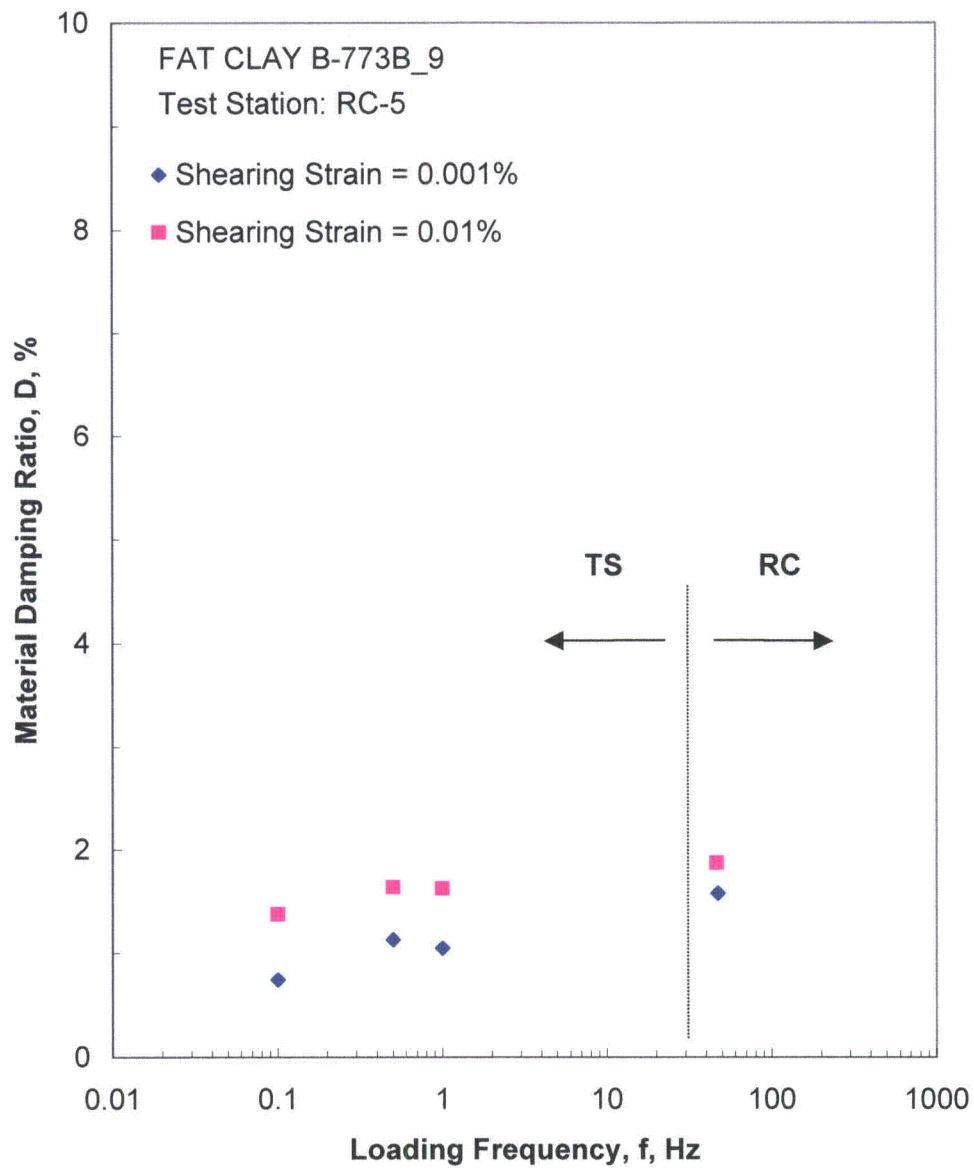


Figure G.15 Comparison of the Variation in Material Damping Ratio with Loading Frequency at an Isotropic Confining Pressure of 3326 psf from the Combined RCTS Tests

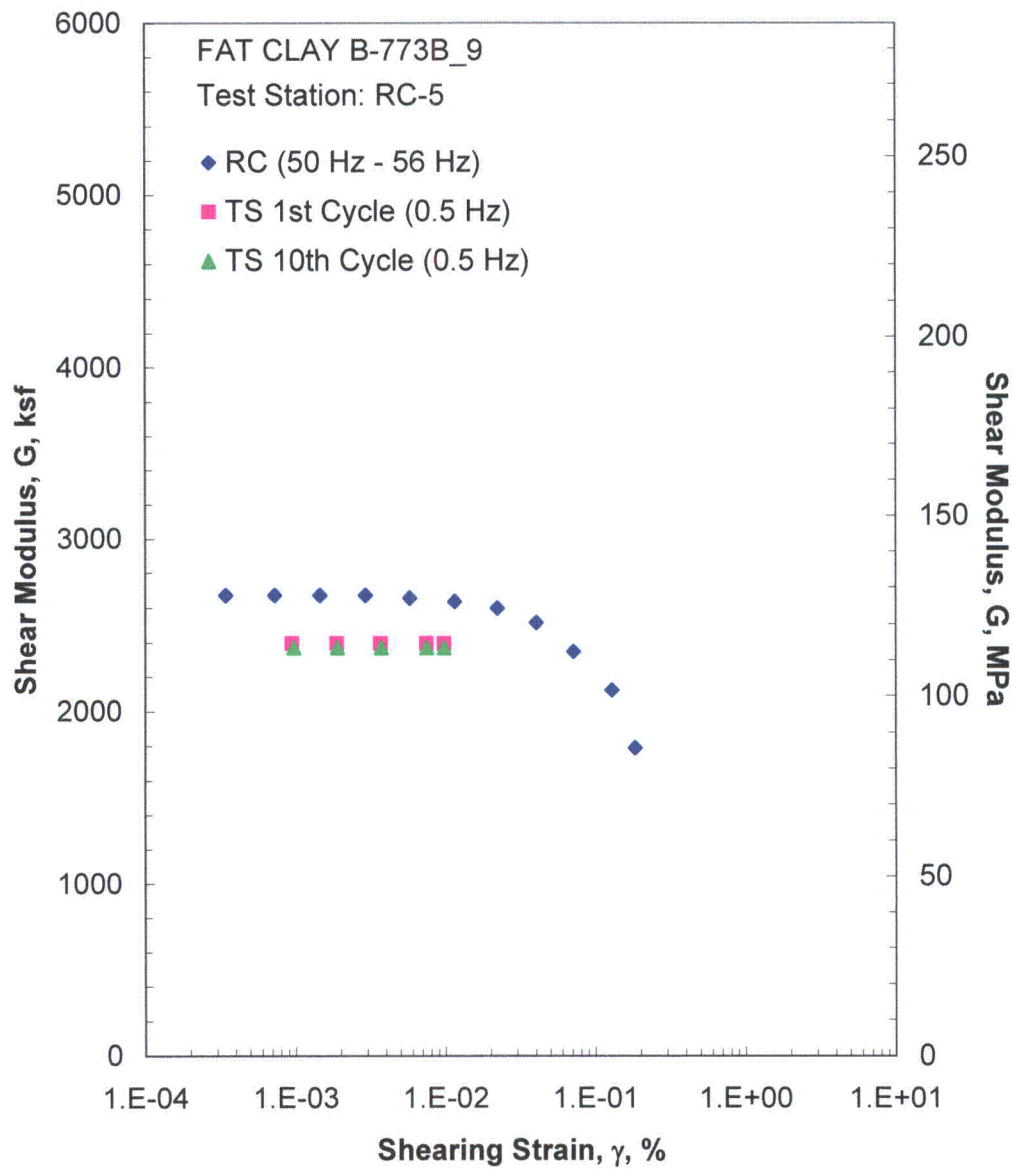


Figure G.16 Comparison of the Variation in Shear Modulus with Shearing Strain at an Isotropic Confining Pressure of 13334 psf from the Combined RCTS Tests

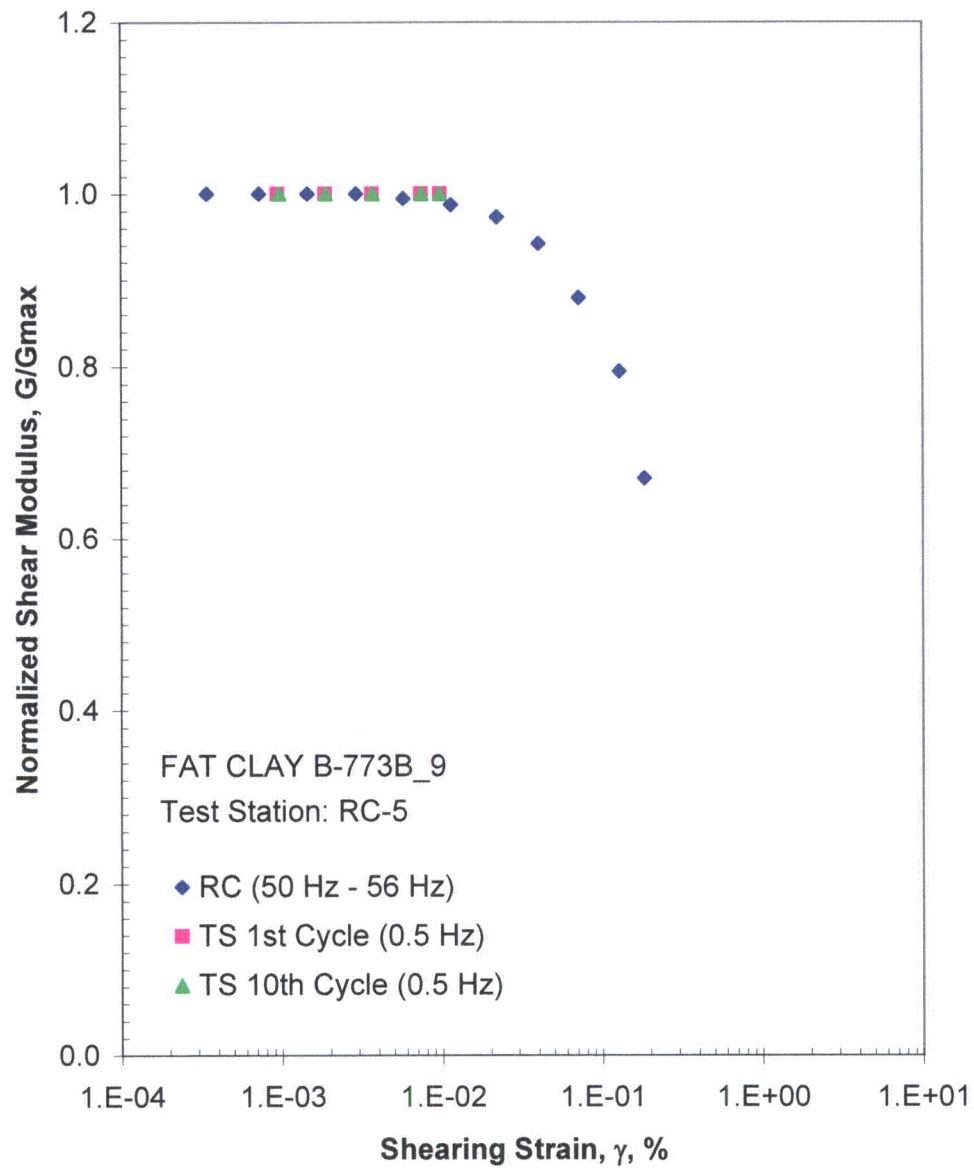


Figure G.17 Comparison of the Variation in Normalized Shear Modulus with Shearing Strain at an Isotropic Confining Pressure of 13334 psi from the Combined RCTS Tests

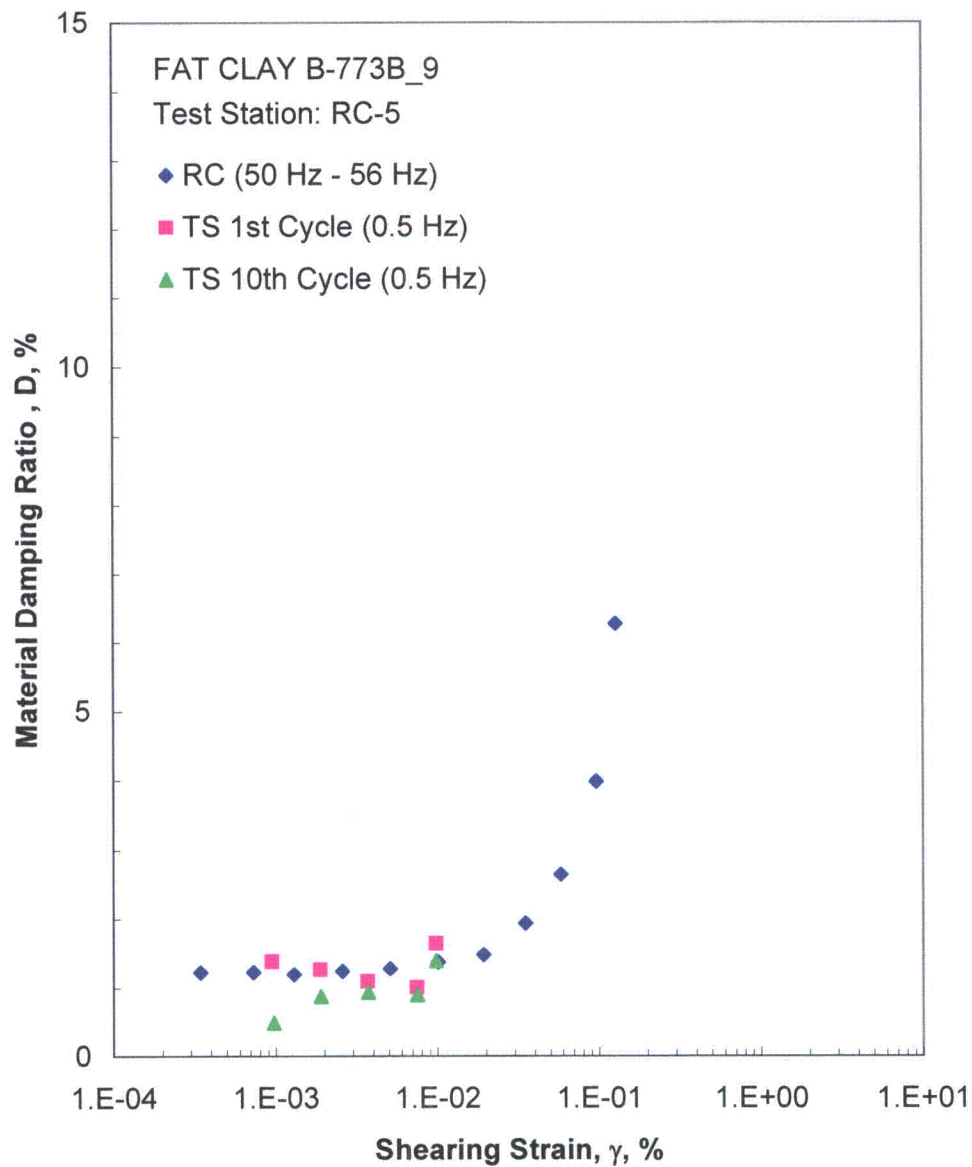


Figure G.18 Comparison of the Variation in Material Damping Ratio with Shearing Strain at an Isotropic Confining Pressure of 13334 psf from the Combined RCTS Tests

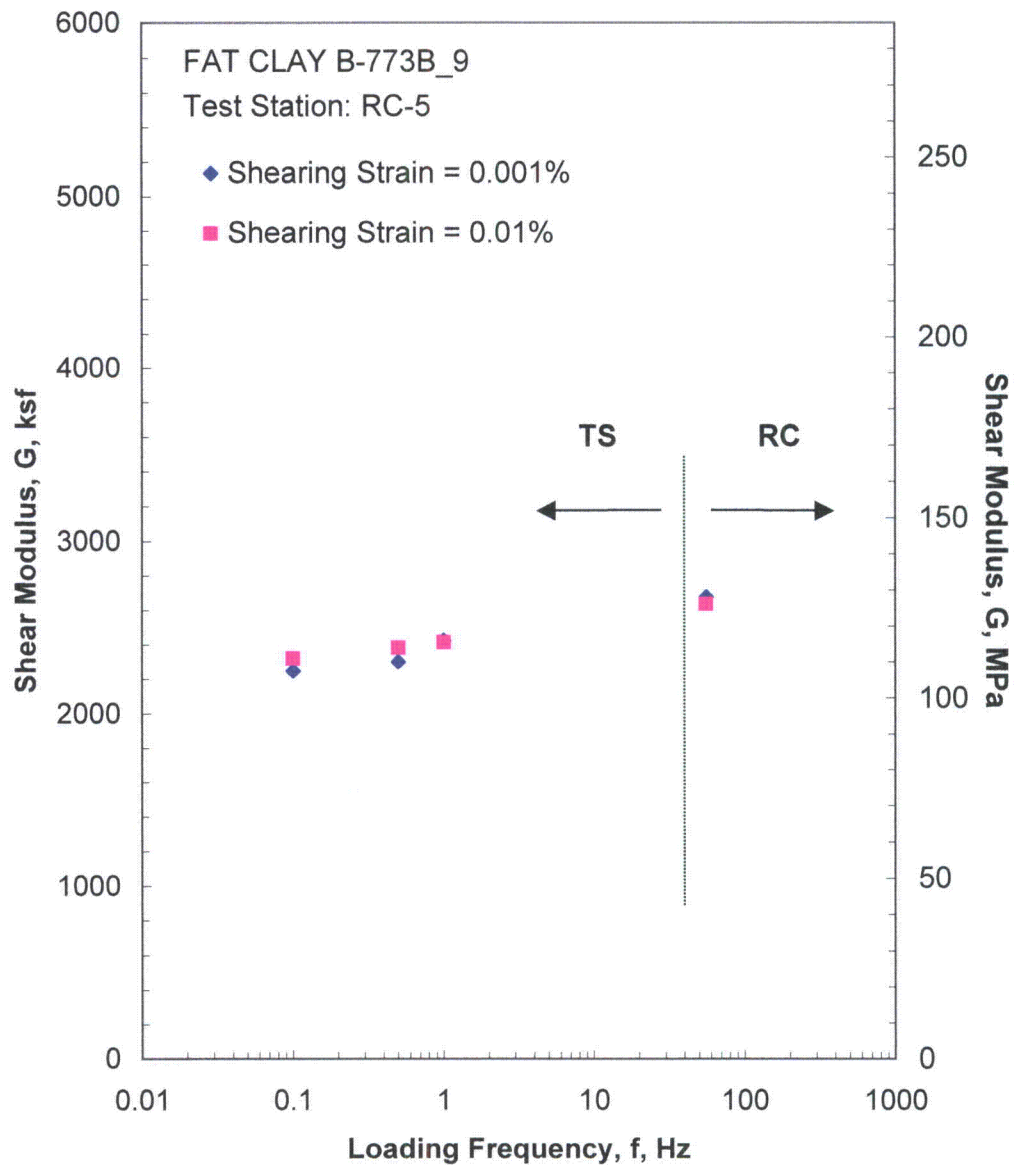


Figure G.19 Comparison of the Variation in Shear Modulus with Loading Frequency at an Isotropic Confining Pressure of 13334 psf from the Combined RCTS Tests

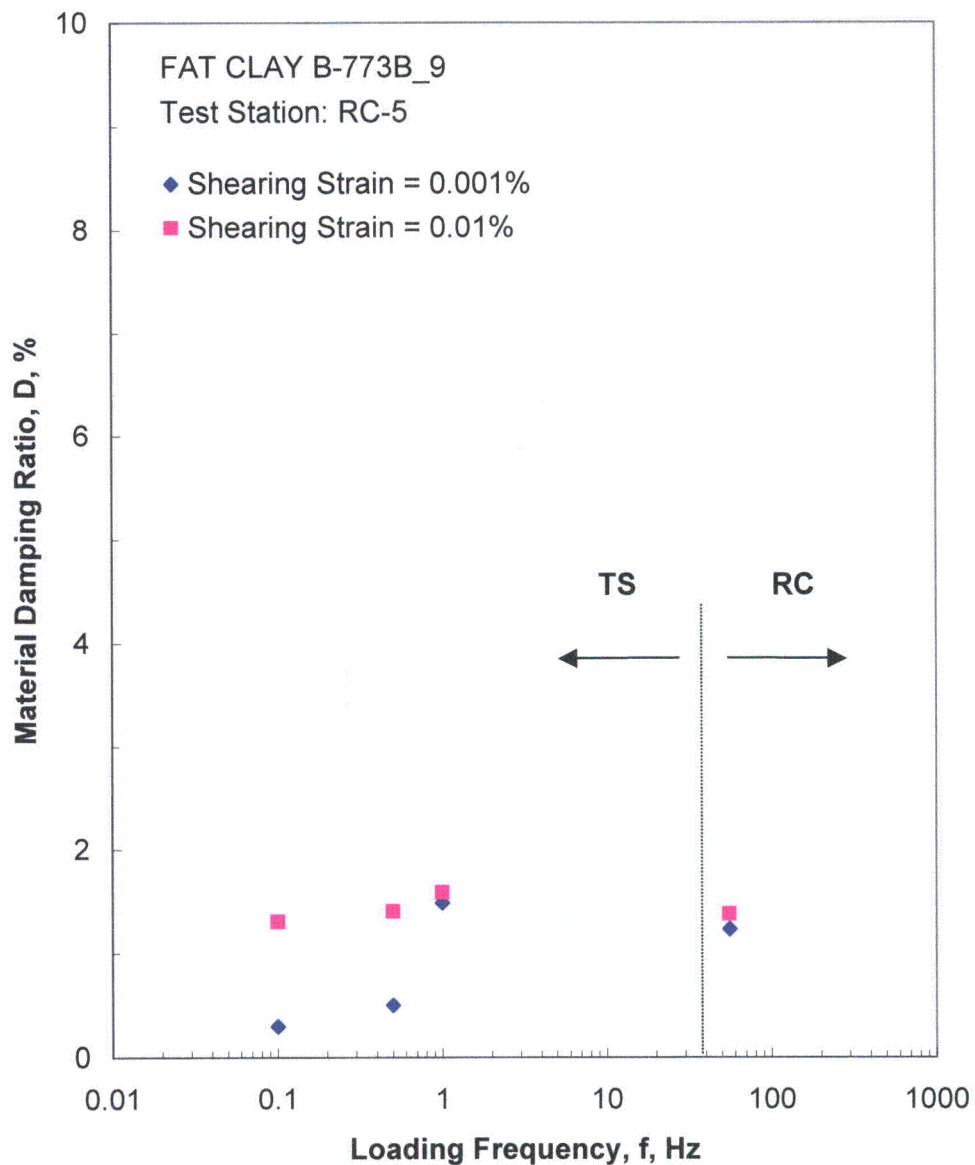


Figure G.20 Comparison of the Variation in Material Damping Ratio with Loading Frequency at an Isotropic Confining Pressure of 13334 psf from the Combined RCTS Tests

Table G.1 Variation in Low-Amplitude Shear Wave Velocity, Low-Amplitude Shear Modulus, Low-Amplitude Material Damping Ratio and Estimated Void Ratio with Isotropic Confining Pressure from RC Tests of Specimen B-773B-9

Isotropic Confining Pressure, σ_o			Low-Amplitude Shear Modulus, G_{max}		Low-Amplitude Shear Wave Velocity, V_s	Low-Amplitude Material Damping Ratio, D_{min}	Estimated Void Ratio, e
(psi)	(psf)	(kPa)	(ksf)	(MPa)	(fps)	(%)	
6	835	40	1683	81	737	1.78	1.70
12	1670	80	1755	84	753	1.63	1.69
23	3326	159	1922	92	788	1.58	1.69
46	6667	319	2207	106	844	1.42	1.69
93	13334	638	2675	128	929	1.23	1.69

Table G.2 Variation in Shear Modulus and Material Damping Ratio with Shearing Strain from RC Tests of Specimen B-773B-9; Isotropic Confining Pressure, $\sigma_o = 3326$ psf

Peak Shearing Strain, %	Shear Modulus, G, ksf	Normalized Shear Modulus, G/G_{max}	Average ⁺ Shearing Strain, %	Material Damping Ratio ^x , D, %
4.81E-04	1910	1.00	4.81E-04	1.58
1.00E-03	1910	1.00	1.00E-03	1.58
2.01E-03	1910	1.00	1.69E-03	1.58
4.02E-03	1892	0.99	3.41E-03	1.58
7.80E-03	1873	0.98	6.71E-03	1.65
1.49E-02	1854	0.97	1.25E-02	1.87
2.86E-02	1799	0.94	2.37E-02	2.18
5.23E-02	1674	0.88	4.19E-02	2.89
9.51E-02	1523	0.80	7.04E-02	4.34

⁺ Average Shearing Strain from the First Three Cycles of the Free Vibration Decay Curve

^x Average Damping Ratio from the First Three Cycles of the Free Vibration Decay Curve

Table G.3 Variation in Shear Modulus, Normalized Shear Modulus and Material Damping Ratio with Shearing Strain from TS Tests of Specimen B-773B-9; Isotropic Confining Pressure, $\sigma_o = 3326$ psf

First Cycle				Tenth Cycle			
Peak Shearing Strain, %	Shear Modulus, G, ksf	Normalized Shear Modulus, G/G_{max}	Material Damping Ratio, D, %	Peak Shearing Strain, %	Shear Modulus, G, ksf	Normalized Shear Modulus, G/G_{max}	Material Damping Ratio, D, %
9.79E-04	1906	1.00	1.28	9.74E-04	1914	1.00	1.12
1.98E-03	1879	0.99	0.81	1.95E-03	1908	1.00	1.00
3.97E-03	1877	0.99	0.89	3.98E-03	1870	0.98	1.00
9.92E-03	1818	0.95	1.59	9.97E-03	1809	0.95	1.63

Table G.4 Variation in Shear Modulus and Material Damping Ratio with Shearing Strain from RC Tests of Specimen B-773B-9; Isotropic Confining Pressure, $\sigma_0 = 13334$ psf

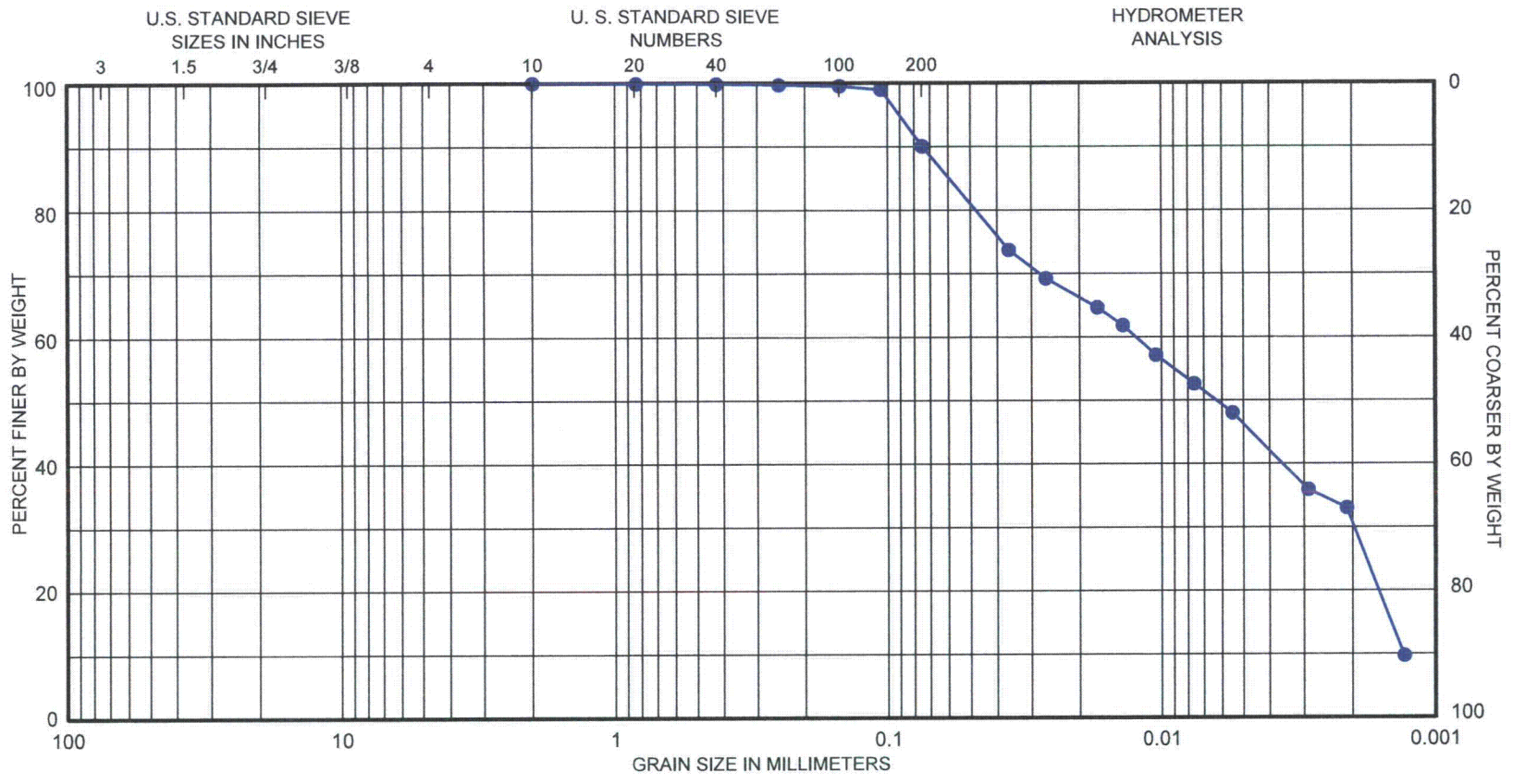
Peak Shearing Strain, %	Shear Modulus, G, ksf	Normalized Shear Modulus, G/G_{max}	Average ⁺ Shearing Strain, %	Material Damping Ratio ^x , D, %
3.44E-04	2671	1.00	3.44E-04	1.23
7.27E-04	2671	1.00	7.27E-04	1.23
1.46E-03	2671	1.00	1.30E-03	1.19
2.92E-03	2671	1.00	2.57E-03	1.24
5.78E-03	2656	0.99	5.09E-03	1.28
1.15E-02	2637	0.99	1.01E-02	1.38
2.21E-02	2599	0.97	1.92E-02	1.49
4.02E-02	2515	0.94	3.50E-02	1.94
7.14E-02	2348	0.88	5.78E-02	2.65
1.28E-01	2122	0.79	9.61E-02	3.99
1.84E-01	1790	0.67	1.27E-01	6.27

⁺ Average Shearing Strain from the First Three Cycles of the Free Vibration Decay Curve

^x Average Damping Ratio from the First Three Cycles of the Free Vibration Decay Curve

Table G.5 Variation in Shear Modulus, Normalized Shear Modulus and Material Damping Ratio with Shearing Strain from TS Tests of Specimen B-773B-9; Isotropic Confining Pressure, $\sigma_o = 13334$ psf

First Cycle				Tenth Cycle			
Peak Shearing Strain, %	Shear Modulus, G, ksf	Normalized Shear Modulus, G/G_{max}	Material Damping Ratio, D, %	Peak Shearing Strain, %	Shear Modulus, G, ksf	Normalized Shear Modulus, G/G_{max}	Material Damping Ratio, D, %
9.44E-04	2395	1.00	1.39	9.74E-04	2369	1.00	0.49
1.89E-03	2395	1.00	1.27	1.90E-03	2369	1.00	0.88
3.69E-03	2395	1.00	1.10	3.72E-03	2369	1.00	0.94
7.43E-03	2395	1.00	1.01	7.48E-03	2369	1.00	0.90
9.76E-03	2395	1.00	1.65	9.77E-03	2369	1.00	1.40



GRAVEL		SAND			SILT or CLAY		
Coarse	Fine	Coarse	Medium	Fine			
<u>SYMBOL</u>	<u>BORING</u>	<u>DEPTH, FT</u>	<u>C_c</u>	<u>C_u</u>	<u>D₅₀</u>	<u>D₉₀</u>	<u>CLASSIFICATION</u>
●	B-773B-9	87	0.24	9.54	0.01	0.07	Fat Clay (CH), olive gray

GRAIN SIZE CURVE



APPENDIX H

Specimen B-773B_11

Borehole B-773B

Sample 11

Depth = 107 ft (32.6 m)

Total Unit Weight = 102.5 lb/ft³

Water Content = 55.1 %

FUGRO JOB #: 0411-09-1734
Testing Station: RC6



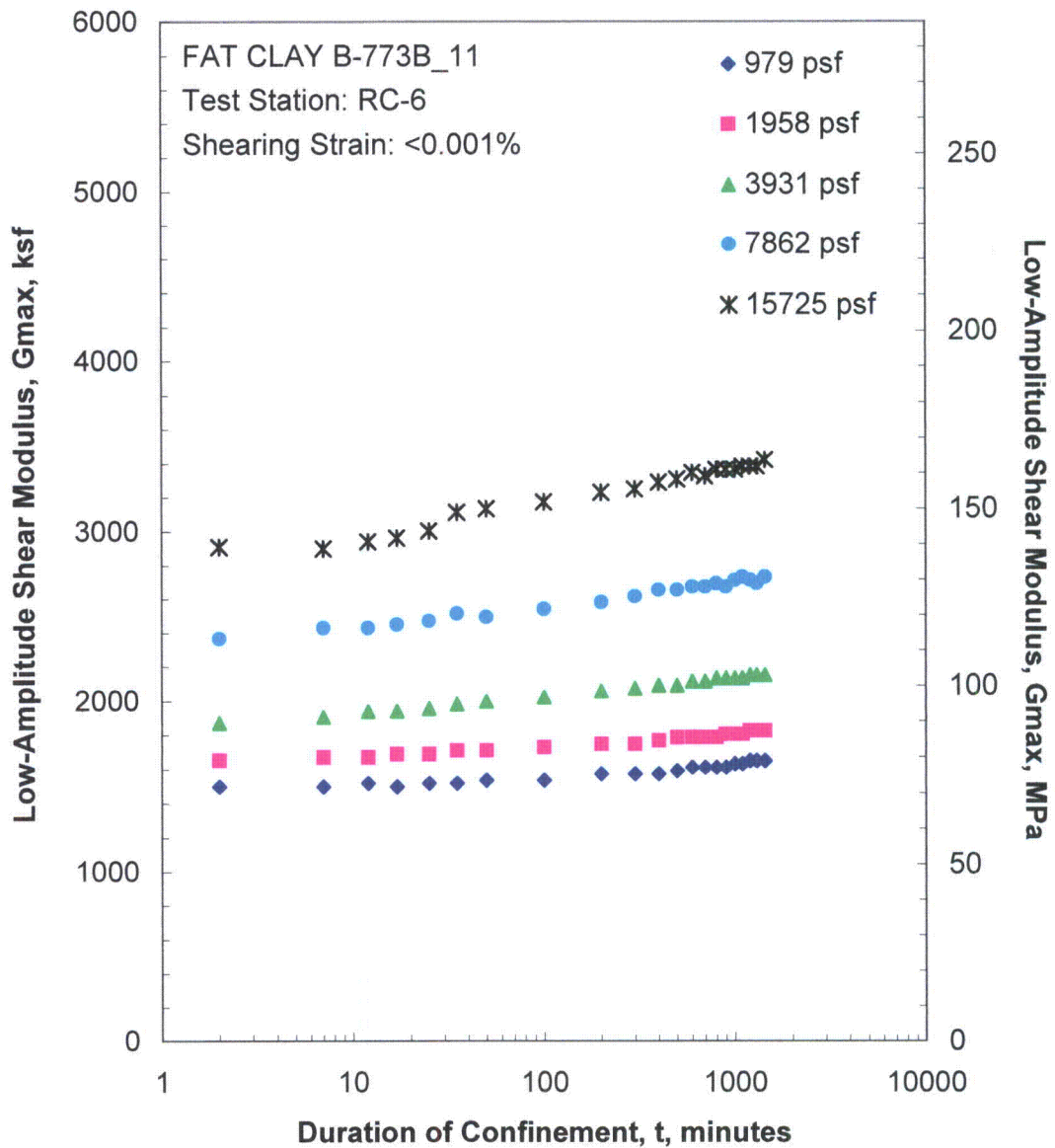


Figure G.1 Variation in Low-Amplitude Shear Modulus with Magnitude and Duration of Isotropic Confining Pressure from Resonant Column Tests

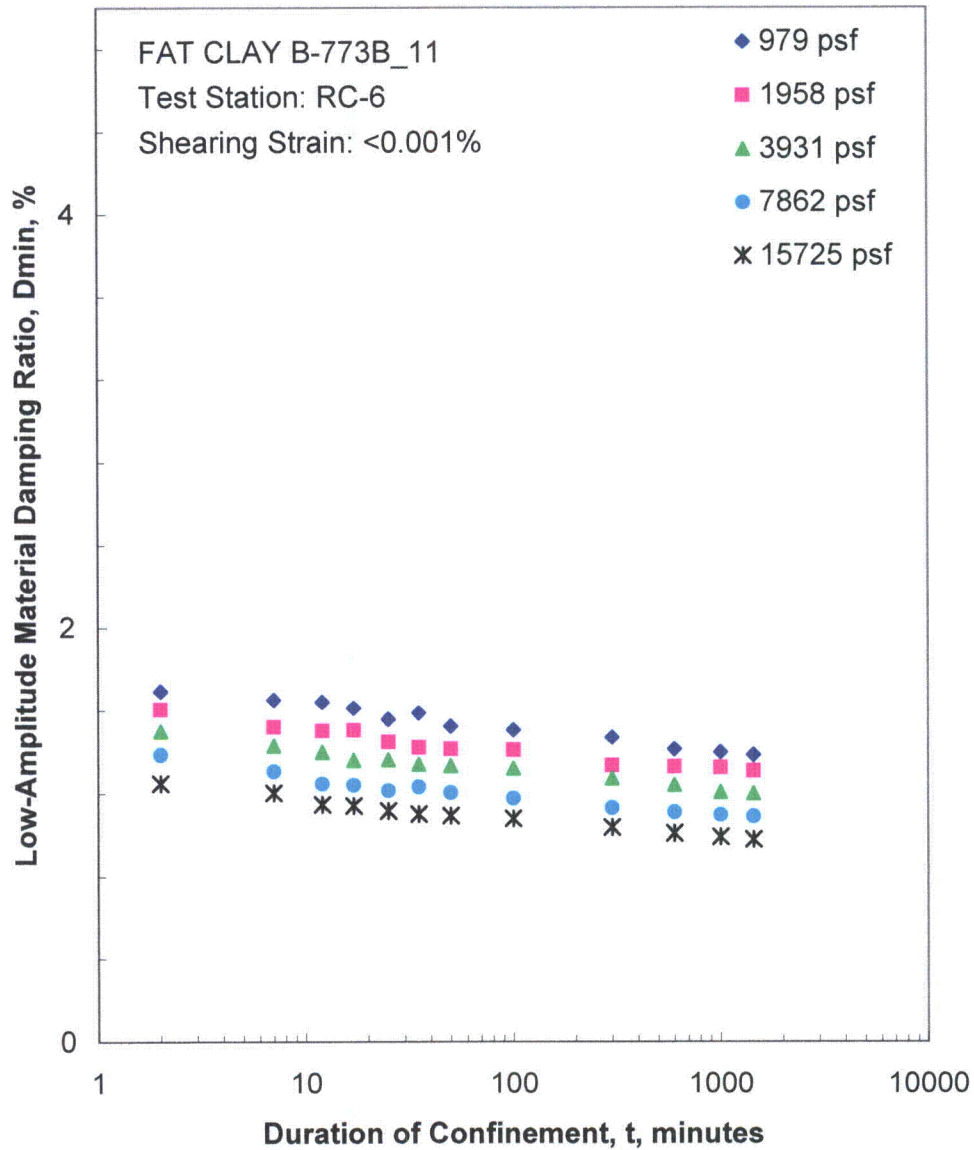


Figure G.2 Variation in Low-Amplitude Material Damping Ratio with Magnitude and Duration of Isotropic Confining Pressure from Resonant Column Tests

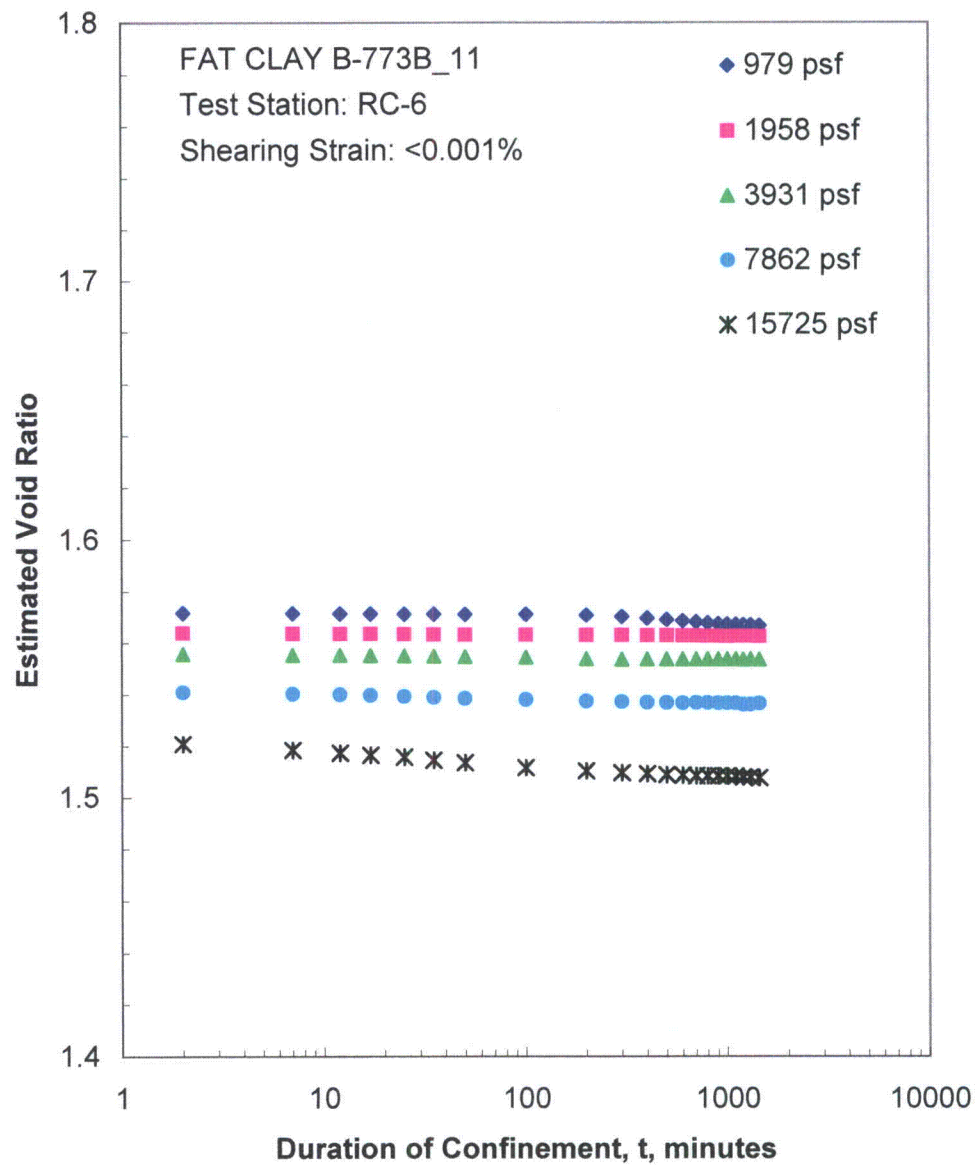


Figure G.3 Variation in Estimated Void Ratio with Magnitude and Duration of Isotropic Confining Pressure from Resonant Column Tests

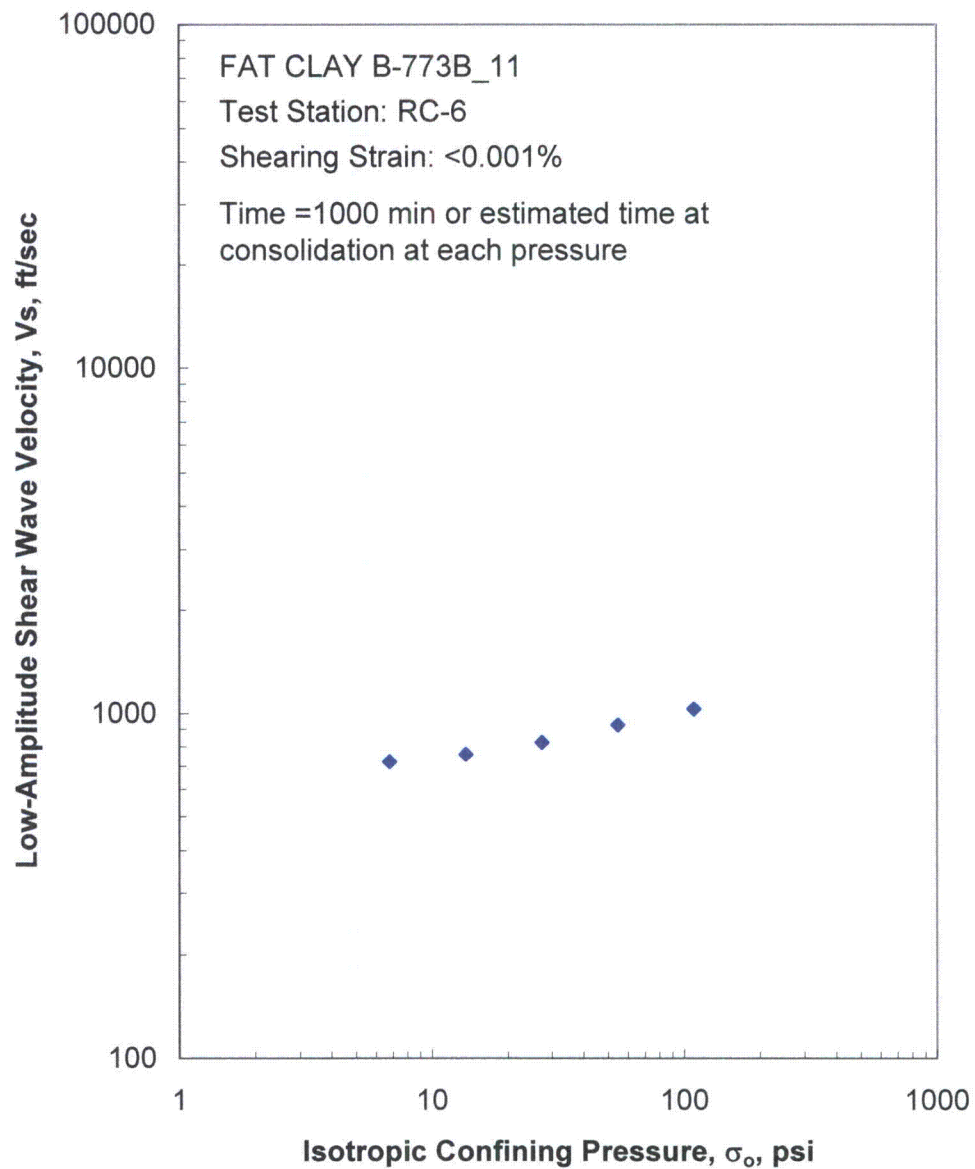


Figure G.4 Variation in Low-Amplitude Shear Wave Velocity with Isotropic Confining Pressure from Resonant Column Tests

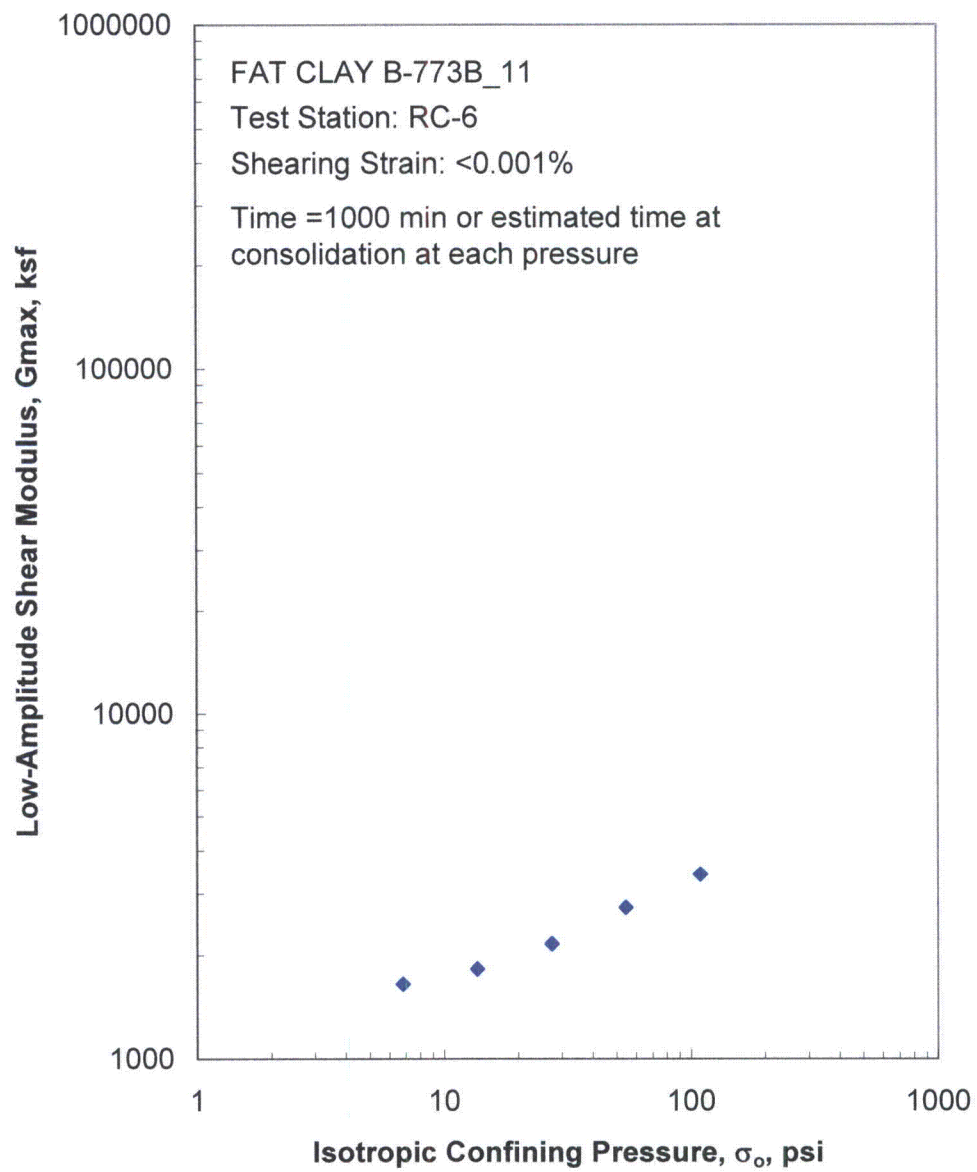


Figure G.5 Variation in Low-Amplitude Shear Modulus with Isotropic Confining Pressure from Resonant Column Tests

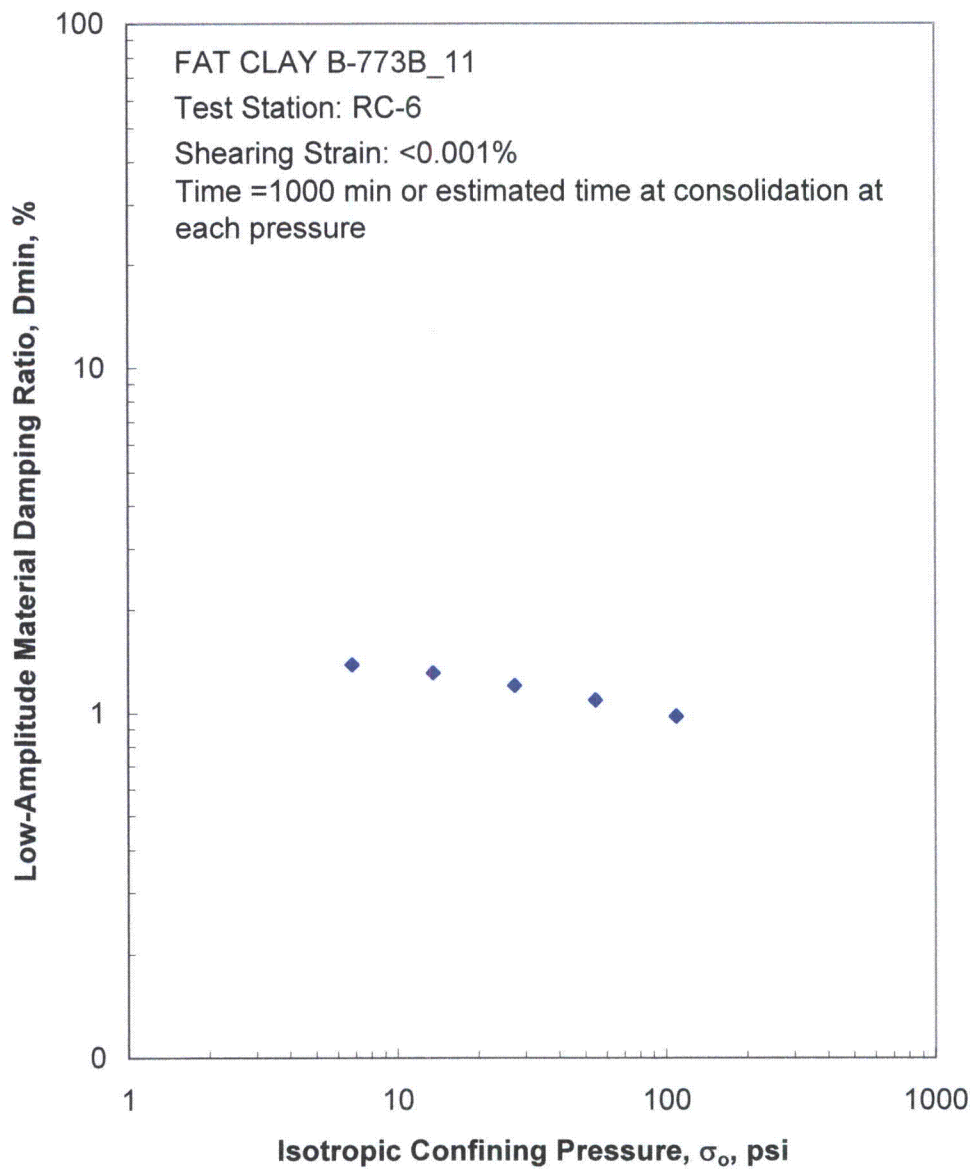


Figure G.6 Variation in Low-Amplitude Material Damping Ratio with Isotropic Confining Pressure from Resonant Column Tests

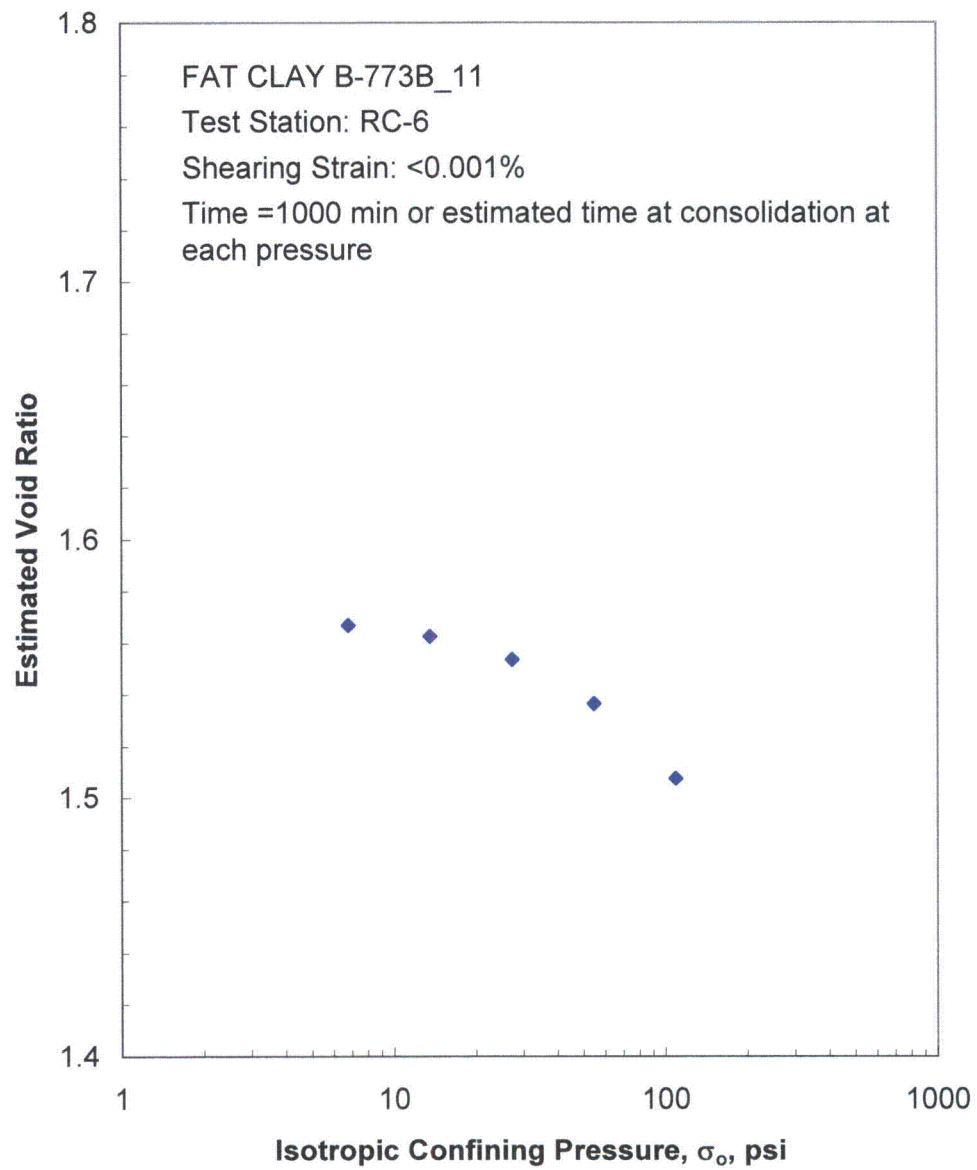


Figure G.7 Variation in Estimated Void Ratio with Isotropic Confining Pressure from Resonant Column Tests

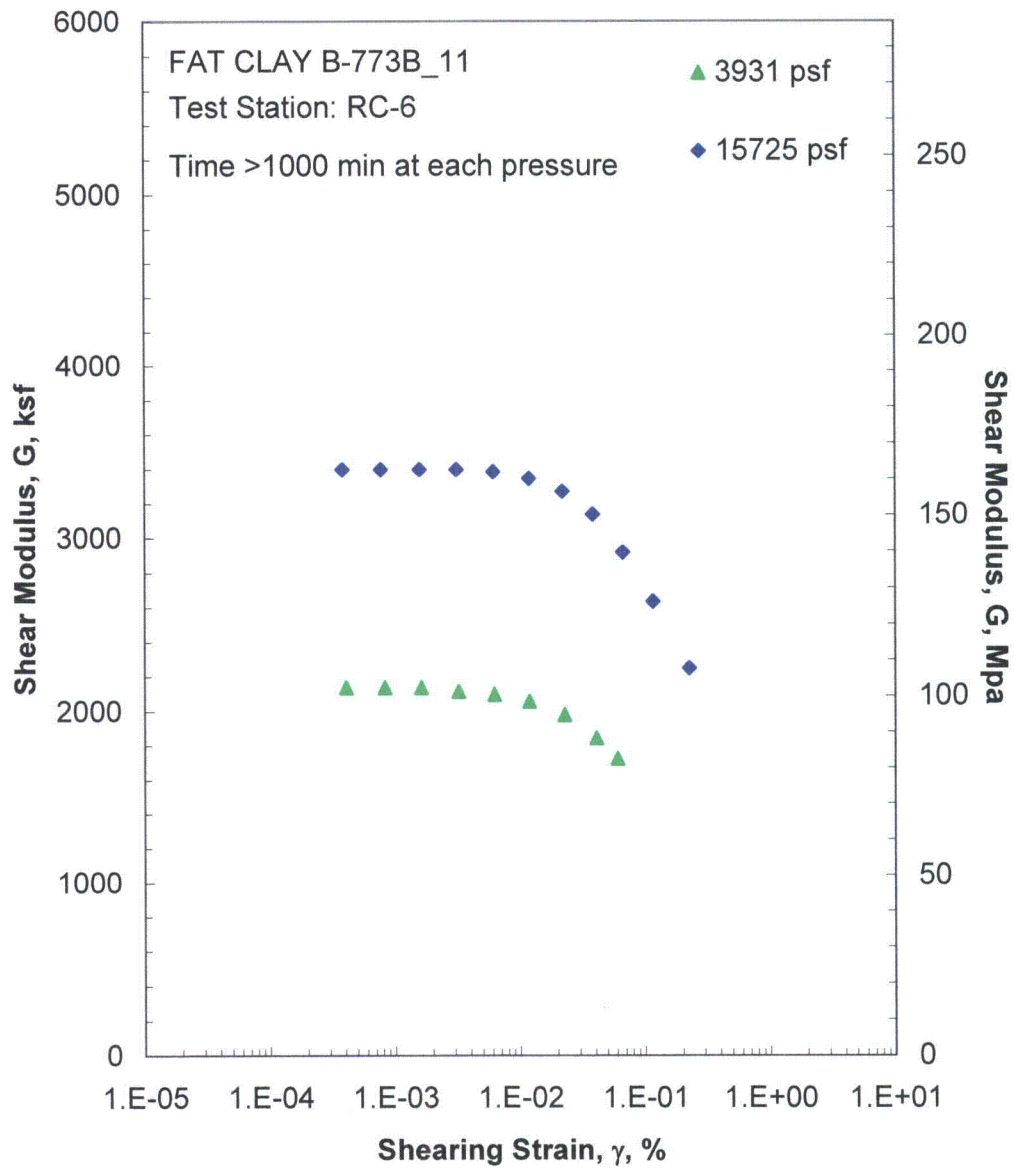


Figure G.8 Comparison of the Variation in Shear Modulus with Shearing Strain and Isotropic Confining Pressure from the Resonant Column Tests

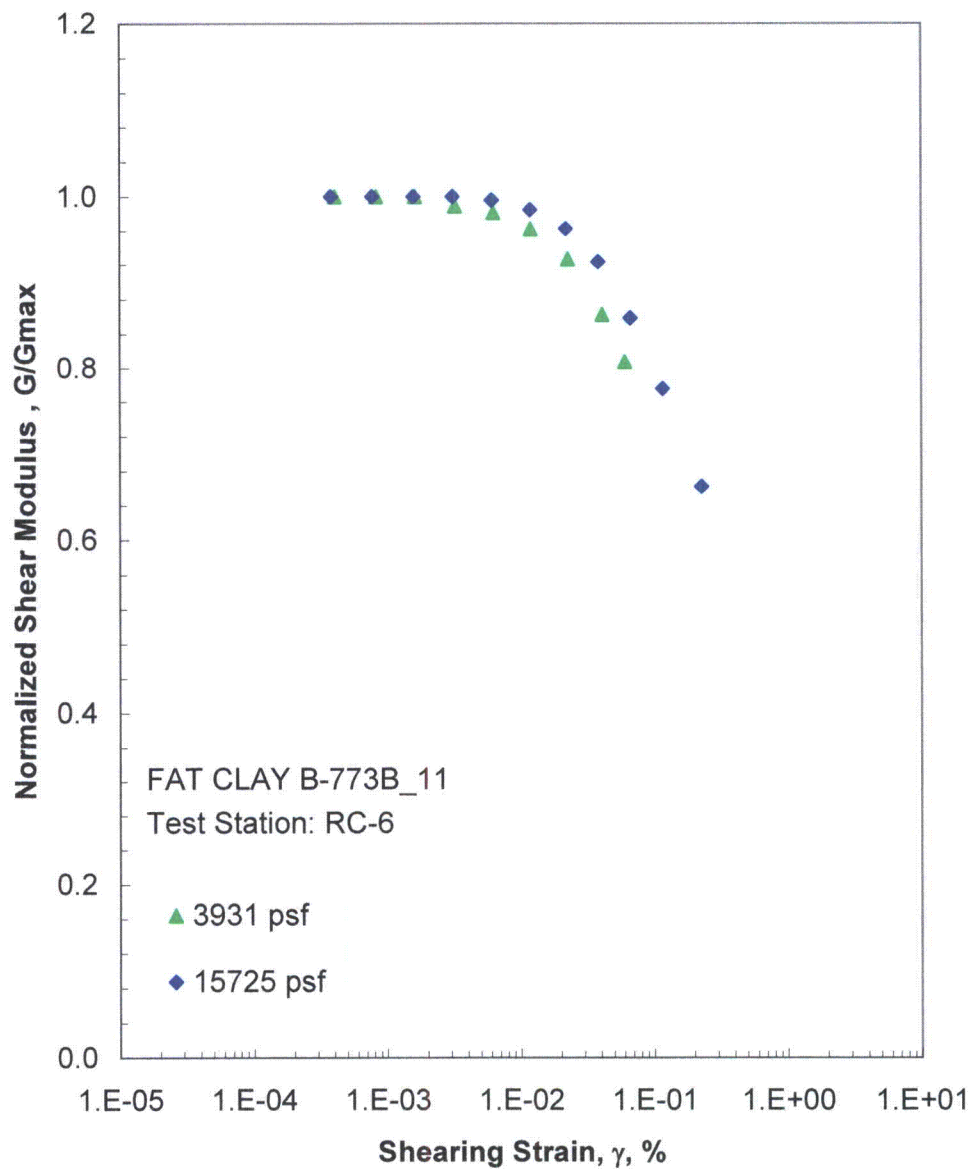


Figure G.9 Comparison of the Variation in Normalized Shear Modulus with Shearing Strain and Isotropic Confining Pressure from the Resonant Column Tests

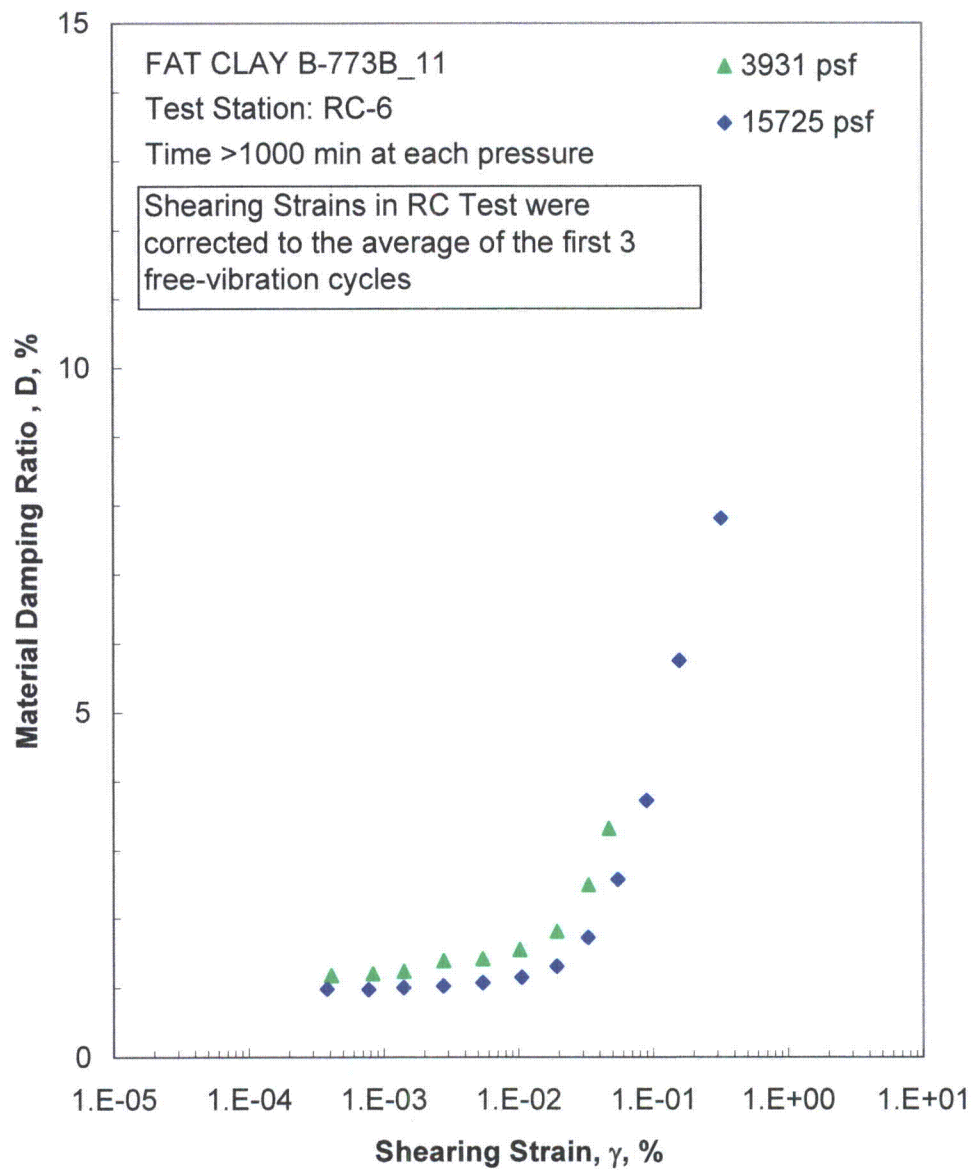


Figure G.10 Comparison of the Variation in Material Damping Ratio with Shearing Strain and Isotropic Confining Pressure from the Resonant Column Tests

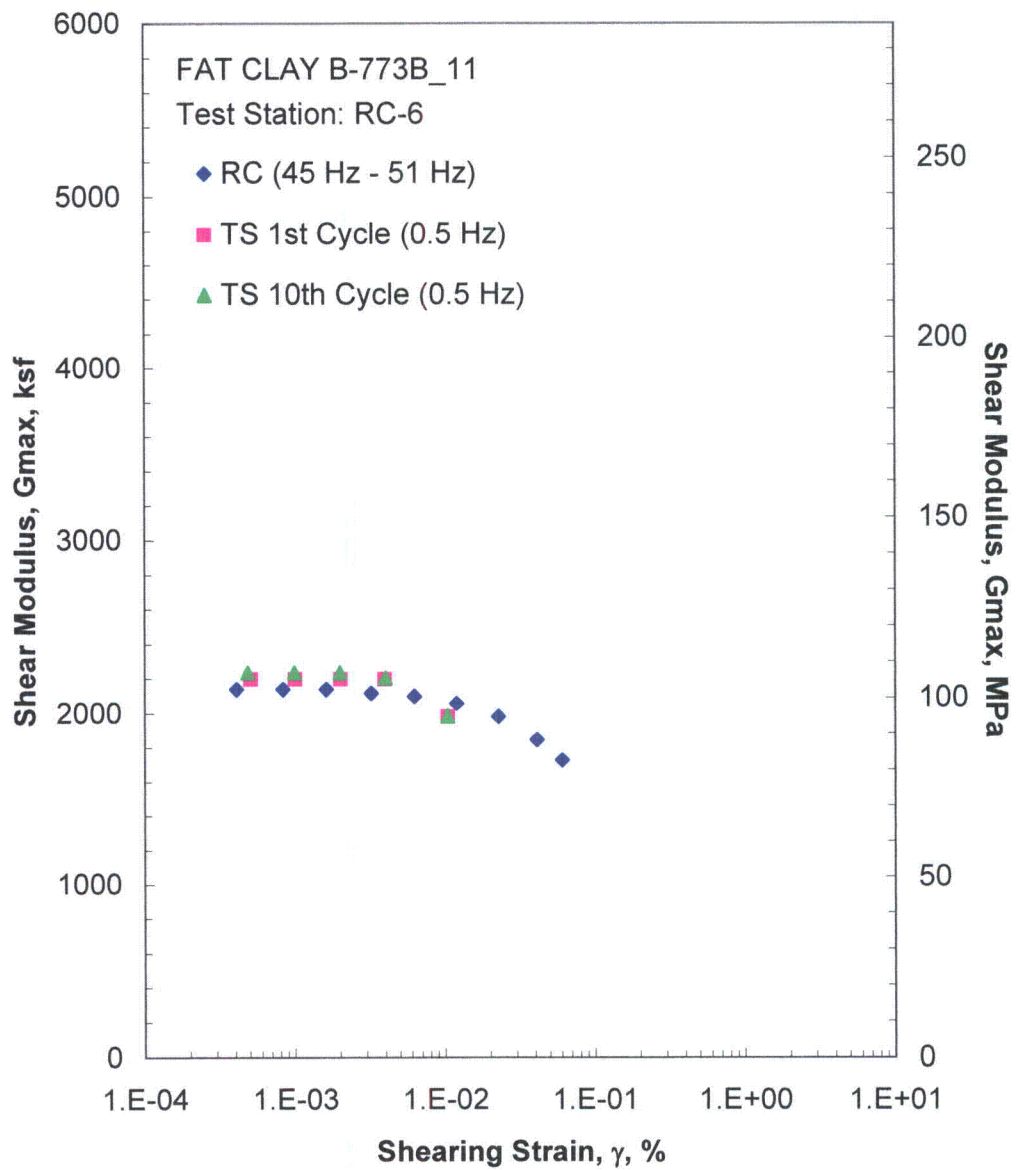


Figure G.11 Comparison of the Variation in Shear Modulus with Shearing Strain at an Isotropic Confining Pressure of 3931 psf from the Combined RCTS Tests

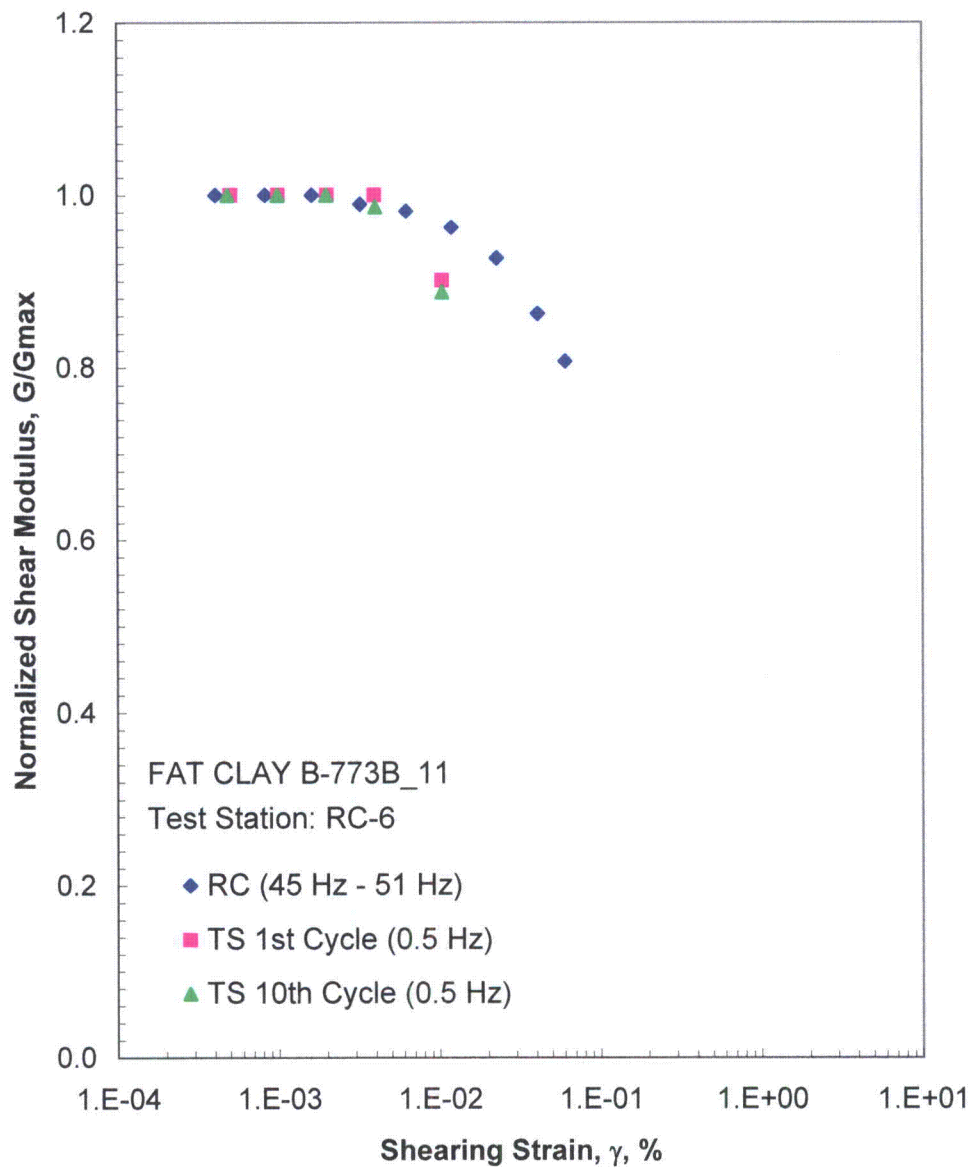


Figure G.12 Comparison of the Variation in Normalized Shear Modulus with Shearing Strain at an Isotropic Confining Pressure of 3931 psf from the Combined RCTS Tests

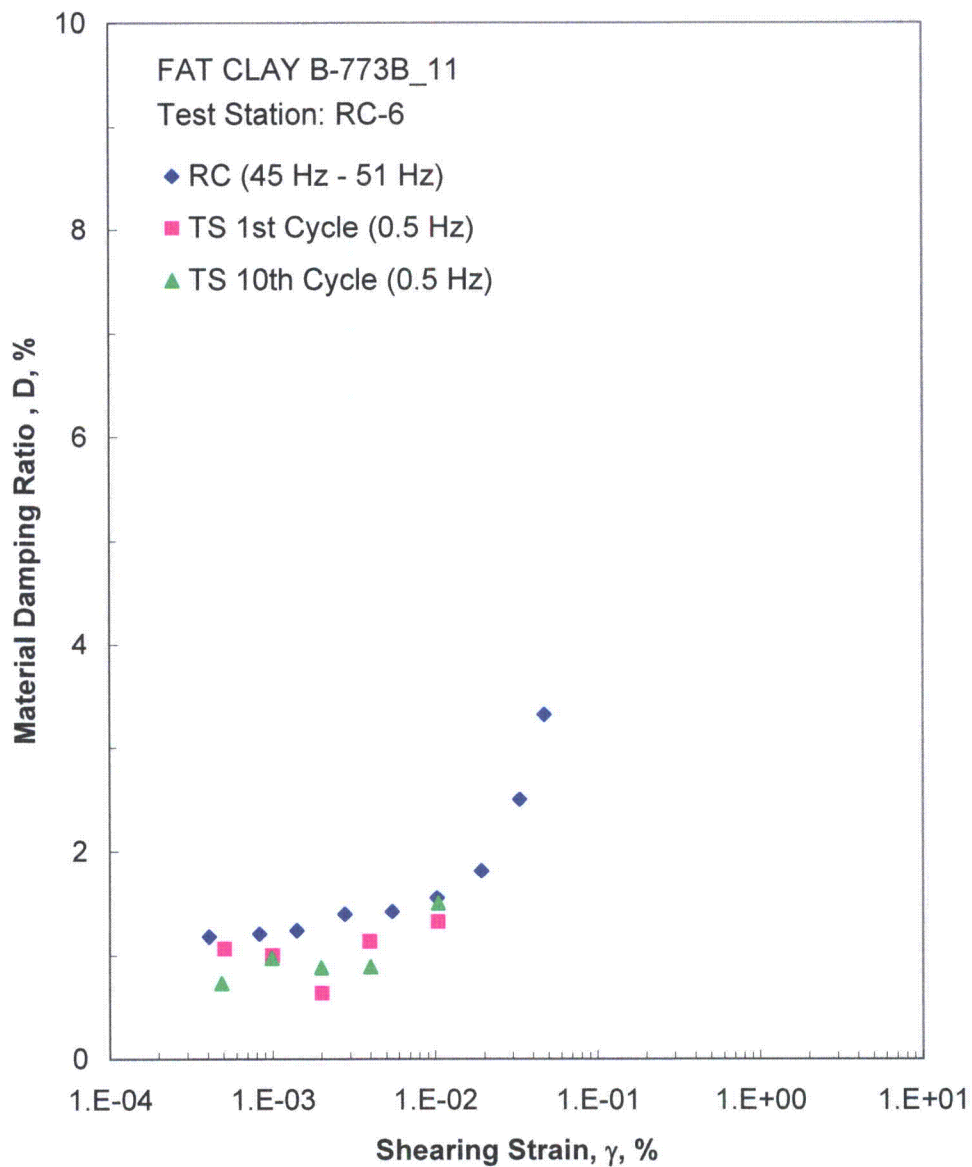


Figure G.13 Comparison of the Variation in Material Damping Ratio with Shearing Strain at an Isotropic Confining Pressure of 3931 psf from the Combined RCTS Tests

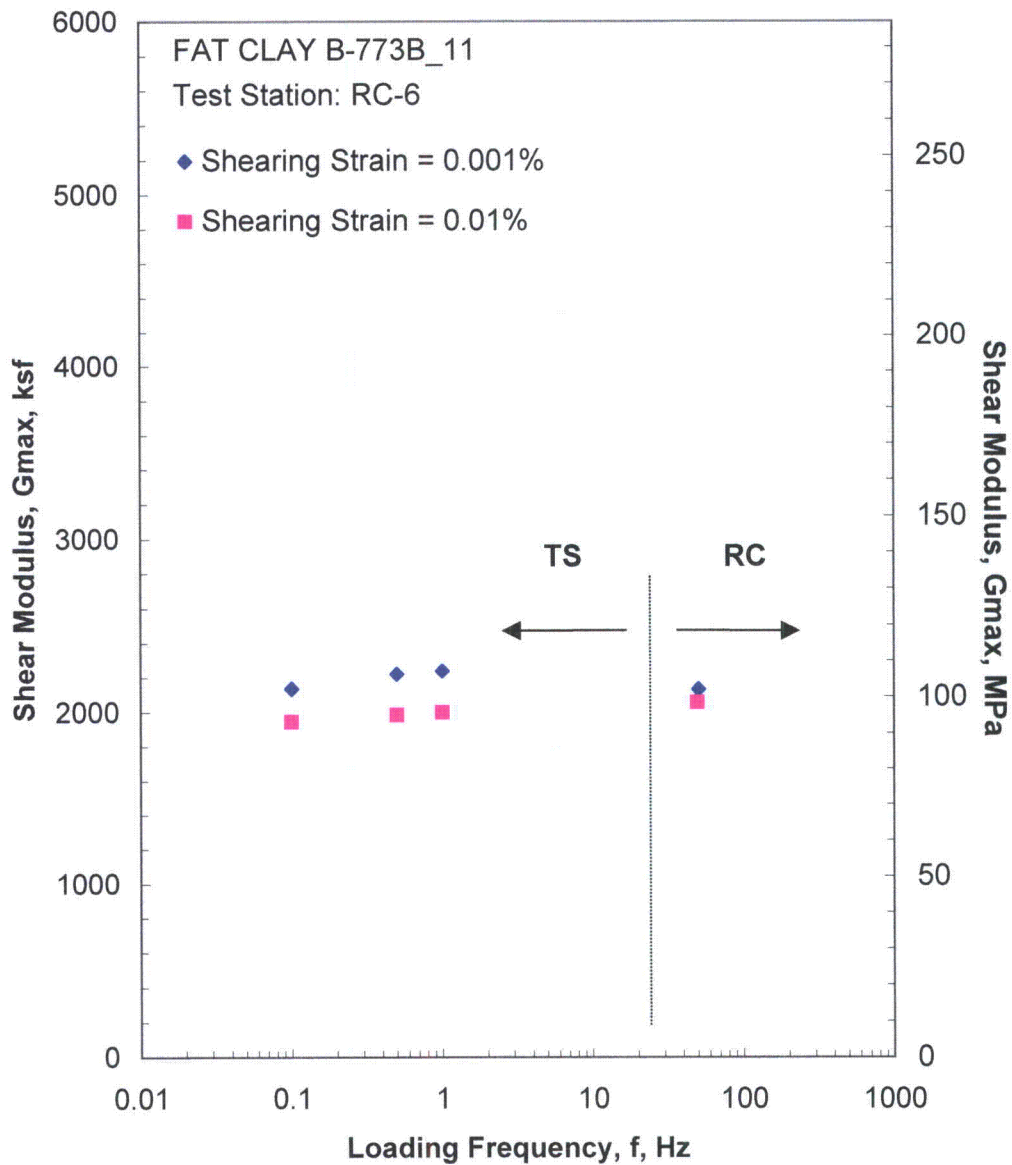


Figure G.14 Comparison of the Variation in Shear Modulus with Loading Frequency at an Isotropic Confining Pressure of 3931 psf from the Combined RCTS Tests

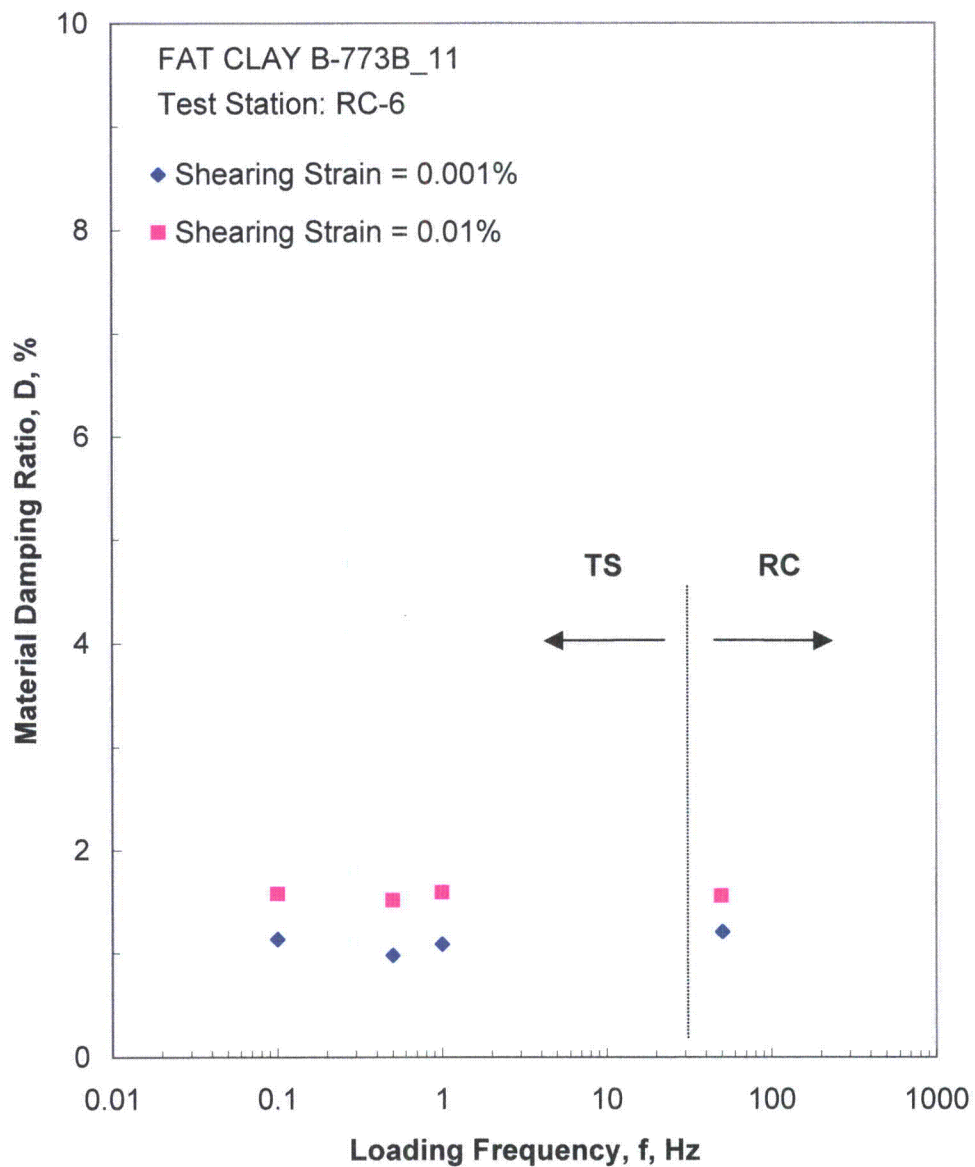


Figure G.15 Comparison of the Variation in Material Damping Ratio with Loading Frequency at an Isotropic Confining Pressure of 3931 psf from the Combined RCTS Tests

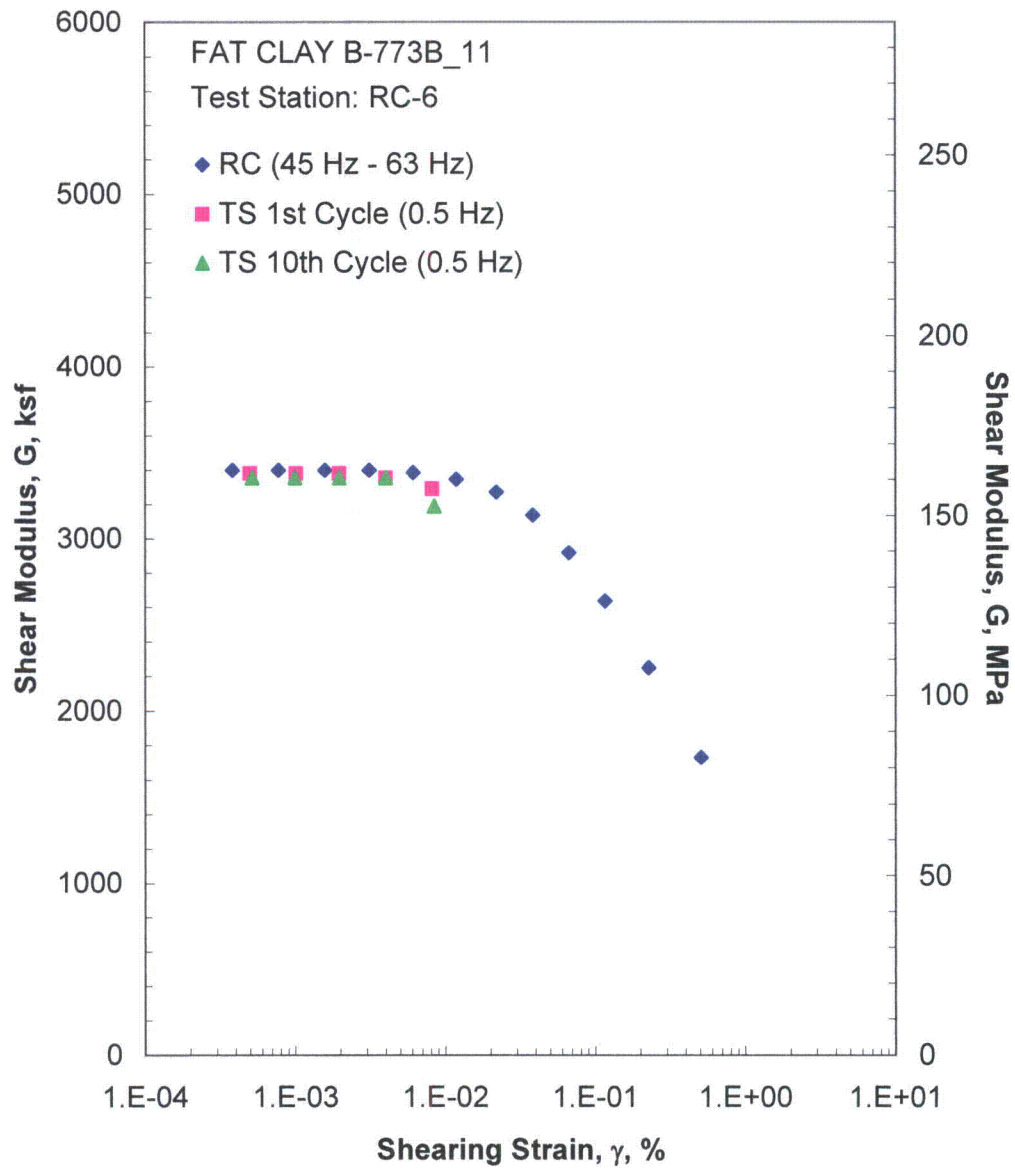


Figure G.16 Comparison of the Variation in Shear Modulus with Shearing Strain at an Isotropic Confining Pressure of 15725 psf from the Combined RCTS Tests

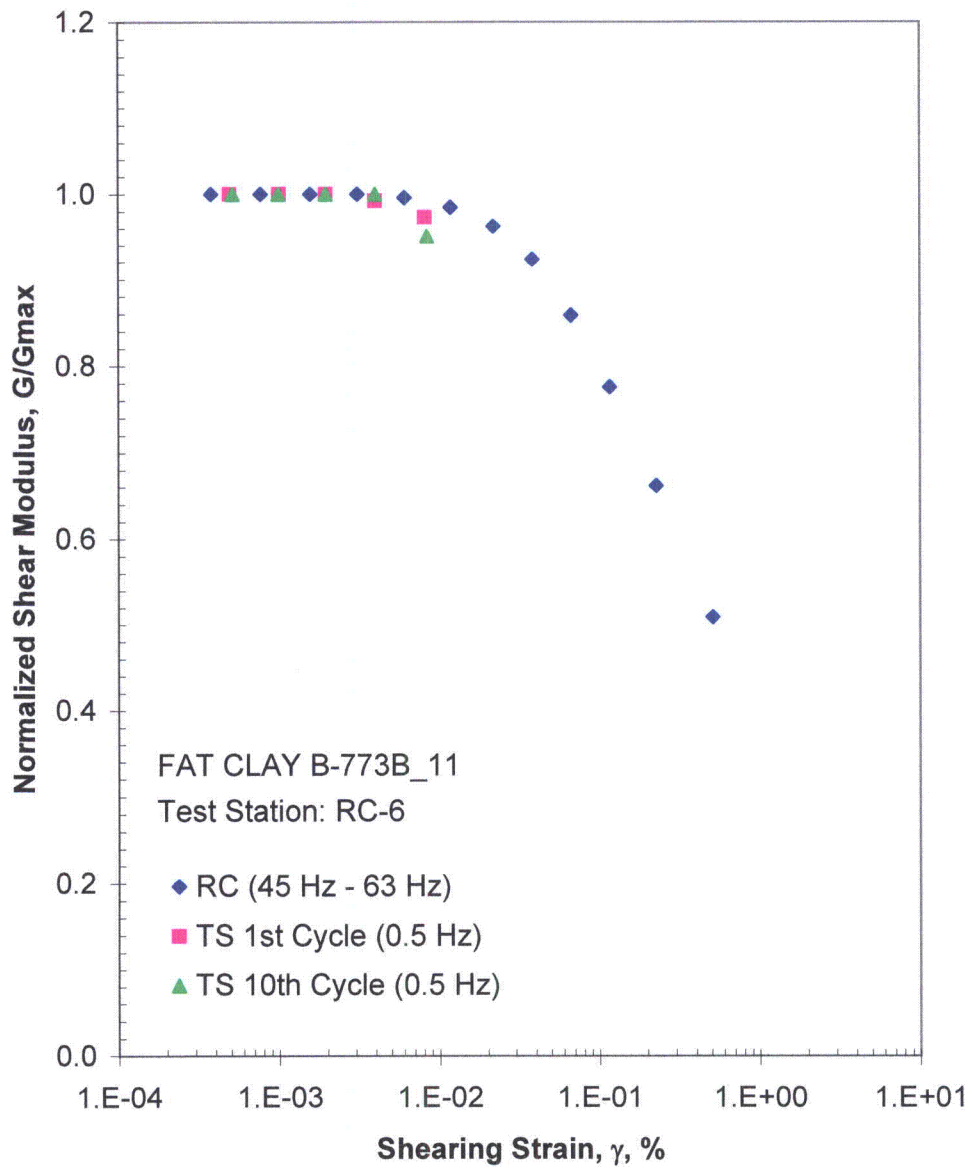


Figure G.17 Comparison of the Variation in Normalized Shear Modulus with Shearing Strain at an Isotropic Confining Pressure of 15725 psi from the Combined RCTS Tests

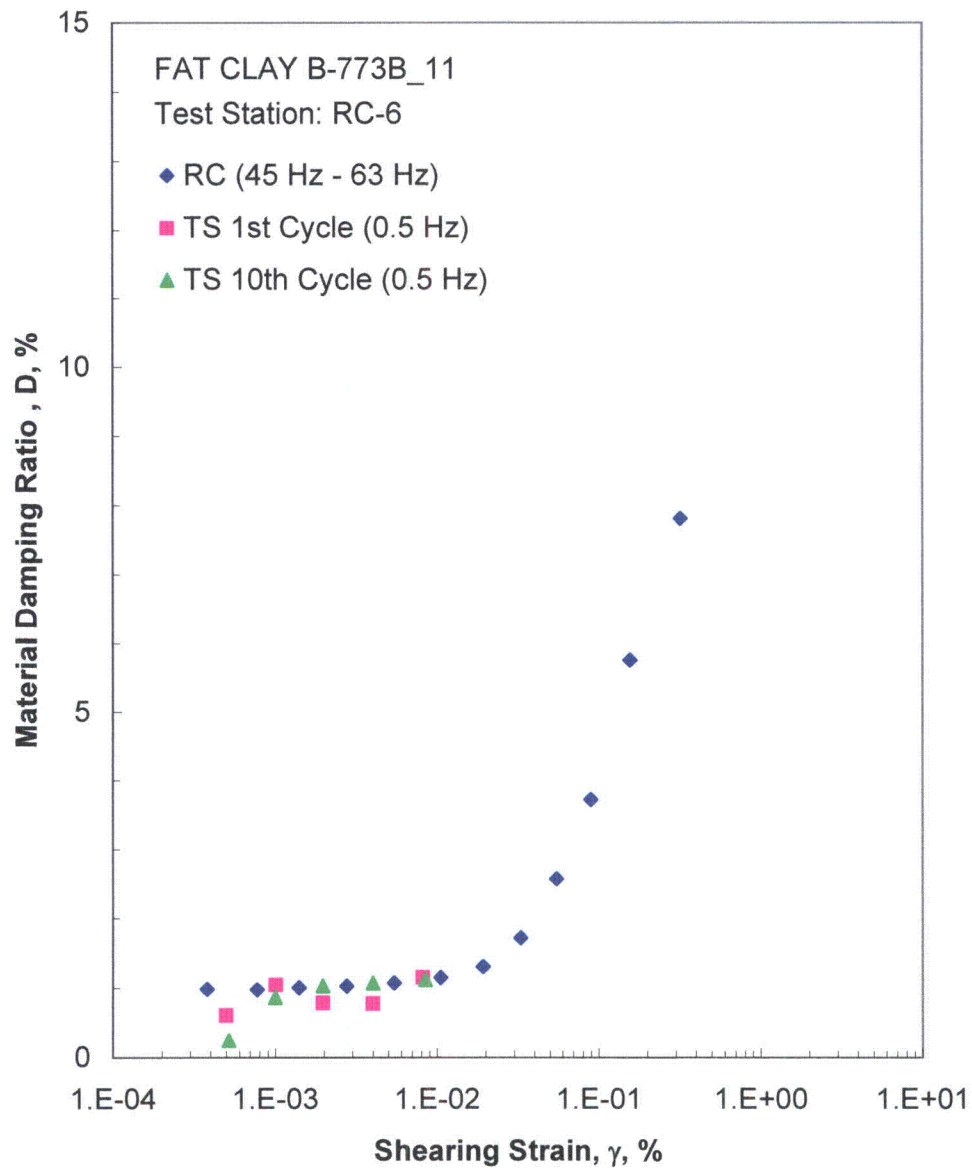


Figure G.18 Comparison of the Variation in Material Damping Ratio with Shearing Strain at an Isotropic Confining Pressure of 15725 psf from the Combined RCTS Tests

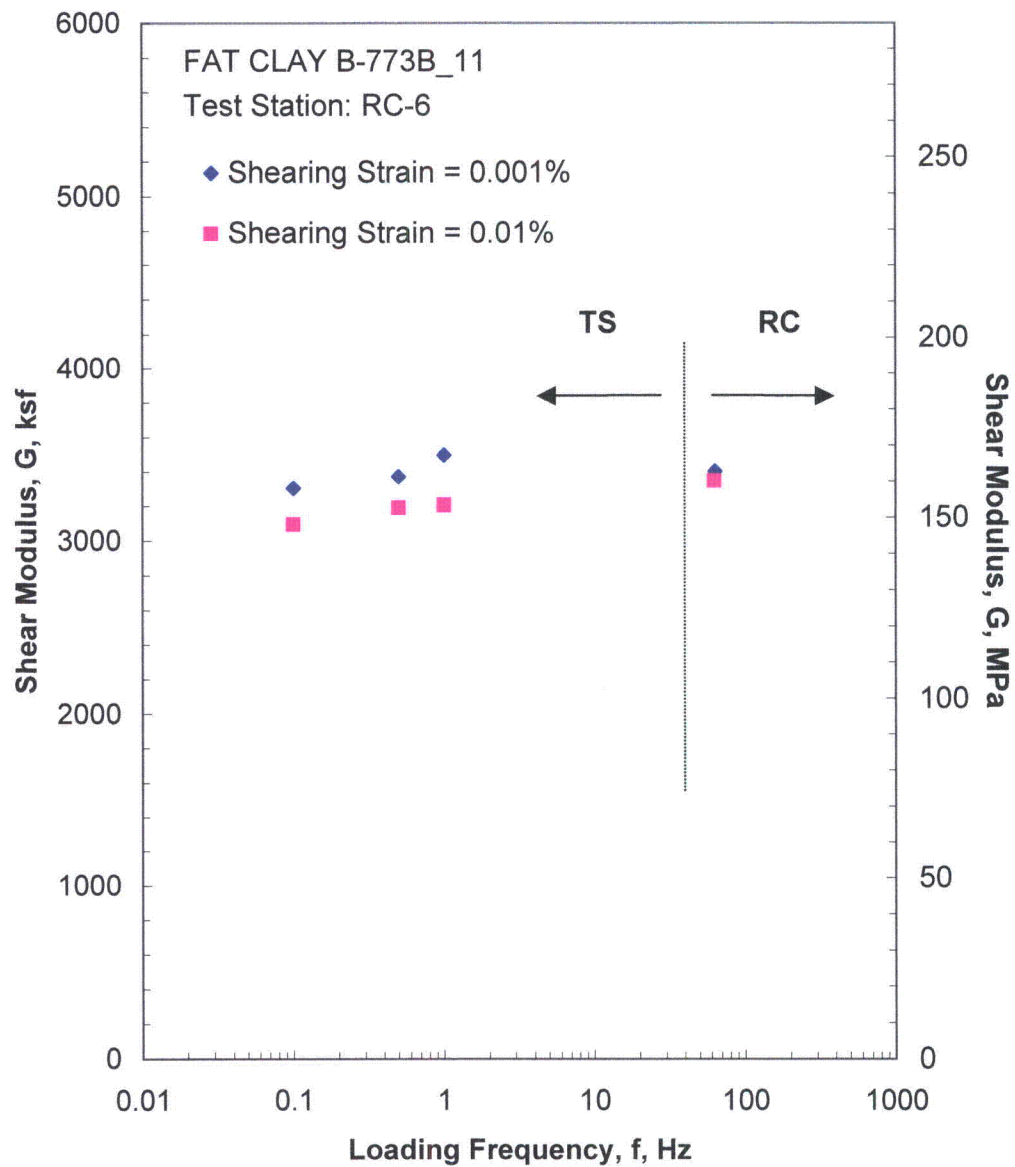


Figure G.19 Comparison of the Variation in Shear Modulus with Loading Frequency at an Isotropic Confining Pressure of 15725 psf from the Combined RCTS Tests

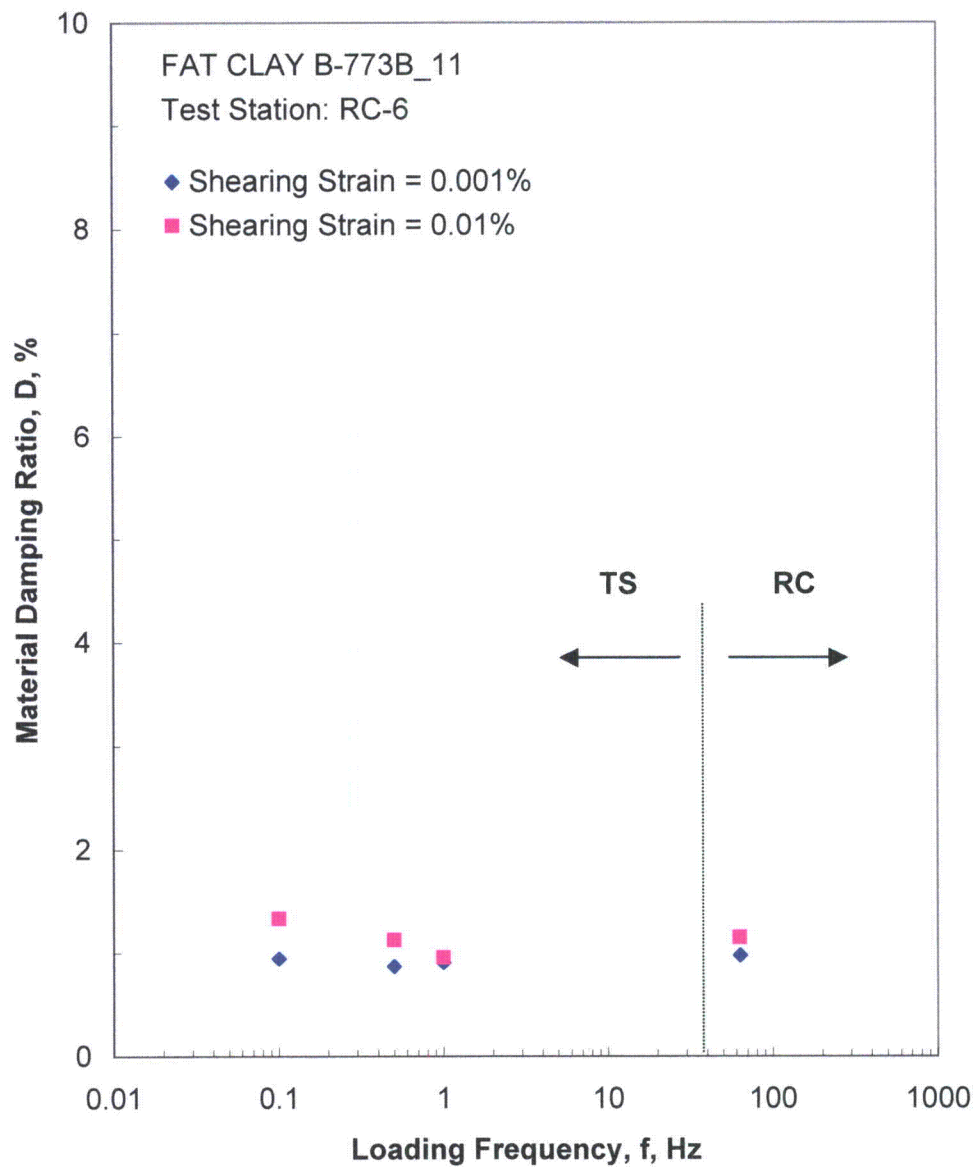


Figure G.20 Comparison of the Variation in Material Damping Ratio with Loading Frequency at an Isotropic Confining Pressure of 15725 psf from the Combined RCTS Tests

Table H.1 Variation in Low-Amplitude Shear Wave Velocity, Low-Amplitude Shear Modulus, Low-Amplitude Material Damping Ratio and Estimated Void Ratio with Isotropic Confining Pressure from RC Tests of Specimen B-773B-11

Isotropic Confining Pressure, σ_o			Low-Amplitude Shear Modulus, G_{max}		Low-Amplitude Shear Wave Velocity, V_s	Low-Amplitude Material Damping Ratio, D_{min}	Estimated Void Ratio, e
(psi)	(psf)	(kPa)	(ksf)	(MPa)	(fps)	(%)	
7	979	47	1649	79	722	1.38	1.57
14	1958	94	1825	88	759	1.31	1.56
27	3931	188	2153	103	823	1.20	1.55
55	7862	376	2732	131	924	1.09	1.54
109	15725	752	3422	164	1028	0.98	1.51

Table H.2 Variation in Shear Modulus and Material Damping Ratio with Shearing Strain from RC Tests of Specimen B-773B-11; Isotropic Confining Pressure, $\sigma_o = 3931$ psf

Peak Shearing Strain, %	Shear Modulus, G, ksf	Normalized Shear Modulus, G/G_{max}	Average ⁺ Shearing Strain, %	Material Damping Ratio ^x , D, %
4.07E-04	2137	1.00	4.07E-04	1.18
8.30E-04	2137	1.00	8.30E-04	1.21
1.62E-03	2137	1.00	1.41E-03	1.24
3.23E-03	2114	0.99	2.77E-03	1.39
6.25E-03	2097	0.98	5.43E-03	1.42
1.19E-02	2056	0.96	1.02E-02	1.55
2.27E-02	1980	0.93	1.93E-02	1.81
4.09E-02	1843	0.86	3.31E-02	2.49
6.04E-02	1726	0.81	4.71E-02	3.32

⁺ Average Shearing Strain from the First Three Cycles of the Free Vibration Decay Curve

^x Average Damping Ratio from the First Three Cycles of the Free Vibration Decay Curve

Table H.3 Variation in Shear Modulus, Normalized Shear Modulus and Material Damping Ratio with Shearing Strain from TS Tests of Specimen B-773B-11; Isotropic Confining Pressure, $\sigma_3 = 3931$ psf

First Cycle				Tenth Cycle			
Peak Shearing Strain, %	Shear Modulus, G, ksf	Normalized Shear Modulus, G/G_{max}	Material Damping Ratio, D, %	Peak Shearing Strain, %	Shear Modulus, G, ksf	Normalized Shear Modulus, G/G_{max}	Material Damping Ratio, D, %
5.07E-04	2198	1.00	1.06	4.84E-04	2235	1.00	0.73
1.00E-03	2198	1.00	1.00	9.91E-04	2235	1.00	0.97
2.01E-03	2198	1.00	0.63	1.99E-03	2235	1.00	0.88
3.96E-03	2198	1.00	1.13	4.00E-03	2204	0.99	0.89
1.04E-02	1979	0.90	1.32	1.04E-02	1983	0.89	1.50

Table H.4 Variation in Shear Modulus and Material Damping Ratio with Shearing Strain from RC Tests of Specimen B-773B-11; Isotropic Confining Pressure, $\sigma_0 = 15725$ psf

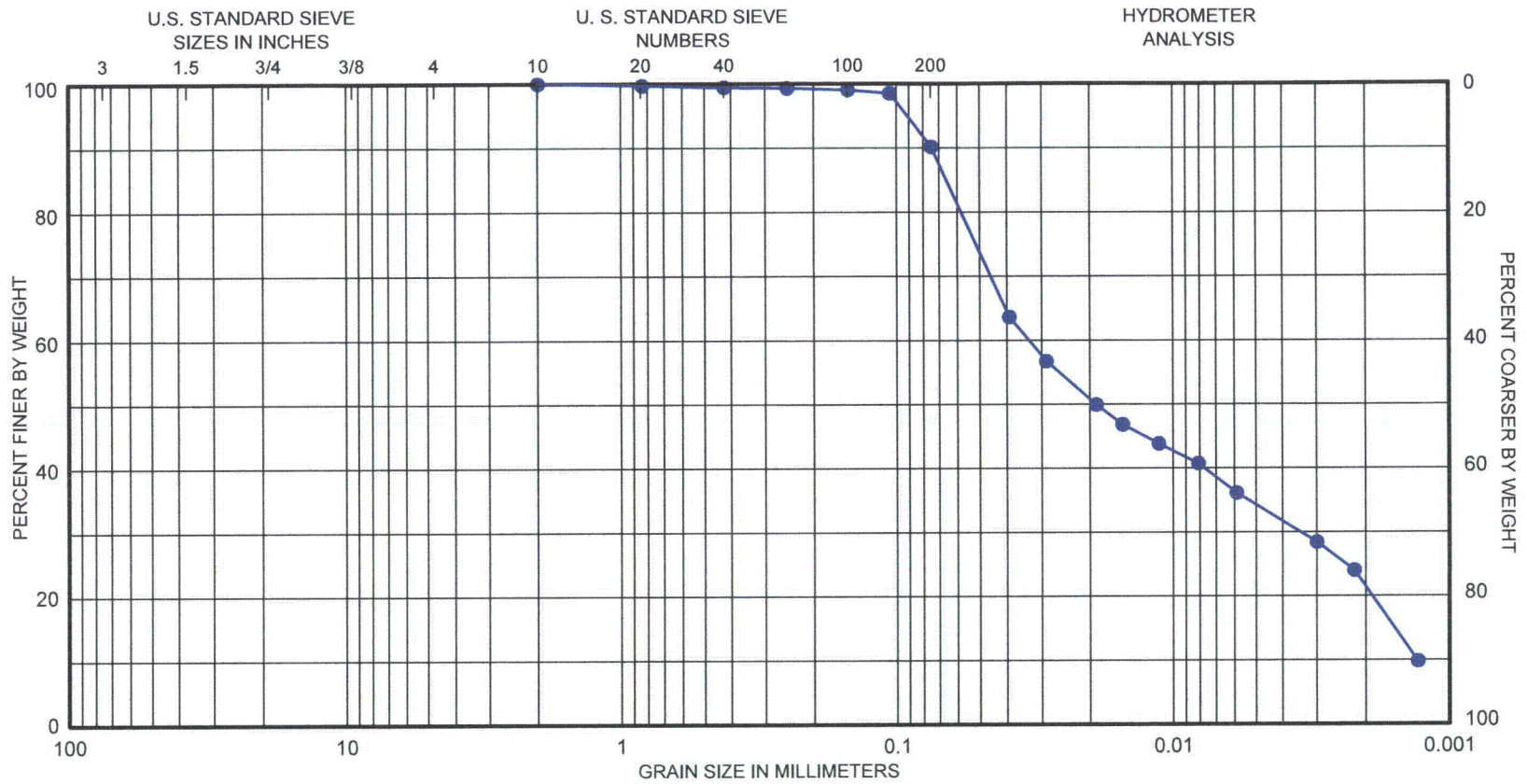
Peak Shearing Strain, %	Shear Modulus, G, ksf	Normalized Shear Modulus, G/G_{max}	Average ⁺ Shearing Strain, %	Material Damping Ratio ^x , D, %
3.80E-04	3398	1.00	3.80E-04	0.98
7.72E-04	3398	1.00	7.72E-04	0.97
1.58E-03	3398	1.00	1.40E-03	1.01
3.10E-03	3398	1.00	2.76E-03	1.03
6.10E-03	3384	1.00	5.43E-03	1.08
1.18E-02	3346	0.98	1.05E-02	1.15
2.19E-02	3271	0.96	1.92E-02	1.31
3.82E-02	3137	0.92	3.29E-02	1.72
6.66E-02	2917	0.86	5.46E-02	2.57
1.16E-01	2635	0.78	8.93E-02	3.72
2.27E-01	2249	0.66	1.56E-01	5.76
5.08E-01	1731	0.51	3.20E-01	7.81

⁺ Average Shearing Strain from the First Three Cycles of the Free Vibration Decay Curve

^x Average Damping Ratio from the First Three Cycles of the Free Vibration Decay Curve

Table H.5 Variation in Shear Modulus, Normalized Shear Modulus and Material Damping Ratio with Shearing Strain from TS Tests of Specimen B-773B-11; Isotropic Confining Pressure, $\sigma_o = 15725$ psf

First Cycle				Tenth Cycle			
Peak Shearing Strain, %	Shear Modulus, G, ksf	Normalized Shear Modulus, G/G_{max}	Material Damping Ratio, D, %	Peak Shearing Strain, %	Shear Modulus, G, ksf	Normalized Shear Modulus, G/G_{max}	Material Damping Ratio, D, %
4.97E-04	3380	1.00	0.60	5.16E-04	3354	1.00	0.24
1.01E-03	3380	1.00	1.04	9.97E-04	3354	1.00	0.86
1.97E-03	3380	1.00	0.78	1.97E-03	3354	1.00	1.03
4.01E-03	3355	0.99	0.77	4.00E-03	3354	1.00	1.07
8.18E-03	3290	0.97	1.15	8.43E-03	3189	0.95	1.12



GRAVEL		SAND			SILT or CLAY		
Coarse	Fine	Coarse	Medium	Fine			
<u>SYMBOL</u>	<u>BORING</u>	<u>DEPTH, FT</u>	<u>C_c</u>	<u>C_u</u>	<u>D₅₀</u>	<u>D₉₀</u>	<u>CLASSIFICATION</u>
●	B-773B-11	107	0.27	25.56	0.02	0.07	Fat Clay (CH), olive gray

GRAIN SIZE CURVE



APPENDIX I

Specimen B-773B_13

Borehole B-773B

Sample 13

Depth = 127 ft (38.7m)

Total Unit Weight = 108.3 lb/ft³

Water Content = 45.2 %

FUGRO JOB #: 0411-09-1734

Testing Station: RC6



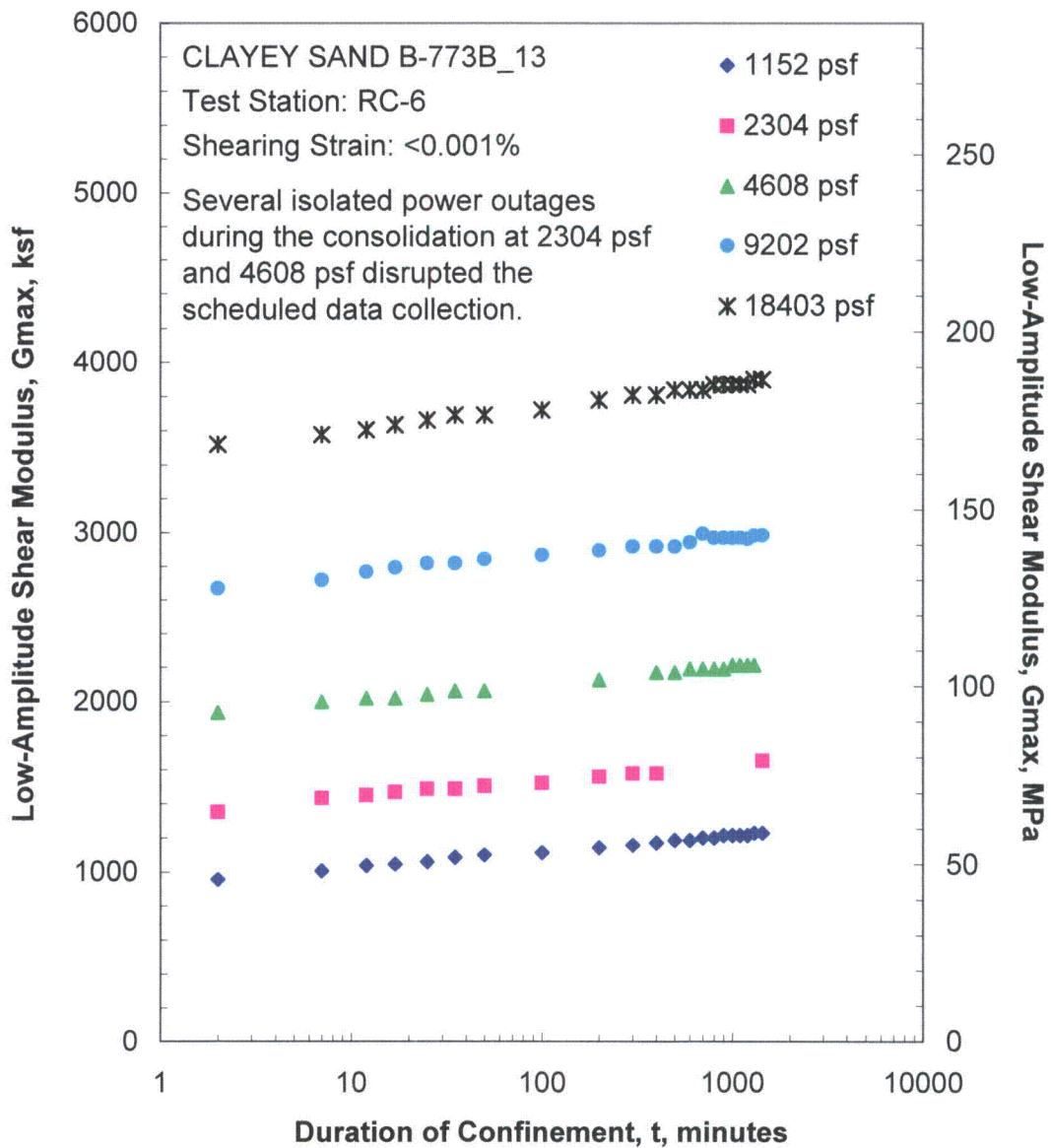


Figure I.1 Variation in Low-Amplitude Shear Modulus with Magnitude and Duration of Isotropic Confining Pressure from Resonant Column Tests

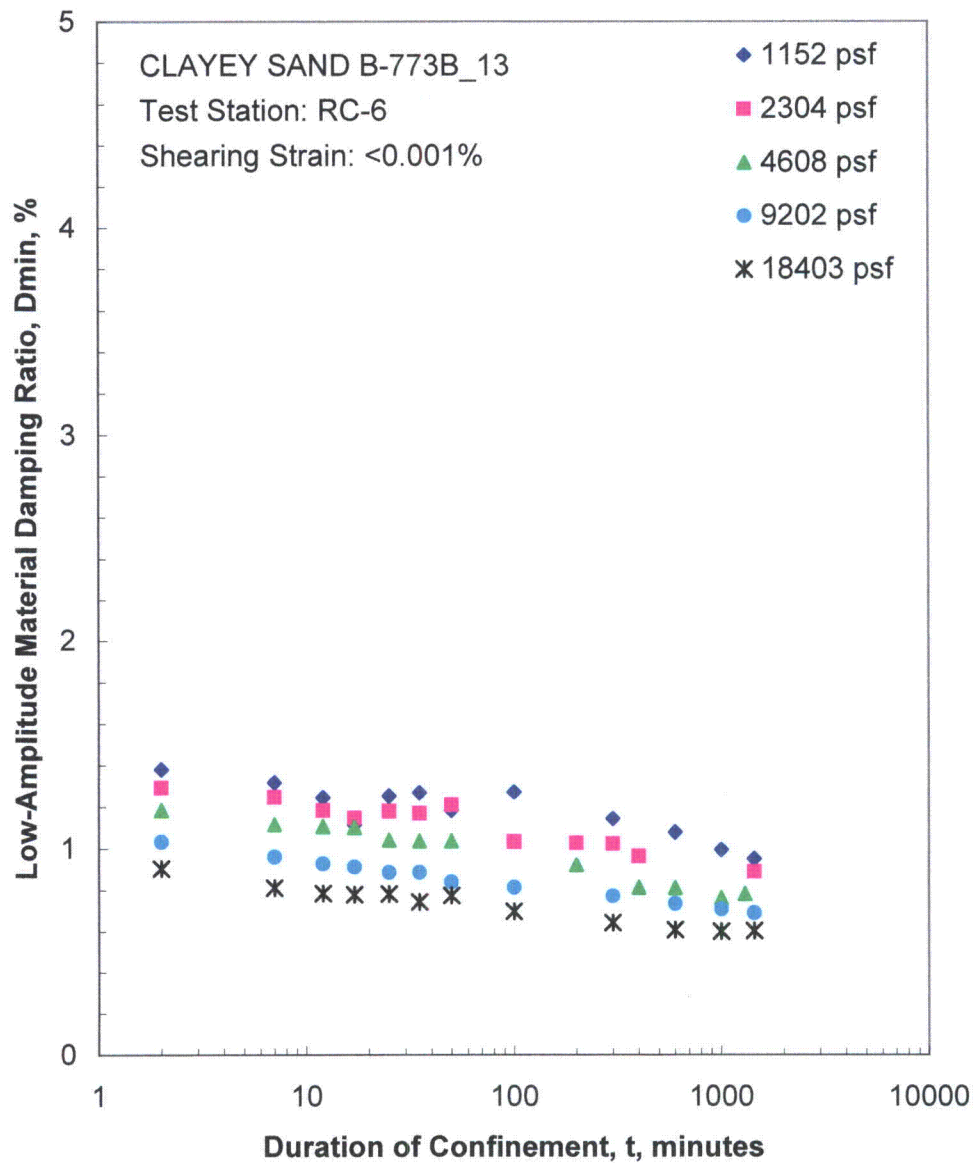


Figure I.2 Variation in Low-Amplitude Material Damping Ratio with Magnitude and Duration of Isotropic Confining Pressure from Resonant Column Tests

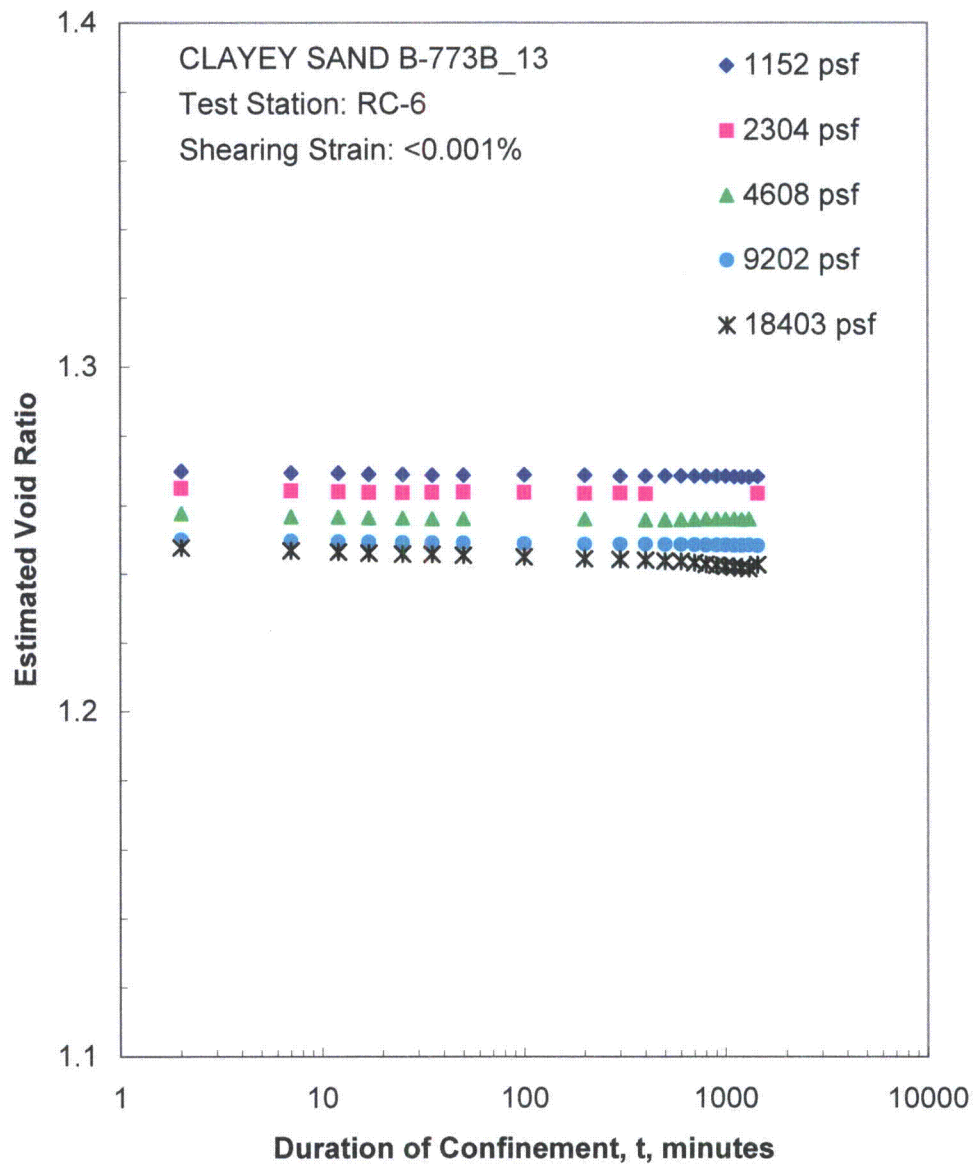


Figure I.3 Variation in Estimated Void Ratio with Magnitude and Duration of Isotropic Confining Pressure from Resonant Column Tests

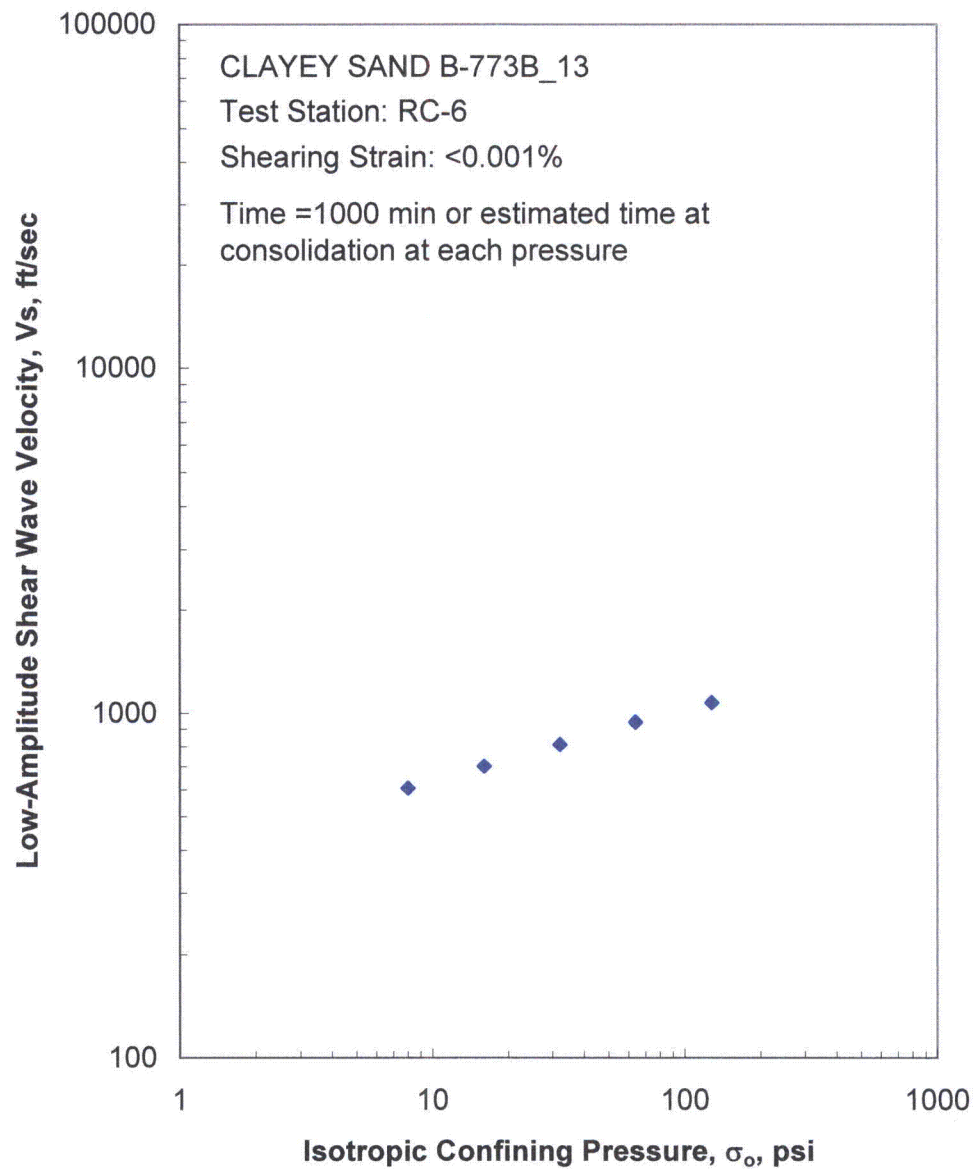


Figure I.4 Variation in Low-Amplitude Shear Wave Velocity with Isotropic Confining Pressure from Resonant Column Tests

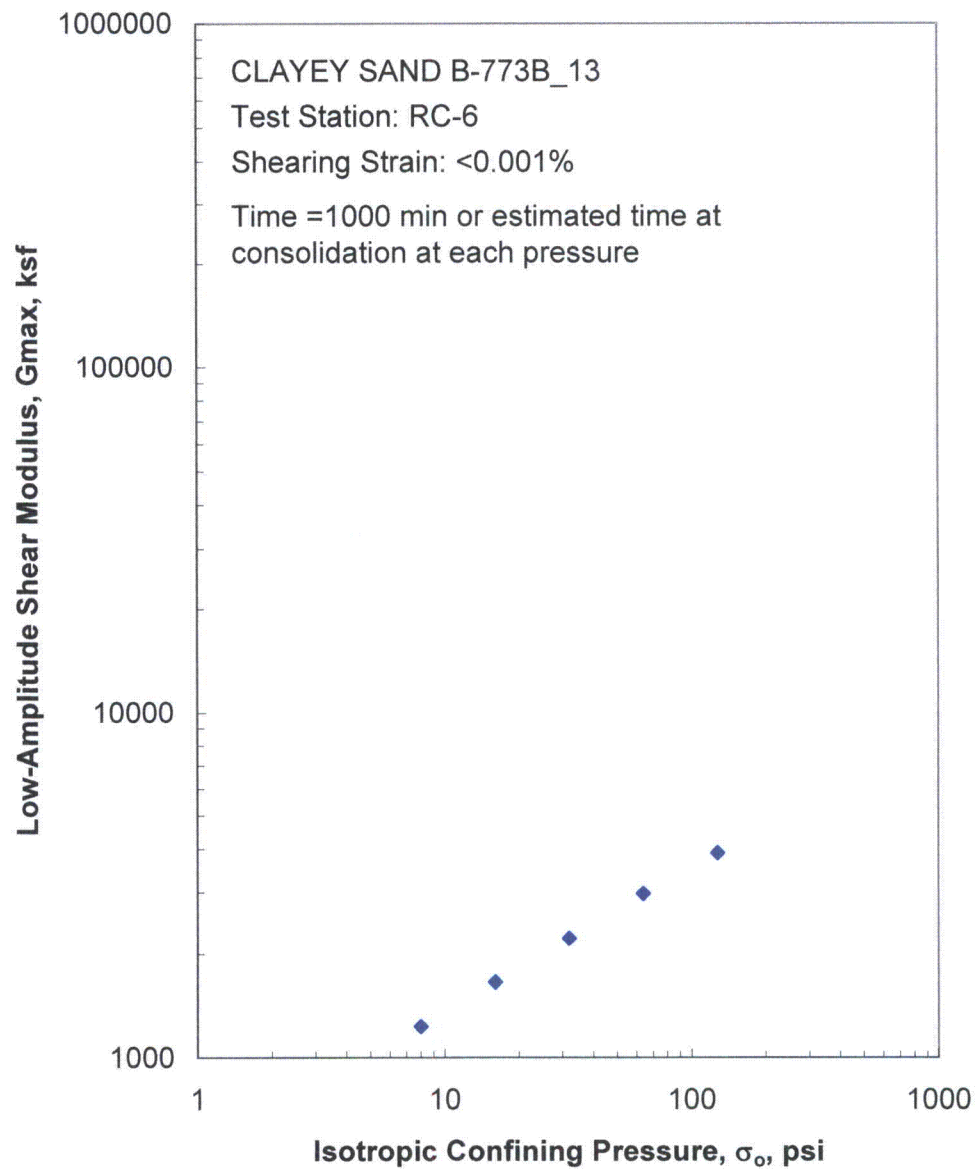


Figure I.5 Variation in Low-Amplitude Shear Modulus with Isotropic Confining Pressure from Resonant Column Tests

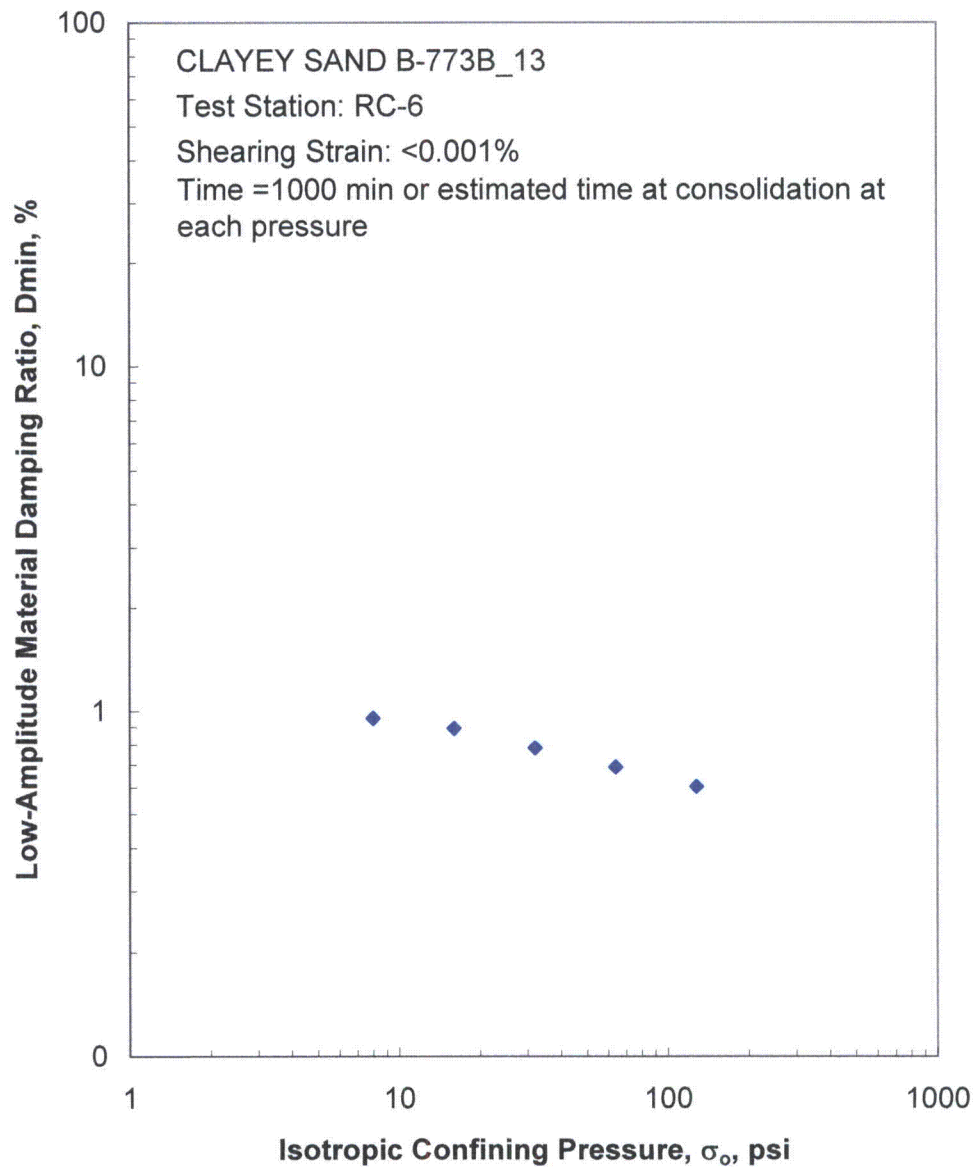


Figure I.6 Variation in Low-Amplitude Material Damping Ratio with Isotropic Confining Pressure from Resonant Column Tests

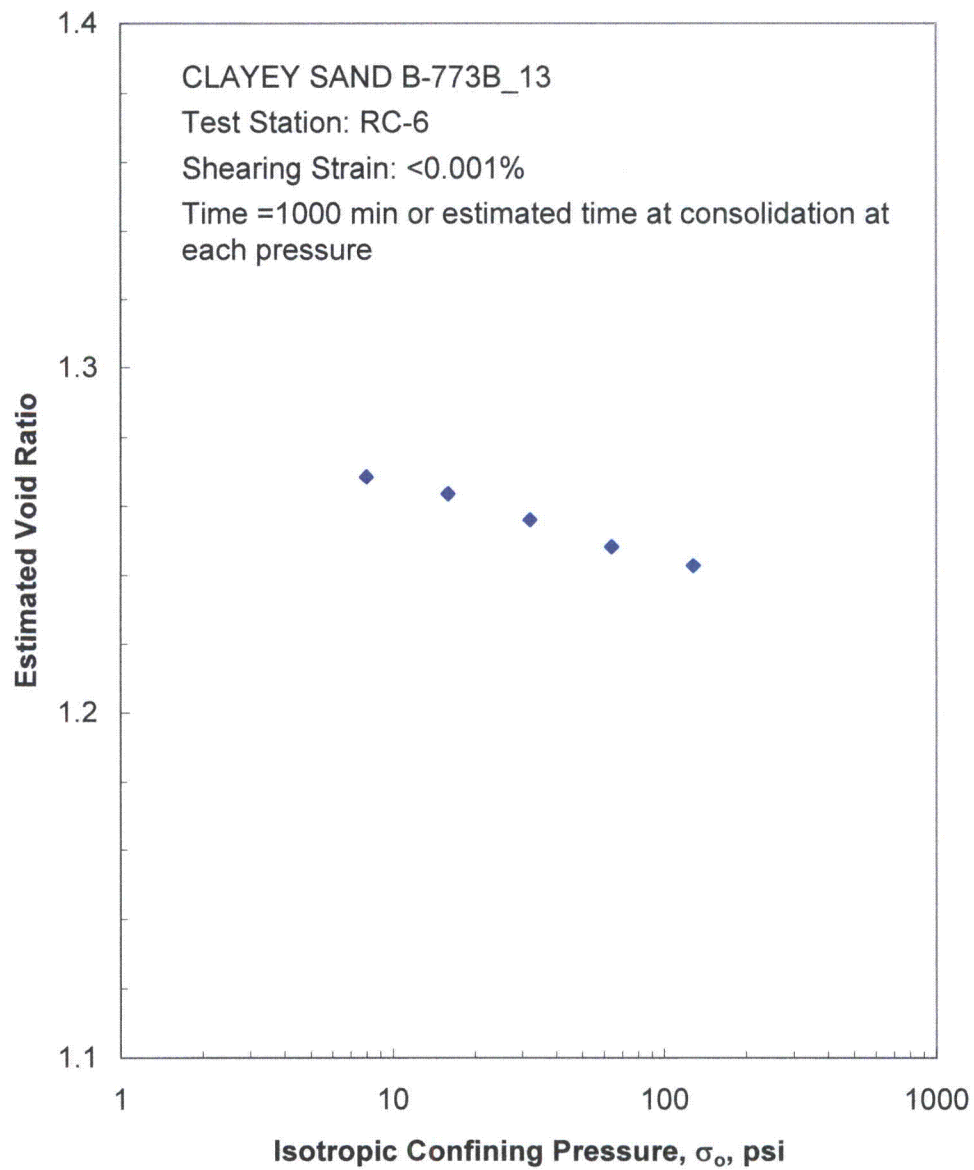


Figure I.7 Variation in Estimated Void Ratio with Isotropic Confining Pressure from Resonant Column Tests

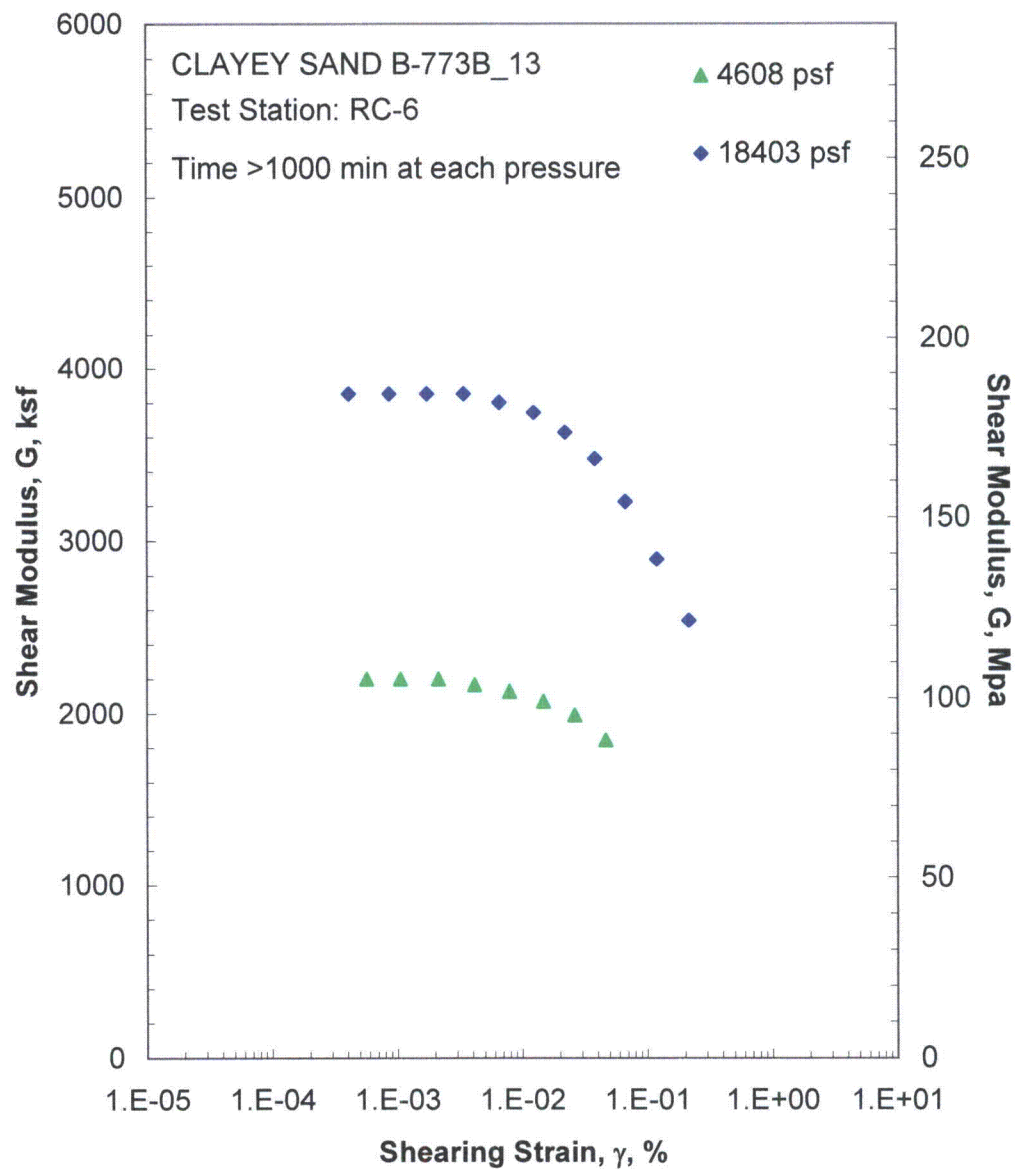


Figure I.8 Comparison of the Variation in Shear Modulus with Shearing Strain and Isotropic Confining Pressure from the Resonant Column Tests

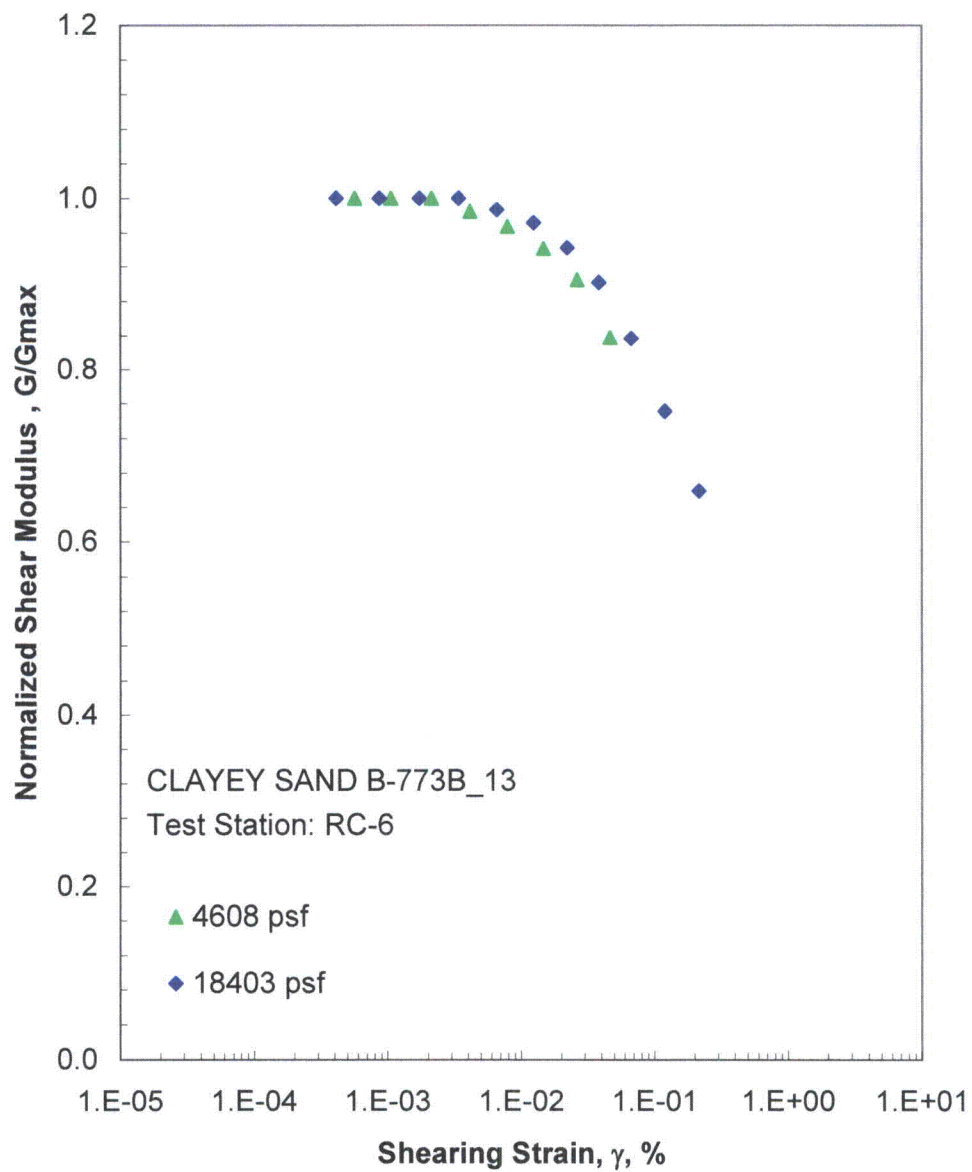


Figure I.9 Comparison of the Variation in Normalized Shear Modulus with Shearing Strain and Isotropic Confining Pressure from the Resonant Column Tests

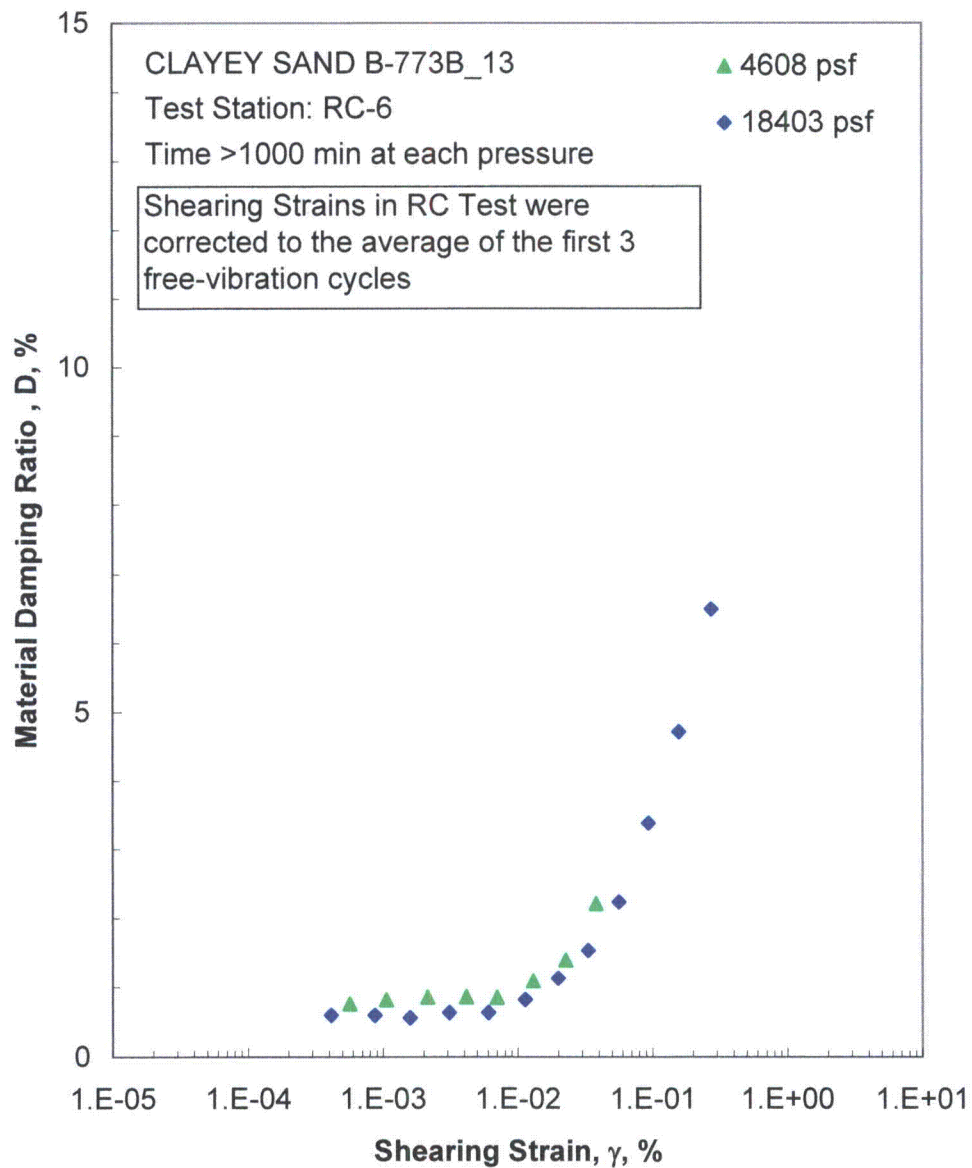


Figure I.10 Comparison of the Variation in Material Damping Ratio with Shearing Strain and Isotropic Confining Pressure from the Resonant Column Tests

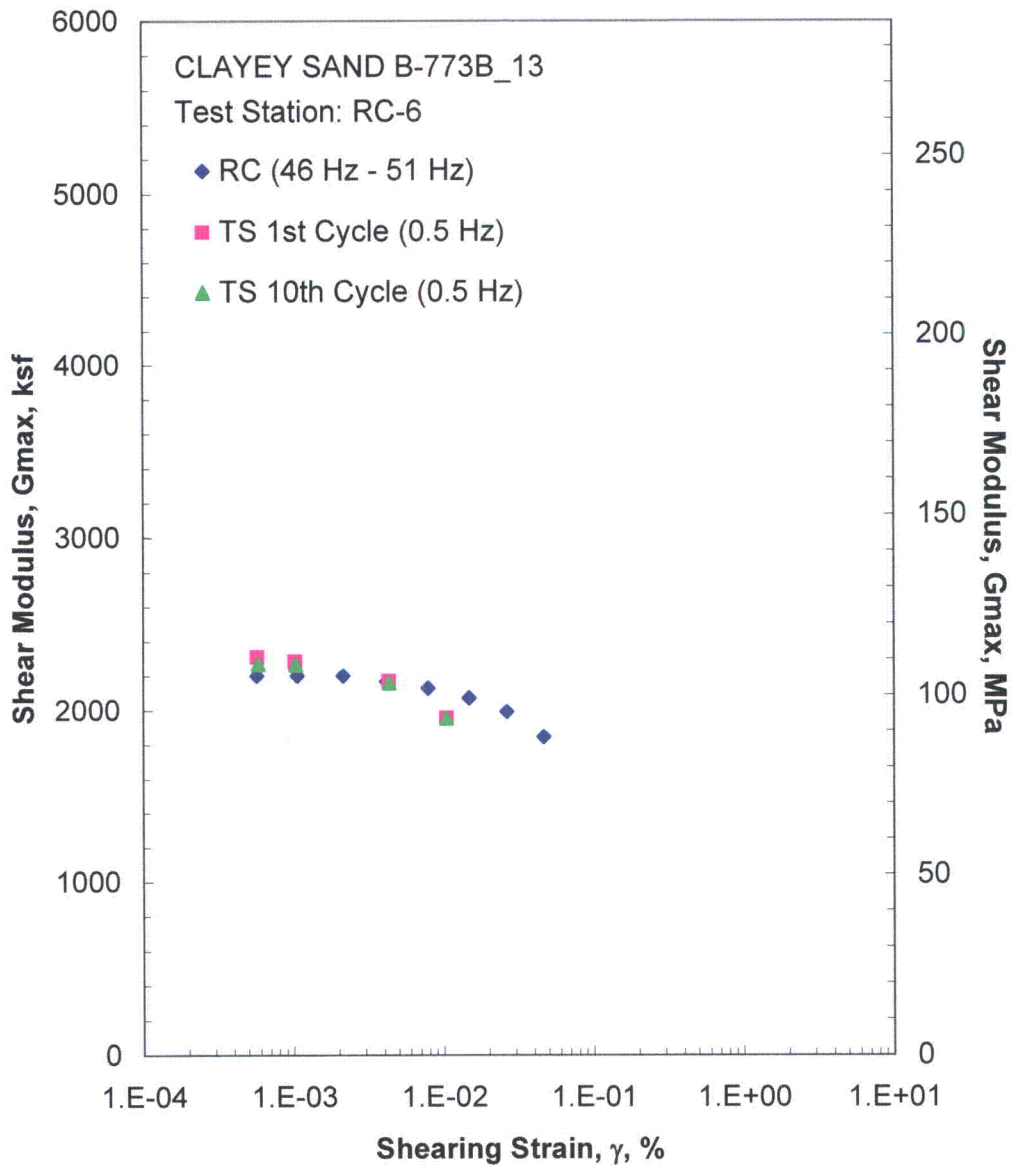


Figure I.11 Comparison of the Variation in Shear Modulus with Shearing Strain at an Isotropic Confining Pressure of 4608 psf from the Combined RCTS Tests

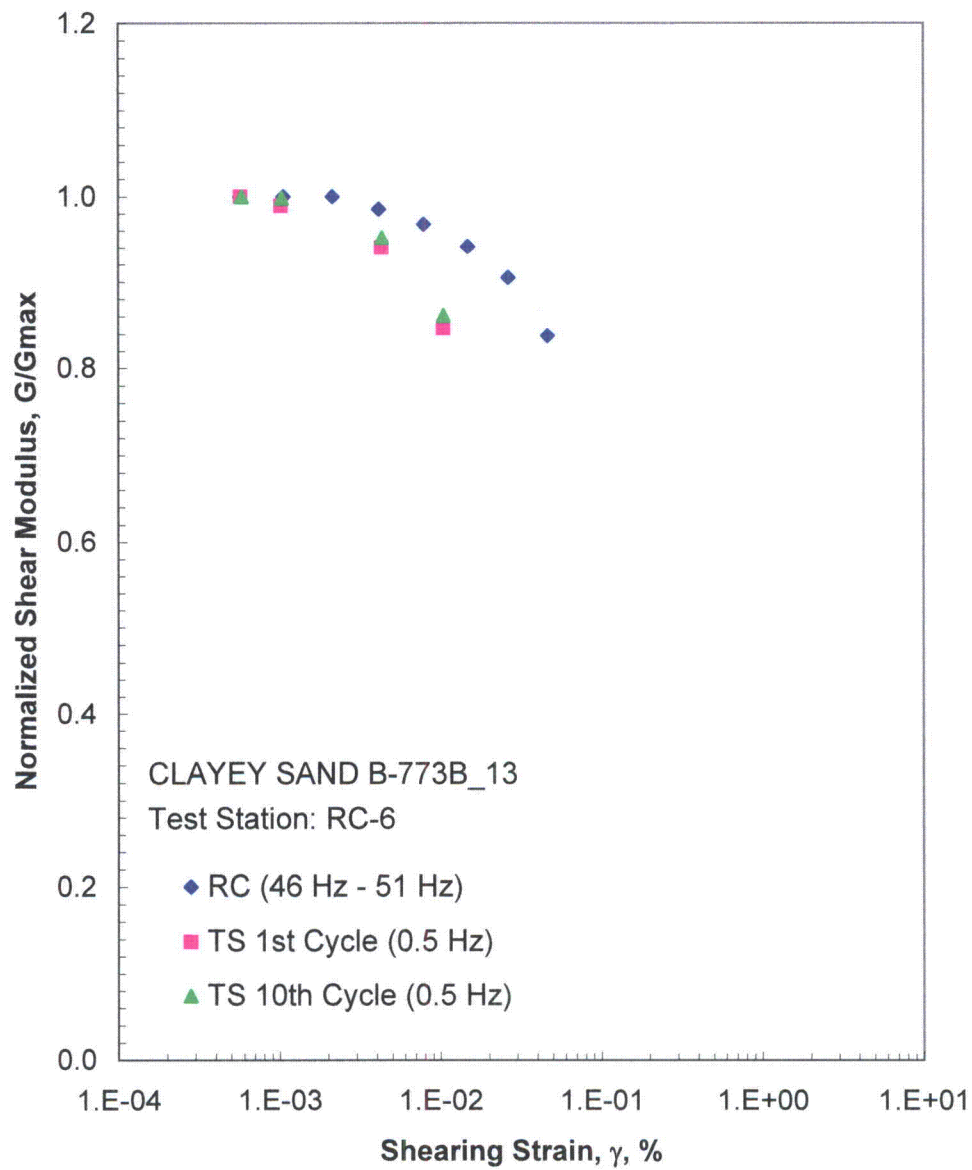


Figure I.12 Comparison of the Variation in Normalized Shear Modulus with Shearing Strain at an Isotropic Confining Pressure of 4608 psf from the Combined RCTS Tests

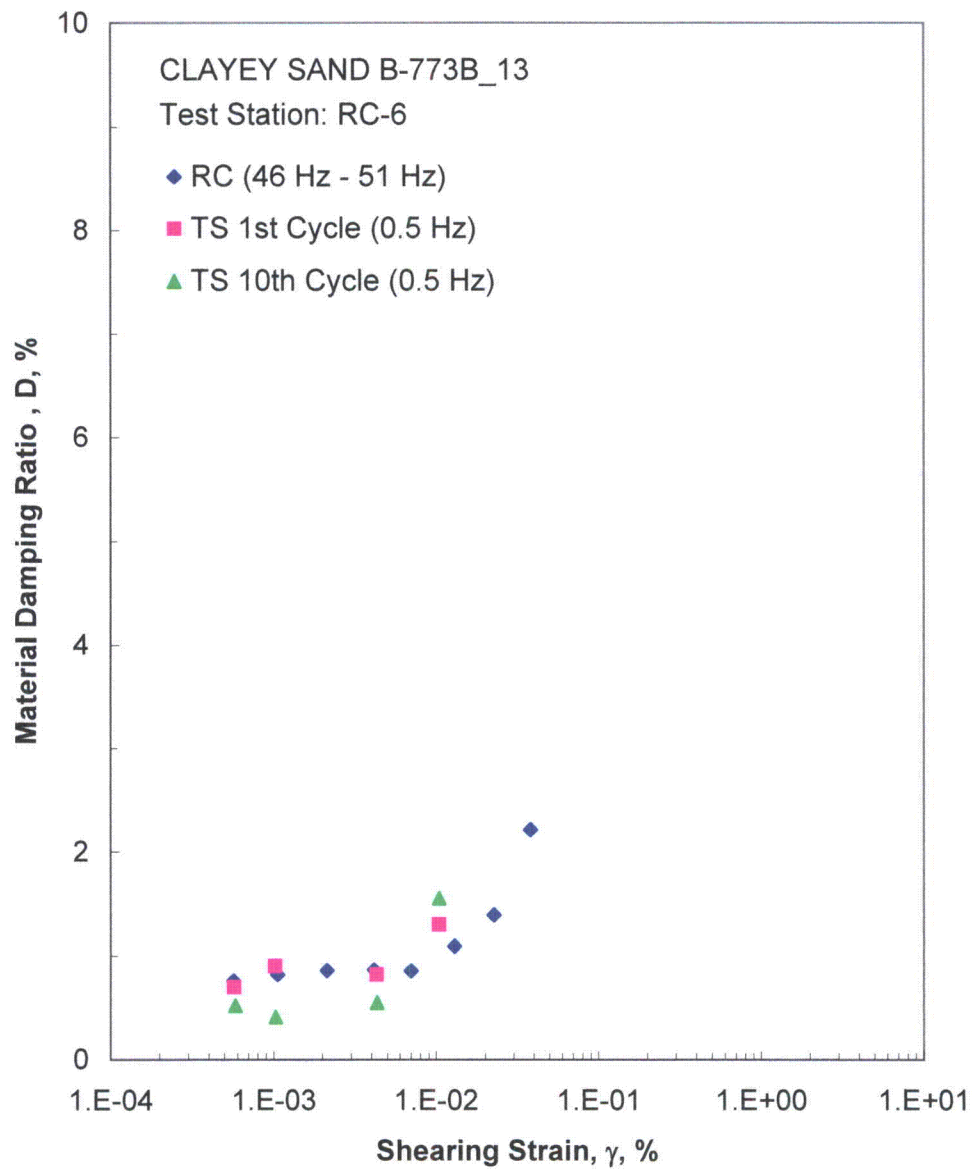


Figure I.13 Comparison of the Variation in Material Damping Ratio with Shearing Strain at an Isotropic Confining Pressure of 4608 psf from the Combined RCTS Tests

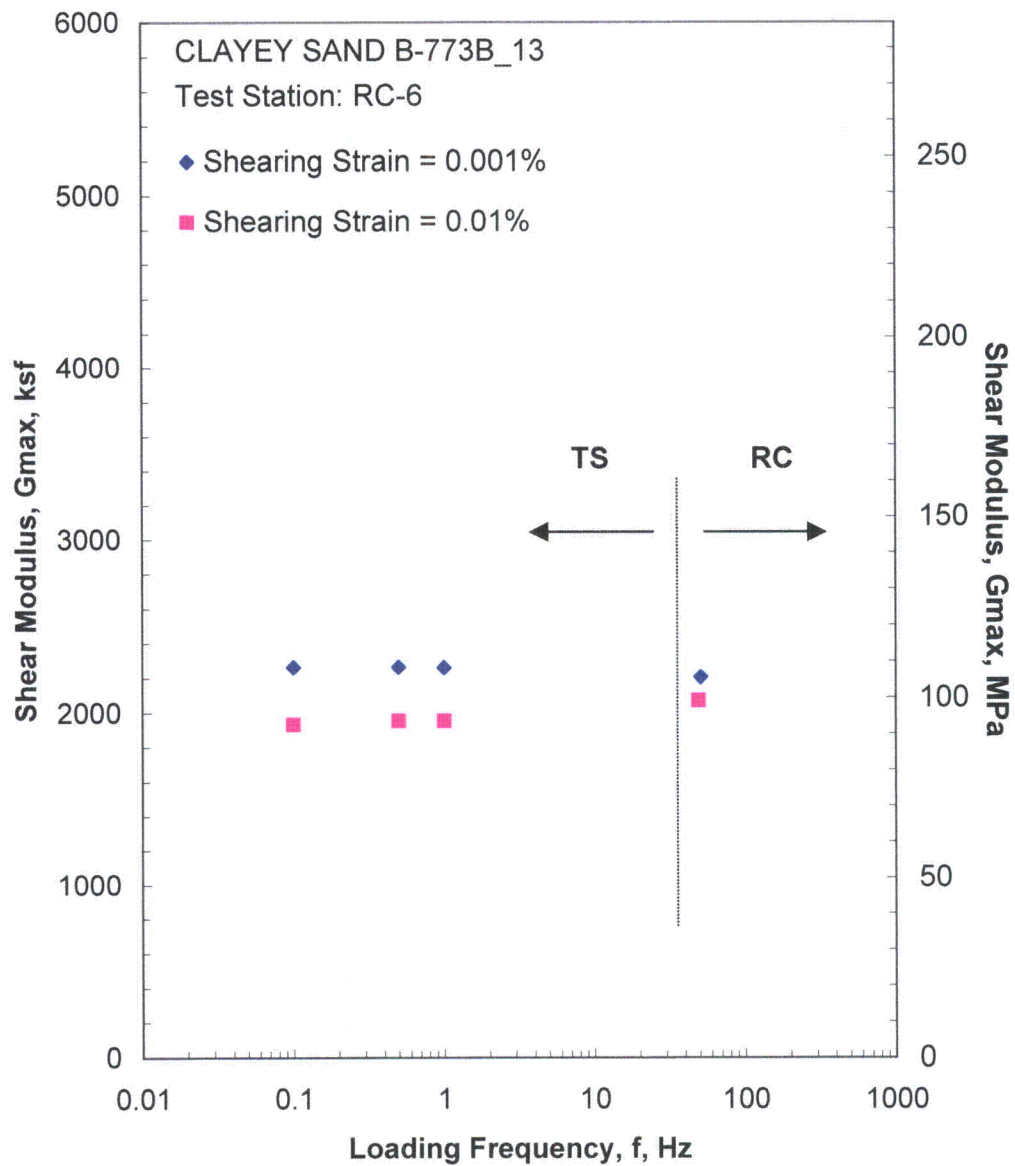


Figure I.14 Comparison of the Variation in Shear Modulus with Loading Frequency at an Isotropic Confining Pressure of 4608 psf from the Combined RCTS Tests

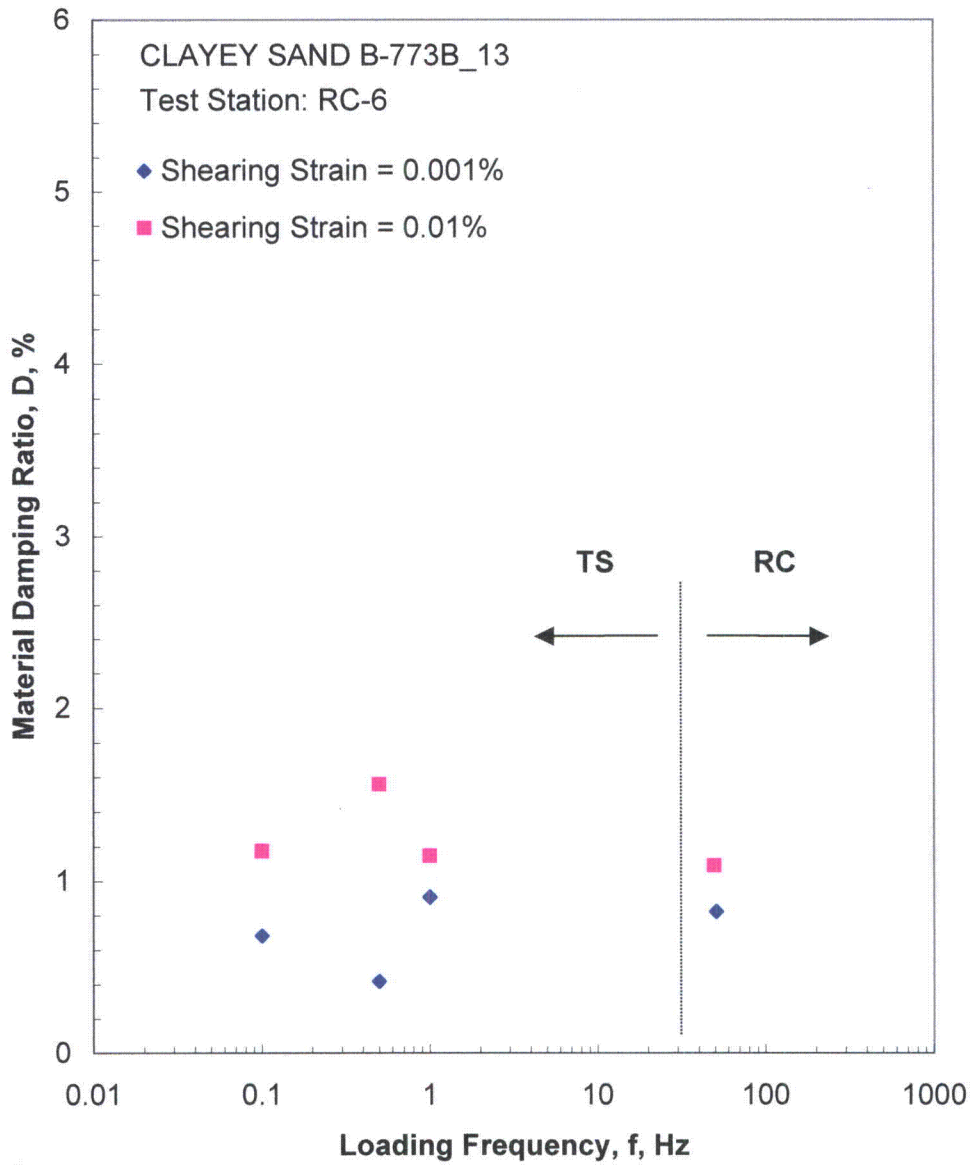


Figure I.15 Comparison of the Variation in Material Damping Ratio with Loading Frequency at an Isotropic Confining Pressure of 4608 psf from the Combined RCTS Tests

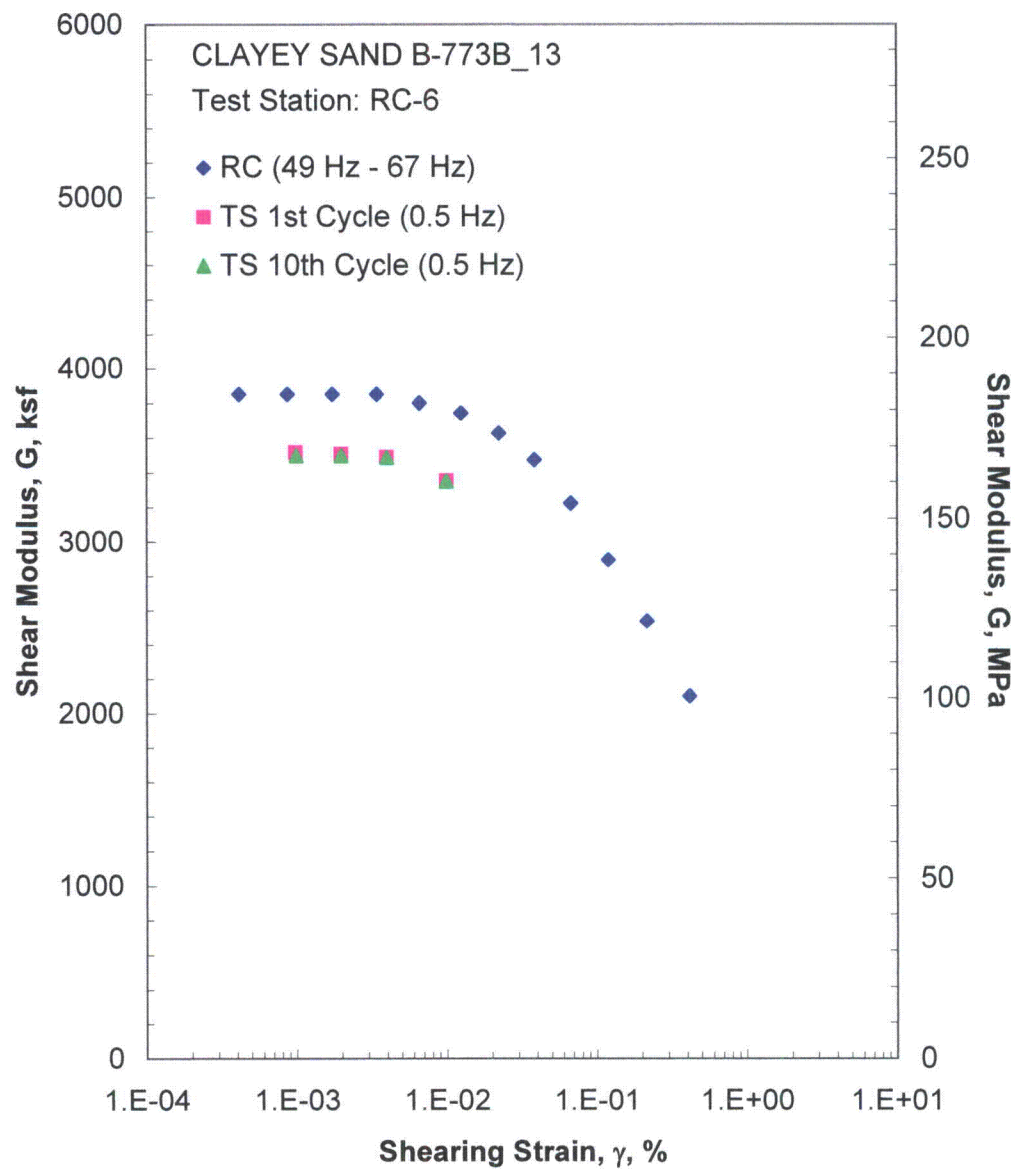


Figure I.16 Comparison of the Variation in Shear Modulus with Shearing Strain at an Isotropic Confining Pressure of 18403 psf from the Combined RCTS Tests

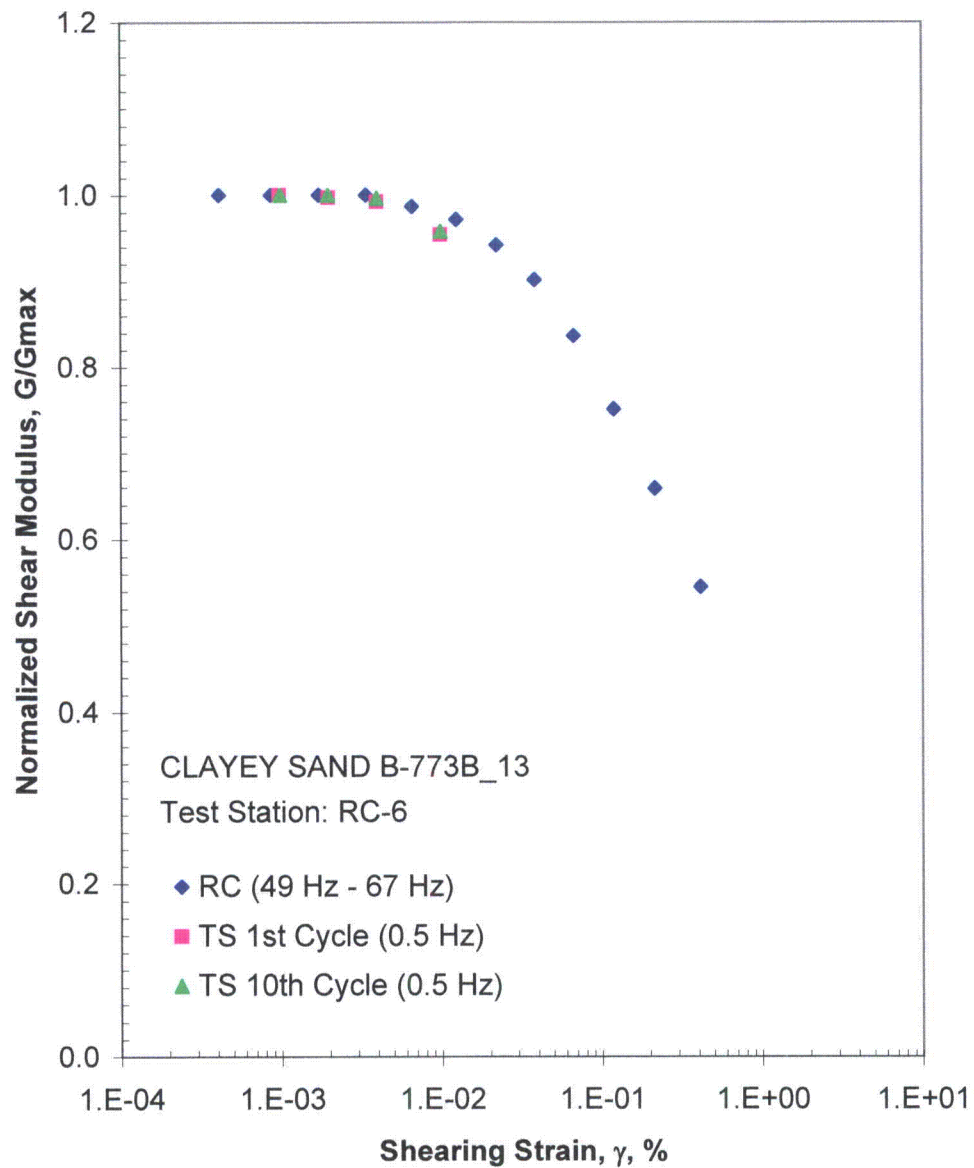


Figure I.17 Comparison of the Variation in Normalized Shear Modulus with Shearing Strain at an Isotropic Confining Pressure of 18403 psi from the Combined RCTS Tests

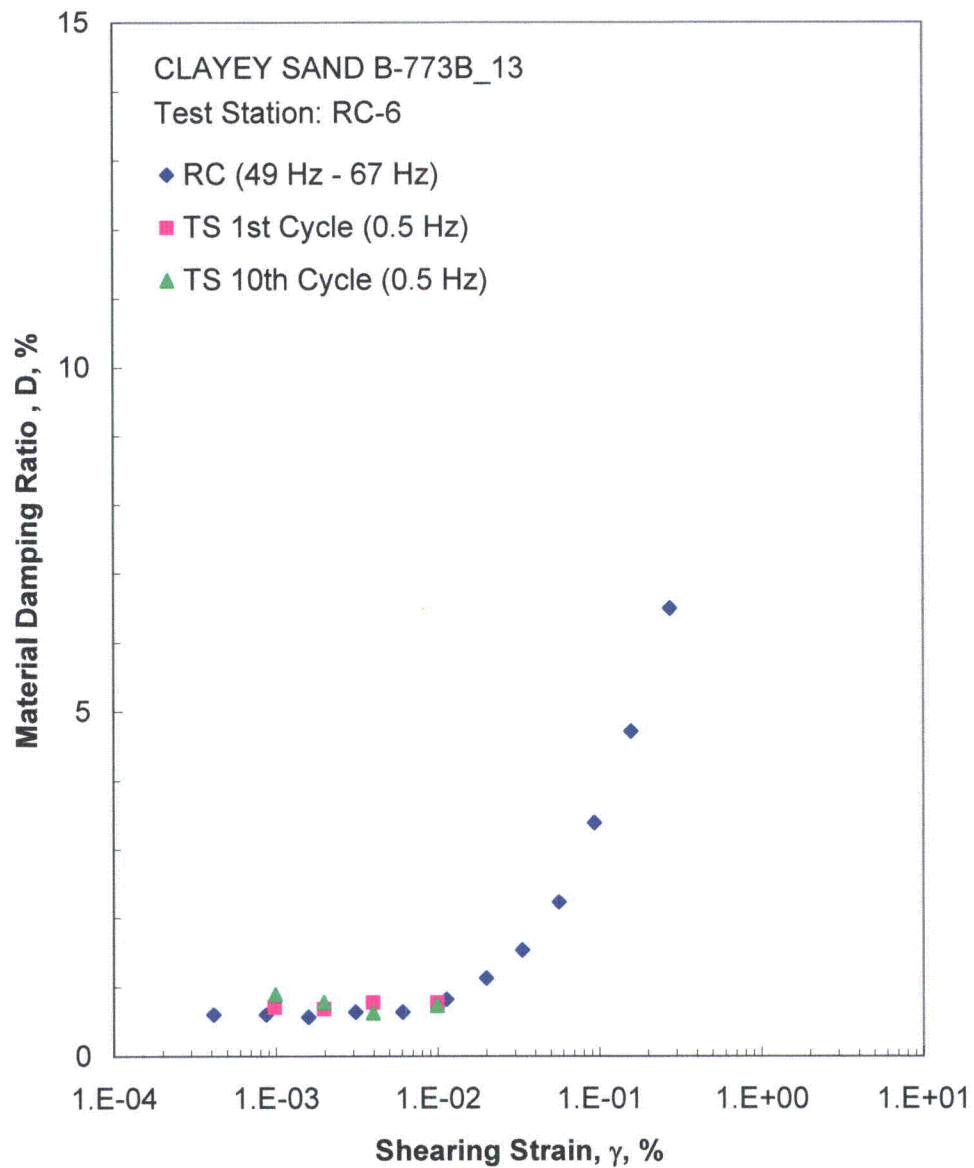


Figure I.18 Comparison of the Variation in Material Damping Ratio with Shearing Strain at an Isotropic Confining Pressure of 18403 psf from the Combined RCTS Tests

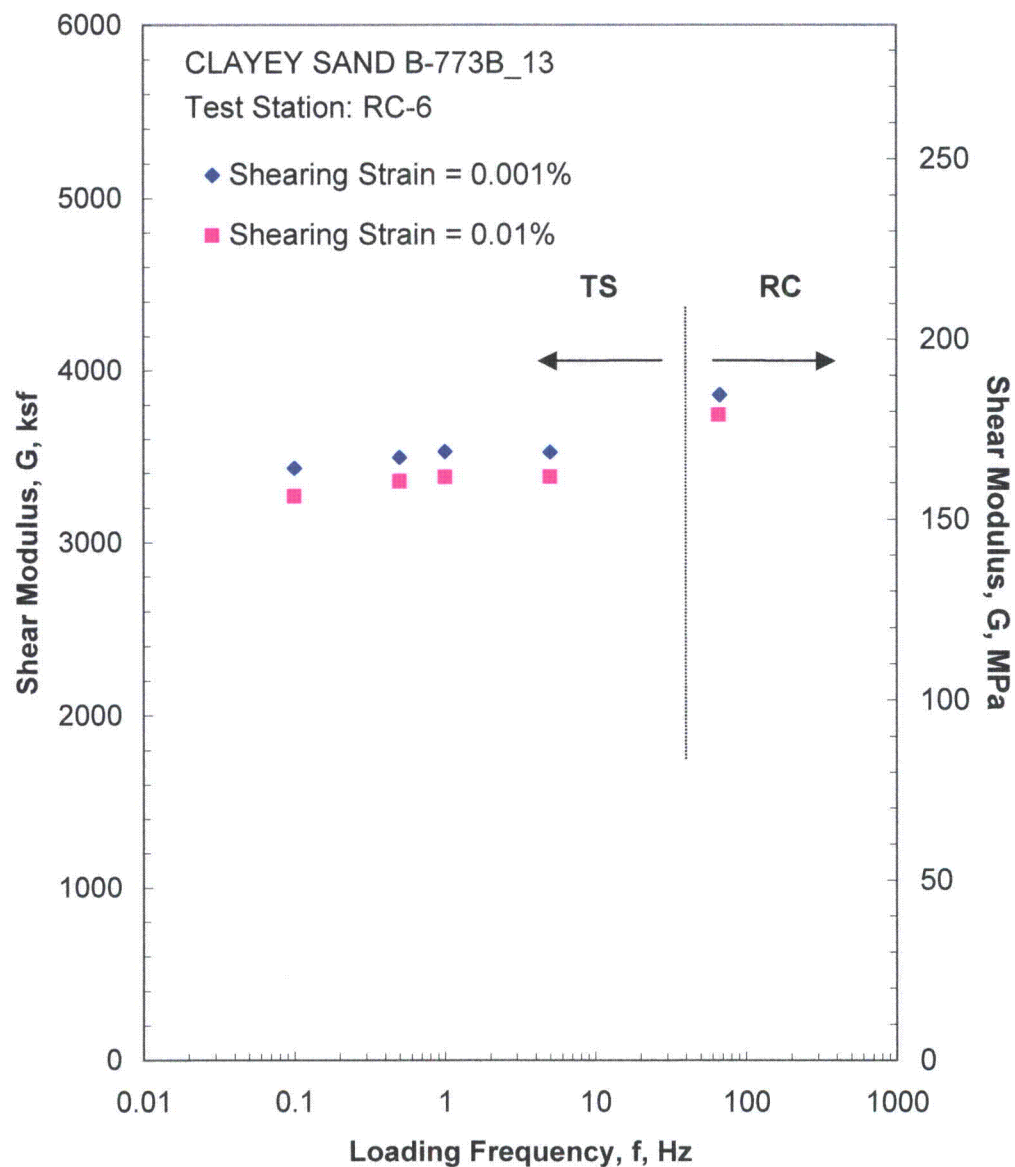


Figure I.19 Comparison of the Variation in Shear Modulus with Loading Frequency at an Isotropic Confining Pressure of 18403 psf from the Combined RCTS Tests

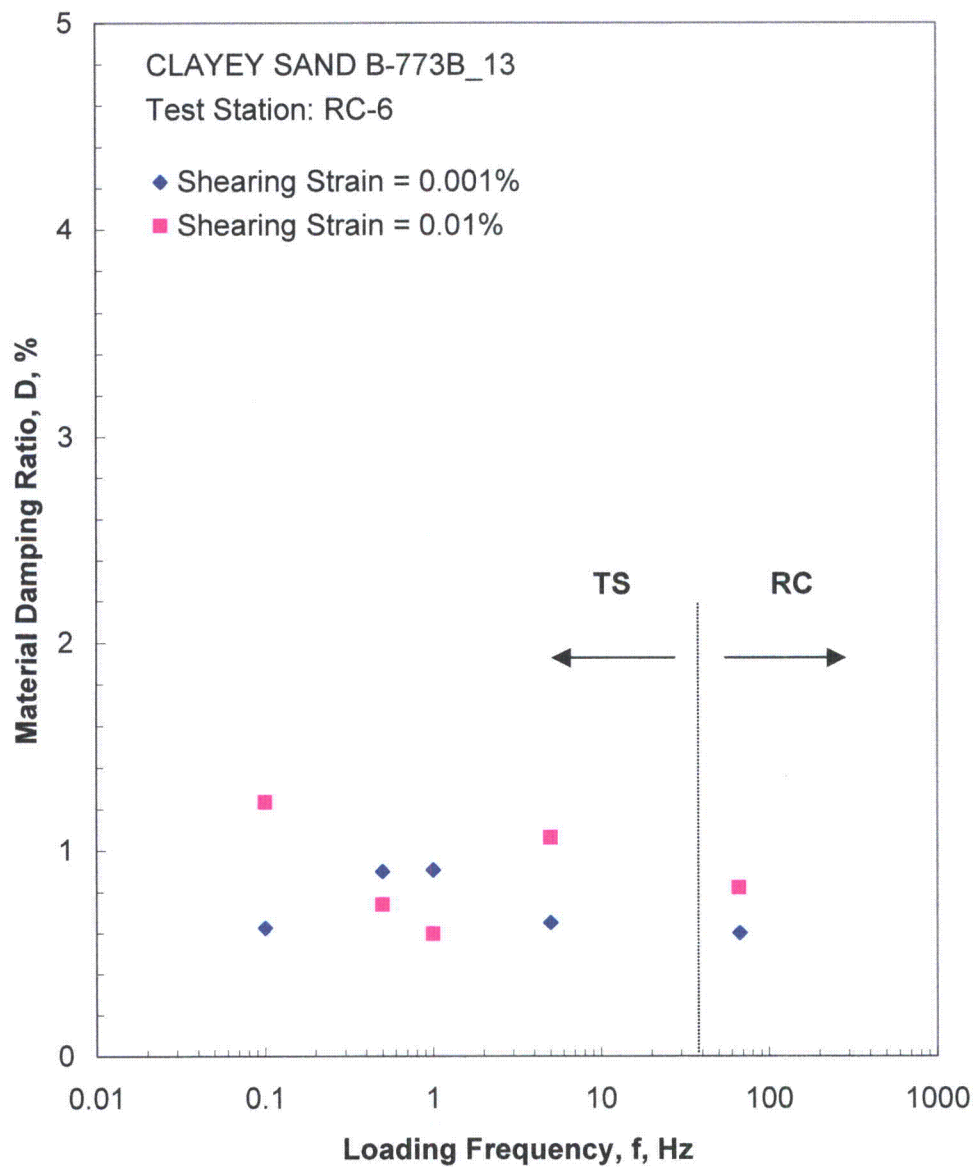


Figure I.20 Comparison of the Variation in Material Damping Ratio with Loading Frequency at an Isotropic Confining Pressure of 18403 psf from the Combined RCTS Tests

Table I.1 Variation in Low-Amplitude Shear Wave Velocity, Low-Amplitude Shear Modulus, Low-Amplitude Material Damping Ratio and Estimated Void Ratio with Isotropic Confining Pressure from RC Tests of Specimen B-773B-13

Isotropic Confining Pressure, σ_o			Low-Amplitude Shear Modulus, G_{max}		Low-Amplitude Shear Wave Velocity, V_s	Low-Amplitude Material Damping Ratio, D_{min}	Estimated Void Ratio, e
(psi)	(psf)	(kPa)	(ksf)	(MPa)	(fps)	(%)	
8	1152	55	1231	59	606	0.95	1.27
16	2304	110	1653	79	701	0.89	1.26
32	4608	220	2214	106	810	0.78	1.26
64	9202	440	2984	143	942	0.69	1.25
128	18403	881	3899	187	1072	0.60	1.24

Table I.2 Variation in Shear Modulus and Material Damping Ratio with Shearing Strain from RC Tests of Specimen B-773B-13; Isotropic Confining Pressure, $\sigma_0 = 4608$ psf

Peak Shearing Strain, %	Shear Modulus, G, ksf	Normalized Shear Modulus, G/G_{max}	Average ⁺ Shearing Strain, %	Material Damping Ratio ^x , D, %
5.68E-04	2201	1.00	5.68E-04	0.76
1.06E-03	2201	1.00	1.06E-03	0.82
2.13E-03	2201	1.00	2.13E-03	0.86
4.15E-03	2168	0.99	4.15E-03	0.87
7.88E-03	2129	0.97	7.01E-03	0.86
1.47E-02	2071	0.94	1.30E-02	1.09
2.63E-02	1991	0.90	2.26E-02	1.39
4.64E-02	1843	0.84	3.80E-02	2.21

⁺ Average Shearing Strain from the First Three Cycles of the Free Vibration Decay Curve

^x Average Damping Ratio from the First Three Cycles of the Free Vibration Decay Curve

Table I.3 Variation in Shear Modulus, Normalized Shear Modulus and Material Damping Ratio with Shearing Strain from TS Tests of Specimen B-773B-13; Isotropic Confining Pressure, $\sigma_0 = 4608$ psf

First Cycle				Tenth Cycle			
Peak Shearing Strain, %	Shear Modulus, G, ksf	Normalized Shear Modulus, G/G_{max}	Material Damping Ratio, D, %	Peak Shearing Strain, %	Shear Modulus, G, ksf	Normalized Shear Modulus, G/G_{max}	Material Damping Ratio, D, %
5.72E-04	2310	1.00	0.70	5.82E-04	2269	1.00	0.52
1.02E-03	2285	0.99	0.90	1.03E-03	2265	1.00	0.41
4.31E-03	2171	0.94	0.82	4.33E-03	2159	0.95	0.55
1.04E-02	1955	0.85	1.30	1.04E-02	1955	0.86	1.55

Table I.4 Variation in Shear Modulus and Material Damping Ratio with Shearing Strain from RC Tests of Specimen B-773B-13; Isotropic Confining Pressure, $\sigma_o = 18403$ psf

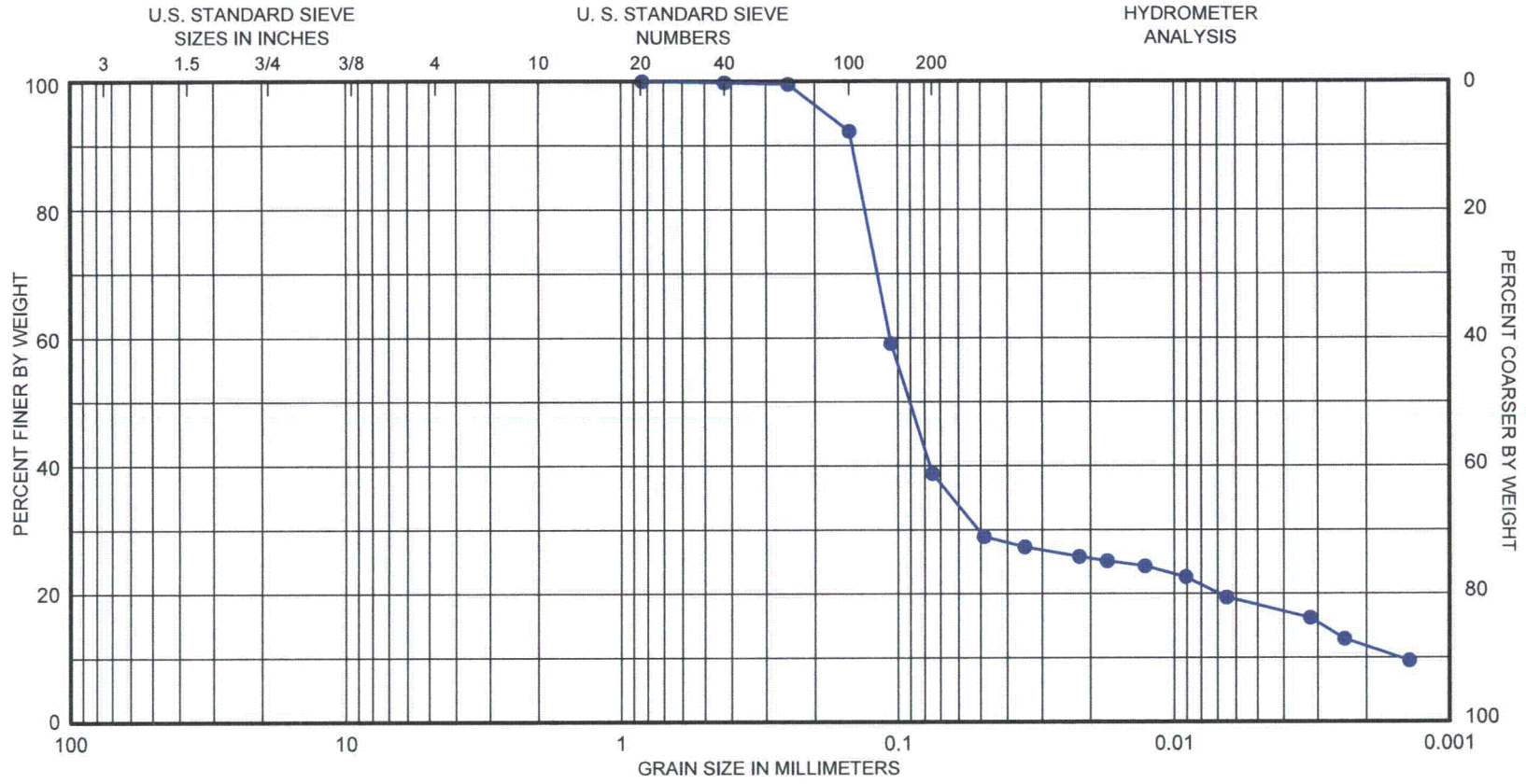
Peak Shearing Strain, %	Shear Modulus, G, ksf	Normalized Shear Modulus, G/G_{max}	Average ⁺ Shearing Strain, %	Material Damping Ratio ^x , D, %
4.12E-04	3852	1.00	4.12E-04	0.60
8.68E-04	3852	1.00	8.68E-04	0.60
1.73E-03	3852	1.00	1.59E-03	0.56
3.40E-03	3852	1.00	3.09E-03	0.64
6.57E-03	3801	0.99	6.05E-03	0.64
1.24E-02	3743	0.97	1.13E-02	0.82
2.22E-02	3629	0.94	1.99E-02	1.13
3.82E-02	3473	0.90	3.32E-02	1.53
6.69E-02	3222	0.84	5.62E-02	2.23
1.19E-01	2894	0.75	9.30E-02	3.39
2.15E-01	2537	0.66	1.57E-01	4.72
4.13E-01	2100	0.55	2.73E-01	6.50

⁺ Average Shearing Strain from the First Three Cycles of the Free Vibration Decay Curve

^x Average Damping Ratio from the First Three Cycles of the Free Vibration Decay Curve

Table I.5 Variation in Shear Modulus, Normalized Shear Modulus and Material Damping Ratio with Shearing Strain from TS Tests of Specimen B-773B-13; Isotropic Confining Pressure, $\sigma_o = 18403$ psf

First Cycle				Tenth Cycle			
Peak Shearing Strain, %	Shear Modulus, G, ksf	Normalized Shear Modulus, G/G_{max}	Material Damping Ratio, D, %	Peak Shearing Strain, %	Shear Modulus, G, ksf	Normalized Shear Modulus, G/G_{max}	Material Damping Ratio, D, %
9.81E-04	3516	1.00	0.70	9.91E-04	3498	1.00	0.89
1.97E-03	3507	1.00	0.68	1.97E-03	3498	1.00	0.78
3.97E-03	3489	0.99	0.77	3.97E-03	3486	1.00	0.62
9.90E-03	3354	0.95	0.77	9.91E-03	3351	0.96	0.73



APPENDIX J

Specimen B-773B_15

Borehole B-773B

Sample 15

Depth = 147 ft (44.8 m)

Total Unit Weight = 101.5 lb/ft³

Water Content = 52.3 %

FUGRO JOB #: 0411-09-1734
Testing Station: RC7



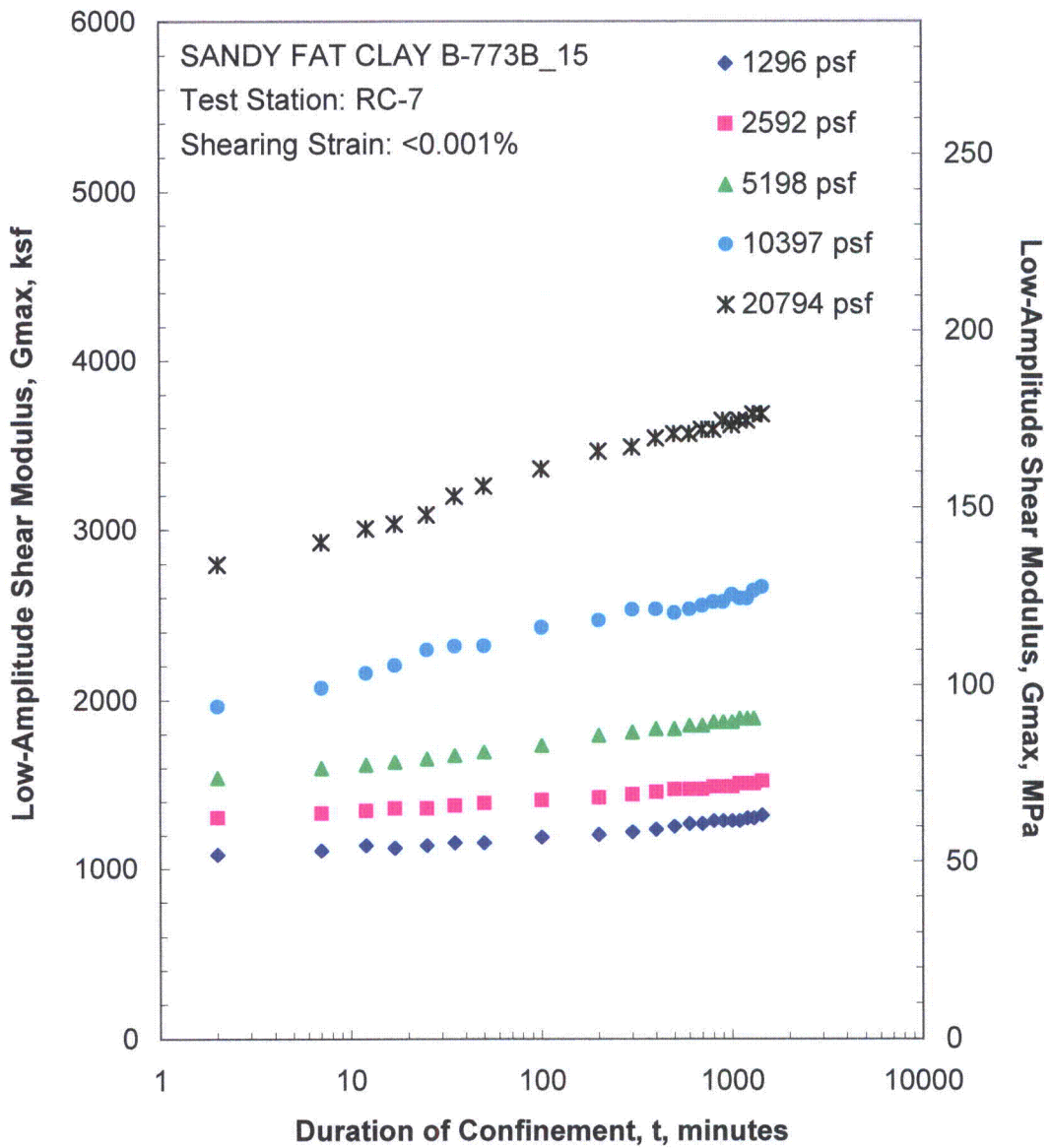


Figure J.1 Variation in Low-Amplitude Shear Modulus with Magnitude and Duration of Isotropic Confining Pressure from Resonant Column Tests

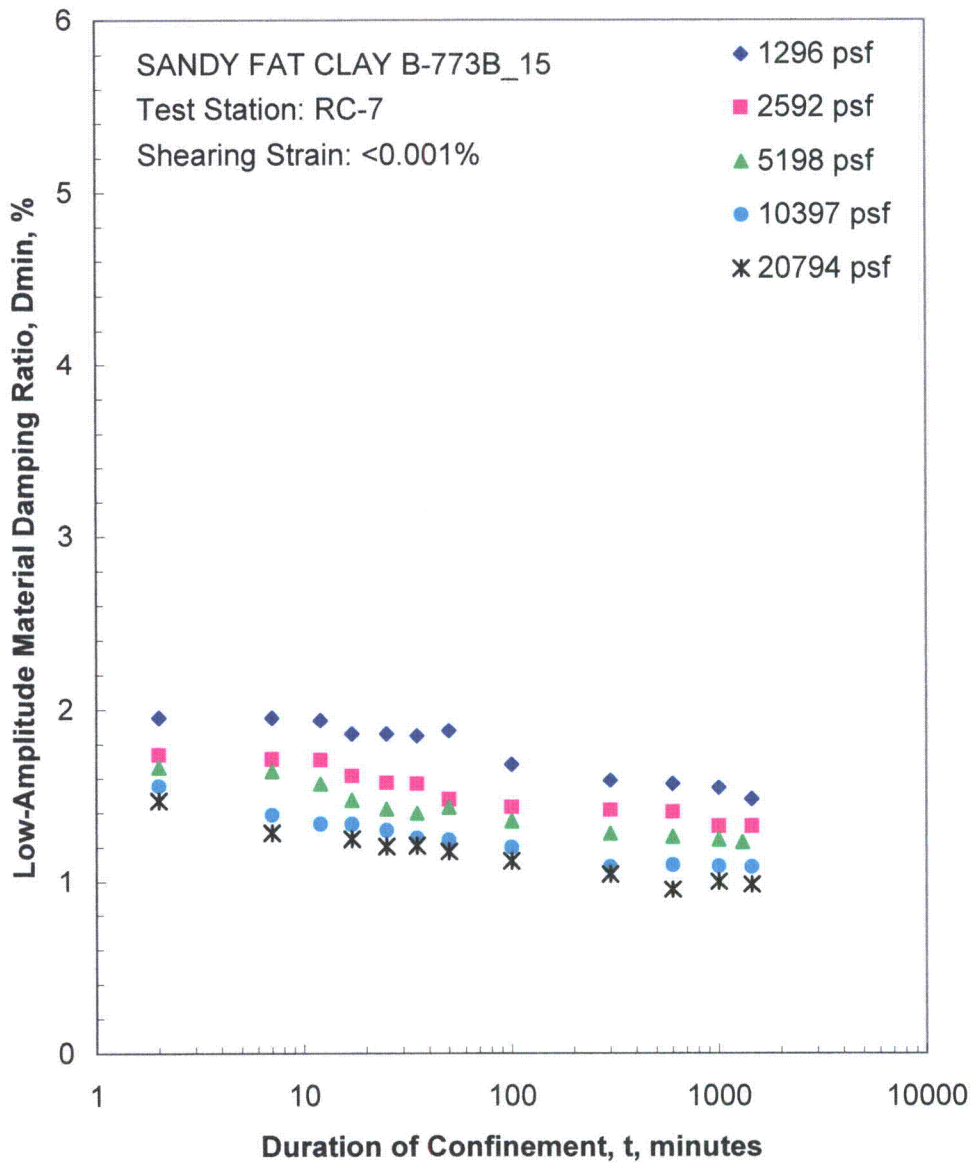


Figure J.2 Variation in Low-Amplitude Material Damping Ratio with Magnitude and Duration of Isotropic Confining Pressure from Resonant Column Tests

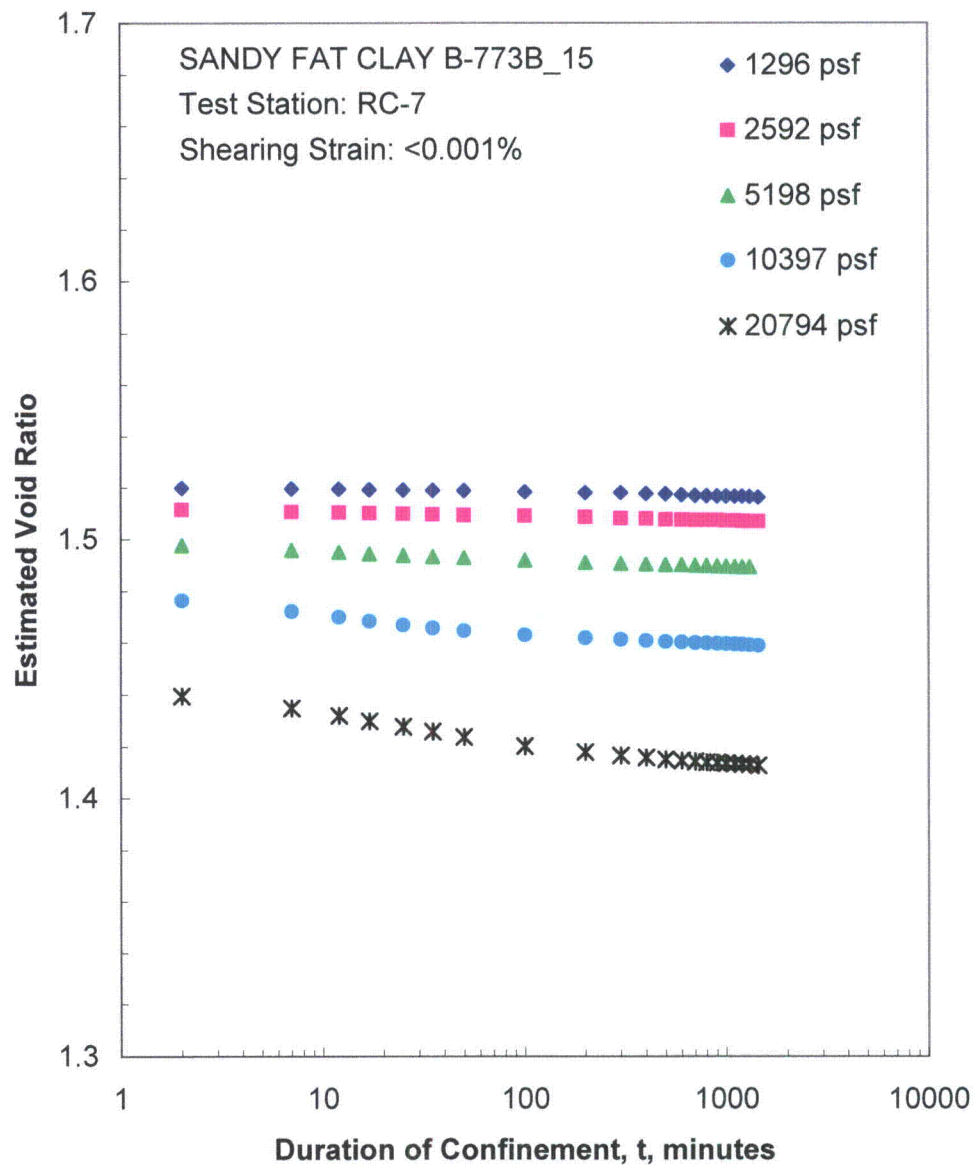


Figure J.3 Variation in Estimated Void Ratio with Magnitude and Duration of Isotropic Confining Pressure from Resonant Column Tests

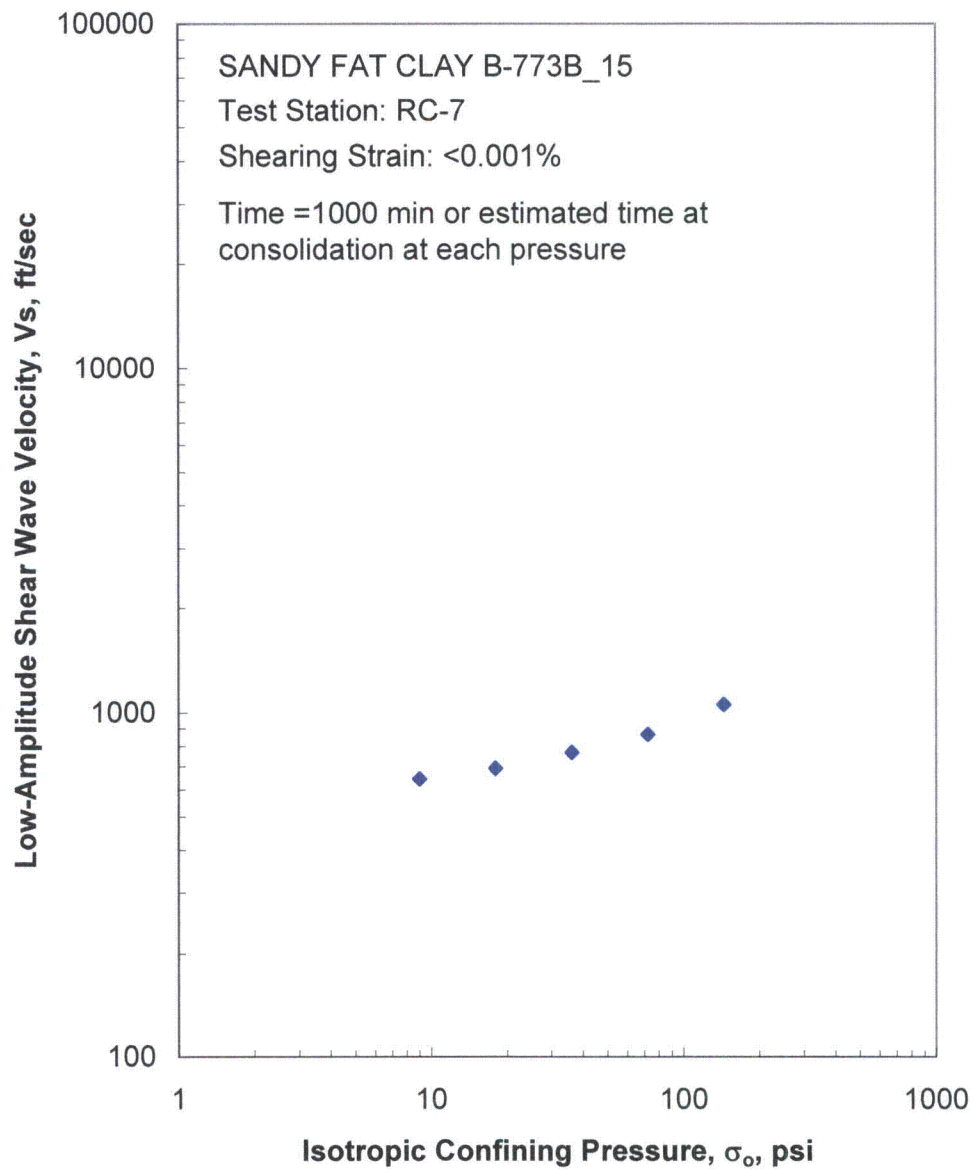


Figure J.4 Variation in Low-Amplitude Shear Wave Velocity with Isotropic Confining Pressure from Resonant Column Tests

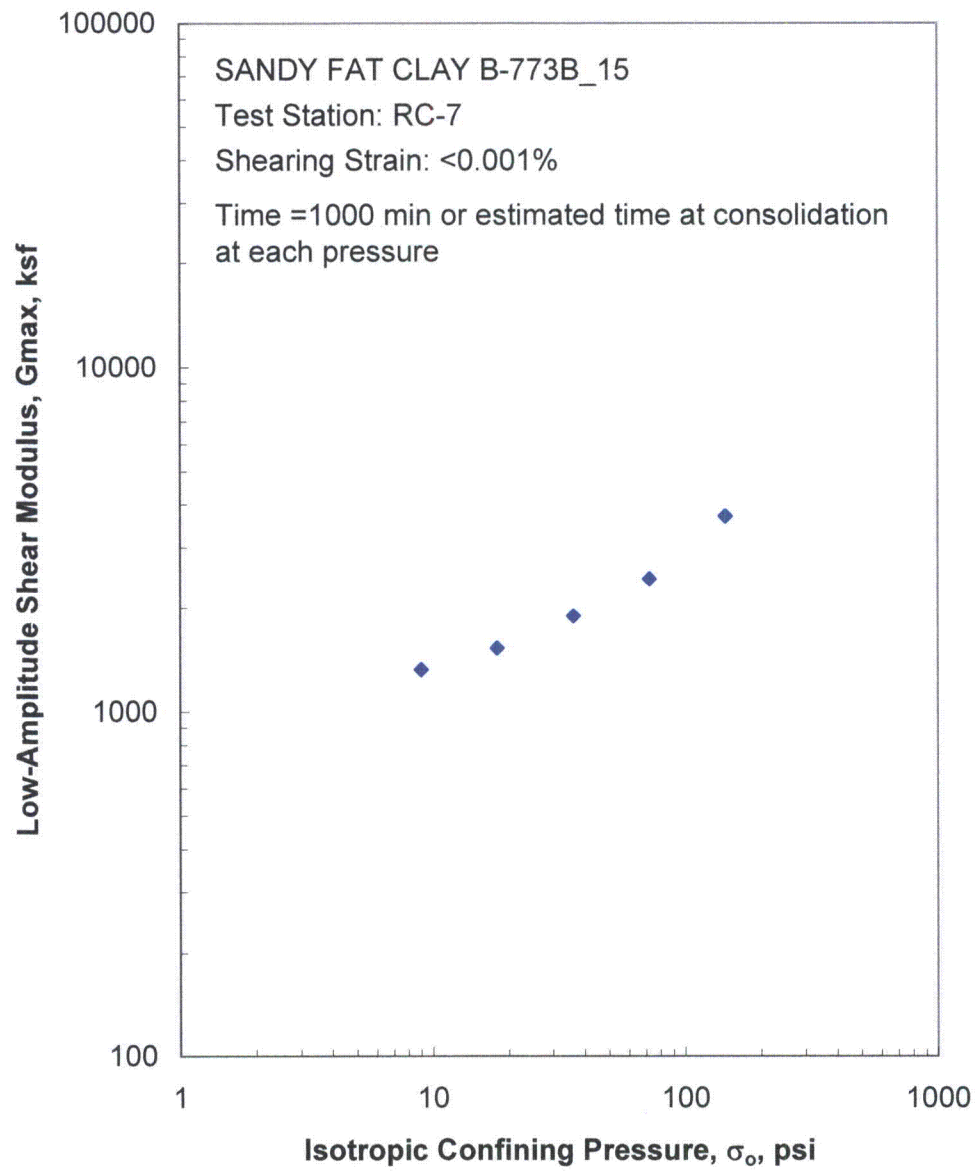


Figure J.5 Variation in Low-Amplitude Shear Modulus with Isotropic Confining Pressure from Resonant Column Tests

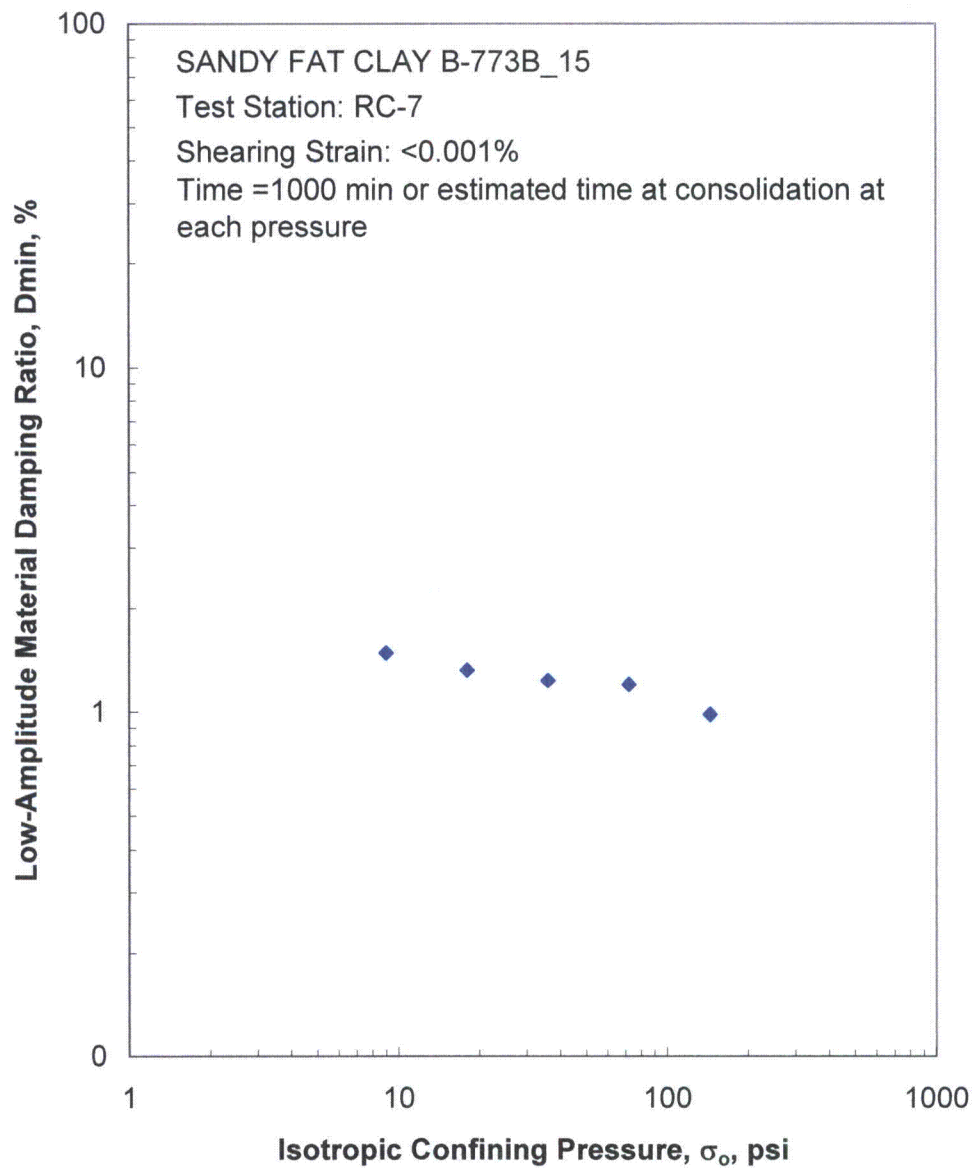


Figure J.6 Variation in Low-Amplitude Material Damping Ratio with Isotropic Confining Pressure from Resonant Column Tests

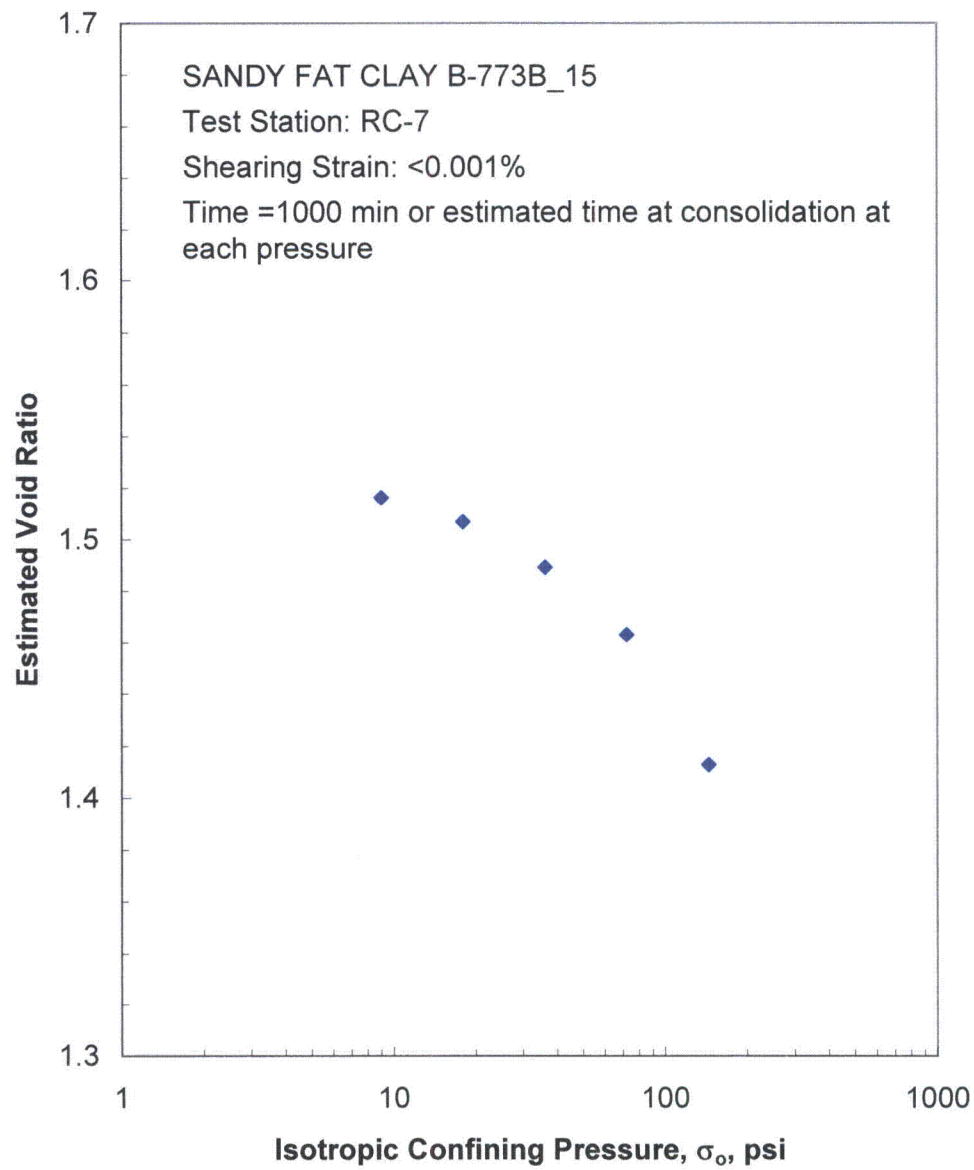


Figure J.7 Variation in Estimated Void Ratio with Isotropic Confining Pressure from Resonant Column Tests

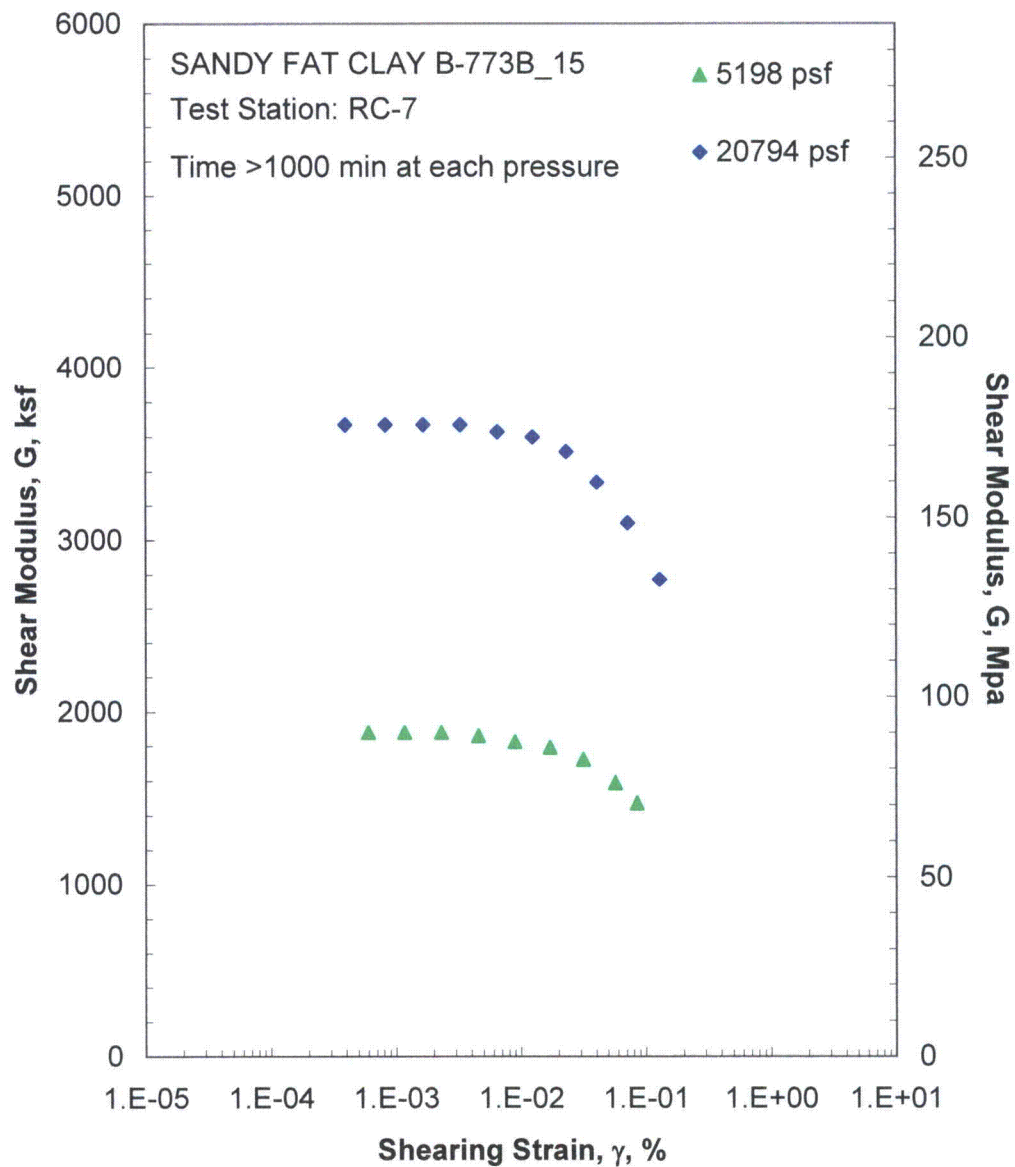


Figure J.8 Comparison of the Variation in Shear Modulus with Shearing Strain and Isotropic Confining Pressure from the Resonant Column Tests

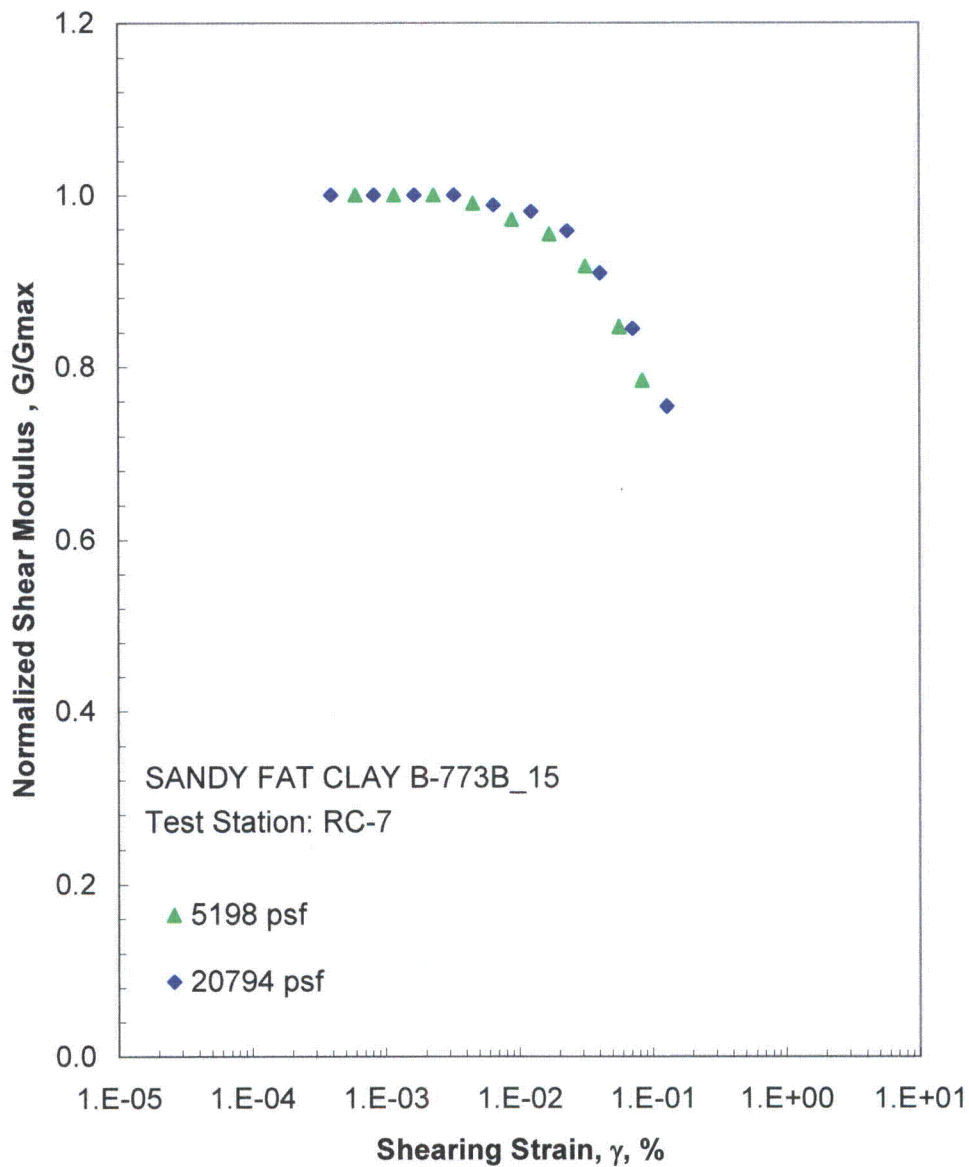


Figure J.9 Comparison of the Variation in Normalized Shear Modulus with Shearing Strain and Isotropic Confining Pressure from the Resonant Column Tests

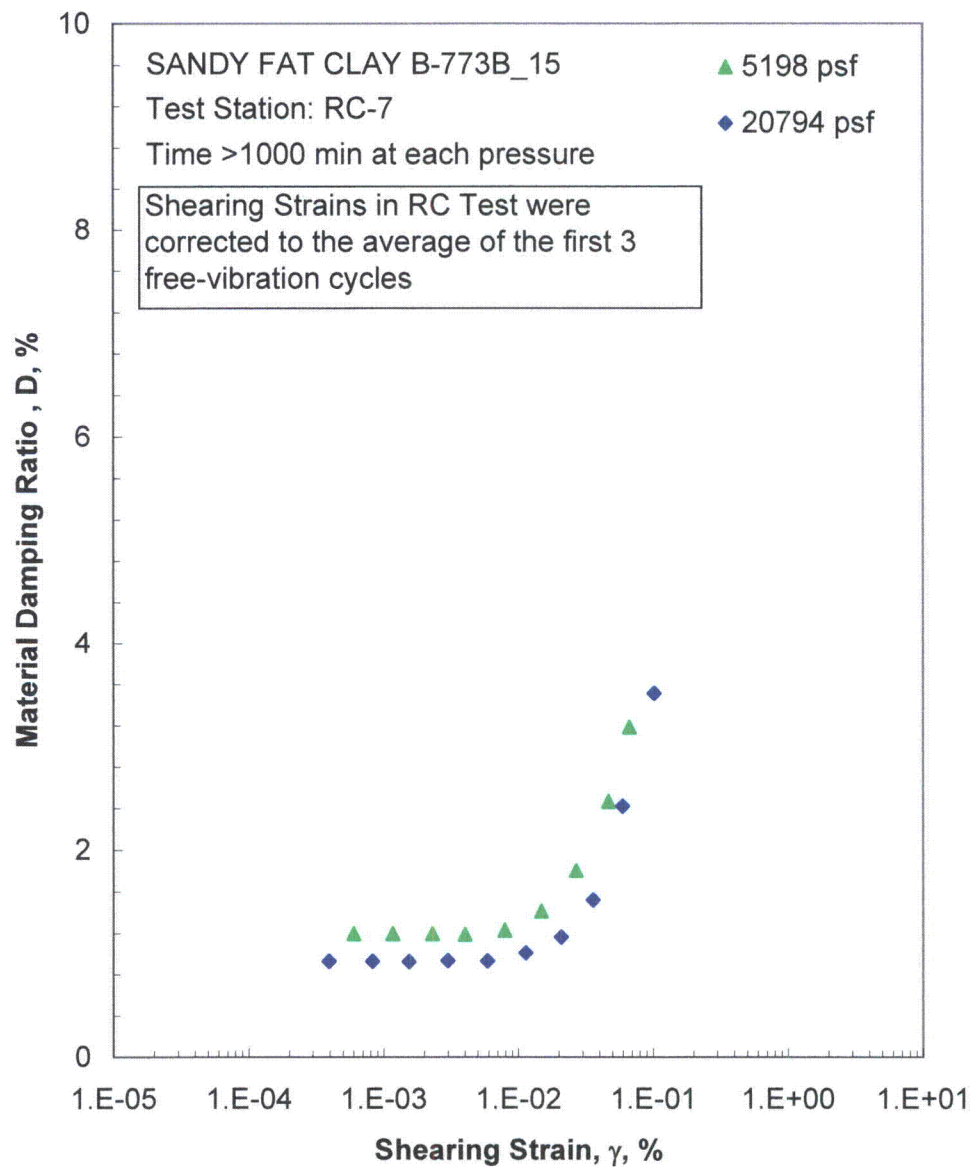


Figure J.10 Comparison of the Variation in Material Damping Ratio with Shearing Strain and Isotropic Confining Pressure from the Resonant Column Tests

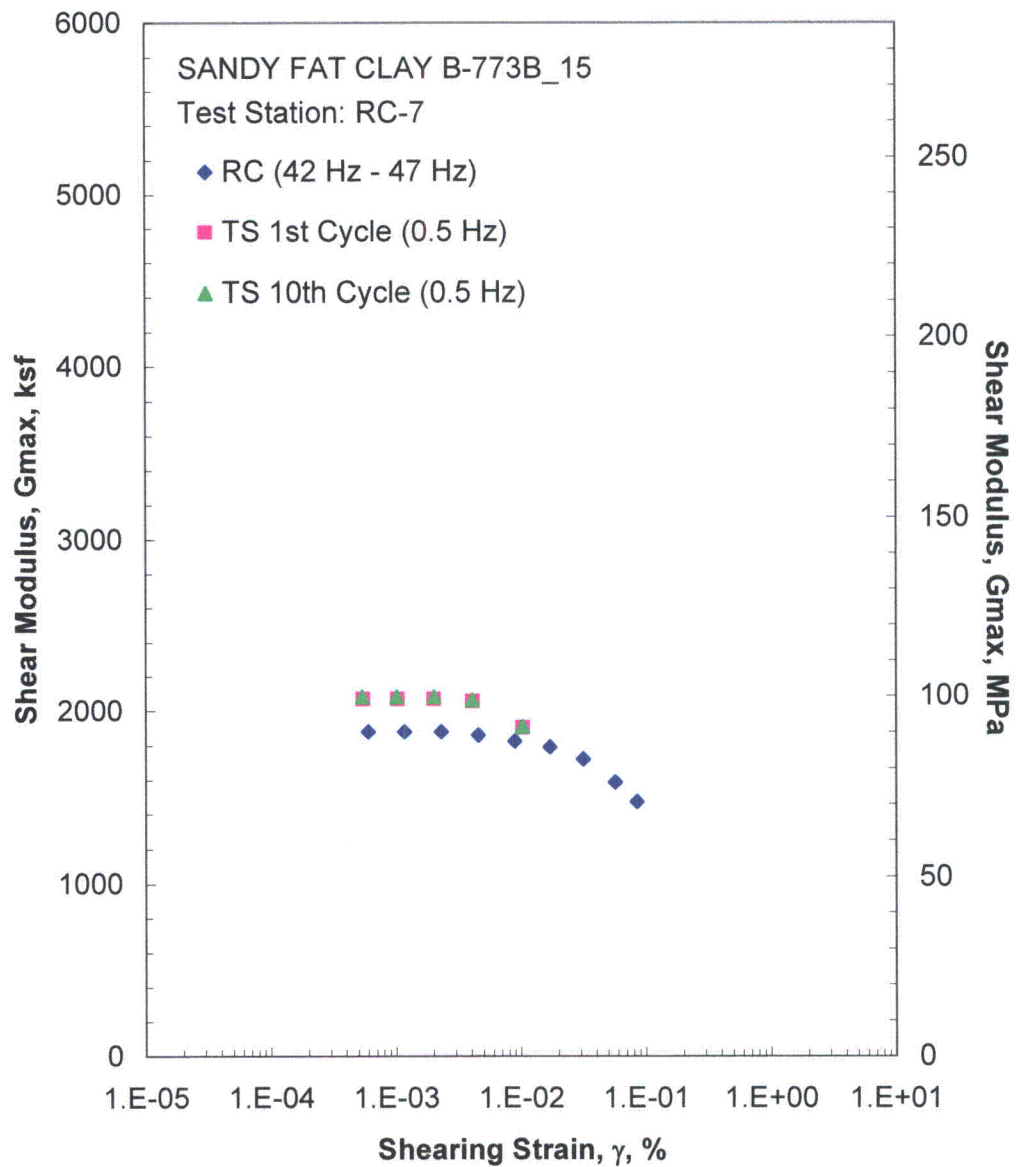


Figure J.11 Comparison of the Variation in Shear Modulus with Shearing Strain at an Isotropic Confining Pressure of 5198 psf from the Combined RCTS Tests

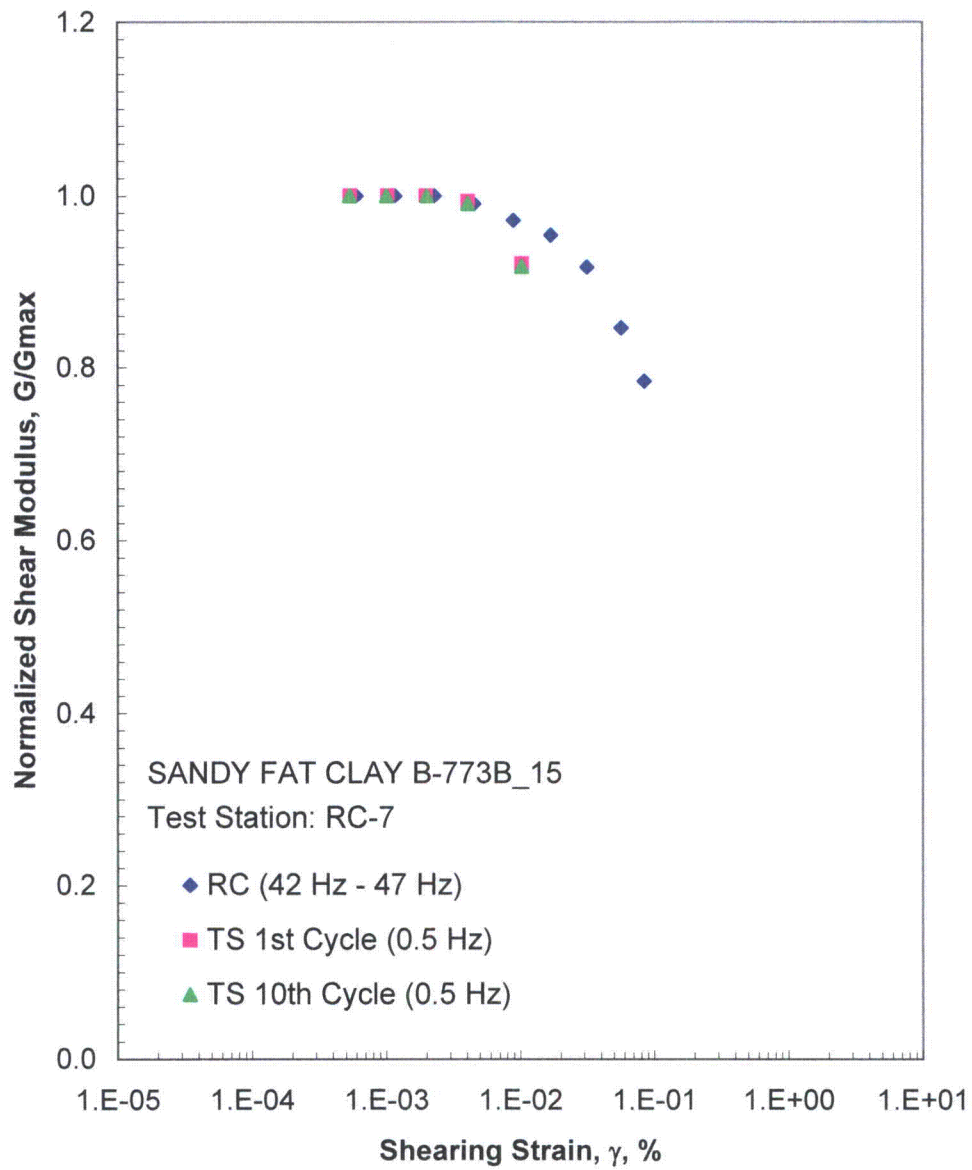


Figure J.12 Comparison of the Variation in Normalized Shear Modulus with Shearing Strain at an Isotropic Confining Pressure of 5198 psf from the Combined RCTS Tests

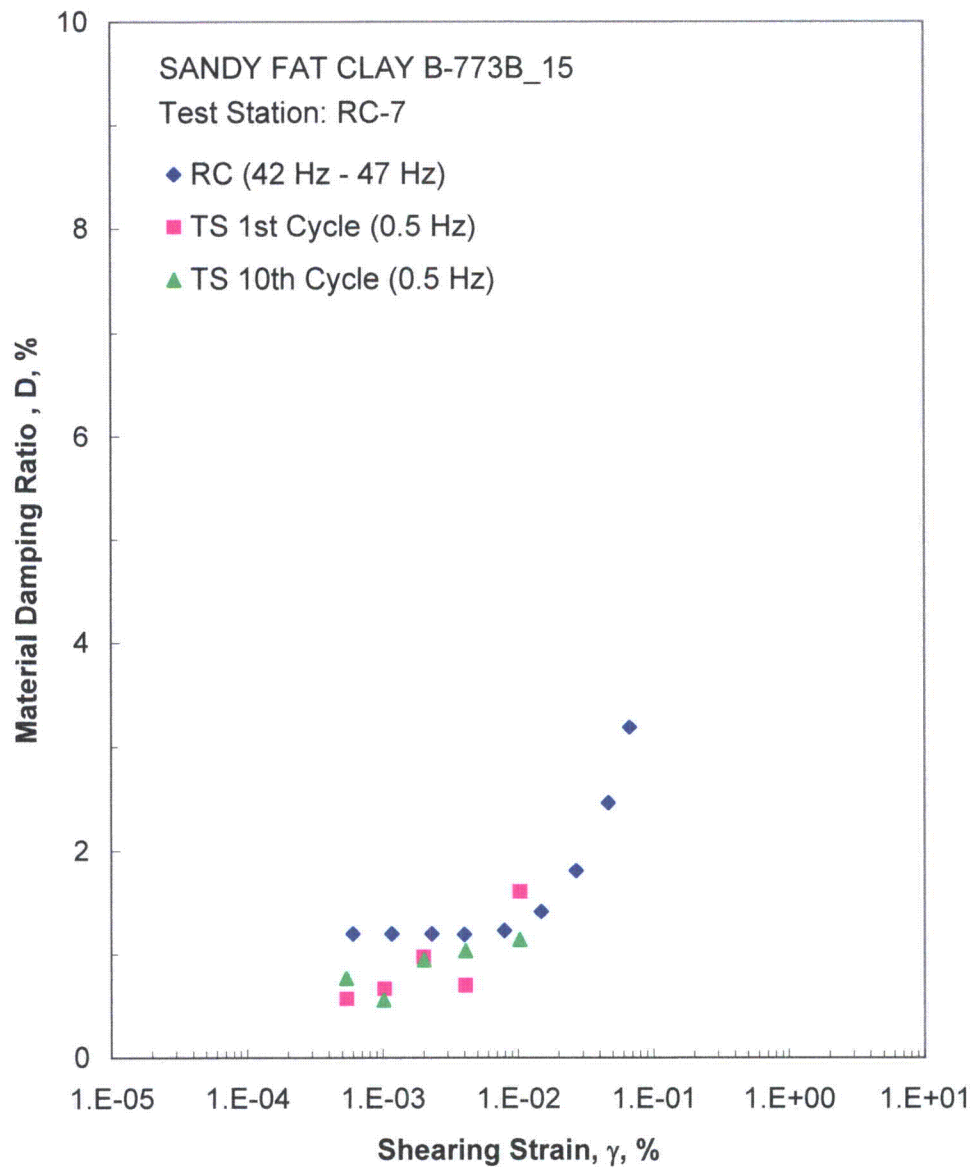


Figure J.13 Comparison of the Variation in Material Damping Ratio with Shearing Strain at an Isotropic Confining Pressure of 5198 psf from the Combined RCTS Tests

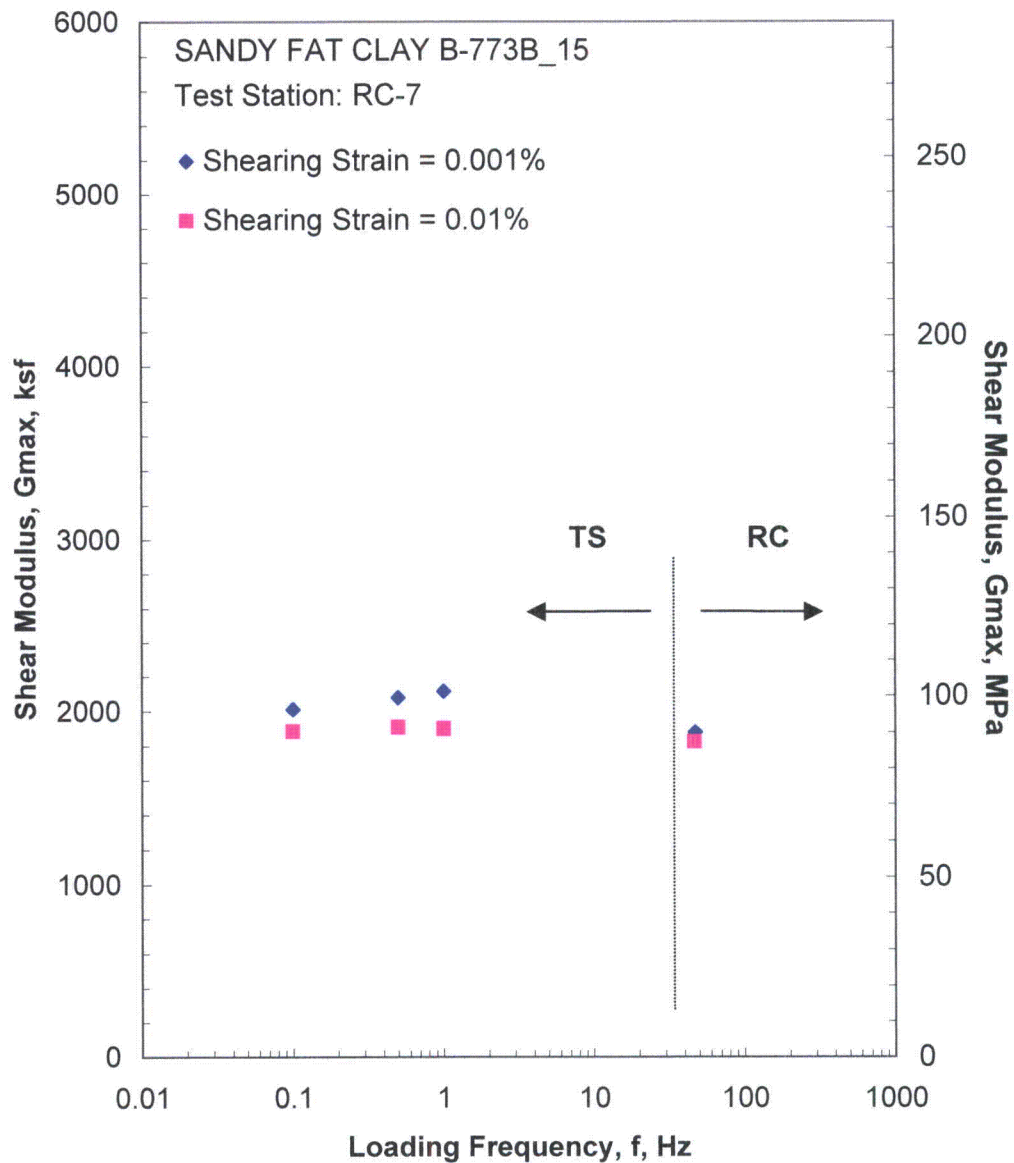


Figure J.14 Comparison of the Variation in Shear Modulus with Loading Frequency at an Isotropic Confining Pressure of 5198 psf from the Combined RCTS Tests

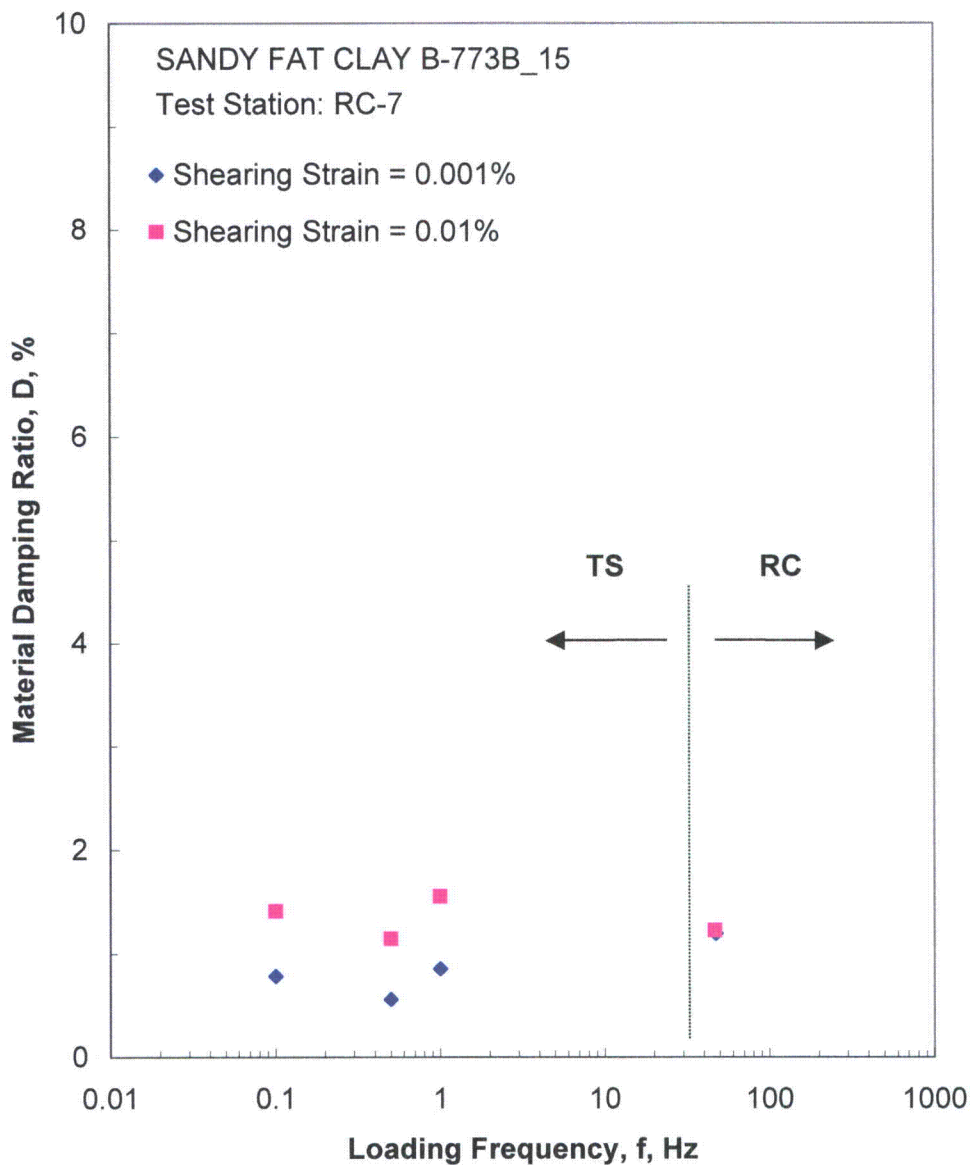


Figure J.15 Comparison of the Variation in Material Damping Ratio with Loading Frequency at an Isotropic Confining Pressure of 5198 psf from the Combined RCTS Tests

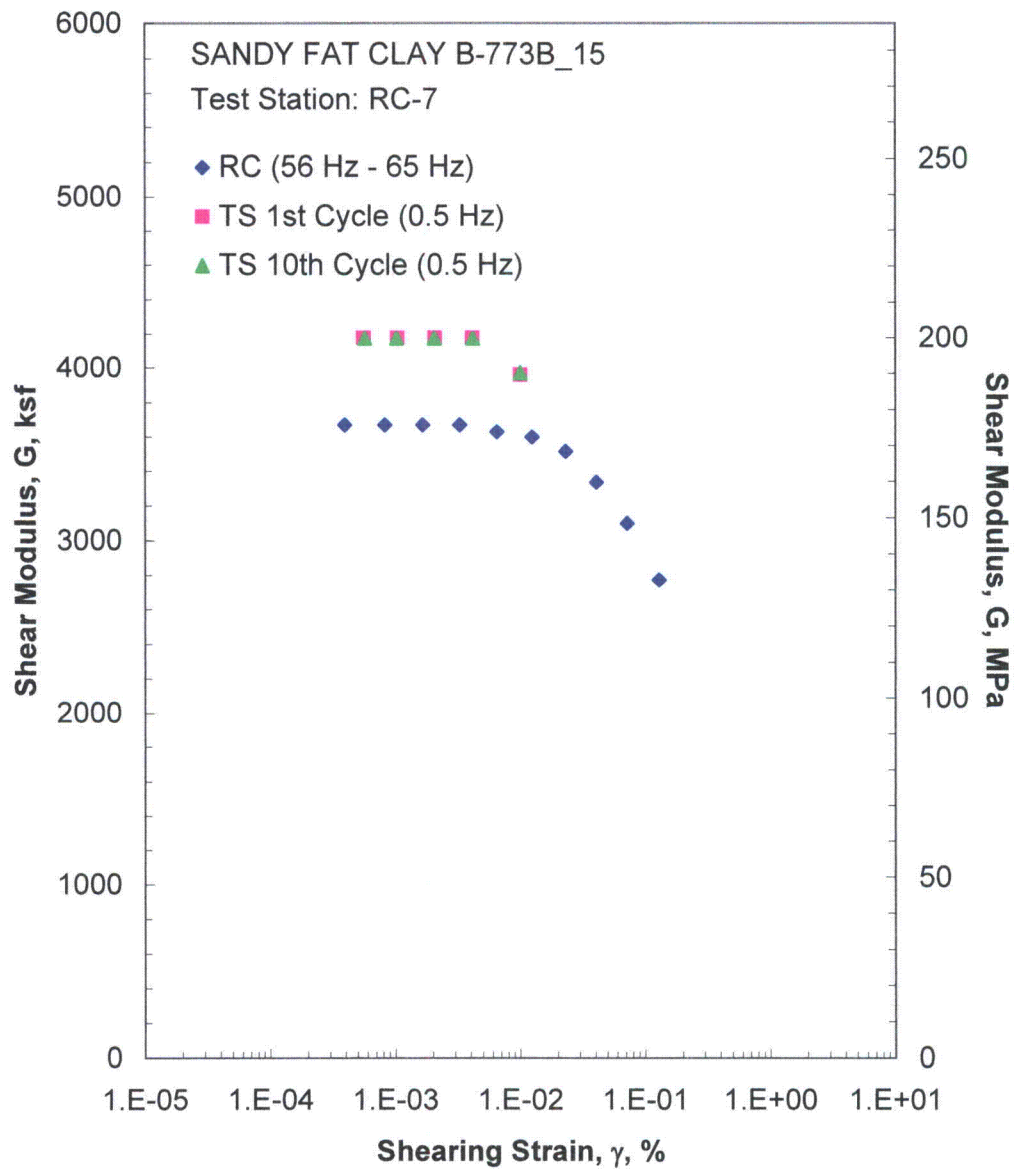


Figure J.16 Comparison of the Variation in Shear Modulus with Shearing Strain at an Isotropic Confining Pressure of 20794 psf from the Combined RCTS Tests

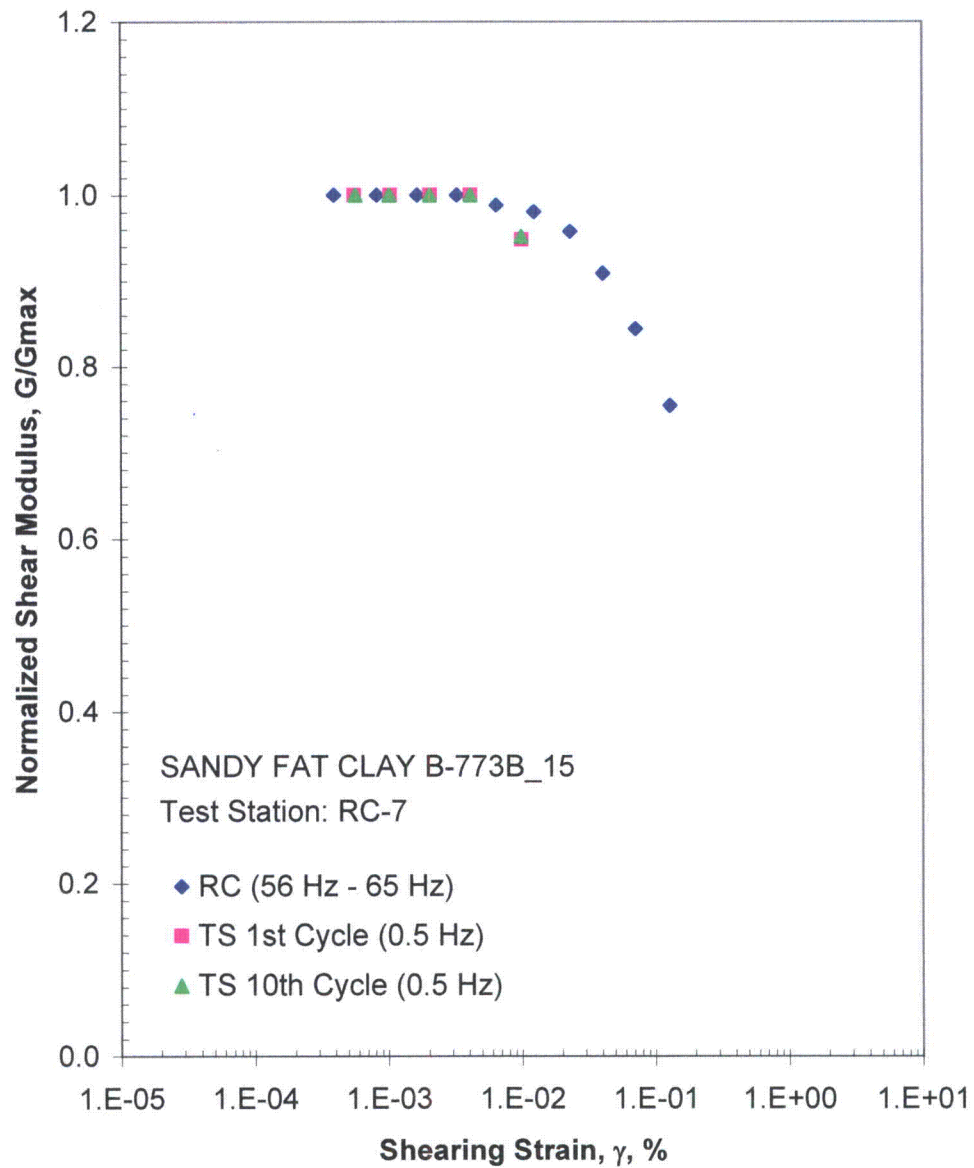


Figure J.17 Comparison of the Variation in Normalized Shear Modulus with Shearing Strain at an Isotropic Confining Pressure of 20794 psf from the Combined RCTS Tests

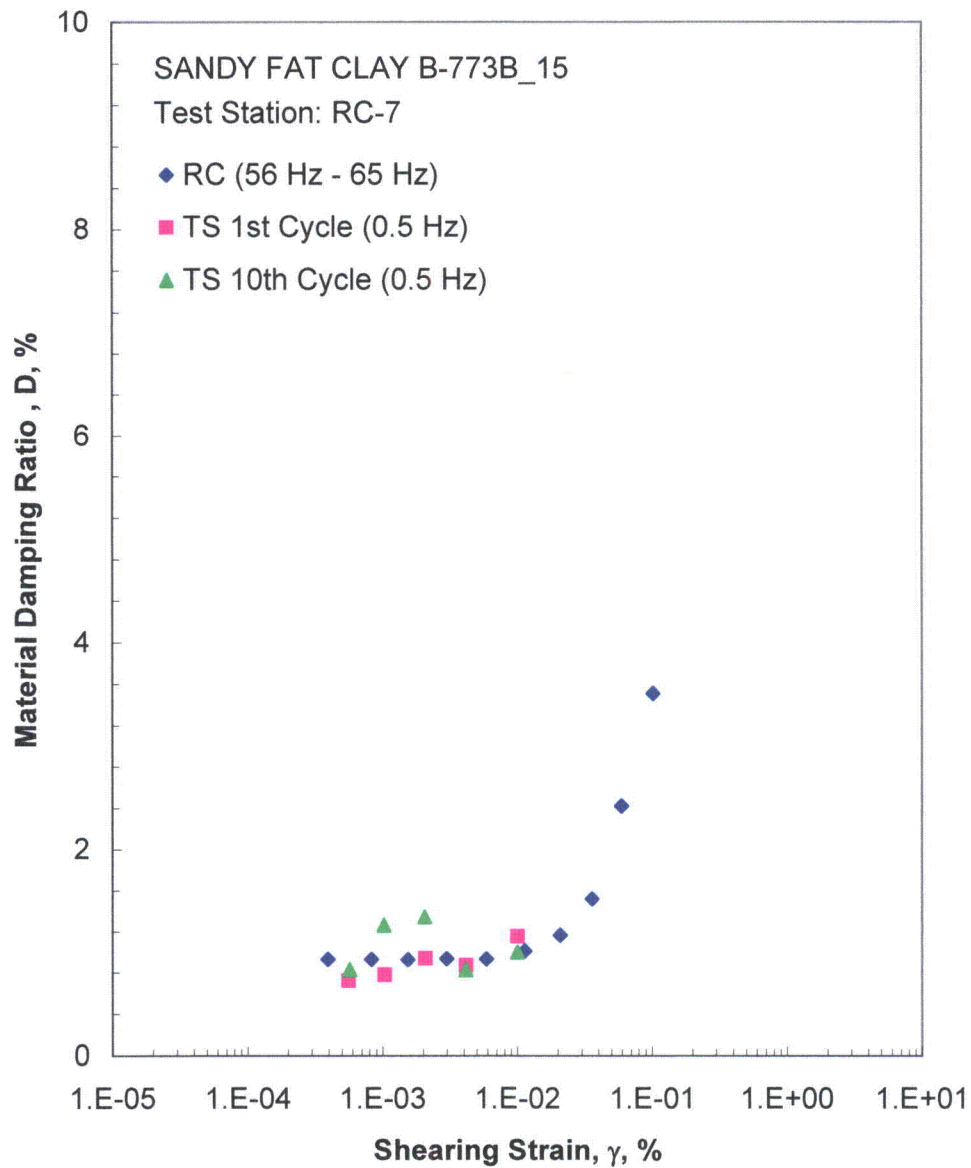


Figure J.18 Comparison of the Variation in Material Damping Ratio with Shearing Strain at an Isotropic Confining Pressure of 20794 psf from the Combined RCTS Tests

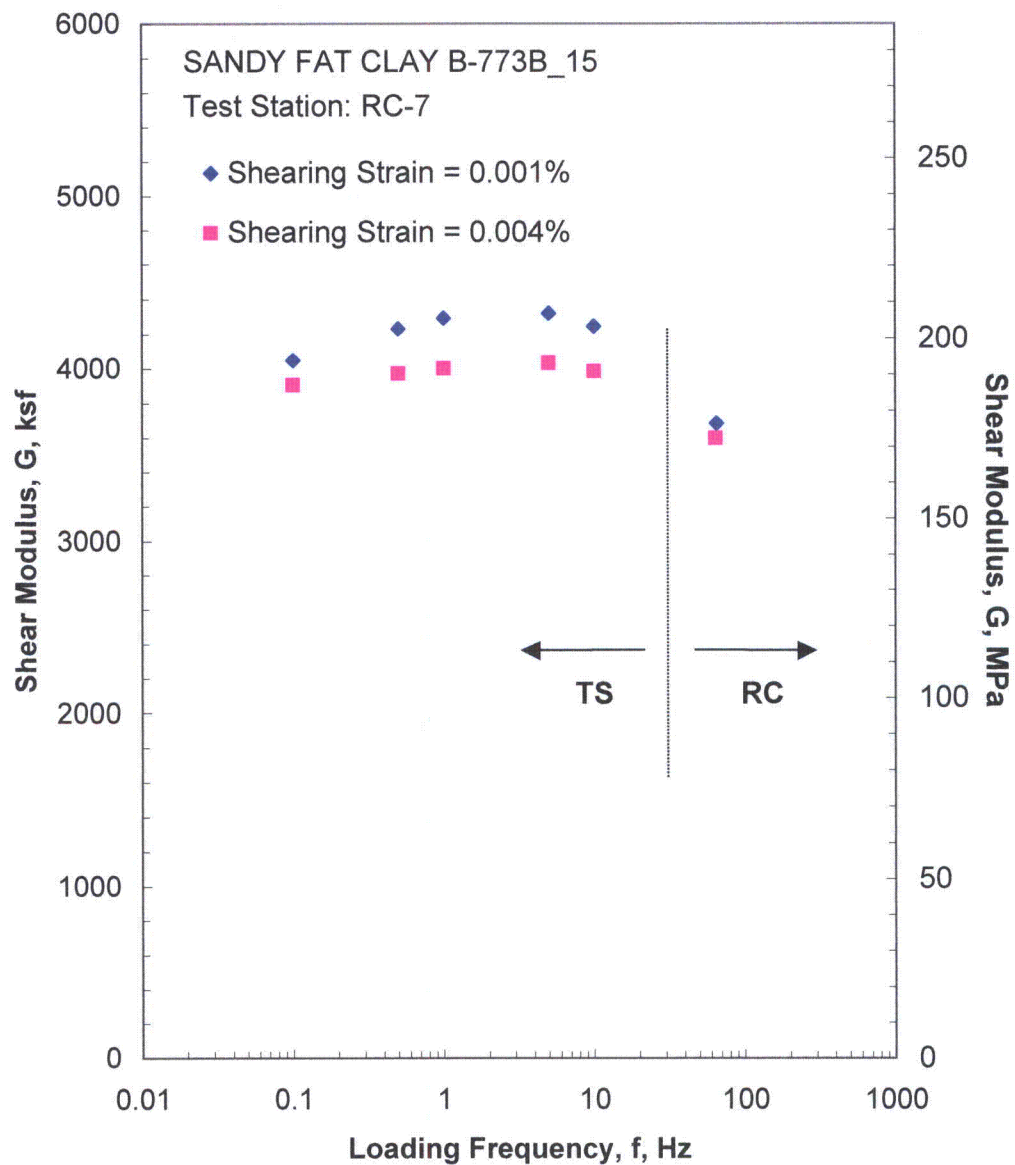


Figure J.19 Comparison of the Variation in Shear Modulus with Loading Frequency at an Isotropic Confining Pressure of 20794 psf from the Combined RCTS Tests

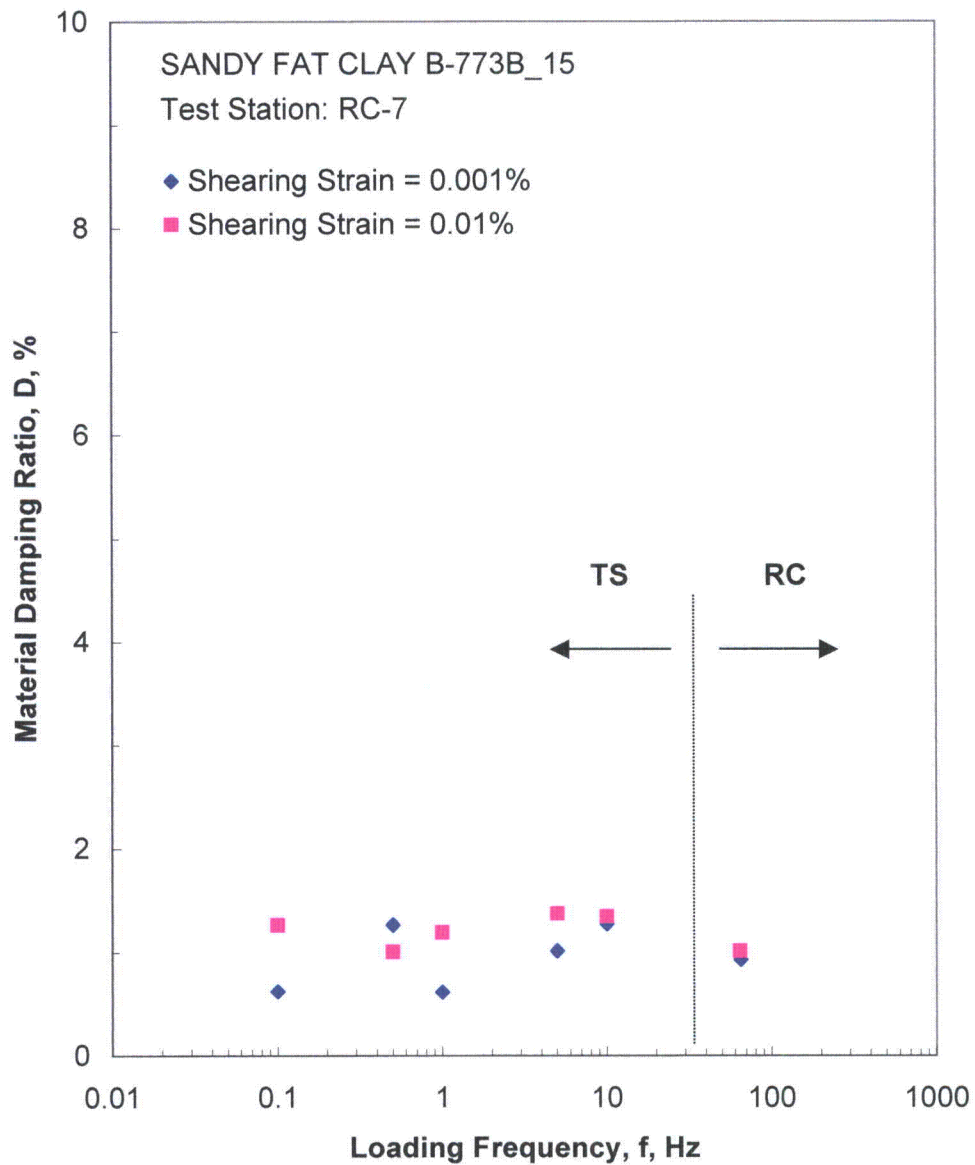


Figure J.20 Comparison of the Variation in Material Damping Ratio with Loading Frequency at an Isotropic Confining Pressure of 20794 psf from the Combined RCTS Tests

Table J.1 Variation in Low-Amplitude Shear Wave Velocity, Low-Amplitude Shear Modulus, Low-Amplitude Material Damping Ratio and Estimated Void Ratio with Isotropic Confining Pressure from RC Tests of Specimen B-773B-15

Isotropic Confining Pressure, σ_o			Low-Amplitude Shear Modulus, G_{max}		Low-Amplitude Shear Wave Velocity, V_s	Low-Amplitude Material Damping Ratio, D_{min}	Estimated Void Ratio, e
(psi)	(psf)	(kPa)	(ksf)	(MPa)	(fps)	(%)	
9	1296	62	1320	63	645	1.48	1.52
18	2592	124	1522	73	692	1.32	1.51
36	5198	249	1892	91	768	1.23	1.49
72	10397	497	2425	116	865	1.20	1.46
144	20794	995	3685	177	1056	0.98	1.41

Table J.2 Variation in Shear Modulus and Material Damping Ratio with Shearing Strain from RC Tests of Specimen B-773B-15; Isotropic Confining Pressure, $\sigma_0 = 5198$ psf

Peak Shearing Strain, %	Shear Modulus, G, ksf	Normalized Shear Modulus, G/G_{max}	Average ⁺ Shearing Strain, %	Material Damping Ratio ^x , D, %
6.00E-04	1878	1.00	6.00E-04	1.20
1.17E-03	1878	1.00	1.17E-03	1.20
2.30E-03	1878	1.00	2.30E-03	1.20
4.55E-03	1860	0.99	4.00E-03	1.19
8.88E-03	1824	0.97	7.90E-03	1.23
1.70E-02	1792	0.95	1.48E-02	1.41
3.16E-02	1721	0.92	2.68E-02	1.80
5.66E-02	1590	0.85	4.64E-02	2.47
8.44E-02	1473	0.78	6.67E-02	3.19

⁺ Average Shearing Strain from the First Three Cycles of the Free Vibration Decay Curve

^x Average Damping Ratio from the First Three Cycles of the Free Vibration Decay Curve

Table J.3 Variation in Shear Modulus, Normalized Shear Modulus and Material Damping Ratio with Shearing Strain from TS Tests of Specimen B-773B-15; Isotropic Confining Pressure, $\sigma_0 = 5198$ psf

First Cycle				Tenth Cycle			
Peak Shearing Strain, %	Shear Modulus, G, ksf	Normalized Shear Modulus, G/G_{max}	Material Damping Ratio, D, %	Peak Shearing Strain, %	Shear Modulus, G, ksf	Normalized Shear Modulus, G/G_{max}	Material Damping Ratio, D, %
5.42E-04	2068	1.00	0.56	5.38E-04	2081	1.00	0.76
1.03E-03	2068	1.00	0.66	1.01E-03	2081	1.00	0.55
2.00E-03	2068	1.00	0.97	2.01E-03	2081	1.00	0.94
4.09E-03	2055	0.99	0.69	4.08E-03	2062	0.99	1.03
1.03E-02	1904	0.92	1.60	1.03E-02	1909	0.92	1.14

Table J.4 Variation in Shear Modulus and Material Damping Ratio with Shearing Strain from RC Tests of Specimen B-773B-15; Isotropic Confining Pressure, $\sigma_o = 20794$ psf

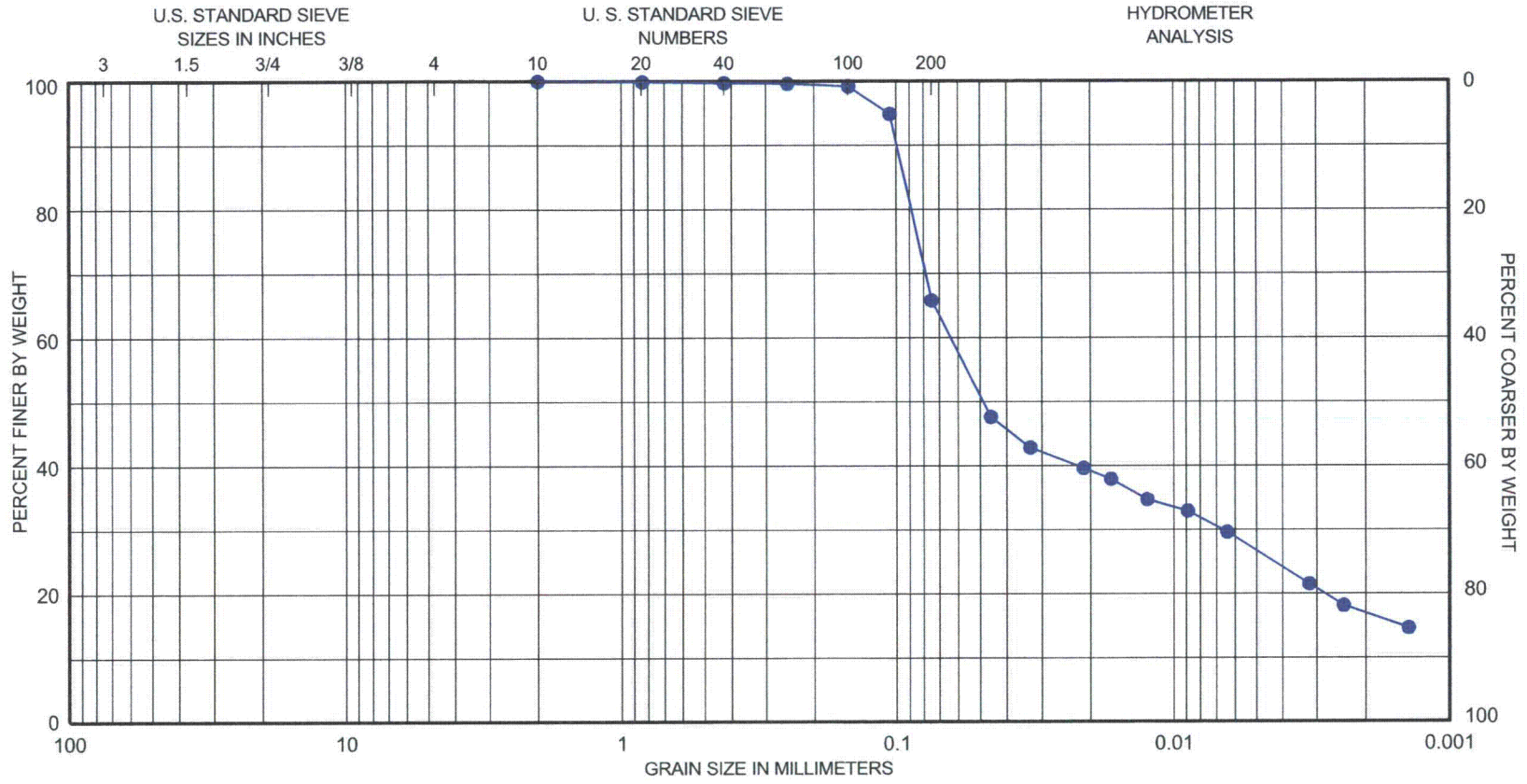
Peak Shearing Strain, %	Shear Modulus, G, ksf	Normalized Shear Modulus, G/G_{max}	Average ⁺ Shearing Strain, %	Material Damping Ratio ^x , D, %
3.94E-04	3671	1.00	3.94E-04	0.93
8.25E-04	3671	1.00	8.25E-04	0.93
1.66E-03	3671	1.00	1.54E-03	0.93
3.29E-03	3671	1.00	2.99E-03	0.94
6.48E-03	3628	0.99	5.90E-03	0.94
1.24E-02	3599	0.98	1.13E-02	1.01
2.31E-02	3515	0.96	2.08E-02	1.16
4.07E-02	3335	0.91	3.58E-02	1.52
7.15E-02	3099	0.84	5.93E-02	2.42
1.29E-01	2770	0.75	1.02E-01	3.51

⁺ Average Shearing Strain from the First Three Cycles of the Free Vibration Decay Curve

^x Average Damping Ratio from the First Three Cycles of the Free Vibration Decay Curve

Table J.5 Variation in Shear Modulus, Normalized Shear Modulus and Material Damping Ratio with Shearing Strain from TS Tests of Specimen B-773B-15; Isotropic Confining Pressure, $\sigma_o = 20794$ psf

First Cycle				Tenth Cycle			
Peak Shearing Strain, %	Shear Modulus, G, ksf	Normalized Shear Modulus, G/G_{max}	Material Damping Ratio, D, %	Peak Shearing Strain, %	Shear Modulus, G, ksf	Normalized Shear Modulus, G/G_{max}	Material Damping Ratio, D, %
5.59E-04	4176	1.00	0.72	5.71E-04	4171	1.00	0.83
1.04E-03	4176	1.00	0.78	1.03E-03	4171	1.00	1.26
2.07E-03	4176	1.00	0.94	2.06E-03	4171	1.00	1.34
4.14E-03	4176	1.00	0.87	4.15E-03	4171	1.00	0.83
1.00E-02	3958	0.95	1.15	9.98E-03	3971	0.95	1.00



GRAVEL		SAND			SILT or CLAY		
Coarse	Fine	Coarse	Medium	Fine			
<u>SYMBOL</u>	<u>BORING</u>	<u>DEPTH, FT</u>	<u>C_c</u>	<u>C_u</u>	<u>D₅₀</u>	<u>D₉₀</u>	<u>CLASSIFICATION</u>
●	B-773B-15	147	NA	NA	0.05	0.1	Sandy Fat Clay (CH), olive gray

GRAIN SIZE CURVE